The Effect of Potential Large-Scale Bioreactor Environmental Heterogeneities during Fed-Batch Culture on the Performance of an Industrially-Relevant GS-CHO Cell Culture, Producing an IgG Antibody

By

William Harry Scott

A thesis submitted to The University of Birmingham for the degree of DOCTOR of PHILOSOPHY

School of Chemical Engineering

College of Engineering and Physical Sciences

Abstract

This work aimed to study the effect of potential large-scale bioreactor environmental heterogeneities during fed-batch culture on the performance of an industrially-relevant GS-CHO cell culture, producing an IgG antibody. Heterogeneity was created by applying, for the first time in animal cell culture, a two-compartment scale-down model, using a combination of a well-mixed stirred tank reactor (STR) and plug flow reactor (PFR). Feeding of glucose substrate and alkali for pH control to the PFR was analogous to feeding them to the liquid surface of a large-scale bioreactor. The flow rate through the PFR was controlled with a peristaltic pump so that the mean residence time in the PFR was equal to typical mixing excursions at the ~20 m^3 scale. In this way, perturbations created in the PFR were analogous to perturbations created by poor mixing typical of the large-scale. The results obtained were compared with controls in which either just the STR was used; or in which circulation took place but all feeds were introduced directly into the STR. In addition to the standard parameters, antibody titre and quality were measured and flow cytometry was used to indicate cell viability and the mode of cell death. For the latter, viability was monitored by dual staining with Calcein-AM and Propidium Iodide (Calcein-AM/PI) and the mode of death by dual staining with Annexin V conjugated to phycoerythrin and Sytox Green (AV-PE/SG).

Typically, growth was continued for ~20 days and for the STR/PFR runs, this required continuous pumping for this time with a peristaltic pump. Durable neoprene was used in the pump head and the PFR tube was silicone. The results essentially fell into two categories: those without circulation and those with it. In all cases with recirculation, whether nutrients and alkali were added into the STR or the PFR, significantly decreased culture duration (~48 hours shorter) and antibody titre (~20% decrease) were found compared to those runs without circulation. All other key process indicators were the same for all cases, with or without recirculation, including death by necrosis. The equivalence of antibody quality in even those cases with greatly decreased viability provided strong evidence for robust antibody production in this cell line.

Clearly, in this study, it was not possible to conclude anything concerning the impact of bioreactor heterogeneities with this cell line. On the other hand, damage associated with peristaltic pumping has relevance to the many aspects of cell culture processes that require transfer of cells in suspension; for example, inoculation and harvest steps. For large culture volumes, pumping duration may be of significant duration. It is considered that the ‘squeezing’ motion by which peristaltic pumps cause flow may impose sufficient mechanical stress on the cells to cause the relatively poor performance. It is of course possible that it may be due to long term chemical leaching or other features of the flow loop but with the high biocompatibility of the materials used in this study, this reason is considered to be less likely.

Acknowledgements

I thank all three of my supervisors, Professors Colin Thomas, Alvin Nienow and Chris Hewitt for their expert advice and guidance over the years. Your guidance kept me focused and gave me a new perspective on research. Our discussions often provided me with a broader view and opened avenues of inquiry that would never have occurred to me. I hope to emulate your dedication and insight.

Thanks to my industrial supervisors at MedImmune, Gareth Lewis and Ray Field, for their invaluable support. Special thanks to all those at MedImmune who were confronted with a PhD student and a tight schedule, but gave their valuable time generously. I appreciate your patience and very hard work. The technical and analytical expertise that you provided was crucial for the satisfactory completion of my thesis.

I would like to thank Hazel Jennings and Elaine Mitchell for suffering my near constant demands with good grace. As well as support with my laboratory work, your fine sense of humour and ready supply of chocolates (yes, I ate them all!) always perked me up when things were not going quite to plan. Thanks to Lynn Draper for smoothing my path over the years.

I owe much of my learning, not to mention a lot of entertainment, to my fellow students, especially Boyen Isailovic and Ken Lee – masters of the flow cytometer. I was fortunate to know so many who were not only generous with their time and knowledge, but also with their food...

Mum and Dad, thank you for all your help and sacrifices. I know you sometimes wondered why I didn't just stay in gainful employment. Sometimes, I wondered the same. But the PhD was worth it.

Steven Meier at Genentech, I would like to thank you for helping to round off my rough edges and show me what it takes to be the very best kind of engineer.

A final *muchas gracias/ merci beaucoup/ ತಾಣಕ್ ಯೌ ಡಿಯರ್/ big ol' thank ya'* to my good friends at *Chez Juju* in San Francisco, Chaitra, '*Julien*' (Fr) and Julien (US), for your support, *tolerance* and, dare I say it, fine company. Your encouragement and careful administration of high-quality IPA provided much needed relief from the rigours of writing-up.

Contents

Figures

Tables

Nomenclature

Abbreviations and Acronyms

6SRGT	6 blade Scaba radial turbine
ATP	Adenosine tri-phosphate
AV	Annexin-V
AV-FITC/PI	Annexin V conjugated to fluorescein isothiocynate used in conjunction with propidium iodide
AV-PE	Annexin V conjugated to Phycoerythrin
AV-PE/SG	Annexin V conjugated to Phycoerythrin used in conjunction with Sytox Green (Dual Stain)
BD	Becton, Dickinson and Company
Calcein-AM	Calcein acetoxymethylester
Calcein-AM/PI	Calcein acetoxymethylester used in conjunction with propidium iodide (Dual Stain)
CCCP	Carbonyl cyanide m-chlorophenyl hydrazone
CFD	Computational fluid dynamics
CHO	Chinese hamster ovary
CM-H_2XRos	Chloromethyl-X-rosamine
dH_2O	Deionised water
$DiOC_6(3)$	3,3'dihexiloxocarboxyanine iodide
$DiOC_6(3)$/PI	3,3'dihexiloxocarboxyanine iodide used in conjunction with propidium iodide (Dual Stain)
DMSO	Dimethyl sulfoxide
DTT	Dithiothreitol
EB	Ethidium bromide
EC	Endothelial cells
EDTA	Ethylenediaminetetraacetic acid
ESI-Q-TOF	Electrospray ionisation quadrapole time of flight (Mass spectrometry)
FACS	Fluorescence activated cell sorting
FC	Flow cytometry/Flow cytometer (Multiparameter)
FCCP	Carbonyl cyanide p-(trifluoromethoxy) phenylhydrazone
FDA	Fluorescein diacetate
FITC	Fluorescein isothiocynate
FS	Forward scatter light
FS-SS	Forward scatter light v side scatter light

Fuc	Fucose
Gal	Galactose
GF	Green fluorescence
GF-RF	Green fluorescence v red fluorescence
GlcNAc	N-acetyl glucose amine
GS	Glutamine synthetase
GS-CHO	Glutamine synthetase chinese hamster ovary
GS-NS0	Glutamine synthetase murine myeloma hybridoma
HC	Haemocytometry/Haemocytometer
HL-60	Human promyelocytic leukemia cells
HPLC	High-pressure liquid chromatography
IEF	Isoelectric focusing
IgG	Immunoglobulin G
JC-1	5,5',6,6'-tetrachloro-1,1',3,3' tetraethylbenzimidazolcarbocyanine iodide
LC	Liquid chromatography
LDA	Laser Doppler anemometry
LDH	Lactate de-hydrogenase
Man	Manose
MSX	Methionine sulfoximine
MWCO	Molecular weight cut off
NP-HPLC 2-AB	Normal phase high pressure liquid chomatography with 2-aminobenamide
NS0	Murine myeloma hybridoma
PBS	Phosphate buffered saline (pH 7.4)
PE	Phycoerythrin
PFR	Plug flow reactor
PI	Propidium iodide
pI	Isoelectric point
PMT	Photomultiplier tube
PS	Phosphatidylserine
PTM	Post translational modification
RF	Red fluorescence
ROS	Reactive oxidative species
RQ	Respiratory quotient

SDS-PAGE	Sodium dodecyl sulfate polyacrylamide gel electrophoresis
Sf-9/Sf-21	*Spodoptera frugiperda*
SG	Sytox green
SS	Side scatter light
STR	Stirred tank (bio)reactor
TB	Trypan blue
TC	Torture chamber (a flow constriction device).

Units and Measures

A	Interfacial area for gas exchange (m^2)
B	Impeller clearance from the bottom of the reactor (m)
barg	Bar (gauge)
C	Oxygen concentration in the liquid phase (mg L^{-1})
c	Concentration of gas dissolved in solution (M)
*C**	Saturation concentration of oxygen in liquid (mg L^{-1})
cells mL^{-1}	Cells per millilitre
%CV	Coefficient of variation (%)
D	Impeller diameter (m)
d^{-1}	Bioreactor (STR) medium volumes per day
DCN	Dead cell number (1 x 10^5 cells mL^{-1})
DCN FC	Dead cell number attained by flow cytometry (1 x 10^5 cells mL^{-1})
DCN FC	Dead cell number attained by haemocytometry (1 x 10^5 cells mL^{-1})
DOT	Dissolved oxygen tension (% of air saturation, referred to as % saturation and %)
Fi	Volume fraction of gas component *i* (%/100)
g	Acceleration due to gravity (9.81 m s^{-2})
g $mole^{-1}$	Gram per mole
h	Hour
h^{-1}	Per hour
k	Equilibrium constant (dimensionless)
kDa	KiloDalton
k_La	Mass transfer coefficient (h^{-1})
L	Litre
M	Molar (mole per litre)
mg mL^{-1}	Microgram per millilitre
mL	Millilitre

mM	Millimolar
mmHg	Millimeters of mercury
mOsm kg^{-1}	Milliosmoles per kilogram
mW	Milliwatt
N	Agitation speed (rev s^{-1})
N m^{-2}	Newtons per metre square (1 Pa)
nM	Nanomolar
^{o}	Degrees (angle)
^{o}C	Degrees Celcius
OUR	Oxygen uptake rate (mg m^{-3} s^{-1})
P	Power input imparted by the impeller (W)
Pa	Pascals (1 x 10^4 Pa approximates to 75 mmHg)
pg $cell^{-1}$ h^{-1}	Picograms per cell per hour
Pn	Total pressure (Pa)
Po	Dimensionless impeller power number
pPi	Partial pressure of gas component *i* (Pa)
qAmmonia	Specific rate of ammonia production (pg $cell^{-1}$ h^{-1})
Q_G	Gas flowrate (m^3 s^{-1})
qIgG	Specific rate of immunoglobulin G production (pg $cell^{-1}$ h^{-1})
qLactate	Specific rate of lactate production (pg $cell^{-1}$ h^{-1})
rev s^{-1}	Impeller revolutions per second
rpm	Impeller revolutions per minute
RT	Mean residence time (s^{-1})
Sc	Schmidt number (dimensionless)
T	Diameter of STR (m)
TCN	Total cell number (1 x 10^5 cells mL^{-1})
TCN FC	Total cell number attained by flow cytometry (1 x 10^5 cells mL^{-1})
TCN FC	Total cell number attained by haemocytometry (1 x 10^5 cells mL^{-1})
U	Units
V	Volume of STR (m^3)
VCN	Viable cell number (1 x 10^5 cells mL^{-1})
VCN FC	Viable cell number attained by flow cytometry (1 x 10^5 cells mL^{-1})
VCN FC	Viable cell number attained by haemocytometry (1 x 10^5 cells mL^{-1})
VCN_{max}	Maximum viable cell number (1 x 10^5 cells mL^{-1})
Viability FC	Viability attained by flow cytometry (%)

Viability HC	Viability attained by haemocytometry (%)
v/v	Volume per volume
W kg^{-1}	Watts per kilogram
w/v	Weight per volume

Greek Symbols

ΔC	Driving force (C*-C)
$\Delta Viability$	Viability FC - Viability HC (%)
ΔDOT	Drop in dissolved oxygen tension (% saturation)
$\mathfrak{d}$	Diffusivity (m^2 s^{-1})
ΔVCN	*VCN* FC - *VCN* HC (1 x 10^5 cells mL^{-1})
ΔDCN	*DCN* FC - *DCN* HC (1 x 10^5 cells mL^{-1})
ΔTCN	*VCN* FC - *VCN* HC (1 x 10^5 cells mL^{-1})
$\Delta\Psi$	Plasma membrane potential (mV)
$\Delta\Psi m$	Mitochondrial membrane potential (mV)
λk	Kolmogoroff micro-scale of turbulence (m)
μ	Specific growth rate (h^{-1})
η	Viscosity (Pa s)
µL	Microlitre
µM	Micromolar
ν	Kinematic viscosity (m^2 s^{-1})
v_s	Superficial gas velocity (m s^{-1})

Energy Dissipation Rate Symbols

$(\bar{\varepsilon}_T)_I$	Mean specific energy dissipation rate from the impeller (W kg^{-1})
$(\varepsilon_T)_I$	Local specific energy dissipation rate from the impeller (W kg^{-1})
$(\varepsilon_T)_{Imax}$	Maximum local specific energy dissipation rate from the impeller (W kg^{-1})
ε_T	Local specific energy dissipation rate (W kg^{-1})
$\bar{\varepsilon}_T$	Mean specific energy dissipation rate (W kg^{-1})
$(\varepsilon_T)_{max}$	Maximum local specific energy dissipation rate (W kg^{-1})
$(\varepsilon_{TC})_{max}$	Median of the maximum specific energy dissipation rate provided by the torture chamber (W kg^{-1})
$E_{max,pipe}$	Maximum energy dissipation rate in tubing (W m^{-3})
$\varepsilon_{max,pipe}$	Maximum energy dissipation rate in tubing (W kg^{-1})

Chapter 1: Literature Survey

1.1 Motivation and Hypothesis

In large-scale stirred tank reactors (STR) (Section 1.4), feeds such as acid, base and nutrients (nutrient feed referred to from here as substrate) are normally added to the liquid surface immediately below the feeding entry-point in the STR head-plate. This has been shown to result in significant, deleterious perturbations that are initially localised in the area around the feeding point (Section 1.7). Such perturbations have been shown to decrease final product concentration (titre) in microbial cell culture (Namdev and Thompson, 1992; Larsson et al., 1996; Langheinrich and Nienow, 1999). Feeding to the impeller region shortens the dispersion time of feeds significantly (Byland et al., 1998; Langheinrich and Nienow, 1999), but is generally considered impracticable for clean-in-place (CIP) sterility (Christi and Moo-Young, 1994). In large-scale microbial culture, very high cell concentrations and the economic and practical restraints on power input for agitation mean that vessel heterogeneity is difficult to avoid. These restraints are also relevant in large-scale animal cell culture; however, poor mixing has typically resulted from a deliberate curb on power input for impeller agitation motivated by concerns over hydrodynamic cell damage ('shear') (Varley and Birch, 1999; Lara et al., 2006; Nienow, 2006). The extent of concern has been shown to be misplaced (Kunas, 1990; Zhang and Thomas, 1993; Nienow and Langheinrich, 1996) and often instead attributable to bubble-bust-damage (Oh et al., 1989; Boulton-Stone, 1995; Ma et al., 2004). Nevertheless, power input is still often relatively low (Nienow, 2006) and it is evident that animal cells are typically less robust that microbial cells.

Furthermore, greater understanding of animal cell culture requirements continues to increase the maximum attainable cell concentration, which will increase vessel heterogeneity (Nienow, 2006).

In microbial culture, two-compartment laboratory scale-down methods (Section 1.8) have been used to conduct laboratory-scale research on the effect of conditions like those found at the large-scale (Namdev and Thompson, 1992; George et al., 1993; Hewitt et al., 2000; Amanullah et al., 2001). Research at the large-scale (e.g., 20 m^3) is limited by cost. For animal cells, only one such two-compartment scale-down study has been conducted (Osman et al., 2002) and the consequences of STR heterogeneity are poorly understood. This is troubling because animal cell culture is the predominant means for production of high-value complex therapeutic proteins and successful transfer from laboratory-scale development to large-scale production is important for the commercial success of the drug pipeline (Birch, 2005; Birch and Racher, 2006).

Thus, it is hypothesised that a two-compartment scale-down model, like that used for scale-down of microbial cell culture, can be used to generate, and study the influence of, perturbations in pH and substrate that sufficiently resemble those that occur in a large-scale stirred tank reactor (STR) for commercial production of therapeutic proteins from animal cell culture. Further, it is hypothesised that these perturbations will influence important aspects of the culture performance, such as antibody concentration (titre) and antibody characteristics (antibody quality). In this study, a stirred tank reactor and plug flow reactor (STR+PFR) scale-down model was chosen because the PFR is well suited to simulation of perturbations created by additions to the feeding zone in a large-scale STR (Section 1.8.4).

Chapter 1: Literature Survey

The principle aim of this study was to investigate the effects of pH and substrate gradients, which are typical of a poorly mixed large-scale STR used for animal cell culture (Section 1.7.1 and Section 1.7.4), on biological performance of an industrially relevant culture of glutamine synthetase Chinese hamster ovary cells (GS-CHO, Section 1.3), using scaled down experiments (Section 2.7). Special consideration was given to the effects of the scale-down on antibody titre and antibody quality (such as glycosylation) (Section 1.1.1), as both are typically of great importance in commercial drug production (Section 1.4).

Flow cytometry (FC) was used with the aim of investigating the physiology of cells in scaled down experiments in greater depth than would be possible with the traditional haemocytometer method (Section 1.9). An understanding of how perturbations like those that are expected to occur in large-scale culture vessels influence cell physiology, antibody titre and antibody quality should allow for better decisions regarding process development, scale-up and operation.

1.2 Monoclonal Antibodies

Antibodies can distinguish between cells of individual members of a species and in some cases can distinguish between proteins that differ by only a single amino acid. Such exquisite binding specificity makes them ideal for directed therapy in the body. By engineering antibodies in the laboratory, it is possible to create highly directed therapeutic agents that are used, amongst other things, to deliver toxic substances to cancer cells leaving normal cells unscathed, and to interrupt and block an autoimmune response in diseases such as Crohn’s (Waldmann, 2003).

1.1.1 Antibody Quality

Therapeutic antibodies require complex posttranslational modifications (PTMs) for efficient secretion, drug efficacy and stability. Common modifications include glycosylation, misfolding and aggregation, oxidation of methionine, deamidation of asparagine and glutamine, and proteolysis (Jenkins, 2007). The nature and extent of PTMs that determine the efficacy of the antibody as a drug are influenced by production conditions, such as culture environment. Product consistency is therefore often reliant on successful control of crucial process parameters within specified limits (Kozlowski and Swann, 2006).

To expedite the drug approval process it is important to establish the protein's characteristics during process development and to ensure that they remain unaltered during scale-up to commercial production (Jenkins et al., 1996). A scale-down model capable of creating large-scale conditions might therefore provide a useful insight into the effects of scale-up on antibody quality. Antibody characteristics are reportedly influence greatly by those aspects of culture environment, such as pH and substrate concentration, which scale-up may alter.

1.2.1.1 Mass Heterogeneity

Mass heterogeneity is primarily introduced by antibody aggregation and chemical modifications. Within the cell, process conditions can cause aggregation by altering protein folding and secretion (Zhang et al., 2004; Chaderjian et al., 2005) and, once the complete antibody is secreted into the culture medium, by subjecting the protein to chemical (such as pH and salt concentration) and physical (such as shear stress) degradation (Chi et al., 2003; Cromwell et al., 2006). Aggregation often increases at alkali pH (Liu et al., 2008).

Protein aggregation is highly undesirable for therapeutic antibodies, because the aggregates might result in an immunogenic reaction (small aggregates), or complications following drug administration (particulates) (Hermeling et al., 2004; Cromwell et al., 2006). The chemical modifications of interest typically alter protein charge (Section 1.2.1.2). Glycosylation does not typically alter charge but is important in its own right (Section 1.2.1.3).

1.2.1.2 Charge heterogeneity

Charge heterogeneity is primarily introduced by deamidation and C-terminal lysine microheterogeneity (Tsai et al., 1993; Perkins et al., 2000). The antibody studied here was without a C-terminal lysine: any change in charge was attributed to deamidation. Deamidation of asparagine and glutamine introduces an additional negative charge to the antibody and generates acidic species that decrease the protein's isoelectric point (pI) (Liu et al., 2008).

Deamidation of asparagine forms isoaspartate, which is not a natural amino acid and can potentially be immunogenic (Jenkins, 2007). Furthermore, a decrease to, or complete loss of, activity has been reported for IgG (Harris et al., 2001) and other proteins such as recombinant DNAse (Cacia et al., 1993) and recombinant soluble CD4 (Teshima et al., 1991). Like protein aggregation (Section 1.2.1.1), the rate of non-enzymatic deamidation is reportedly accelerated at alkaline pH (Usami et al., 1996; Jenkins, 2007; Liu et al., 2008), and hyperosmotic stress has also been found to decrease the isoelectric point (Schmelzer and Miller, 2002).

1.2.1.3 Glycosylation

Glycosylation can play a crucial role in the activity of therapeutic proteins: the majority glycan groups are attached to the Fc fragment, where they influence the pharmacokinetics, bioactivity, secretion, *in vivo* clearance and solubility recognition (Jenkins and Curling, 1994; Jenkins et al., 1996; Sinclair and Elliott, 2004).

Quantitative and qualitative aspects of glycosylation can be altered by many aspects of the production process. The following are chosen for their relevance: the type of culture vessel and culture method; for example, STR, perfusion, suspension culture or attached culture on beads (Maiorella et al., 1993); critical culture parameters, such as pH, pCO_2, pO_2 and 'shear' (Goochee and Monica, 1990; Senger and Karim, 2003); and glucose concentration (Hayter et al., 1992a; Wong et al., 2004). Furthermore, many alterations and effects are likely to be specific to the host cell line (Sheeley et al., 1997).

1.3 GS-CHO

Chinese hamster ovary (CHO) cells are widely used to produce recombinant antibodies, often using either the DHFR (dihydrofolate reductase) or GS (glutamine synthetase) expression systems (Butler, 2005a; Merten, 2006). This research project used a suspension variant (SV) of the CHO-K1 cell line (CHOK1SV), transfected for GS gene expression, GS-CHO (Section 2.1). The GS gene expression system provides a consistent means of rapidly generating high producing cell lines. Glutamine synthetase (GS) is the enzyme responsible for the biosynthesis of glutamine from glutamate and ammonia, and without it there is no pathway for glutamine formation in a mammalian cell. Normally, unlike NS0 cells, CHO cell lines express sufficient quantities of GS to survive without exogenous glutamine

(Barnes et al., 2000). Recombinant cell selection is made using a GS inhibitor, methionine sulphoximine (MSX), to decrease endogenous GS activity, rendering it insufficient, such that only transfectants that have stably incorporated the GS expression vector into a transcriptionally active locus will survive (Birch and Racher, 2006). The genetic linkage between GS and the transfected gene of interest ensures that the transgene is co-amplified, enhancing the selection of high producing strains (Birch and Racher, 2006).

1.4 Large-Scale

After the successful selection of a recombinant CHO cell line that produces the desired antibody at high concentrations the cell culture must be characterised and the production process developed to assure robust production at commercial manufacturing scales. Depending on the application and dose concentration, some proteins may be required in very large quantities (possibly hundreds of kg per year). To meet the current great demand for therapeutic proteins in a profitable manner, large-scale production has been intensified in ways that clearly increase the potential for differences in culture performance in the development laboratory-scale vessel (~5 L) and large-scale vessel (~20000 L: 20 m^3) used for industrial production. Stirred tank reactor (STR) scale has been increased, to benefit from economies of scale; and volumetric throughput (i.e., cell concentration) of reactors has been increased to improve volumetric productivity. Optimisation of processes during development in the laboratory has therefore become paramount (Varley and Birch, 1999). Indeed, STR scale has increased from only 8 m^3 a few decades ago to 20 m^3 (Lonza, Portsmouth/NH facility) and typical maximum cell concentration has increased to the order of 10^7 cells mL^{-1}. Vessel scale and cell concentration are

predicted to continue increasing while demand for therapeutic proteins is high (Birch and Racher, 2006; Nienow, 2006).

Considering the difference in STR size (scale), it is unsurprising that the transfer from laboratory-scale development reactors to large-scale production reactors may be accompanied by alterations to antibody titre and quality. Such changes are often undesirable, but even ostensibly desirable changes to the cultures' characteristics upon scale-up, such as increased glycosylation, may raise difficulties for regulatory compliance. A considerable factor in the possible change in performance during scale-up is likely to be the far greater heterogeneity that is typical of the large-scale (Namdev and Yegneswaren, 1991; Larsson et al., 1996; Nienow and Langheinrich, 1996; Bylund et al., 1999; Amanullah et al., 2001).

Increased heterogeneity is the corollary of increased mixing time, θ_{m}, that is typically caused by a decrease in agitation speed, *N*, made as part of the transfer to the large-scale. The reasons for the decrease to *N* are twofold. Firstly, the required *N* to satisfy O_2 mass transfer requirements is lower than at the laboratory-scale. Secondly, the ratio of impeller diameter, *D*, to vessel diameter, *T*, (*D/T*) is typically held constant at scale-up; at constant *N* any increase to *D* very substantially increases mean specific energy dissipation rate from the impeller, $(\overline{\varepsilon}_T)_I$, impacting on concerns over hydrodynamic damage or 'shear' (referred to as shear, while acknowledging that this usage may be considered imprecise, Section 1.6). Indeed, concern over shear may often be the key consideration when setting *N*, even if shear may not be as great a problem as is generally believed (Nienow, 2006). Thus, scale-up is often made with a near constant mean specific energy dissipation rate from the

impeller, $(\overline{\varepsilon_T})_I$, and, consequently, greatly increased mixing time, θ_{m} (Osman et al., 2001; Nienow, 2006).

Increased environmental heterogeneity caused by the far greater θ_{m} that is typical in a large-scale stirred tank reactor (STR) used for the industrial production of therapeutic antibodies by animal cell culture can result in perturbations, decreased control and, consequently, unpredictable process performance. Of primary concern is that such perturbations may decrease antibody titre and change antibody quality (Section 1.1.1). An understanding of the implications of poor mixing and STR heterogeneity is therefore essential to surmount this problem and is the main thrust of this thesis.

1.5 Mixing and Reactor Heterogeneity

Mixing time, θ_{m}, can be approximated using a reasonably simple method: tracer is added to the STR, and its concentration plotted against the time since addition; concentration is measured by one or more suitable probes at fixed points in the STR (Coulson and Richardson, 2000). Over time, under idealised conditions, the probe shows a periodic concentration variation above and below the equilibrium tracer concentration, with constant wavelength and diminishing amplitude. The period of the wave is often termed the ‘circulation time’.

θ_{m} is defined as the time at which the amplitude has decreased to within a specified deviation from the equilibrium concentration. When additions of tracer are made to the liquid surface, the duration of mixing is greatly increased because intensive mixing is typically localised to the impeller region

Cutter (1966) found that 70% of energy dissipation took place in the 'impeller zone', creating a well-mixed impeller zone and poorly mixed bulk zone (Figure 1-2). Note that the impeller region is loosely defined and the percentage of the energy dissipation is dependent on the size of impeller region chosen. It is unsurprising that maximum local specific energy dissipation rate from the impeller, $(\varepsilon_T)_{\mathrm{Im}ax}$, is close to the impeller.

It is logical to assume that local gradients of velocity close to the impeller are orders of magnitude higher than the average values in the vessel (Midler and Finn, 1966). The higher local specific energy dissipation rate, $(\varepsilon_T)_I$, in this region close to the impeller has led some groups to define an impeller region based on a subjective choice of a volume close to the impeller. Defined by Zhou and Kresta (1996) as 4.87% of the total volume into which 28.2% of the total energy is dissipated, and in a recent study by Mollet et al. (2004) as a 'square ring' that contains 5.74% of the total liquid in the vessel into which 27.8% of the total energy is dissipated.

Cutter (1966) was the first to quantify the variation in $(\varepsilon_T)_I$ throughout a STR. Using a photographic method, Cutter (1966) found that in a tank stirred with a Rushton turbine the ratio of the local specific energy dissipation rate to the mean specific energy dissipation rate, $(\varepsilon_T)_I$ to $(\overline{\varepsilon}_T)_I$, or $(\varepsilon_T / \overline{\varepsilon}_T)_I$, varied from 0.25 in the bulk region of the tank to 70 near to the impeller. Showing that $(\varepsilon_T)_{\mathrm{Im}ax}$ was 280-fold greater than in the bulk of the tank. Similarly, Costes and Couderc (1988) found that $(\varepsilon_T)_{\mathrm{Im}ax}$ was 200-fold greater, and Mollet et al. (2004) found that it was 60-fold greater. The mean specific energy dissipation rate from the impeller, $(\overline{\varepsilon}_T)_I$, is therefore a poor indicator of the most turbulent environment in a STR.

It is established that as cells circulate randomly around the STR, following turbulent flow patterns, they will be exposed to a continuous variation in $(\varepsilon_T)_I$. Further, that the $(\varepsilon_T)_I$ in the STR may, nevertheless, be considered as divided into two distinct regions: the bulk of the STR, where $(\varepsilon_T)_I$ is often lower than $(\overline{\varepsilon}_T)_I$, and the impeller region, where $(\varepsilon_T)_I$ may be at least 50-fold greater than $(\overline{\varepsilon}_T)_I$.

In the impeller zone, micromixing predominates, so blending is fast down to the molecular scale, where it becomes limited by the rate of molecular diffusion; in the bulk of the STR, macromixing that is controlled by convective bulk diffusion and eddy diffusion is predominant (Manning et al., 1965; Brodkey and Reuss, 1982). Thus, blending or mixing of the entire STR contents is limited by the rate of turbulent diffusion in the bulk of the STR, independent from the agitator.

Feeding is typically restricted to the liquid surface of the STR by practical limitations of clean-in-place (CIP) techniques (Christi and Moo-Young, 1994); surface feeding creates a third zone that is transiently localised around the feeding point— the feed zone. A conceptual model of feeding to a poorly mixed STR might segregate the fluid contents of the STR into three-zones: the impeller zone, the bulk zone, and the feed zone, as proposed by Namdev and Thompson (1992).

High concentration zones are predominantly formed around the feeding points farthest from the impeller, where inefficient mixing fails to disperse the feed rapidly – substrate and alkali often form high concentration regions in this way. Langheinrich and Nienow (1999) used alkali plus an appropriate indicator to show elegantly that plumes of elevated pH are created around the point of feeding of a large-scale reactor; the dispersal of the purple plume was recorded. Evidently, until the concentrated plume is completely dispersed a portion of the culture volume, and

the cells within that volume, will be exposed to an elevated pH, i.e., cells will be exposed to perturbations for a duration approximating to θ_{m}.

Low concentration zones will be created when the rate of consumption by cellular activity is greater than the mixing rate - substrate and O_2 can form low concentration regions in this way. Furthermore, the two regions are not mutually exclusive: the creation of O_2 limitations within the glucose feed zone is a problem that, for the time being, is considered restricted to microbial reactors, because of their high cell concentration cultivation. However, it will almost certainly occur in mammalian cell culture eventually, as increased understanding of cell culture requirements allows for increased cell concentrations to increase volumetric productivity.

Elevated substrate in the feed zone might also create localised accumulation of metabolic by-products (metabolites) that alter pH and further exacerbate STR heterogeneity (George et al., 1993). Concerns surrounding the shear sensitivity of animal cells mean that scale-up is typically made at constant $(\varepsilon_T)_{I\max}$, at the expense of greatly increased θ_{m}, and increased heterogeneity (Section 1.7). A discussion of current research on animal cell shear sensitivity will now be made to inform the subsequent section on the creation of bioreactor heterogeneity.

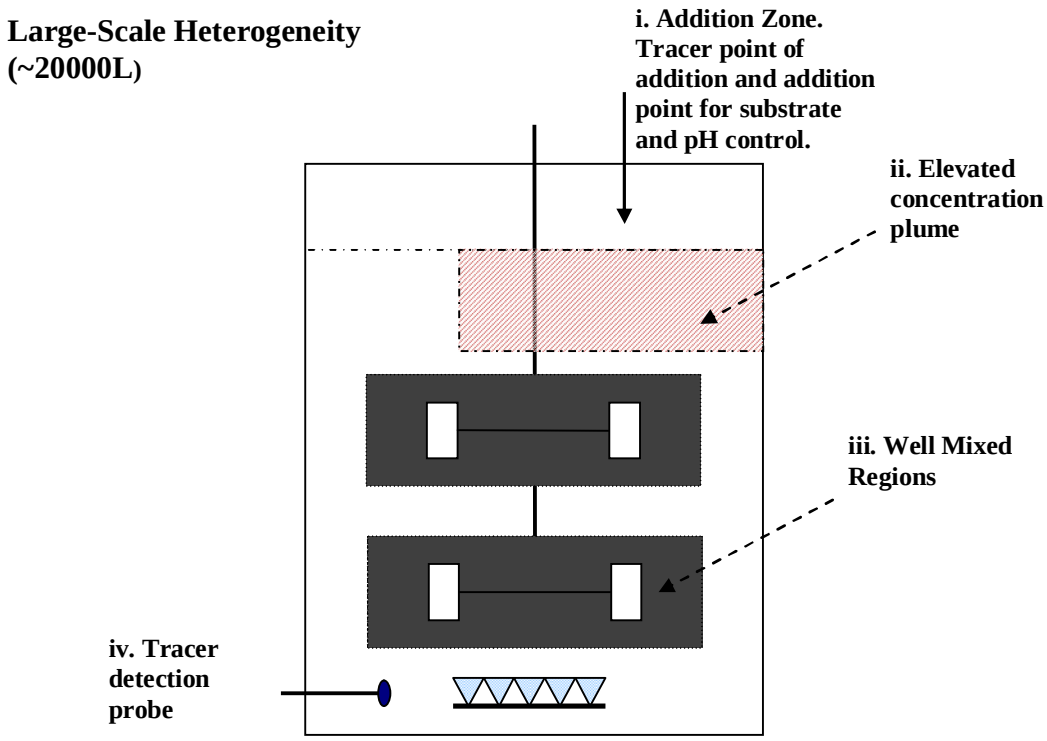

Figure 1-1: Large-scale (~20 m^3) stirred tank reactor (STR) with shading to identify mixing zones: i) addition point at liquid surface; ii) elevated concentration in the addition zone; iii) well mixed impeller region; iv) probe for detection of tracer addition. This schematic is an adaption of the two-compartment model proposed by Oosterhuis and Kossen (1984).

1.6 Energy Dissipation Rate and 'Shear'

In the large-scale culture of animal cells 'shear' and accompanying 'shear sensitivity' has been a subject of considerable debate. 'Shear' here refers generally to any hydrodynamic or mechanical mechanism that may damage the cell, and the term shear will be used, in place of 'shear', while acknowledging that it does not refer directly to shear stress or shear rate, which are difficult to define for the turbulent flow present in a typical STR. The mean specific energy dissipation rate from the impeller, $\left(\bar{\varepsilon}_T\right)_I$, is considered a better means to characterise the turbulent flow in a STR (Pohorecki et al., 1998).

In spite of the contrary evidence (Telling and Elsworth, 1965; Augestein et al., 1971), perceived cell fragility (Midler and Finn, 1966; Nevaril el al., 1968; Bluestein and Mockros, 1969) led to excessive caution in the design of large-scale culture systems, which still suffer from restricted agitation and, consequently, poor mixing (Nienow, 2006). Early concerns around the generation of damaging shear by impeller agitation are now considered largely misplaced, thanks to numerous demonstrations of consistent cell growth and productivity in STR agitated at significantly higher speeds than are commonly used in industry (Oh et al., 1989; Kunas, 1990; Nienow and Langheinrich, 1996). Two studies that effectively demonstrated the resilience of animal cells to shear were conducted by Zhang and Thomas (1993). In one study, they found that hybridoma cells were viable after exposure to 1500 rpm (4 W kg^{-1}) in an un-aerated tank with no air/liquid interface, showing that agitation alone is much less damaging than many thought. In a study of NS1 myeloma cells, passage through capillary tubes was used to demonstrate cell

integrity until specific energy dissipation rates, ε_T, as high as 10^5-10^6 W kg^{-1} were reached (Zhang and Thomas, 1993).

In the literature, it is now established with little doubt that most of the cell damage is not a direct result of shear created by agitation and instead was caused when cells became entrained with bubbles and were exposed to bubble bursting, which can generate ε_T in the order of 10^4-10^5 W kg^{-1}. Fortunately, this damage can be mitigated by surfactants, such as Pluronic-F68, that decrease cell attachment to bubbles and thereby limit exposure to hydrodynamic damage created by bubble bursting (Oh et al., 1989; Boulton-Stone, 1995; Kioukia et al., 1995; Wu, 1995). More recent work (Ma et al., 2002) using a flow constriction device to expose cells to a range of $\overline{\varepsilon}_T$ has shown that CHO cell viability was not lowered until $\overline{\varepsilon}_T$ was raised to 10^4-10^5 W kg^{-1}, several orders of magnitude higher than the $(\varepsilon_T)_{\max}$ generated by impellers in a typical large-scale STR, but equivalent to the $(\varepsilon_T)_{\max}$ found during bubble bursting (Boulton-Stone and Blake, 1993). The insensitivity of animal cells to ε_T even several orders of magnitude greater than is typical at the large-scale is contested by two recent studies that report a noteworthy sub-lethal influence of shear.

The first study (Senger and Karim, 2003), found that the proportion of Type II recombinant tissue type plasminogen activator protein, r-tPA, was ‘maximised under damaging levels of shear stress.’ Unfortunately, they do not specify the $(\overline{\varepsilon}_T)_I$ in their STR and instead provide the Reynolds number, Re, as an indicator of the levels of shear that might be expect. Nevertheless, they do provide the STR dimensions and agitation speed of their experimental case with greatest shear (N =

200 rpm, D = 0.045 m, V = 1.5 x 10^{-3} m^3) and state that a pitched blade (45°) impeller was used. By assuming Po = 1.7 (the Po for a 6SRGT radial impeller; note that for a Rushton turbine Po = 5.5 (Nienow, 1998)) and ρ = 1000 kg m^{-3} (equal to water) then from their STR dimensions power input from the impeller, P, can be found from Equation 1-1:

$$P = Po\rho_L N^3 D^5$$

$$P = 1.7 \text{ x } 1000 \text{ x } (3.33)^3 \text{ x } (0.045)^5$$

$$P = 0.012 \text{ W}$$

And mean specific energy dissipation, $\left(\bar{\varepsilon}_T\right)_I$, rate from Equation 1-4:

$$\left(\bar{\varepsilon}_T\right)_I = P / \rho_L V$$

$$\left(\bar{\varepsilon}_T\right)_I = 0.012/ (1000 \text{ x } 1.5 \text{ x } 10^{-3})$$

$$\left(\bar{\varepsilon}_T\right)_I = 8 \text{ x } 10^{-3} \text{ W kg}^{-1}.$$

It is surprising that this low $\left(\bar{\varepsilon}_T\right)_I$ resulted in extensive cell death, as this is contrary to the findings of many of the studies discussed above. Since their experiment was conducted with an air/liquid interface, it is possible that increased bubble entrainment and the subsequent bubble disengagement damage was responsible for the elevated cell death found at greater N.

The second study to report an altered glycosylation profile at elevated shear (Godoy-Silva et al., 2009a) generated elevated shear by circulation through a modified version of the flow constriction device developed by Ma et al. (2002), and now referred to as the torture chamber. The torture chamber (TC) generated shear in the laminar flow region by forcing cells suspended in medium through a 227 μm gap

(throat) in a stainless steel plate. The TC was used to test the following $(\varepsilon_{TC})_{\max}$: 60, 2.9 x 10^2 , 2.3 x 10^3, 6.4 x 10^3 W kg^{-1}. (Note: they gave $(\varepsilon_{TC})_{\max}$ values in W m^{-3}).

Recirculation began from day 4 of a 14-day fed-batch process. The industrially relevant recombinant CHO line (provided by Pfizer) was repeatedly exposed to shear by recirculation from the STR, through the TC, and back into the STR. An increase in antibody glycosylation was found for all $(\varepsilon_{TC})_{\max}$, increasing the number of galactose groups present in the N-glycosylation of the antibody product. Cell concentration, viability and antibody titre were unaltered, compared to a control case with recirculation and negligible shear (TC with throat widths of 1.2 mm and 2.0 mm were used to generate $(\varepsilon_{TC})_{\max}$ of 9 x 10^{-2} W kg^{-1} and 1.2 W kg^{-1}, respectively). Increased glycosylation with shear is an interesting result.

In part, the Godoy-Silva et al. (2009a) study hoped to simulate the circulation of cells through $(\varepsilon_T)_{\mathrm{Im}ax}$ close to the impeller of a large-scale STR. In spite of this aim, the $(\varepsilon_{TC})_{\max}$ used in their study significantly exceeded those found at the large-scale: the lowest tested $(\varepsilon_{TC})_{\max}$ was, at 60 W kg^{-1}, about 60-fold greater than the typical $\left(\overline{\varepsilon}_T\right)_I$ currently used at the large-scale. This was acknowledged, and they suggested testing $(\varepsilon_{TC})_{\max}$ of between 1 W kg^{-1} and 60 W kg^{-1} for further studies, with the aim of finding the minimum $(\varepsilon_{TC})_{\max}$ at which glycosylation was increased. Regardless of its applicability to scale, their results imply that, for some cell lines and therapeutic products, elevated shear of the sort generated by the TC might be a lever for glycosylation.

However, it should be noted that in an earlier study by the same group (Godoy-Silva et al., 2009b), using the same methods but with the CHO 6E6 cell line

, no alteration to glycosylation was observed and viable cell number (*VCN*), viability and antibody titre were observed to decrease with increasing shear. Since both studies were purportedly performed in the same manner, the contrary results of the two studies imply that there is a cell line specific response to the type of shear generated by recirculation through the TC. Further study is necessary. Shear continues to be an issue of ambiguity and the spectre of a sub-lethal influence to product quality is unfortunately likely to invigorate efforts to minimise shear rather than to maximise vessel homogeneity.

1.7 Creation of Heterogeneity on Scale-Up

It was stated above (Section 1.5) that blending or mixing of the entire STR contents is limited by the rate of turbulent diffusion in the bulk of the reactor, well away from the agitator. This forms the basis of the turbulence model of STR mixing, which states that under turbulent flow conditions, the time required to homogenise the contents of a STR, θ_m (s), is independent of impeller type and is related to agitation parameters by the equation (Nienow, 1997),

$$\theta_m = 5.9\left(\bar{\varepsilon}_T\right)_g^{-1/3}\left(D/T\right)^{-1/3}T^{2/3} \qquad \textbf{1-1}$$

when $H=T$. For STR with an aspect ratio, AR (=H/R)>1, then (Nienow, 1997),

$$\theta_m \mu \left(H/D\right)^{2.43} \qquad \textbf{1-2}$$

It was assumed that the density of the medium is close to that of water (1000 kg m^{-3}) and that the Reynolds number is greater than 1 x 10^4. $\mathrm{Re} = \rho_L N D^2/\eta$, where ρ_L is the media density, η is the viscosity, *D* is the impeller diameter and *N*, its speed (rev s^{-1}). Furthermore, it is assumed that the very low gas flow rate used in animal cell culture, to date, does not alter the impeller performance, so that $Po_g \approx Po$

(Langheinrich et al., 1998). It is clear from Equation 1-1 that θ_m is proportional to vessel diameter ($T^{2/3}$) and at constant $(\bar{\varepsilon}_T)_I$ will therefore increase on scale-up to a geometrically similar STR, for which *D/T* is the same as the laboratory-scale.

Indeed, to maintain a constant θ_{m} with an increase in the STR scale by only a factor of 10 with dimensional consistency (constant *D/T*) will increase $(\bar{\varepsilon}_T)_I$ significantly. The calculation of the actual value follows.

The power input, *P* (W), to the STR, imparted by the impeller, is given by

$$P = Po\rho_L N^3 D^5 \qquad \textbf{1-3}$$

and the mean specific energy dissipation rate (W kg^{-1} or m^2 s^{-3}) from the impeller is given by

$$\left(\bar{\varepsilon}_T\right)_I = P / \rho_L V \qquad \textbf{1-4}$$

where V is the volume of medium in the STR and in a cylindrical tank is given by

$$V = \left(\pi / 4\right) T^3 \qquad \textbf{1-5}$$

Since D/T is constant, $V \propto D^3$ and from Equation 1-4

$$(\bar{\varepsilon}_T)_I \propto N^3 D^2 \qquad \textbf{1-6}$$

Thus, for a constant θ_{m}, *N* is constant and *D* increases by a factor of 10, increasing $(\bar{\varepsilon}_T)_I$ by 100-fold. This substantial increase in $(\bar{\varepsilon}_T)_I$ impacts on concerns around the 'shear sensitivity' of animal cells, and it is therefore likely that a greatly decreased *N* will be chosen for scale-up, increasing θ_{m} (Equation 1-9).

Furthermore, the increase of $(\bar{\varepsilon}_T)_I$ with scale means that a decrease in N need not leave O_2 mass transfer requirements unmet, and it may be considered desirable to maintain O_2 mass transfer characteristics on scale-up. The O_2 mass

transfer coefficient $k_L a$ (s^{-1}) is related to the gassed mean specific energy dissipation rate $(\bar{\varepsilon}_T)_{Ig}$ (gas from sparging) and the superficial gas velocity, v_s, by,

$$k_L a = A(\bar{\varepsilon}_T)_{Ig}^{\alpha}(v_s)^{\beta} \qquad \textbf{1-7}$$

Equation 1-7 applies independent of the impeller type and scale; α and β are usually about 0.5 ± 0.1, whatever the medium. A is extremely sensitive to medium composition (Nienow, 2003). Thus for a linear scale-up, maintaining geometric similarity and medium consistency, it is possible to meet O_2 transfer requirements with a decreased N, so long as v_s is maintained.

Scale up criterion	Designation		Constant *P/V*	Constant *N*	Constant U_T	Constant *Re*
Power Input or Energy Dissipation Rate	P	$P \alpha N^3 D^5$	1000	10^5	100	0.1
Mean Specific Energy Dissipation Rate	P/V	$P/V \alpha N^3 D^2$	**1**	100	0.1	10^{-4}
Impeller Rotational Speed	N		0.22	**1**	0.1	0.01
Impeller Diameter	$\boldsymbol{D}$		**10**	**10**	**10**	**10**
Mixing Time	$\boldsymbol{\theta_m}$	$\boldsymbol{\theta_m \alpha N^{-1}}$	**4.64**	**1**	**10**	**100**
Maximum Impeller Tip Speed	U_T	$U_T \alpha ND$	2.2	10	**1**	0.1
Reynolds Number	Re	$Re \alpha ND^2$	22	100	10	**1**

Table 1-1: The effect of scale-up criteria for a 10-fold linear scale-up maintaining geometric similarity on mixing parameters that impact on stirred tank reactor (STR) performance. Adapted from Amanullah (1994).

Cell fragility concerns in animal cell culture often overshadow proper consideration of θ_m and have resulted in the acceptance of constant impeller tip-speed (U_T) and constant $(\bar{\varepsilon}_T)_I$ as scale-up criteria.

Maintenance of U_T is acknowledged by Varley and Birch (1999) as a scale-up criterion, despite a 10-fold increase in θ_m:

$$U_T = \pi ND \qquad \textbf{1-8}$$

Since $(\bar{\varepsilon}_T)_I \propto N^3 D^2$ and $\theta_{\mathrm{m}} = 5.9\left(\bar{\varepsilon}_T\right)^{-1/3}\left(D/T\right)^{-1/3} T^{2/3}$, for constant D/T

$$\theta_{\mathrm{m}} \propto \left(N^3 D^2\right)^{-1/3}\left(D\right)^{2/3} \qquad \textbf{1-9}$$

and therefore

$$\theta_{\mathrm{m}} \propto N^{-1} \qquad \textbf{1-10}$$

for a constant (D/T), and if N is held constant and D decreased for constant U_T

$$\theta_{\mathrm{m}} \propto D^{-1} \qquad \textbf{1-11}$$

Thus, as Nienow (2006) states, 'maintaining constant tip speed is a major constraint on scale-up with severe implications for mass transfer as well as homogeneity.' Yet there is little evidence to support the assertion that tip speed has a critical effect in terms of shear; indeed, Amanullah et al. (2003) found in a mycelium fermentation that damage went down on scale-up, despite an increase in tip speed.

To restrict hydrodynamic shear created by the impeller, scale-up is often conducted with constant $(\bar{\varepsilon}_T)_I$ as the criterion, but since

$$(\bar{\varepsilon}_T)_I \propto N^3 D^2 \qquad \textbf{1-12}$$

and D increases 10-fold, then N^3 must decrease by 100-fold, so by finding x,

$$100\left(\frac{N}{x}\right)^3 = N_{smallscale} \qquad \textbf{1-13}$$

it is found that θ_{m} is decreased by 4.64-fold. If STR heterogeneity is not a concern this may seem appealing, since thanks to the low O_2 uptake rate (*OUR*) of animal cells, even at this decreased agitator speed, N, it is easy to meet the O_2 demands of the culture.

It is important to note the implications of Equation 1-3: because $P \propto D^5$, a 10-fold increase in *T* (constant *D/T*) when constant θ_m (constant *N*) is desired will increase the power required for agitation, *P*, by a factor of 10^5. Thus, if the laboratory-scale motor consumes 100 Watts (W), as stipulated by Applikon (www.applikon-bio.com), a STR manufacturer, then to achieve the same θ_m an equivalent commercial-scale motor will consume 10 MW—approximately equal to the power output of a large wind farm (MacKay, 2009). Clearly, scale-up at constant θ_m is impracticable.

The combination of practical and economic restraints coupled to the perceived and debatable possibility of shear damage has severely restricted impeller agitation speeds, and sometimes impeller diameter, in mammalian cell cultures, so that upon scale-up there is a significant increase in θ_m (Table 1-2). θ_m in a 5 L laboratory-scale mammalian cell culture was reported by Kenty et al. (2005) as between 2 and 5 seconds (s), which creates an almost ideally mixed STR that does not suffer from significant heterogeneity. The 20 L pilot plant θ_m was reported by Kenty et al. (2005) as between 20 and 80 s. At the manufacturing scale of 12 m^3, θ_m was reported by Kiss et al. (1994) to be between 120 and 380 s. The greatly increased θ_m is certain to result in considerably greater STR heterogeneity.

1.7.1 pH

1.7.1.1 How pH heterogeneity occurs in large-scale reactors

Langheinrich and Nienow (1999) showed that the pulsed surface addition of 2M Na_2CO_3 (pH 11.7) to large-scale, 8 m^3, STR created pH increases of up to 0.8 pH

units, 0.6 units in excess of the desired 0.2 units step change for control. Having coloured the alkali, they were able to observe an alkali plume covering a significant portion of the upper half of the vessel. Larsson et al. (1996) estimated a total feed zone volume of 10% in a 30 m^3 STR (created by glucose feed to the liquid surface) during *Saccharomyces cerevisiae* (*S. cerevisiae*) cultivation to 20 g L^{-1}. In high cell concentration culture, pH excursions have been shown to occur even in laboratory-scale reactors: Ozturk (1996) observed the formation of a viscous 'snow-ball' close to the addition point of concentrated alkali feed and this was clearly the result of cell lysis (Nienow, 2006). Excursions in pH may not always have such dramatically visible effects on cell culture, but they are certain to expose cells to a sub-optimal growth environment.

1.7.1.2 The effect of pH on CHO cell culture

The effect of pH on CHO cell growth, protein production and protein glycosylation has been established by several research groups. Borys et al. (1993) investigated the effect of culture pH on a CHO cell culture producing a recombinant mouse placental lactogen (mPL-I), and found that protein expression rate and extent of glycosylation were maximum between pH 7.6 and 8.0, while glycosylation was observed to decrease below pH 6.9 and above 8.2. Yoon et al. (2004) and Trummer and Fauland (2006) have completed similar, but more comprehensive, studies of the effect of pH on CHO culture that revealed pH effects on substrate consumption and protein yield; both observed a specific protein yield decrease when the pH was decreased below optimal for cell growth and viability.

Reactor Type	Reactor Configuration	Scale	Organism	Mixing Time (seconds)	Reference
Cell Culture					
STR	-	5 L	*CHO*	2-5	Kenty et al. (2005)
STR	-	8.5 L	*Plant Cells*	3-6	Leckie et al. (1991)
STR	Helical Ribbon	11 L	*Plant Cells*	18-25	Jolicoeur et al. (1992)
STR	-	20 L	*CHO*	20-80	Kenty et al. (2005)
STR	-	8 m^3	*Mammalian Cells*	40-200	Langheinrich et al. (1998)
STR	-	10 m^3	*Plant Cells*	20-200	Doran (1993)
STR	-	12 m^3	*Mammalian Cells*	120-360	Kiss et al. (1994)
STR	Spin filter, Hydrofoil impeller, 20 rpm	10 L	*CHO*	120	Jem et al. (1994)
STR		250 L	*CHO*	120	Jem et al. (1994)
STR	Spin filter, Pitched Blade impeller, 80 rpm	250 L	*CHO*	1620	Jem et al. (1994)
STR	spin filter, Hydrofoil impeller, mixed through spin filter	1 m^3	*CHO*	3120	Jem et al. (1994)
Bubble Column	-	15 L	*Plant Roots*	2400	Curtis (2000)
Airlift	-	10 m^3	*Plant Cells*	200-1000	Doran (1993)
Microbial Culture					
STR	Three Rushton impellers	12 m^3	*Microorganisms*	10-50	van der Lans et al. (2000)
STR	Three Scaba impellers	12 m^3	*Microorganisms*	10-30	van der Lans et al. (2000)
STR	Three Rushton impellers	30 m^3	*Microorganisms*	125-250	van der Lans et al. (2000)
STR	Three Scaba impellers	30 m^3	*Microorganisms*	70-110	van der Lans et al. (2000)
Bubble Column	-	2 m^3	*Microorganisms*	18	Schugerl (1993)
Airlift	-	2 m^3	*Microorganisms*	80	Schugerl (1993)
Airlift tower loop	-	4 m^3	*Baker's Yeast*	100-175	Schugerl (1993)
Bubble Column	-	40 m^3	*Microorganisms*	80	Schugerl (1993)
Airlift	-	40 m^3	*Microorganisms*	100	Schugerl (1993)
Bubble Column	-	150 m^3	*Baker's Yeast*	10-1000	Sweere et al. (1987)

Table 1-2: Based on Table 2 (Reported Mixing Times) in Lara et al. (2006). This table shows the mixing times, θ_m, in several types of stirred tank reactor (STR) in a range of sizes. Note that in the 5 L (laboratory-scale) STR used to culture CHO cells θ_m is reported to be only 2-5 seconds, which can be considered almost instantaneous; at the pilot plant scale the θ_m is 20-80 seconds and therefore not ideal, but at manufacturing-scale it is reported to be in excess of 120 seconds, which will allow considerable STR heterogeneity. m^3 used in place of 1000 L, for brevity.

Glucose and lactate production rates were found by Trummer and Fauland (2006) to have increased nearly twofold by elevating the pH value from 6.8 to 7.2, in accordance with the findings of Yoon et al. (2004). Trummer and Fauland (2006) also found that specific glutamine consumption rates also increased from pH 6.8 to 7.3, but to a lesser extent than specific glucose consumption rates. The specific ammonia production rate, *qAmmonia*, decreased as pH was increased from 6.8 to 7.1, and remained constant thereafter; Yoon et al. (2004) found no influence on glutamine and ammonia metabolism of CHO cells for a pH range between 6.85 and 7.60. Decreased antibody sialylation (a type of glycosylation, Section 1.2.1.3) was observed by Borys et al. (1993) below pH 6.9 and above pH 8.2, while Trummer and Fauland (2006) found that between pH 6.8 and pH 7.3 the degree of sialylation remained constant.

An investigation of pH perturbations similar to those found in large-scale animal cell reactors has been conducted by Osman et al. (2002) using a two-compartment technique to create pH excursions similar to those that occur when alkali is added to poorly mixed large-scale reactors. Their study is the only one of its type to be conducted with mammalian cells; the details of the method are discussed (Section 1.8.3). Osman et al. (2002) investigated the effect of single and multiple pH perturbations on the growth of glutamine synthetase murine myeloma (GS-NS0) cell culture. In two separate experiments, cells were exposed to single and multiple pH perturbations. Single perturbations were created by a single shift in pH from pH 7.3 to either pH 8.0 or 9.0 for durations ranging from 0 to 90 minutes. No measurable decrease in cell viability was found for pH 8.0 perturbations lasting from 0 to 90 minutes; pH 9.0 perturbations lasting for 10 minutes caused a 15% decrease in

viable cell number (*VCN*). Cells proved less robust when exposed to multiple perturbations similar to those created in a large-scale vessel, exhibiting 28% cell death when exposed to 10 perturbations at pH 9.0, each lasting for 200 seconds (s) and made with a frequency of 6 minutes.

1.7.2 CO_2/Osmolality

1.7.2.1 How CO_2/Osmolality Heterogeneity Occurs in Large-Scale Reactors

At the large-scale, to prevent the partial pressure of CO_2 (pCO_2) increasing above the often desirable 'physiological range' (approximately 40-80 mmHg) it usually necessary for CO_2 to be displaced ('stripped') by a more inert gas ('ballast'), such as nitrogen or air. Unfortunately, to minimise the potential damage caused to cells by bursting bubbles, the volumetric gas flow rate is often restricted and a pure oxygen feed may be used instead of an air to enhance the driving force, increasing mass transfer, k_La, (Equation 1-7) and thereby permitting a further decrease in gas flow rate. (Note: often oxygen and air are blended). Under such conditions, pCO_2 can range from 150 to 200 mmHg (deZengotita et al., 2002a).

Mostafa and Xuejun (2003) observed a pCO_2 increase from 68 mmHg at the 5 L laboratory-scale STR to 179 mmHg at the 1 m^3 pilot-scale STR in a CHO cell culture producing a therapeutic protein. Garnier et al. (1996), working with insect cells *Spodoptera frugiperda* (Sf-9), found that pCO_2 accumulated to 114 mmHg when they transferred their process from the laboratory-scale (~5 L) to a 110 L STR.

1.7.2.2 Effect of CO_2 and Osmolality on Cell Culture

If CO_2 is allowed to accumulate in the medium, it will readily diffuse back across the cell membrane into the cell where it can hydrate and dissociate into H^+ and HCO_3^-

and alter the cell's pHi (Alberts et al., 1989). If cellular control of pHi is lessened or manipulated, viability and productivity will likely decrease and protein processing be altered (deZengotita et al., 2002b).

Accumulation of CO_2 in solution decreases the pH of the STR, and subsequent pH control by alkali addition creates a concomitant increase in medium osmolality. Osmolality is an important process variable that is ideally maintained between 260 and 320 milliosmoles (mOsm kg^{-1}), to mimic the osmolality of serum at 290 mOsm kg^{-1} (Ozturk and Palsson, 1990). Reports of the effect of pCO_2 and osmolality on CHO cell growth, protein production and glycosylation are present in the literature. Zhu et al. (2005) explored the effects of high pCO_2 and osmolality on CHO cell growth and production of antibody-fusion protein B1 in a laboratory-scale STR. At a controlled osmolality (~350 mOsm kg^{-1}), cells were exposed to an elevation in pCO_2 from 50 to 150 mmHg; this resulted in a specific growth cell growth rate, μ, fall of 9%; an elevation in osmolality from 316 to 450 mOsm kg^{-1}, at a constant pCO_2 of 50 mmHg, led to a 60% decrease in μ. At osmolality levels above 500 mOsm kg^{-1} cell viability decreased but antibody titre remained unaltered, indicating an increased specific productivity at hyperosmolality. The stress of elevated pCO_2 (160 mmHg) was exacerbated by elevated osmolality (450 mOsmkg^{-1}), causing a larger decrease in cell viability than exposure to each separately. These results are in accordance with those of Kimura and Miller (1996) who also explored the effects of elevated pCO_2 and osmolality on growth and recombinant production of CHO cells.

Osmolality and pCO_2 may both alter the pHi of the cell's organelles, but they appear to have surprisingly little influence on protein glycosylation: tissue

plasminogen activator (tPA) produced in CHO cell culture at elevated pCO_2 had only around 1-2% decrease in the amount of N-glycolyl-neuramic acid as a fraction of total sialic acid (Kimura and Miller, 1997). Negligible impact of pCO_2 on glycosylation was also observed in hybridoma culture, where pCO_2 did not significantly alter cells' production and processing of the antibody. Glycosylation was found to be less robust under the influence of hyperosmotic stress, which increased the heterogeneity of the protein distribution, increasing the isoelectric point by 0.41 pH units at 435 $mOsmkg^{-1}$ (Schmelzer and Miller, 2002).

1.7.3 Oxygen

1.7.3.1 How Oxygen Heterogeneity Occurs in Large-Scale Reactors

In a poorly mixed bioreactor, heterogeneity may result in O_2 limitations in parts of the STR where the O_2 transfer rate is exceeded by the cells' rate of O_2 consumption. Dissolved O_2 gradients do not yet occur in large-scale mammalian cell culture because the O_2 uptake rate (*OUR*) is still much less than typical microbial culture, at about 5×10^{-17} mole O_2 s^{-1} $cell^{-1}$ (Gray et al., 1996; Carvlhal et al., 2003), which at 1×10^{7} cells mL^{-1} equates to an *OUR* of 5×10^{-14} mole O_2 L^{-1} s^{-1}, compared to microbial culture, which consume around 1.5×10^{-6} mol O_2 s^{-1} g of dry cell weight $(DCW)^{-1}$ (Noguchi et al., 2004), which at 100 g $(DCW)L^{-1}$ equates to an *OUR* of 1.5×10^{-4} mole O_2 L^{-1} s^{-1}. Indeed the presence of O_2 gradients and O_2 limitations in the large-scale microbial culture, where cell concentration can reach 200 g (DCW) L^{-1} in high cell concentration culture (Lee, 1996), is a recognised problem (Oosterhuis and Kossen, 1984; Amanullah, 1994). However, agitation and sparging are limited in animal cell culture by the prospect of hydrodynamic damage and as the cell

concentration of the cultures used for large-scale production are increased significant O_2 gradients in mammalian cell cultures are expected by Nienow and Langheinrich (1996). Their prediction is based on a comparison of the characteristic θ_m to the rate of O_2 mass transfer and rate of O_2 uptake by cells (regime analysis, Sweere et al. (1987)) in an 8 m^3 STR used to culture CHO320 and NS0 at low cell densities of 4 x 10^5 and 2 x 10^6 cells mL^{-1}, for CHO and NS0 respectively. Potential O_2 limitations were observed for NS0 culture at a mean specific energy dissipation rate from the impeller, $(\overline{\varepsilon}_T)_I$, of 0.0135 W kg^{-1}. They note that this $(\overline{\varepsilon}_T)_I$ is around the low end of the range used in practice. Since cell cultures have been taken to over 1 x 10^7 cells mL^{-1} for some time (Birch et al., 1985) and further gains in maximum cell concentration are predicted (Birch and Racher, 2006), O_2 limitation should be anticipated.

1.7.3.2 The Effect of Oxygen on CHO cell culture

Oxygen is essential for efficient mammalian cell energy generation by aerobic metabolism in mitochondria, where it is the terminal electron receptor during oxidative phosphorylation. Cells must modulate their consumption of O_2 to meet energy demands, and to do this they must adapt to the O_2 tension of their environment (Batandier et al., 2002).

The observed impact of dissolved oxygen tension, *DOT*, as a percentage of air saturation (% saturation, referred to here as %) on CHO cell culture performance has not been universal across several studies; notably, those studies conducted in STR where O_2 demand was met by sparging observed the least effect on cell culture. Kurano et al. (1990a) found that *DOT* did not significantly influence cell viability

until O_2 limitation occurs at very low *DOT* (anoxic exposure) of about 5% saturation, or when hypoxic exposure occurs at *DOT* above 90%. The most recent study was conducted by Trummer and Fauland (2006), who found that cell viability and product titre were not significantly influenced between 30% and 90%. The lowest cell viable cell number (*VCN*) was observed at a *DOT* of 10%. No effect on antibody specific productivity was observed. These findings contrast with those made by Link et al. (2004), who observed that a *DOT* of 40% gave the highest antibody titre, and Chotigeat et al. (1994), who observed a correlation between *DOT* and productivity. Their results must, however, be treated with caution because these two studies were made using culture methods that may not be analogous to large-scale STR cell culture. Link et al. (2004) used silicon tubing to provide O_2; Chotigeat et al. (1994) studied a perfusion culture, a culture method that is currently rarely used for large-scale production.

Trummer and Fauland (2006) observed no connection between *DOT* and cell metabolism until the *DOT* was taken to 10% and below; cell growth decreased and both glucose consumption and lactate production increased by 20%. Glutamine and other amino acids were reportedly unaltered, even at a *DOT* of 10%. Kurano et al. (1990a) found that glucose utilisation was most efficient between 50% and 100%.

The few studies that explored the effect of *DOT* on glycosylation profile of the protein observed alterations: Trummer and Fauland (2006) found a loss of protein sialylation at a *DOT* of 100%, and no effect on sialylation at any other tension, including anoxic growth. A positive correlation between sialyltransferase activity in CHO cells and *DOT* was reported by Chotigeat et al. (1994).

1.7.4 Substrate

1.7.4.1 How Substrate Heterogeneity Occurs in Large-Scale Reactors

During fed-batch cultures, substrate addition is generally made to the liquid surface of the culture in the same manner as alkali additions (Section 1.7.1). Unlike alkali, which is added in small batches as required for control, substrate addition is often made continuously at a low flow rate, calculated based on cell growth. One would therefore expect an accompanying high concentrate plume, as occurred during alkali additions to the surface. The substrate plume would be persistent and likely of relatively low magnitude, compared to the transient alkali plume. No studies on substrate heterogeneity of mammalian cell culture are found in the literature, but a high nutrient concentration plume that lowered protein titre and increased by-product formation has been observed in microbial culture (Bylund et al., 1998; Enfors et al., 2001). It is probably only a matter of time until rising cell densities in large-scale animal cell culture that are needed to increase volumetric therapeutic protein production make substrate gradient a concern (Nienow, 2006).

1.7.4.2 The Effect of Substrate and Metabolites on Cell Culture

The carbon sources glucose and glutamine are the most widely used substrates in cell culture (Butler, 2005a); their catabolysis by cells releases energy and precursors for biosynthesis. An overabundance or inefficient use of these substrates results in the excretion of the metabolic by-products (metabolites) lactic acid (lactate), from glucose, and ammonia from glutamine.

1.7.4.3 Lactate

Entry of glucose into the glycolytic pathway leads to the formation of pyruvate as the product. In animal cells, pyruvate can either be shuttled into the TCA cycle or converted into lactate. Aerobic lactate production is atypical for normal diploid cell strains (Mulukutla et al., 2010); cancer cells, however, have been shown to produce lactate in fully aerobic condition, termed the Warburg effect (Warburg, 1930). Indeed, it is likely that glycolytic lactate production is connected to their proliferative capabilities (Xu et al., 2005; Vazquez et al., 2010). Cell lines developed for industrial cell culture share similar continuous growth abilities with cancer cells and they too typically produce lactate under fully aerobic conditions (Mulukutla et al., 2010). Lactate production under aerobic conditions is usually attributed to the high flux of glucose to pyruvate and supposed inefficient coupling between glycolysis and the tricarboxylic acid (TCA) cycle (Tsao et al., 2005). Recently, lactate consumption has been reported in industrial cell culture, and is considered desirable, by lowering concentrations of this potentially deleterious metabolite (Tsao et al., 2005; Mulukutla et al., 2010).

Several studies of CHO and NS0 cell culture have reported a strong negative influence of lactate on viability and weak or positive influence on protein productivity (Kurano et al., 1990a; Newland et al., 1990; Ozturk et al., 1992; Xing et al., 2008). Nevertheless, several contrary studies found little or no negative effect (Reuveny et al., 1986; Reuveny et al., 1987; Kurano et al., 1990a; Lao and Toth, 1997).

There is some evidence that lactate acts indirectly by increasing osmolality (Kurano et al., 1990b). After correcting for osmolality, Lao and Toth (1997)

attributed 25% of the observed growth inhibition to lactate. The increased antibody production that has been attributed to accumulation of lactate was instead likely caused by elevated osmolality, both from the lactate itself and, probably to greater extent, the alkali required to increase pH (Kimura and Miller, 1996; Vivian et al., 2002; Zhu et al., 2005). In poorly controlled vessels, and perhaps in localised regions of those with poor mixing, lactate concentration may also be sufficient to cause a detrimental fall in pH (Kubicek, 2001).

1.7.4.4 Ammonia

Accumulation of ammonia can disrupt intracellular pH (pHi) decreasing cell growth and recombinant protein productivity (Chen and Harcum, 2005). Several studies have shown ammonia inhibition of cell growth in CHO culture (Kurano et al., 1990a; Chen and Harcum, 2005; Xing et al., 2008), while antibody yield was not investigated; ammonia is known to decrease cell growth and antibody yield in hybridoma cells (Reuveny et al., 1986). However, a similar study (Yang and Butler, 2000) exploring the effects of ammonia on CHO cells during erythropoietin production (EPO) found cell growth inhibition above a concentration of 5 mM ammonia, but observed an increase to EPO yield. In general, ammonia accumulation was found to create a significant increase in glycoform heterogeneity and decrease in terminal sialylation (Andersen and Goochee, 1994; Zanghi et al., 1998; Yang and Butler, 2000).

1.7.4.5 Glucose and Glutamine Level

Consistent low concentration of glucose and glutamine has been shown to increase cell viability and productivity while decreasing metabolite formation. Unfortunately,

glycosylation levels of recombinant proteins are also decreased: glucose starvation creates a shortage of glucose-derived nucleotide sugars, which are replaced by smaller species derived from alternate glycosylation pathways (Rearick et al., 1981; Gu and Wang, 1998). In glucose limited chemostat CHO culture, Hayter et al. (1992a) observed a decrease in the glycosylation of gamma interferon. Their finding is supported by Wong et al. (2004) who conducted a series of fed-batch studies exploring limited substrate concentration on CHO culture, again producing human interferon gamma (IFN-γ): glucose and glutamine molalities below critical values of 0.7 mM and 0.1 mM, respectively, decreased sialylation and increased hybrid and high mannose type glycans.

Thus, cells are prone to inhibition of cell growth and formation of potentially deleterious metabolites at elevated concentration of substrate, and incomplete protein glycosylation at a dearth of substrate. Process development entails steps to optimise the substrate concentration for antibody titre and quality, but heterogeneity in a typical poorly mixed large-scale animal cell STR may expose cells to suboptimal concentrations, with the clear potential to decrease antibody titre and alter antibody quality.

1.8 Scale-Down Methods

The aim of scale-down is to create, at the laboratory or pilot-scale, conditions present at the large-scale. The type of scale-down considered here seeks to replicate the heterogeneity of a large-scale STR in laboratory-scale STR, which otherwise has near perfect mixing and STR homogeneity. Creation of heterogeneity like that experienced during large-scale production, should provide some useful insight into the expected performance of the cell culture process under conditions like those that

occur during manufacturing, without the considerable cost and difficulty of performing large-scale runs. Further, it should be possible to optimise potentially problematic process parameters and thereby improve the chances of a successful and predictable scale-up.

To study cell behaviour effectively on scale-up a scale-down method is required to simulate the conditions of large-scale heterogeneity with a reasonable degree of accuracy. Several different methods of scale-down have been used to simulate the O_2, pH and substrate gradients in the cultivation of a range of different organisms. The method is approached by adopting either a one or a two-compartment system: single STR and loop reactors belong to the former, while STR linked to another STR (STR+STR) and STR linked to a plug flow reactor, PFR, (STR+PFR) to the latter.

In the following sections, relevant examples from the literature will be used to discuss the relative merits of approaches to scale-down. Only a single study has attempted a two-compartment scale-down of large-scale mammalian culture, using the STR+STR method to create pH perturbations (Osman et al., 2002), so most of following discussion will unavoidably centre on microbial scale-down studies, of which there are many.

1.8.1 Single-Compartment Models

In a single-compartment scale-down, it is possible to model temporal gradients in STR concentration, but not spatial gradients, as they would occur at the large scale. Spatial gradients cannot be created in the laboratory-scale STR because it is not compartmentalised and perturbations must therefore occur throughout the whole reactor. In spite of this limitation, it does provide a simple method to explore the

effect of cell exposure to repeated process perturbations. The two-compartment model was used in this study because of its greater suitability for modelling of repeated perturbations throughout the duration a production cell culture. A review of single-compartment scale-down can be found in Osman et al. (2002).

1.8.2 Two-compartment Models

The two-compartment model is usually founded on the premise that when cells cycle around a heterogeneous large-scale STR they are effectively exposed to two aggregated regions (zones) (Section 1.5). As a result of inefficient mixing, one zone is subject to perturbations in the concentration of some fundamental parameter and the other zone is not. Perturbations are created by either elevated or depleted levels of a fundamental parameter. Primarily, elevated concentration is caused by inefficient dispersal of feeds from a poorly mixed zone, and depleted concentration, by inefficient mixing of a feed into a zone.

Two-compartment systems seek to recreate these separate zones, using two homogeneous vessels. Accordingly, one vessel is controlled to simulate the conditions in a well-mixed zone; the other vessel, to simulate a poorly mixed region. Heterogeneity is introduced by cycling the cell culture between the two vessels (Figure 1-3). Within the limits of the model, its efficacy as a simulation of large-scale heterogeneity is largely dependent on the type and size of vessels, the location of feed-points, and the cycle rate between them. Note that two-compartment scale-down models provide only an approximation to conditions that actually occur in a large-scale vessel; furthermore, the flow and dispersion conditions in the region surrounding the feeding positions are not characterised.

Scale-Down Method	Heterogeneity	Organism	Comparison to Large-Scale Performance	Author(s)
Single Compartment				
STR	Oxygen	*Penicillium chrysogenum*		Varder and Lilly (1982)
STR	Oxygen	*Gluconobacter oxydans*		Oosterhuis (1985)
STR	pH	*AB2-143.2 Hybridoma Cells*		Miller et al. (1988)
STR	Oxygen	*Saccharomyces cerevisiae*		Sweere et al. (1988)
STR	Oxygen	*Saccharomyces cerevisiae*		Namdev et al. (1991)
STR	Oxygen	*Aspergillus niger*		Trager et al. (1991)
STR	Oxygen	*Streptomyces clavuligerus*		Yegneswaran and Gray (1991)
STR	Oxygen	*Bacillus subtilis*		Suphantharika et al. (1995)
STR	Oxygen	*Spodoptera frugiperda*		Rhiel and Murhammer (1995)
Loop	Oxygen	*A. pullulan*		McNiel and Kristiansen (1987)
Loop	Oxygen	*Saccharomyces cerevisiae*		McNiel and Kristiansen (1990)
Two-compartment				
STR+STR	Oxygen	*Gluconobacter oxydans*	Good	Oosterhuis et al. (1983)
STR+STR	Oxygen	*Gluconobacter oxydans*	Good	Oosterhuis et al. (1985)
STR+STR	Oxygen	*Saccharomyces cerevisiae*	Not Made	Sweere et al. (1988)
STR+STR	Oxygen and pH	*Bacillus subtilis*	Not Made	Amanullah (1993) (PhD thesis)
STR+STR	Oxygen	*Enterobacter aerogenes*	Not Made	Byun (1994)
STR+STR	**pH**	***NSO***	**Not Made**	**Osman et al (2002)**
STR+PFR	Glucose	*Saccharomyces cerevisiae*	Not Made	Fowler and Dunlop (1989)
STR+PFR	Oxygen	*Penicillium chrysogenum*	Not Made	Larsson and Enfors (1985)
STR+PFR	Oxygen	*Escherichia coli*	Not Made	Larsson and Enfors (1993)
STR+PFR	Oxygen	*Saccharomyces cerevisiae*	Not Made	Larsson and Enfors (1993)
STR+PFR	Glucose	*Escherichia coli*	Fair	Larsson and Enfors (1999)
STR+PFR	Glucose	*Saccharomyces cerevisiae*	Not Made	Namdev et al. (1992)
STR+PFR	Oxygen and pH	*Bacillus subtilis*	Not Made	Amanullah (1993) (PhD thesis)
STR+PFR	Glucose and Oxygen	*Escherichia coli*	Good	Hewitt et al. (2000)
STR+PFR	Glucose and Oxygen	*Escherichia coli*	Good	Hewitt et al. (2001)

Table 1-3: Based on Table 1 in Osman et al. (2002). The majority of the scale-down studies in the literature are presented. It can be seen that few studies have simulated pH heterogeneity, despite the importance of this parameter in process optimisation. Only one study has explored the effect of heterogeneity on mammalian cell culture: that of Osman et al. (2002).

Nevertheless, two-compartment scale-down should provide an improvement on process development conducted entirely in perfectly mixed STR without due regard to the problems that large-scale STR heterogeneity might present. Two-compartment models have been created by connecting two STR together, and by connecting a STR to a PFR.

1.8.3 STR+STR

Two stirred tank reactors (STR), usually a large STR and a small STR, are connected by a small length of piping (time spent in the pipe should be insignificant). Flow between the two vessels is typically mediated by peristaltic pumps and is analogous to the interchange between the well-mixed impeller region the poorly mixed region. In effect, the fluid flow created by the impeller in a large-scale vessel is replaced by the pumped flow in the scale down model (Amanullah, 1994). The mean residence time (*RT*) in each compartment is dependent on two factors: the size of the vessel and the flow rate provided by pumping.

The STR+STR model has been used by several groups working at the laboratory-scale to simulate the O_2 heterogeneity expected in large-scale microbial reactors (Oosterhuis and Kossen, 1984; Amanullah, 1994; Byun et al., 1994). Amanullah (1994) used a highly aerated small STR to model the impeller region, and to model the poorly oxygenated bulk zone of a large-scale STR, a larger STR was stripped of O_2 by sparging with nitrogen. Circulation rates from 15 to 300 s between the two STR were used to explore the response of *Bacillus subtilis* (*B. subtilis*) to degrees of large-scale heterogeneity.

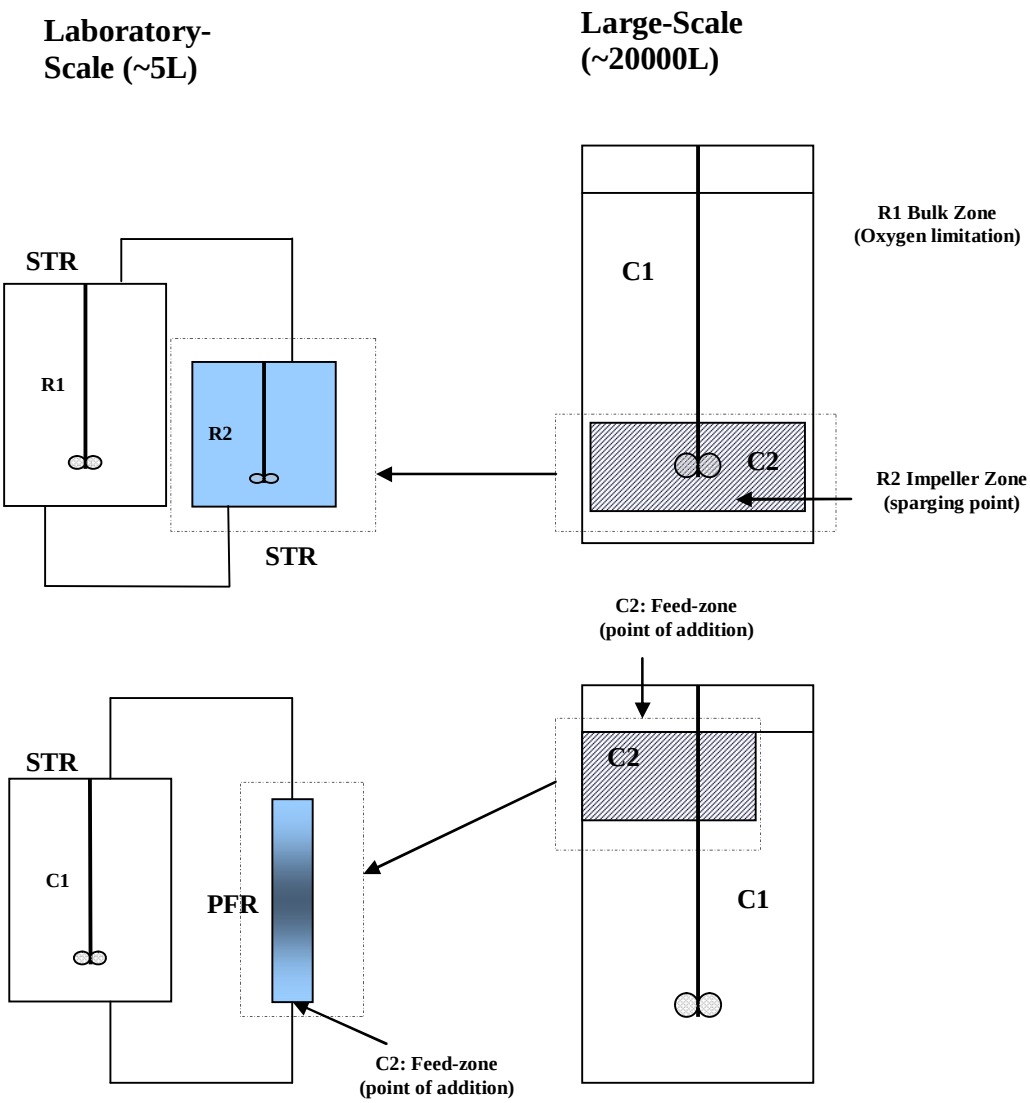

Figure 1-2: Scale-down simulation schematic (based on Hewitt et al., 2000): the two-compartment model allows heterogeneity to be introduced to the laboratory-scale. Examples of two-compartment scale-down with two stirred tank reactors (STR+STR). STR+STR being used to simulate O_2 limitation: region 1 (R1) represents the bulk of the large-scale reactor; thus, it is not sparged with air or O_2 and may be sparged with nitrogen to increase the degree of heterogeneity; R2 is sparged with air and/or O_2 and represents the well-mixed impeller zone. Stirred tank reactor and a plug flow reactor (STR+PFR) being used to simulate the feed zone at in a large-scale STR: compartment 1 (C1) is not exposed to significant concentration perturbations; feed is added to C2 so that it alone is exposed to elevated concentrations.

The same culture and laboratory-scale vessels were also used to explore pH heterogeneity (Amanullah et al., 2001). In this case, the small STR, controlled at pH 6.5, represented the feeding zone of a poorly mixed large-scale STR; the large STR, controlled at pH 7.2, represented the bulk, away from the feeding zone. To maintain the two connected vessels at differing pH values required almost continuous addition of alkali to the larger STR and acid to the smaller STR. This balancing act inevitably increased osmolality so that it may have overwhelmed the effects of cycling through a moderate pH excursion. Furthermore, the creation of a continuously elevated pH in the small STR does not replicate the transient, irregular pH excursions in large-scale reactors, which are created by batch alkali additions and added at irregular intervals as required for pH control.

A part solution to the problem of osmolality increase created by successive pH perturbations, or continuous alkali addition, is offered by Osman et al. (2002). They connected a 2 L STR (large) and a 1 L STR (small) to investigate the effect of perturbation frequency, duration and number on GS-NS0 cell growth. To produce a perturbation, a predetermined volume of alkali (2M NaOH) was added to the small STR to increase pH from 7.3 to either 8.0 or 9.0; a simultaneous equimolar addition of acid to the large vessel maintained its pH at 7.3. Since the pH excursions were transient and made to a small STR (an advantage over the single STR model), the amount of alkali required was insufficient to create deleterious increases to osmolality. To control for osmolality, an experimental case was performed in which alkali was substituted for NaCl. Performance was equivalent to a control without NaCl addition.

Unlike Amanullah et al. (2001), Osman et al. (2002) used their scale-down to produce transient pH perturbations; however, perturbation regularity was set arbitrarily and did not therefore simulate pH perturbations as they occur when batch additions of alkali are made to control pH in a large-scale reactor. A better scale-down should be achieved by adding alkali to the small STR only when it is required for control of the culture; this is accomplished in several studies that used STR+PFR (Section 1.8.4).

In both of the above studies the perturbation zone was one third of the total culture volume, which is large compared to the feed zone ratio used by several other studies: Bylund et al. (1999) and Hewitt and Nebe-Von-Caron (2001) used a 10% feed zone ratio and only 5% was used by Namdev and Yegneswaren (1991) and by Amanullah et al. (2001) in further studies. Studies using a 5-10% feed zone were not conducted using the STR+STR model that probably restricted the vessel size available to Amanullah (1994) and Osman et al. (2002), but with the STR+PFR model that is more flexible thanks to the simpler fabrication of a PFR at various sizes.

1.8.4 STR+PFR

In the same manner as the STR+STR configuration, flow between the two vessels is provided by peristaltic pumping, which is conceptually analogous to impeller pumping in the large-scale STR. The plug flow reactor, PFR, is well suited to simulation of perturbations created by addition to a quiescent feeding zone in a reactor: in an ideal PFR, mixing will be radial but not axial, allowing the creation of a step change in concentration that persists and travels along the length of the PFR. The mean residence time, *RT*, in the PFR can then be manipulated to simulate the

duration of a perturbation in the large-scale STR. Perturbations are created by adding the feed (be it substrate or alkali) to the entry point of the PFR. In an ideal PFR, feed then travels along the PFR as a pulse of high concentration. Often, however, there is some degree of longitudinal dispersion and the pulse concentration 'spreads' into a Gaussian curve (Levenspiel, 1999). Once the volume of the PFR is fixed, the recirculation rate dictates frequency at which cells enter the PFR and the exposure time of cells within the perturbation as it travels down the length of the PFR.

The method has been used by several groups to simulate O_2, nutrient, and pH perturbations (Table 1-3). O_2 limitation is created either by metabolic consumption of O_2 within the unaerated PFR or by using nitrogen to strip O_2 from the medium as it flows into the PFR.

Namdev and Thompson (1992) used an STR+PFR configuration to investigate the effects of substrate addition to the feeding zone on *S. cerevisiae* culture at the large-scale. The PFR was fed intermittently, in accordance with the Monte-Carlo method (Namdev and Yegneswaren, 1991), which attempts to account for the time fluid elements spend in the bulk region of the STR as they cycle between the feed zone and the impeller zone. By feeding in this way, they sought to replicate the circulation time distribution of cells, and their resultant exposure times to the feed zone that is found in a large-scale vessel.

A survey of the literature shows that the Monte-Carlo method of feeding is not used in the majority of two-compartment studies. It was not used, for example, by Hewitt et al. (2000) in a novel study that applied flow cytometry (FC) to determine the physiological response of *E. coli* in a scale-down of substrate

heterogeneity that produced a good correlation to the culture's performance in a 20 m^3 large-scale fed-batch STR, characterised in earlier work by Hewitt et al. (1998). Interestingly, substrate heterogeneity actually increased cell viability. The PFR used by Hewitt et al. (2000) was developed by George et al. (1993) as part of a series of scale-down studies (Table 1-3). Neither Namdev and Thompson (1992) nor Hewitt et al. (2000) characterised their PFR so it is unknown if plug flow was achieved. Nevertheless, George et al. (1993) established plug flow that was well characterised and because they adapted the same method it can therefore be assumed that the PFR used by Hewitt et al. (2000) was also in plug flow.

In one of the few studies that have investigated pH perturbations, Amanullah et al. (2001) used the STR+PFR to model pH addition to the surface of a poorly mixed large-scale STR during *B. subtilis* cultivation. Alkali was added to the PFR by the STR control system when required to maintain pH at the controller set-point. Characterisation of the PFR showed that stagnant zones were present at the flow rate used to create a theoretical mean residence time of 120 s; small deviations from plug flow were assumed and the axial dispersion model with a Gaussian flow distribution (described by Levenspiel, 1999) was used to characterise the flow.

Decreased cell viability, the ratio of live cells to total cells, is often reported when cells are exposed to concentration gradients that occur in heterogeneous culture. Viability is typically found using Trypan Blue exclusion on the haemocytometer (HC); however, this method is slow and subjective and does not provide any additional information on cell physiology. In this study, HC will be compared to a rapid objective analysis and quantification of cells provided by multi-parameter flow cytometry (FC). This powerful technique shall be applied, for the

first time, to characterise the cell population in a scale-down of large-scale mammalian cell culture, with the aim of improving the understanding of how GS-CHO cultures respond to STR heterogeneity commensurate to that found in large-scale vessels (Section 1.1).

1.9 Flow Cytometry

1.9.1 Why Flow Cytometry?

Flow cytometry (FC) facilitates the rapid monitoring (100-1000 cells s^{-1}) of individual cell physiological states. The judicious selection and application of a mixture of fluorescent stains (in the literature, also referred to as fluorophores and fluorescent dyes) that stain cells in a manner dependent on the cell's physiological state enables a high degree of differentiation of the cell population based on the cells' physiological characteristics. High throughput and precise analysis enables the assessment of large numbers of cells on a cell-by-cell basis, providing a great degree of statistical resolution in the characterisation of heterogeneous cell culture populations and identification of sub-populations. FC has been used to study changes in DNA, RNA, protein, IgG, mitochondrial activity, cell cycle and cell size - enabling a comprehensive analysis of cell culture (Omerod, 1999). FC can thus be used to identify and characterise the morphological and biochemical heterogeneity of cell populations.

1.9.2 What is Flow Cytometry?

At the heart of the machine lies the flow-cell. When analysis is made, cells in suspension are withdrawn from the sample-tube and forced by a stream of sheath fluid, which is either water or an isotonic saline solution, to flow through a passage

in the flow-cell that hydro-dynamically restricts the movement of the cells and forces them to flow in single file through the focal point of the laser with an accuracy of 1 µm. This is referred to as hydrodynamic focusing. A cell travelling through the flow-cell has light focused upon it by a series of lenses; it is the scatter and reflection of this light from the cell that is collected and amplified, and finally interpreted to characterise the cell (Figure 1-3).

An exhaustive description of the instrumentation present in a FC can be found in Omerod (1999) and Shapiro (2003b). To understand how the interaction of a light source with a cell provides the necessary information for characterisation of properties as varied as cell size and mitochondrial membrane potential consideration must be given to light scattering and fluorescence.

1.9.3 Light Scattering

When a laser beam travels through a cell the photons are scattered at all angles. The intensity of light scattered between 0.5^{o} and 5.0^{o} is approximately correlated to both the refractive index and cross-sectional area of the cell; this allows a relative comparison of cell sizes. Light scattered at acute angles is collected by the photodiode in-line with the illumination beam and is referred to as forward scatter light.

The intensity of light scattering between 15° and 150° is correlated to the roughness, irregularity or granularity of the surface and internal constituents of the cells, but only as an approximate evaluation, and can thereby provide information on cell viability and levels of intracellular structures, including DNA and protein (Al-Rubeai, 1999; Shapiro, 2003b). Light scattered at between 15° and 150° is referred to as side scatter light.

Figure 1-3: Flow cytometer (FC) layout (adapted from that found in Omerod (1999) the argon-ion laser emits blue light (488 nm) focused on the stream of suspended cells in the flow cell. Photo Multiplier Tubes (PMT) collect side scattered light from cells passing through the laser; the PMT measure four different colours, typically scattered primary-light (blue) and green, orange and red. In the forward direction, a photodiode measures forward scatter light (FS).

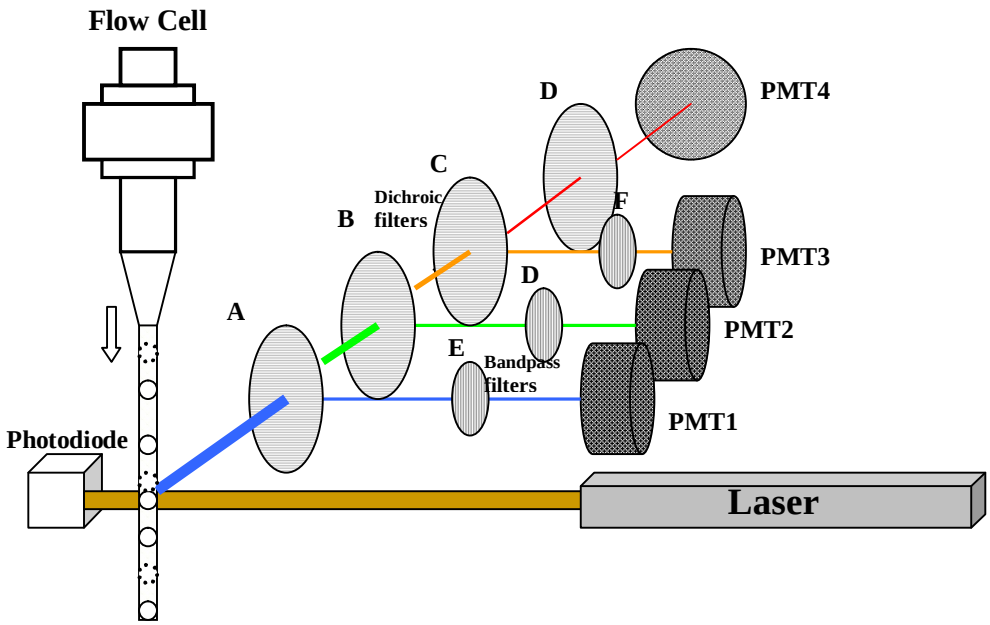

The application of this sophisticated equipment to measure forward and side scatter is useful to gauge cell size and granularity, and is an effective, and often essential, method to discriminate cells from debris, but is often peripheral to the collection and amplification of fluorescent light emissions.

1.9.4 Fluorescence

Fluorescence occurs in a FC when molecules of a fluorescent stain (stain) within the cell absorb energy from the laser and their electron energy state is increased from ground to excited; the energy that is lost when the electron returns to its ground state is emitted as light (a radiative transmission) at a range of longer wavelengths, referred to as the emission spectrum.

By careful stain selection, it is possible to detect fluorescence simultaneously from two, three or even four compounds fluorescing at different wavelengths, enabling several parameters to be measured at once. Multi-parametric analysis permits a greater degree of cell characterisation

1.10 Cell Characterisation Using Fluorescent Stains

1.10.1 Stain Selection

Characterisation of multiple cell parameters with a number of stains potentially enhances our knowledge of the cell's specific physiological responses to heterogeneity. In some cases, it was not possible to obtain information on the exact structure and chemistry of a stain because such information remains proprietary. All of the following stains are excited by the 488 nm spectral line of an argon-ion laser.

1.10.2 Plasma Membrane Integrity Stains

The mode of cell death can often be identified by cytoplasmic membrane permeability: apoptotic cells are reported to retain their cytoplasmic membrane integrity until cell degradation and secondary necrosis occurs in late-apoptotic cells; necrotic cell death is accompanied by significant membrane degradation. A measure of the permeability of a cell's cytoplasmic membrane ('membrane permeability') is therefore an effective method to discriminate between viable/early-apoptotic cells and necrotic/late-apoptotic cells (Catchpoole and Stewart, 1993; Zamai et al., 1996). Membrane disruption or permeability is now an established viability indicator in mammalian cell culture (Altman et al., 1993; Al-Rubeai et al., 1996; Al-Rubeai, 1999) and is typically revealed by cellular staining with one of the two popular membrane impermeable cationic stains, PI and EB.

1.10.2.1 Propidium Iodide

PI has two positive charges carried on its heterocyclic ring structure; EB is similarly structured, but, unlike PI, has only one positive charge and may not therefore be fully excluded by an intact cytoplasmic membrane. Once PI enters the cell it is attracted to negatively charged cell constituents such as glycosaminoglycans and nucleaic acids, and will intercalate between the bases of double stranded nucleic acids. When bound to DNA its red fluorescent emission is enhanced by from 20- to 30-fold by the reducing environment. In this state, its excitation and emission maxima are 535 nm and 617 nm, respectively. Since PI should effectively stain only dead cells it provides a simplistic assay for the live and dead cell population, which, when used on a FC, may be regarded as a more rapid and precise alternative to manual counts using the Trypan Blue (TB) exclusion on a haemocytometer

(Darzynkiewicz, 1992; Al-Rubeai, 1996). The same could be said of Sytox Green, which will also be used in this study, in conjunction with Annexin-V/PE (Section 1.10.5).

1.10.2.2 Sytox Green

Like PI, Sytox Green (SG) has a high affinity for nucleic acid, easily penetrates and stains cells with compromised cytoplasmic membranes and yet will not cross the cytoplasmic membrane of live cells (Haugland, 2002). SG is considerably more impermeable even than PI. Its structure has not yet been published but its impermeance is recognised and attributed to the presence of at least three positively charged groups (Shapiro, 2003b). When bound to DNA, the green fluorescence of SG is enhanced more than 500-fold, demonstrating considerably higher quantum efficiency than PI. Furthermore, it has been reported, for cell cycle analysis of yeast, to exhibit improved coefficients of variation (*%CV*) and an improvement on PI in its correlation between DNA content and fluorescence (Haase, 2004). SG is widely used as a dead-cell stain in conjunction with Annexin V (AV) to discriminate effectively between apoptotic and necrotic cell death in various cell types (Haugland, 2002; Mukhopadhyay et al., 2007). FC facilitates the use of a second stain to provide a positive control or counter-stain and, where possible, a combination of stains has been used in this study.

1.10.3 Viability Stain

1.10.3.1 Calcein-AM

‘As a general rule, cells that become stained with TB or PI are dead, but cells that don’t are not necessarily viable’ (Shapiro, 2003b). To confirm the viability of cells

in this study, they were counter-stained with Calcein acetoxymethylester (Calcein-AM), which reportedly requires activation by cellular processes and has a fluorescent emission spectrum that is well separated from PI (Weaver, 1998).

Calcein-AM is a highly lipophilic vital stain, that lacks charge and thus rapidly enters live cells where the lipophilic acetoxymethyl (AM) blocking group is cleaved by non-specific esterases; after removal of its blocking group (AM), Calcein produces a bright fluorescent green that is relatively insensitive to pH in the physiologic range (Bratosin et al., 2005); it is also negatively charged and well retained by intact cell membranes. Its excitation and emission maxima are 494 nm and 517 nm, respectively (Haugland, 2002).

Calcein-AM is widely used as a viability assay for a variety of cell types (Haugland, 2002), but has yet to find widespread use for analysis of mammalian cells in STR culture, although it has been used by Isailovic et al. (2007) in conjunction with PI to investigate cell-population heterogeneity in *Spodoptera frugiperda* 21 culture grown in a 3 L STR. They describe three cell populations: viable (Calcein-AM positive, PI negative), dead (Calcein-AM negative, PI positive) and recently dead (Calcein-Am positive, PI positive). The latter, dual stained population (DSP), was attributed by Isailovic (2007) to a greater uptake rate for PI than the rate of Calcein-AM diffusion out of dead cells.

1.10.4 Mitochondrial Function Stains

If one considers the fundamental role of mitochondria and, thereby, $\Delta\Psi m$ in energy generation, it should not be altogether surprising that $\Delta\Psi m$ can be used to monitor metabolic integrity and assess the viability of the cell (Campbell et al., 1995; Kluck et al., 1997; Shapiro, 2000). For example, in the early stages of apoptosis continued

energy generation preserves ΔΨm, while necrotic cells, in contrast, are reported to exhibit early ΔΨm depreciation caused by mitochondrial membrane damage (Darzynkiewicz et al., 1996). Fluorescent stains that reveal ΔΨm should therefore provide a sensitive indication of cell metabolism and viability.

Fluorescent lipophilic cationic stains are ideal for measurement of ΔΨm as they are drawn towards the highly negative membrane environment present in functional mitochondria. If equilibrium is established with the stain then its uptake by the mitochondria should be correlated to the potential difference across the membrane, and cells that are suffering from some metabolic stress or damage to their mitochondrial membrane that decreases ATP production will be observed to have lower ΔΨm by a decrease in their stain uptake and, consequently, their fluorescence (Shapiro, 2000).

1.10.4.1 $DiOC_6(3)$

3,3-dihexyloxacarbocyanine iodide ($DiOC_6(3)$) is a lipophilic cationic stain that easily penetrates viable cells and at concentrations below 1 nm is reportedly localised in the mitochondria. Its green fluorescence permits dual staining with red fluorescent PI so that separation (by gating) of live and dead cells can be performed and ΔΨm of live cells found. Its concentration in the mitochondria and therefore the intensity of its green fluorescence has been observed to correlate with ΔΨm at concentrations below 1 nm, above this very low concentration correlation with ΔΨm was lost (Petit et al., 1995; Zamzami et al., 1995; Metivier et al., 1998). Loss of correlation was attributed to the stain's association with other cytoplasmic lipids; evidence that supports this hypothesis was later found by Zuliani et al. (2003) when, using fluorescent microscopy, they observed diffuse cytoplasmic fluorescence for

$DiOC_6(3)$. Salvioli et al. (1997) and Zuliani et al. (2003) found that $DiOC_6(3)$ was considerable less efficient than JC-1 (Section 1.10.4.2) at tracking changes in ΔΨm, and they suggest JC-1 be used in preference. Isailovic (2007) observed dual staining with $DiOC_6(3)$ and PI, which was attributed to cytoplasmic staining of dead cells. In this study, comparison of $DiOC_6(3)$ and JC-1 will be made, and their efficacy as probes for ΔΨm in GS-CHO cell culture established.

1.10.4.2 JC-1

5,5'6,6'-tetrachloro-1,1'3,3'-tetraethylbenzimidazolcarbocyanine iodide (JC-1) is also a lipophilic cationic stain that easily penetrates the intact cell membrane and exhibits ΔΨm dependent accumulation in the mitochondria, but it should not create a false indication of ΔΨm even when cytoplasmic binding occurs: a colour change from green (525 nm) to red (590 nm) that is caused by the aggregation of the stain monomer at highly localised concentrations that occur only in mitochondria eliminates fluorescence contribution from cytoplasmic membrane binding. Indeed, staining of the cell with the green fluorescent monomer is expected and convenient, because it is the ratio of green to red fluorescence that indicates ΔΨm. Using the ratio of two colours should effectively exclude the effect of factors, such as mitochondrial size, shape and density, that can influence fluorescent measures of ΔΨm reliant solely on the stain's intensity (Cossarizza et al., 1993; Cossarizza et al., 1994). Zuliani et al. (2003) observed using fluorescent microscopy that cells stained with JC-1 have a bright green stained cytoplasm that contains distinctive red mitochondria. Furthermore, JC-1 has been used successfully to monitor changes in ΔΨm caused by mitochondrial depolarisation and apoptosis inducing agents (Salvioli et al., 1997; Zuliani et al., 2003). Both JC-1 and $DiOC_6(3)$ facilitate

characterisation of mitochondrial activity by their correlation with ΔΨm, and this is a useful measure that can be used to infer the mitochondrial integrity and respiratory activity, but it does not provide a direct measure of respiration – for this CM-H_2XRos was used in this study (Section 1.10.4.3).

1.10.4.3 Mitotracker Red CM-H_2XRos

Cellular respiration by oxidative phosphorylation in the mitochondria generates reactive oxidative species (ROS) (Batandier et al., 2002); and their concentration is a strong indicator of mitochondrial function. Indeed, several studies have reported that the amount of ROS in healthy cells roughly correlate with activity of respiration (Poot et al., 1996; Poot and Pierce, 1999b; Degli Esposti, 2002); this is corroborated by research showing that when ΔΨm is lost production of ROS drops considerably (Loschen et al., 1971; Chance et al., 1979; Korshunov et al., 1997).

Measurements of ROS have been reported using (8-(4'-chloromethyl) phenyl-2, 3, 5, 6, 11, 12, 14, 15-octahydro-1H, 4H, 10H, 13H-diquinolizino-8H-xanthene) (CM-H_2XRos for short). CM-H_2XRos has no charge or fluorescence when it enters the cell, and only when it is oxidised within the cell by one or more reactive oxidative species generated during mitochondrial respiration does it reveal a positive charge and a red fluorescence that is sensitive to local oxidative activity. Owing to its positive charge the oxidised form is sequestered by the mitochondria where it binds to mitochondrial proteins, its red fluorescence can then be used to monitor the degree of oxidative activity. Poot and Pierce (1999a) and Haugland (2002) used antimycin A inhibition of electron flux to show the correlation between CM-H_2XRos and oxidative turnover, or 'respirative activity', in viable cells. They also observed that CM-H_2XRos fluorescence, and thus respirative activity, was unaltered during

the early stages of camptothecin induced apoptosis; in late-stage apoptotic cells loss of CM-H_2XRos fluorescence indicated that respiration had ceased. In an earlier study (Poot et al., 1996), depressed CM-H_2XRos fluorescence was observed when respiration was inhibited with rotenone and antimycin A. These studies provide convincing evidence that there exists a strong correlation between CM-H_2XRos fluorescence and cellular respiration. Nevertheless, Isailovic (2007) observed a poor correlation to respiratory activity in SF-21 STR culture, which was attributed to oxidation of the stain during storage. This stain has not yet been used to monitor mitochondrial function of mammalian cells exposed to the particular stresses of culture in a STR.

1.10.5 Apoptosis Indicator Stain

1.10.5.1 Annexin-V/PE used in conjunction with Sytox Green.

In viable mammalian cells, the phospholipid phosphatidylserine (PS) is normally located on the cytosolic facing side of the cytoplasmic membrane; during apoptosis it translocates to face the cell exterior (Fadok et al., 1992; Koopman et al., 1994). It is not observed to translocate during necrosis (Darzynkiewicz et al., 1996). PS can be bound by the vascular anticoagulant α (VACα,), referred to as Annexin V (AV), which was found to preferentially bind to negatively charged phosphlipids such as PS (Andree et al., 1990).

Simply by dual staining with AV conjugated to fluorescein isothiocyanate (FITC), referred to here as AV-FITC, and the non-vital stain PI (AV-FITC/PI). Vermes et al. (1995) and Ishaque and Al-Rubeai (1998) revealed three distinct sub-populations using the dual stain on a FC: non-apoptotic cells (AV-FITC negative, PI

negative), apoptotic cells (AV-FITC positive, PI negative), late apoptotic and/or necrotic cells (AV-FITC positive, PI positive). Note that this result would be entirely applicable were SG used instead of PI and PE used instead of FITC, as in this study, since the action of these stains is equivalent. Indeed, Koopman et al. (1994) conducted their study using EB instead of PI, with the same result as specified above. It is important to note that the above studies established that necrotic cells could also be stained with AV (probably because of severe membrane disintegration) and, without dual staining with PI can be misclassified as apoptotic.

Studies in the literature using the AV assay have reported PS translocation at some point *en-route* to cell death by apoptosis in a variety of cell types; for example, human lymphocytes (Castedo et al., 1996) murine hybridoma (TB/C3) (Ishaque and Al-Rubeai, 1998) and HSB2-2 human leukaemia cells (Vermes et al., 1995), although there remains some contention surrounding the timing of PS translocation (Ishaque, 2000). Furthermore, the notable absence of PS translocation in cells over expressing apoptosis inhibitors, bcl-2 and abl, corroborates those studies that reported PS translocation as a fundamental characteristic of apoptotic cell death (Martin et al., 1995). However, Frey (1997) contends that AV does not reveal apoptosis in some cell lines (Raji, U937 and HL-60), perhaps because of differences in lipid composition of the cytoplasmic membrane.

Chapter 2: Materials and Methods

2.1 Cell Line

This research project used a suspension variant (SV) of the CHO-K1 cell line (CHOK1SV), pre-adapted to suspended growth in chemically defined medium and transfected for GS gene expression, GS-CHO (Section 1.3). Glutamine synthetase Chinese hamster ovary (GS-CHO) is a recombinant cell line using the glutamine synthetase expression system that is proprietary to Lonza Biologics (Lonza). The GS-CHO cell line used in this study has been engineered to produce an IgG antibody for therapeutic purposes.

2.2 Cell Culture Maintenance

GS-CHO cells were grown as a suspension culture in polycarbonate Erlenmeyer shake flasks with vented lids (Corning Incorporated, USA). Cells were grown in the defined proprietary medium formulation CDCHO (Sigma-Aldrich, UK). An incubator (LC12 –LEEC, UK) was used to maintain culture conditions at 36.5^{o}C and 5% CO_2, agitation of the flasks at a rate of 130 revolutions per minute (rpm) was made by an orbital shaker (Denley Instruments, UK) placed onto a shelf of the incubator. Flask volumes were progressively increased from 125 mL to 250 mL, 500 mL, 2 L containing a medium volume equal to one fifth of the flask volume; this stepwise escalation in volume provided the necessary viable cell number (*VCN*) for inoculation of the 3 L STR. The initial inoculum-flask was inoculated to 3 x 10^5 cells mL^{-1}; subsequent flasks were inoculated with sufficient volume to ensure between 2 x 10^5 and 3 x 10^5 cells mL^{-1}.

Flask passages were made during the middle of the rapid growth phase after either 3 or 4 days of growth in the incubator. Thus, the 125 mL was passaged after 4 days, the 250 mL flask after 3 days, the 500 mL after 4 days and after 3 days the 2 L was used to inoculate the 3 L STR. To ensure consistency and that the passage number was constant for each experiment, a fresh vial was revived from the frozen working cell bank for each inoculum chain. This cell bank was sufficient to inoculate all of the experiments of this study. All cell work was conducted in a laminar flow class II safety cabinet (ICN Gelaire BSB3-SS – ICN Biomedicals, UK).

2.3 Cell Banking

Cells in their rapid growth phase (Figure 3-8) with a viability of more than 95% were centrifuged (MSE Mistral 2000) in 50 mL centrifuge tubes at 179 *g* for 5 minutes. Supernatant was discarded, leaving the cell pellet, which was resuspended to a concentration of 1.5 x 10^7 cells mL^{-1}. A mixture of 90% fresh medium and 10% dimethyl sulfoxide (DMSO), percentage volume/volume (v/v), both at room temperature, was used for re-suspension.

The cell-suspension was aliquoted to 1 mL in each 1.5 mL cryovial (Nunc – Gibco, UK). A 'Mr Frosty' freezing container (Nalgene, Sigma Aldrich, UK) with an external jacket containing isopropyl alcohol was used to control the rate of freezing of the cryovials in a -80°C freezer over 24 hours (h), after which cells were immediately transferred to liquid nitrogen at a temperature of about -190°C. To maximise cell viability, the transfer of cells from the incubator to the -80°C freezer was completed within 1 h.

2.4 Revival of Cells from Cell Bank

No more than two cryovials were removed from liquid nitrogen at a time. On removal, vials were placed in a 36.5^{o}C water bath to be thawed. Immediately upon cells' thawing, vials were sprayed with ethanol and placed into the laminar flow cabinet. The entire contents of the vial were then transferred into 25 mL of CDCHO medium at 36.5^{o}C in a 125 mL shake flask. Inoculated flasks placed were placed into the incubator and maintained as described (Section 2.2).

2.5 Shake Flask Study

Shake flask studies were made in 2 L shake flasks in an incubator maintained at 36.5^{o}C, 5% CO_2 and 130 rpm, as detailed (Section 2.2).

2.5.1 CCCP Induced Cell Death Shake Flask Study

Carbonyl cyanide m-chlorophenyl hydrazone (CCCP) at a concentration of 1 mM in dimethylsulphoxide (DMSO) was added to a final concentration of 100 µM to cultures in mid-rapid growth phase (~7 x 10^5 cells mL^{-1}), growing in 250 mL of CDCHO in 1 L vented lid Erlenmeyer flasks. After addition of CCCP, flasks were rapidly returned to the shaker-incubator and incubated at 36.5^{o}C for 12 h. At the end of the incubation period cell physiology was assessed using flow cytometry (FC), dual staining with the following stain couplets: Calcein-AM/PI; AV-PE/SG and $DiOC_6(3)$/PI.

Single staining was made with JC-1, as its dual emission spectrum complicated dual staining. Single staining was made with CM-H_2XRos because it was necessary to fix the staining of the cell with paraformaldehyde, which alters cell

properties for measurement with other stains. Staining methods are detailed (Section 2.11).

2.6 Fed-batch Study

Fed-batch growth took place in a 5 L stirred tank reactor, STR, (Applikon, UK) with a 3 L working volume. STR vessels were glass with rounded bottoms. A single marine (axial flow) impeller was mounted on the shaft; the ratio of the impeller diameter (D) to the vessel diameter (T) was D/T = 1/3. The ratio of the height of the STR culture (H) to the vessel diameter was H/T = 6/5 and the ratio of the distance of the impeller from the vessel bottom (C) to the height of the STR culture was C/H = 1/6. The STR was controlled by a BioController ADI 1030 (Applikon, UK) to conditions set on a BioConsole ADI 1035. Bicarbonate buffer and CO_2 sparging were used to increase or decrease pH, respectively, as necessary for maintenance of pH control within set limits. The buffer had a pH of 9.7 at 21°C.

Feeding of the STR began when either the viable cell number (*VCN*) had reached 1 x 10^6 (measured by Trypan Blue, TB, exclusion) or after day 4 from inoculation of the STR, whichever occurred first. Feeding rate was adjusted after each sample (~ every 24 h) on the basis of specific growth rate, μ, so that cell growth could be predicted for the next 24 h and glucose controlled at 4.5 ± 1.5 g L^{-1}. The substrate had a pH of 2.5 at 21°C.

DOT was controlled at a set % of saturation with air (% saturation). pH and *DOT* were measured using steam-sterilisable probes (Applisens - Applikon, UK). Sparged gas entered the STR via a sparge-pipe, which released the gas underneath the impeller through holes facing the bottom of the STR. The impeller agitation rate

was set to 195 rpm. STR temperature was set at 36.5^{o}C and controlled using an electric heat-jacket.

2.7 Scale-down STR+PFR

The fed-batch STR without recirculation is also included for comparison with the control. In total, 12 STR experiments were made as 6 duplicates at the following different conditions:

1. No recirculation: fed-batch STR without PFR (Section 3.3)
2. Control, with recirculation: STR+PFR 60 s residence, but feeding to the STR
3. STR+PFR 60 s residence, with substrate to the STR and alkali feed to the PFR
4. STR+PFR 60 s residence, with alkali and substrate feed to the PFR
5. STR+PFR 120 s residence, with alkali and substrate feed to the PFR
6. STR+PFR 120 s residence, with 100x higher alkali concentration (compared to experiments 4 and 5) and substrate feed (the same as experiments 4 and 5) to the PFR

The experimental results in this study are presented as a comparison to those obtained in the recirculation control case. The control case consisted of a fed-batch STR with substrate feed and pH control directly to the STR, but with continuous recirculation of the STR contents through the attached plug flow reactor (PFR), with a mean residence time (*RT*) in the PFR of 60 seconds (s). In test cases, alkali and substrate feed additions were made into the PFR.

In all of the STR+PFR experimental cases, the culture was continuously withdrawn from a 5 L STR and pumped through a coiled length of silicone tubing that constituted the PFR (Figure 2-1). The PFR was made from a 1.98 m length of

9.8 mm internal diameter and 1.6 mm wall thickness platinum cured silicone tubing (SLS, UK). A new length of tubing was used for each experiment.

The PFR was coupled to the STR by two sets of tubing: a 15 cm length of 3.2 mm internal diameter silicon tubing connected to a 20 cm length of 3.2 mm internal diameter neoprene tubing (SLS, UK) that was fed through the peristaltic pump. Neoprene tubing was used in the pump-head because its resilience allowed continuous peristaltic pumping without tube damage - silicone tubing was found to wear within 24 hours (h). A further 10 cm length of 3.2 mm internal diameter tubing was bisected by a feeding point and connection to the beginning of the 1.98 m length that constituted the PFR tubing. The feeding point was forked to allow addition of bicarbonate buffer and nutrient feed. The total volume of the tubing after this feeding point was 150 mL, 5% of the 3 L working volume of the 5 L STR, as used by Namdev and Thompson (1992) and Amanullah et al. (2001).

A 15 cm length of 3.2 mm internal diameter and wall thickness tubing connected the end of the PFR back to the STR head-plate. The total volume of connection tubing before the entrance to the PFR, marked by the point from which alkali and substrate additions were made, was ~5% of the PFR volume, an additional 3 s on top of the 60 s PFR residence.

The mean residence time (*RT*) within the PFR was controlled by the pumping rate provided by a peristaltic pump (Watson Marlow 505 S – Watson Marlow Pumps Group, UK). The PFR was submerged in a water-bath controlled at 36.5^{o}C to prevent the contents of the PFR dropping below 36.5^{o}C, as it was important to ensure temperature gradients were not present.

The pump was calibrated using the PFR and connection tubing under the conditions of the model, with a gas liquid mixture entering the PFR. The *RT* in the PFR was controlled by the pumping rate to 60 s or 120 s; these are the approximate expected range of mixing times, θ_m, in a 20 m^3 STR (Table 1-2). A photograph of the scale-down equipment used in this study is provided (Figure 2-2).

2.7.1 Control Study

For the duration of the stirred tank reactor connected to the plug flow reactor, (STR+PFR) control experimental case, alkali and substrate feed additions were made directly to the STR in the same manner detailed for the fed-batch experimental case that was without recirculation through the PFR (Section 2.6). The mean residence time (*RT*) in the PFR was 60 s. In this recirculation control case, no additions were made to the PFR; i.e., all additions were made to the STR.

2.7.2 pH gradients

To study the effect of pH gradients alone, alkali additions for control of pH, as detailed (Section 2.6), were made to the PFR, while nutrient feed (substrate addition) was made to the STR only. Residence time (*RT*) in the PFR was 60 s.

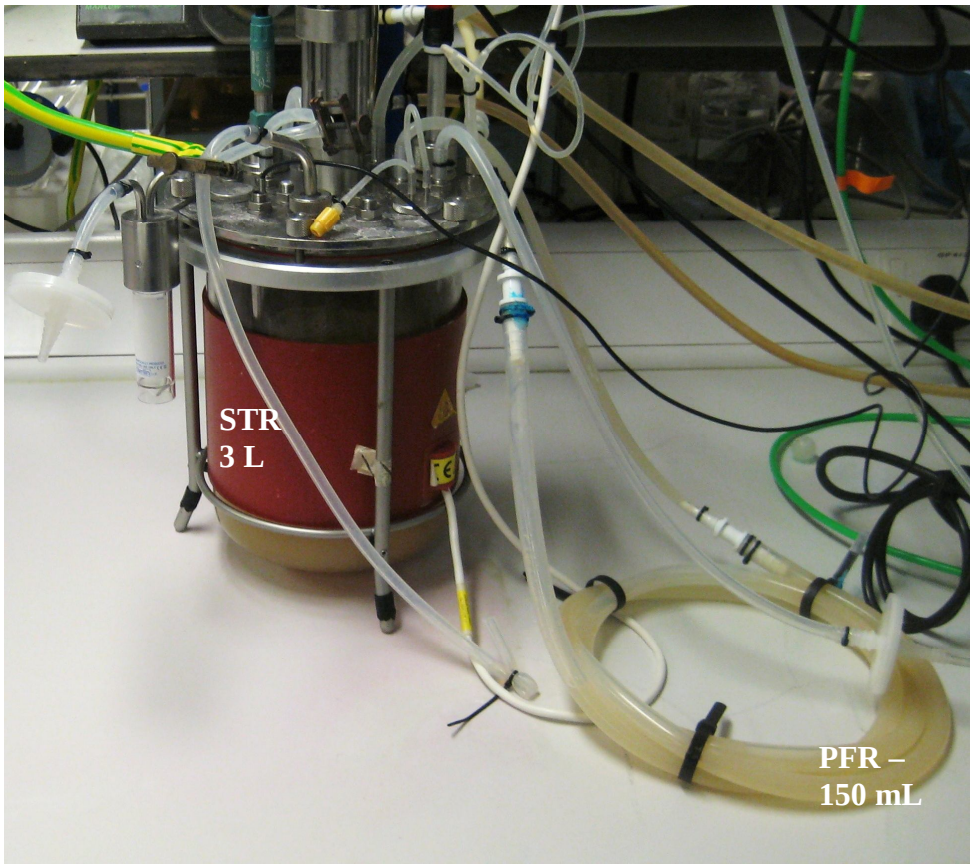

Figure 2-1: Scale-down, showing the 5 L (3 L working volume) stirred tank reactor (STR) connected to the 150 mL plug flow reactor (PFR), referred to as STR+PFR; thus the PFR (and attendant connective tubing, after the point of feed addition) had 5% of the STR working volume. The PFR was made using a platinum cured silicone with following dimensions: 1.98 m length, internal diameter 9.8 mm, external diameter 11.4 mm (Section 2.7).

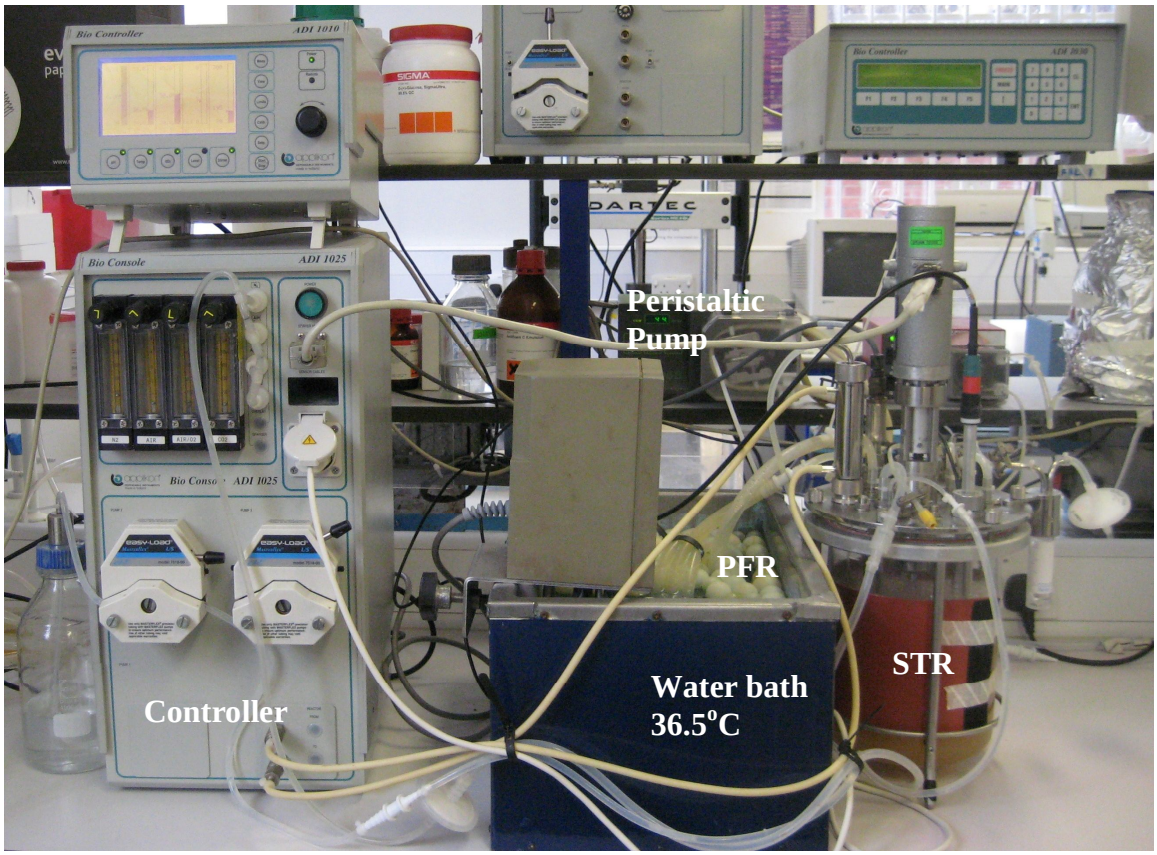

Figure 2-2: Scale-down set up, showing the stirred tank reactor (STR) connected to the plug flow reactor (PFR), referred to as (STR+PFR), with the PFR in a water bath at 36.5°C. The PFR was raised slightly out of the water bath so it could be located in this figure; during the experiments, the PFR was entirely submerged.

2.7.3 pH and Nutrient gradients

Two pH and nutrient gradient scale-down studies were conducted:

1. To study the combined effect of expected pH and nutrient gradients created in a large-scale STR's feed-zone, alkali and nutrient addition (referred to as substrate feed) for control of pH and glucose concentration were made to the PFR (Section 2.6). For scale-down test experimental cases, no additions were made directly to the STR and all additions were made to the PFR. Over separate experiments, *RT* in the PFR was set at 60 s and 120 s.

2. Often a higher alkali concentration is used at the large-scale to decrease volumes and associated costs; for this reason, a second pH and nutrient gradient study was also conducted with 2 M Na_2CO_3, which is 100x more concentrated that the alkali used for all other experimental cases, (pH of 12.3 at 21°C). As in the first study above, the alkali was added with the substrate as necessary for control. *RT* in the PFR was set at 120 s; this represented the 'worst case scenario' for creation of addition zone (Section 1.5) associated heterogeneity in a 20 m^3 STR.

2.8 STR Setup

After each experiment, pH and O_2 probes were checked and calibrated before their return to the STR. Before beginning a run, sterile medium in the STR, agitated at 195 rpm, was heated to 36.5^{o}C, a sample was taken, its pH was measured with an offline pH meter (SevenEasy™ - Mettler Toledo, UK) and the calibration of the STR's pH-probe was corrected, if off line pH differed from online pH by ± 0.02. The STR was then set to the control pH at the setpoint (Section 2.6). When the desired pH was attained, the O_2-probe was again calibrated and O_2 control was initiated. Sparging rates were restricted (Section 2.6) to minimise damage from

bubble bursting and to dampen control responses. The STR was inoculated only after control values had been reached and maintained for at least 1 h, ideally, 24 h. With a regularity of at least every 24 h, a sample was taken from the STR and pH was checked offline and corrected as necessary.

2.8.1 Water Bath for Constant PFR Temperature

A 5 L water bath (Fisherbrand – Fisher Scientific, UK) was used to maintain the PFR at 36.5^{o}C. The water bath was filled to the brim with approximately 5 L of deionised water (dH_2O) and covered with floating balls to minimise evaporation. The temperature was verified with a mercury thermometer that remained in the bath. To maintain sterility, 200 g of $CoSO_4$ (Sigma Aldrich, UK) and 100 g of ethylenediaminetetraacetic acid (EDTA) were added, as well as water bath detergent (SigmaClean™ water bath treatment – Sigma Aldrich, UK), as recommended by the manufacturer. The water bath was placed beside the STR so that the PFR could be effectively submerged.

2.9 STR Cleaning Protocol

Scrupulous cleaning of the STR was required to prevent the build-up of deleterious material such as metabolic by-products, cell debris, DNA, and proteases, glycol and proteins.

At the end of each experiment, the STR was steam sterilised at 121°C. After sterilisation, the contents of the STR were disposed of and the pH and O_2 probes removed and carefully cleaned with dH_2O. Sodium hydroxide (NaOH) at a concentration of 1 M was made using dH_2O that was dispensed into the STR through one of the probe ports up to the impeller connection with the drive-shaft.

To prevent damage to the drive shaft's bearings, cleaning solutions were kept below the small openings in the drive shaft. The impeller was then set to 200 rpm and the STR heated to 50°C for a minimum of 12 h.

Following treatment with NaOH, the STR was emptied and cleaned with dH_2O. The ostensibly clean STR was then filled with 0.5 M citric acid, made using dH_2O, and for a minimum of 12 h it was agitated at 200 rpm at a temperature of 50°C. The STR was then emptied and again cleaned with dH_2O. The head-plate of the STR was then dismantled, the rubber washers were carefully removed and placed in dH_2O, and the dismantled head-plate was placed into 0.5 M citric acid and left for a minimum of 12 h. The head-plate and ports were then washed thoroughly in dH_2O to remove every trace of acid. The STR was then put back together; latex gloves wear worn during this procedure to minimise contamination. 50 mL of dH_2O was poured into the STR and it was then sealed, connected with the relevant tubing for control and steam sterilised at 121°C.

2.10 Haemocytometry

Viable cell number (*VCN*) was determined with a haemocytometer (HC) (Neubauer improved, 0.1 mm depth chamber) and Trypan Blue (TB) exclusion. If necessary, cells were diluted with phosphate buffer solution (PBS) at pH 7.4 (Biotechnology performance certified - Sigma Aldrich, UK) to ensure a concentration of less than l x 10^6 cells mL^{-1}; they were then stained with TB (0.5%) at a 1:1 dilution. Dead cells took up the stain and appeared blue when observed at 20x magnification on a standard light microscope (OLYMPUS, Japan). Cells from four grids per slide were counted twice and the *VCN* calculated based on a single grid volume of 10^{-4} mL. The following equation was used to calculate the total cell number, *TCN*:

$$TCN = \left[\left(\frac{Cells\, in\, 4\, squares}{4} \right) \times 2\left(dilution\ \ factor \right) \right] \times 10^4\, cells\, mL^{-1} \qquad \textbf{2-1}$$

From this *TCN*, *VCN* is found by counting unstained cells and dead cell number (*DCN*), by counting stained cells.

2.11 Flow Cytometry

2.11.1 The Instrument

Flow cytometric (FC) analysis was made using a Coulter Epics Elite Analyser (Beckman Coulter, UK) using a 15 milliwatt (mW) argon-ion laser at a wavelength of 488 nanometres (nm). Laser light scattered at small angles (0.5^o-5°) from the incident beam, forward scatter light (FS), traversed a standard cross beam mask and neutral filter before arriving at the FS detector, a photodiode. Light scattered at large angles (15°-150°) to the incident, side scatter light (SS), was collected in a simple collection lens, producing a collimated beam that first passed through a 488 nm band pass filter reflecting light to the first photomultiplier tube (PMT1), where it was converted into an electronically amplified signal. The remaining higher wavelength light was separated for amplification by a series of long pass filters of wavelengths 525 nm (green light region), 575 nm (orange light region) and 635 nm (red light region) that reflected light in to PMT2, PMT3 and PMT4, respectively.

EXPO™ 32 ADC Software for Coulter®, operating on the Windows 98 ™, system was used for collection and presentation of the data produced by the FC. Off-line data analysis was made using WIN MDI 2.9, which was free to download from http://en.bio-soft.net/other/WinMDI.html.

2.11.2 Cleaning Procedure

To prevent debris from accumulating, the flow cell was cleaned at the beginning and end of analysis sessions. Cleaning was performed by running through the system's tubing full test tubes of 70% ethanol, 10-fold diluted bleach and COULTER CLENZ® (Beckman Coulter, UK). A lens tissue was used to apply ethanol for cleaning the exterior of the flow cell, lenses used to collect FS and SS, and beam shaper lenses; light collection filters were cleaned using a dry lens tissue.

2.11.3 Alignment of Fluidics and Optics

Having cleared the flow chamber of debris, the quality of results is dependent on the accuracy of the flow chamber's alignment with the laser beam. The laser beam's focus must be the centre of a stream of cells flowing through the chamber, illuminating whole cells as they pass through the excitation beam; further, the flow chamber must be positioned so that SS is received by the photo-multiplier tubes (PMT).

Alignment was made using fluorescent polystyrene beads (FLOW-CHECK™ fluorospheres - Beckman Coulter, UK) of uniform fluorescence and size (diameter 10 µm) at a concentration of 1 x 10^6 beads mL^{-1} in an aqueous suspension medium containing surfactants and preservatives. When excited by a 488 nm laser the fluorospheres fluoresced at 525-700 nm. The bead solution was run through the flow chamber at a data-rate of 40-50 events per second during acquisition of 10000 gated events.

Following the recommendations of Beckman Coulter, alignment was established when the half-peak coefficient of variance (1/2 *%CV*) on the normal distribution of fluorescence was between 0.8 and 1.5. The percentage coefficient of

variation (*%CV*) is a common measure of the spread of a distribution, found by the following equation:

$$\%CV = \left(standard\ deviation\ /\ mean\ channel\ width\right) x\ 100 \qquad \textbf{2-2}$$

2.11.4 Ratiometric Cell Count

Using a fluorescent bead (fluorospheres) solution containing 1 x 10^6 beads mL^{-1} allowed a simple ratiometric count to find the total cell number (*TCN*) by using the percentage of cells that are found in quadrant 1 (Q1), *% cells*, and the percentage fluorospheres that are found in quadrant 4 (Q4), *% fluorospheres*, (Figure 2-3):

$$TCN = \left(\frac{\%\,cells}{\%\ \ fluorospheres}\right) \times 10^6\ cells\ mL^{-1} \qquad \textbf{2-3}$$

To 600 µL of PBS at pH 7.4 (Biotechnology performance certified, Sigma Aldrich, UK) 25 µL of fluorospheres and 25 µL of the cell sample were added. After agitation, to ensure homogeneity, the mixture was analysed on the FC. The region of interest was defined by 'gating' on the forward scatter light v side scatter light, FS-SS, cytograph, excluding debris and electronic noise from the information before its further analysis. Gated information was viewed on a green fluorescence v red fluorescence, GF-RF, cytograph.

The percentage of cells and fluorospheres was defined using a quadrant to separate the two populations (Figure 2-3). Note: cell numbers are presented as 1 x 10^5 cells mL^{-1} throughout the results of this study, not at 1 x 10^6 cells mL^{-1}, which was used for the above calculation (Equation 2-3) because the concentration of fluorescent beads was 1 x 10^6 mL^{-1}.

2.11.5 Viability Assessment

Dual staining with Calcein-AM (Molecular Probes, UK) and PI (Molecular Probes, UK) was used as a viability assay (Calcein-AM/PI). PI was prepared to a concentration of 150 µmolar (µM) in PBS (pH = 7.4), and Calcein-AM to 50 µM in DMSO. Cell culture samples to be stained were diluted in PBS at 36.5^{o}C to a concentration of 1 x 10^6 cells mL^{-1}. A 1 mL aliquot of the cell dilution was used for each analysis. To each 1 mL, 25 µL of PI and 1 µL of Calcein-AM were added, giving concentrations of 3.7 µM and 50 nanomolars (nM), respectively. Immediately after addition of the fluorescent stains, samples were placed in an incubator at 36.5^{o}C in an atmosphere of 5% CO_2 for 15 minutes. Incubated samples were immediately placed in a melting ice bath, ready for analysis on the FC.

Calcein-AM is a recent improvement on fluorescein diacetate (FDA), which is an established viability counter-stain for PI (Szabo et al., 1982; Sugita et al., 1986; Ross et al., 1989; Cocomartin et al., 1992). Calcein-AM was used in preference to FDA because it has a brighter green fluorescence (GF) and better cell retention (Barda-Saad et al., 1997; King, 2000). Calcein-AM has been shown to stain CHO cells effectively for viability assessment (Wang et al., 2008).

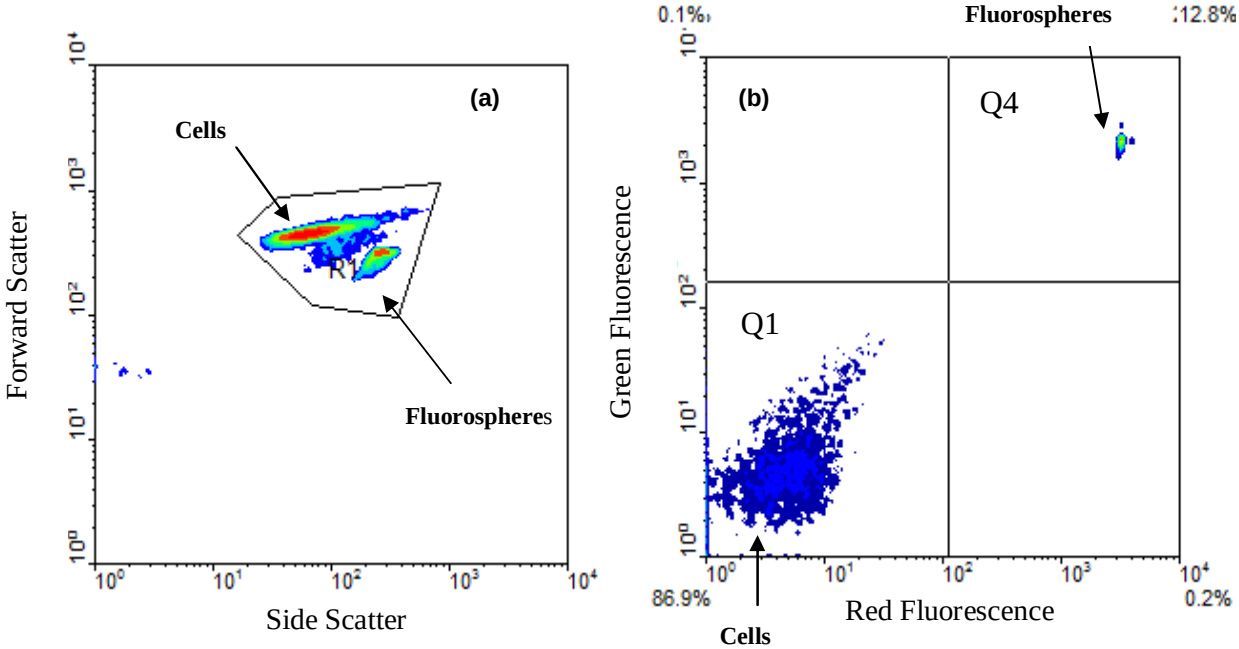

Figure 2-3: Ratiometric counts: (a) FS-SS cytograph was used to gate out cells and fluorospheres (beads) from debris and electronic noise; (b) analysis of the contents of the gate was performed on a GF-RF cytograph that revealed the percentage of cells and beads.

2.11.6 Mode of Cell-Death Assessment

Staining with Sytox Green (SG) and Annexin V (AV), conjugated to R-phycoerythrin (PE) to give (AV-PE), all provided as a kit from Molecular Probes, UK. The dual stain is referred to as AV-PE/SG. Cell culture samples to be stained and analysed on the FC were diluted in PBS at 36.5^{o}C to a concentration of 1 x 10^6 cells mL^{-1}. For each sample analysis, a 1 mL aliquot of the cell dilution was required. These were first centrifuged at 179 *g* for 5 minutes and resuspended in 1 mL of PBS at 36.5^{o}C before being centrifuged again (179 g for 5 minutes) and resuspended in 100 µL of binding buffer solution (10 mM Hepes/NaOH, pH 7.4, 150mM KCl, 1mM $MgCl_2$ and 1.8 mM $CaCl_2$ from Molecular Probes, UK), only then was AV-PE added to each to give a final concentration of 1 µg mL^{-1}. Samples were then incubated at 36.5^{o}C and 5% CO_2 for 15 minutes. SG to a final concentration of 0.01 µM was then added to incubated samples that were immediately placed in a melting ice bath, ready for analysis on the FC.

2.11.7 Evaluation of Mitochondrial Activity and Membrane Potential

Mitochondrial membrane potential ($\Delta\Psi m$) and activity were assayed using the following three molecular probes: 5,5', 6,6'-tetrochloro-1,1,'3,3'–tetraethylbenzimidazolcarbocyanine iodide (JC-1), 3,3'-dihexyloxacarboncyanine iodide ($DiOC_6(3)$) and CM-H_2XRos (Molecular Probes, UK). JC-1 was prepared at a concentration of 1000 µM, $DiOC_6$ (3) to 0.9 µM and Mitotracker red, 50 µM. All three mitochondrial stain concentrates were made using high-grade DMSO (Sigma-Aldrich, UK). Cell culture samples to be stained and analysed on the FC were diluted in PBS at 36.5^{o}C to a concentration of less than or equal to 1 x 10^6 cells mL^{-1}. For each sample analysis, stain was added to a 1 mL aliquot of the culture sample.

JC-1 staining began with the addition of 1 µL of JC-1 concentrate to the 1 mL culture sample to give a final concentration of JC-1 of 1 µM. After addition of the stain, samples were incubated at 36.5^{o}C in an atmosphere of 5% CO_2 for 15 minutes. Incubated samples were immediately placed in a melting ice bath, ready for analysis on the FC.

$DiOC_6(3)$ was used with PI ($DiOC_6(3)$/PI); staining began with the addition of 1 µL of $DiOC_6(3)$ concentrate to the 1 mL culture sample to give a final concentration of 0.9 nM. After addition of the stain, samples were incubated at 36.5^{o}C and 5% CO_2 for 15 minutes. Incubated samples were immediately stained with 25 µL of PI, as for viability assessment (Section 2.11.5), and placed in a melting-ice bath, ready for analysis on the FC.

CM-H_2XRos staining began with the addition of 10 µL of CM-H_2XRos to the 1 mL culture sample to give a final concentration of 500 nM. After addition of the stain, samples were incubated at 36.5^{o}C and 5% CO_2 for 15 minutes. Incubated samples were centrifuged at 500 *g* for 10 minutes, re-suspended in a 4% paraformaldehyde solution at 4°C and then stored at 4°C; this process fixed the stain. Before FC analysis, the samples were centrifuged at 179 g for five minutes and re-suspended in 1 mL of PBS at 4°C.

2.11.8 Flow Cytometric Analysis: Gating on Unstained Control

Cells as whole entities were first gated out in their FS-SS cytograph and transferred to the GF-RF cytographs. The quadrant gate in the GF-RF cytographs was set in such a way that control unstained cells appeared in the bottom left quadrant (Figure 2-3).

2.12 Nutrient and By-Product Analysis

Culture samples were centrifuged at 179 *g* for 10 minutes and the supernatant stored in 1.5 mL sample vial (Eppendorf, UK) at -80°C. For analysis, the samples were thawed at room temperature and run through a Bioprofile 300B analyser (Nova Biomedical, USA) according to the manufacturer's protocols. The analysis included quantification of glucose, lactate, ammonia (NH_3), sodium ion (Na^+), potassium ion (K^+) and osmolality.

2.13 Antibody Quantification

Culture samples were centrifuged at 179 *g* for 10 minutes and the supernatant stored in 1.5 mL sample vials (Eppendorf, UK) at -80°C until they were thawed for analysis. Volumetric product yield was quantified based on the absorption and elution of the mAb to and from a high-pressure liquid chromatography (HPLC) protein A column. mAb in the supernatant selectively bound to a protein A affinity column (PA ImmunoDetection® sensor cartridge; Applied Biosystems, UK) in an Agilent HPLC Series 1200 series HPLC (Agilent, UK); non-bound material was washed from the column and bound product eluted by changing pH from 7.2 to 2.0. For quantification, UV (280 nm) was used by the Agilent HPLC to monitor the elution of the mAb against a matched IgG standard.

2.14 Antibody Characterization

The following four methods were used to assess the effects of the heterogeneity that was introduced by the scale-down on product (mAb) consistency: mass analysis using sodium dodecyl sulphate-polyacrylamide gel electrophoresis (SDS PAGE); highly accurate mass analysis by mass spectrometry using liquid chromatography

(LC) followed by electrospray ionisation (ESI) coupled to a quadrapole time-of-flight (TOF) mass analyser, referred to as ESI-Q-TOF; charge analysis using isoelectric focusing (IEF); glycoform profiling using normal phase high-pressure liquid chromatography (NP-HPLC) using 2-aminobenzamide (2-AB) as the fluorescent tag, referred to as NP-HPLC 2-AB. This suite of antibody characterisation methods provided a comprehensive analysis of antibody quality.

2.14.1 Reducing and Non-Reducing SDS Page: Protein Molecular Weight

SDS PAGE is typically used to reveal mass heterogeneity, and is a sensitive technique for detection of protein aggregation (Jiskoot et al., 1990; Kroon et al., 1992; Lin et al., 2000); reduced SDS PAGE removes disulphide bonds and can therefore be used to determine if they are responsible for aggregation (Liu et al., 2005).

Purified harvest samples (taken at the final time point from each STR experiment, referred to as harvest) were loaded onto precast NuPAGE™ 4-12% BisTris 12 well polyacrylamide gels (Invitrogen, UK). Two separate analyses were performed: non-reduced and reduced. Reduced samples were heated to 95°C in the presence of a reducing agent (Invitrogen, UK); non-reduced samples were heated without the reagent. Proteins were visualized using Coomassie Blue staining to determine antibody purity. Purity is defined as the percentage intact IgG for non-reducing gels and sum of the percentages for the heavy and light chain for reducing gels.

2.14.2 Mass Spectroscopy: Peptide Mapping and Antibody Mass

Mass spectroscopy is the most accurate method for mass analysis (Liu et al., 2008) and is capable of revealing significant chemical modifications; the ESI-Q-TOF used for analysis in this study has a reported mass accuracy of 100 parts per million (ppm) (Zhang et al., 2009). Mass spectroscopy here provided a conformation of the protein's elemental composition, the nature of major modifications and major glycoforms, but it can not readily identify small mass changes such as oxidation (+16 Da) or dehydration (-18 Da), and is certainly unable to identify deamidation (+1 Da) (Zhang et al., 2009). Small mass changes, such as these, alter the protein's charge and should have been indentified by IEF.

Purified harvest samples were dialysed for 18 h against 0.1 M ammonium bicarbonate (NH_4HCO_3) at room temperature in Slide-A-Lyzer 3.5 kDa MWCO (molecular weight cut off) dialysis cassettes (Pierce, USA). After buffer exchange, 100 µg of each sample was concentrated to dryness in a centrifugal vacuum concentrator (miVac DNA, GeneVac, UK). 100 µg of each sample was then dissolved in 50 µL of 0.35 M Tris, pH 8.6 containing 8 M Urea and 4 mM EDTA, providing a 2 mg mL^{-1} solution. 30 mM dithiothreitol (DTT) (1.5 µL of 1 M DTT/50 µL protein sample) was then added to the protein sample and the sample incubated for 4 h at 40°C. After the 4 h incubation, samples were left to cool to room temperature in the dark. Once cooled, 40 mM of iodacetamide (2 µL of 1 M iodacetamide/50 µL protein sample) was added to each sample, which was incubated in the dark for 30 minutes at room temperature.

After the second incubation, the samples were diluted 1:8 with 0.1 M ammonium bicarbonate and immediately transferred to -70°C for 12 h. Samples

were thawed at room temperature and 0.16 units (U – specified by manufacturer) per 1 µg of sequencing grade modified trypsin (Promega, UK) per µg of protein was added, e.g., 100 µg of 4 µL of 4U μL^{-1} solution of trypsin. The samples were then incubated overnight (minimum 18 h, maximum 24 h) at $30^{o}C$.

After the third incubation, digestion of the protein was halted by adding formic acid to a final concentration of ~1% v/v in water. Trypsin specifically cuts lysine and arginine residues to produce a number of peptides.

The digested protein samples were then loaded onto a reverse-phase high pressure liquid chromatography, HPLC (Ultimate 3000 LC – Dionex, USA), attached in-line to an electrospray mass spectrometer (QStar XL Mass Spectometer – Applied Biosystems, USA). In this way, the peptides were separated by reverse-phase HPLC before entering the mass spectrometer, which provided the mass of each peptide fragment.

2.14.3 Isoelectric focusing: Extent of Deamidation

Purified harvest samples were loaded onto a precast IsoGel® Agarose IEF plate (FMC BioProducts, Rockland, ME) with a pH range from 3 to 10 and focused so that the isoelectric pattern created by the antibody's charge could be characterized. Any changes in this pattern are indicative of structural changes in the antibody molecule. For comparison, isoelectric focusing (IEF) standards (LKB Pharmacia) with known isoelectric point (pI) values between pH 3 and pH 10 were also loaded.

2.14.4 Antibody Glycan Analysis

Glycans were removed from the antibody using an enzymatic deglycosylation kit (Prozyme, Inc., USA) and following the manufacturer's instructions. In preparation

for glycan analysis, the purified glycan samples were fluorescently labelled with 2-AB (2-aminobenzamide) by reductive amination, using the Signal 2-AB Labelling Kit (Prozyme, Inc., USA), following manufacturer's instructions. Briefly, prior to labelling the purified glycan samples were aliquoted into 500 µL sample vials (Eppendorf, UK) and dried without heating in a centrifugal vacuum concentrator (miVac DNA - GeneVac, UK); labelling reagent was added and the samples incubated at 65°C for 3 h; excess reagent was removed from the samples using the GlycoClean S Cartridge (Prozyme, USA) in a procedure recommended by the manufacturer. Fluorescently labelled glycan samples were then loaded onto a Glycosep N HPLC and run according to the manufacturer's protocol developed from Guile et al. (1996).

Chapter 3: Results and Discussion of Preliminary Studies

3.1 Development of Characterisation Methods

The suitability of the fluorescent stains chosen to characterise cell physiology during scale-down experiments was explored by using multi-parameter flow cytometry (FC) in conjunction with fluorescent staining protocols developed (Section 2.11) to monitor cell culture during normal shake flask culture (Section 2.2) and during induced cell death (Section 2.5.1).

A preliminary control study to establish the characteristics of each staining protocol during cell death was conducted by treating cells with CCCP (Section 2.5.1). CCCP is a protonophore that renders the mitochondrial inner membrane permeable to protons and causes uncoupling of mitochondria, which means that the transfer of electrons through the electron transport train should no longer be coupled to ATP production, due to the loss of the electrochemical gradient (de Graaf et al., 2004). CCCP has been found to induce apoptotic cell death in a variety of cell types (Armstrong et al., 2001; Mlejnek, 2001; de Graaf et al., 2004) and is recognised within the literature as an effective means for mitochondrial membrane depolarisation (Duchen, 2004; Arimochi and Morita, 2006).

In this study, GS-CHO cell culture was incubated with 100 µM CCCP for 12 h, as used to induce apoptosis in IL3-dependent murine pro-B lymphoid cells (FL5.12) and neomycin resistant Jurkat T-ALL cells (de Graaf et al., 2004); incubation for 10 h with 50 µM CCCP was effectively used to induce apoptosis in HL60 cells (Armstrong et al., 2001). In both their studies, mitochondrial depolarisation and apoptosis were concurrent.

At the end of the incubation period, cell physiology was assessed using FC, staining with Calcein-AM/PI, AV-PE/SG, JC-1, CM-H_2XRos, and DiOC_6(3)/PI. The properties of this selection of stains have been discussed (Section 1.10).

3.2 Characterisation of CCCP Induced Cell Death

3.2.1 Mode of Cell Death with Annexin-V/PE and SG: Apoptosis or Necrosis

By dual staining with Annexin-V conjugated to Phycoerythrin (AV-PE) and Sytox Green (AV-PE/SG) (Section 2.11.6), it was possible to use flow cytometry (FC) to establish the mode of cell death in glutamine synthetase Chinese hamster ovary (GS-CHO) cell culture after incubation with the recognised decoupler and apoptosis-inducing toxin CCCP (Section 2.5.1). Untreated cells were over 90% viable (AV-PE negative, SG negative), and the remaining cells were necrotic (AV-PE positive, SG positive), as identified by their high green fluorescence (GF) (Figure 3-1, a). It is clear from the concurrent red fluorescence (RF) of this population that membrane rupture had revealed phosphatidylserine serine (PS). Necrotic cells are labelled A on the green fluorescence v red fluorescence (GF-RF) cytograph and back-gated so that only light scattering properties of necrotic cells are visible in the forward scatter light v side scatter light (FS-SS) cytographs (Figure 3-1, A). The proportion of necrotic cells (Figure 3-1, B) is shown to increase after incubation with CCCP; this is clear when comparing the size of population A and B (Figure 3-1). There is no apoptotic population (AV-PE positive, SG negative). Note that an apoptotic population would show only high RF.

When viable (AV-PE negative, SG negative) and necrotic cells (AV-PE positive, SG positive) were back gated to FS-SS cytographs (Figure 3-1, A and B)

viable cells corresponded to a distinct population with higher FS and lower SS and necrotic cells to a distinct population with lower FS and higher SS. This is consistent with the light-scattering properties of necrotic cells recently reported (Laporte et al., 2006), but contrary to those reported in a review of cell death (Darzynkiewicz et al., 1992), which observed that necrotic death was generally accompanied by decreased FS paralleled by a decreased SS that was caused by dissolution of the cells' contents. Indeed, apoptotic cells were reported to show decreased FS and an increased SS, reflecting cell shrinkage paralleled by increased granularity.

In this study, however, cells with these light scattering properties were stained with the nucleic acid stain SG, which identifies cells as having a permeable cytoplasmic membrane, and therefore as likely necrotic. Thus, in this study, cells with decreased FS and elevated SS will be referred to as necrotic. The slight increase in SS, seen here in necrotic cells, may be caused by the disintegration of cellular organelles; perhaps, dissolution of cellular contents was insufficient to decrease FS.

Were it not for staining with SG that proved that the cytoplasmic membrane was not intact, and that the cells could not therefore be early-apoptotic, the observed light scattering might be misinterpreted as indicative of the early stages of apoptotic death. Demonstrably, light scattering changes must be interpreted with caution and accompanied by the more specific staining assay.

There are three possible reasons for the absence of an identified apoptotic population: first, that, at the culture conditions used in this study, CCCP does not induce apoptosis in this cell line; second, that the AV-PE/SG staining method is flawed and incapable of detecting apoptotic cells that do exist; third, that the GS-

CHO cell line used studied here does indeed die only by necrosis. Each will be addressed below.

As noted, CCCP has been proven to induce apoptotic cell death in a variety of cell types (Armstrong et al., 2001; Mlejnek, 2001; de Graaf et al., 2004). Apoptotic death induced by CCCP has also been identified by dual staining with AV conjugated to green fluorescent fluorescein isothiocynate (FITC) and red fluorescent PI (AV-FITC/PI) (de Graaf et al., 2004), and this dual stain is analogous to AV-PE/SG. In view of its reported efficacy as an inducer of apoptosis, it is concluded that CCCP does reliably induce apoptosis. Note that in this study the stain colours and the corresponding attributes were the opposite way around from the many studies using AV-FITC/PI: in this study, using AV-PE/SG, RF indicated PS translocation (indicative of apoptosis, if GF negative) and GF indicated cytoplasmic membrane rupture.

Comparison of FS-SS cytographs derived from each of the staining protocols showed that the method used to stain with AV-PE/SG decreased the viable cell population significantly more than other staining protocols, compared to unstained cells (Figure 3-1 to Figure 3-5).

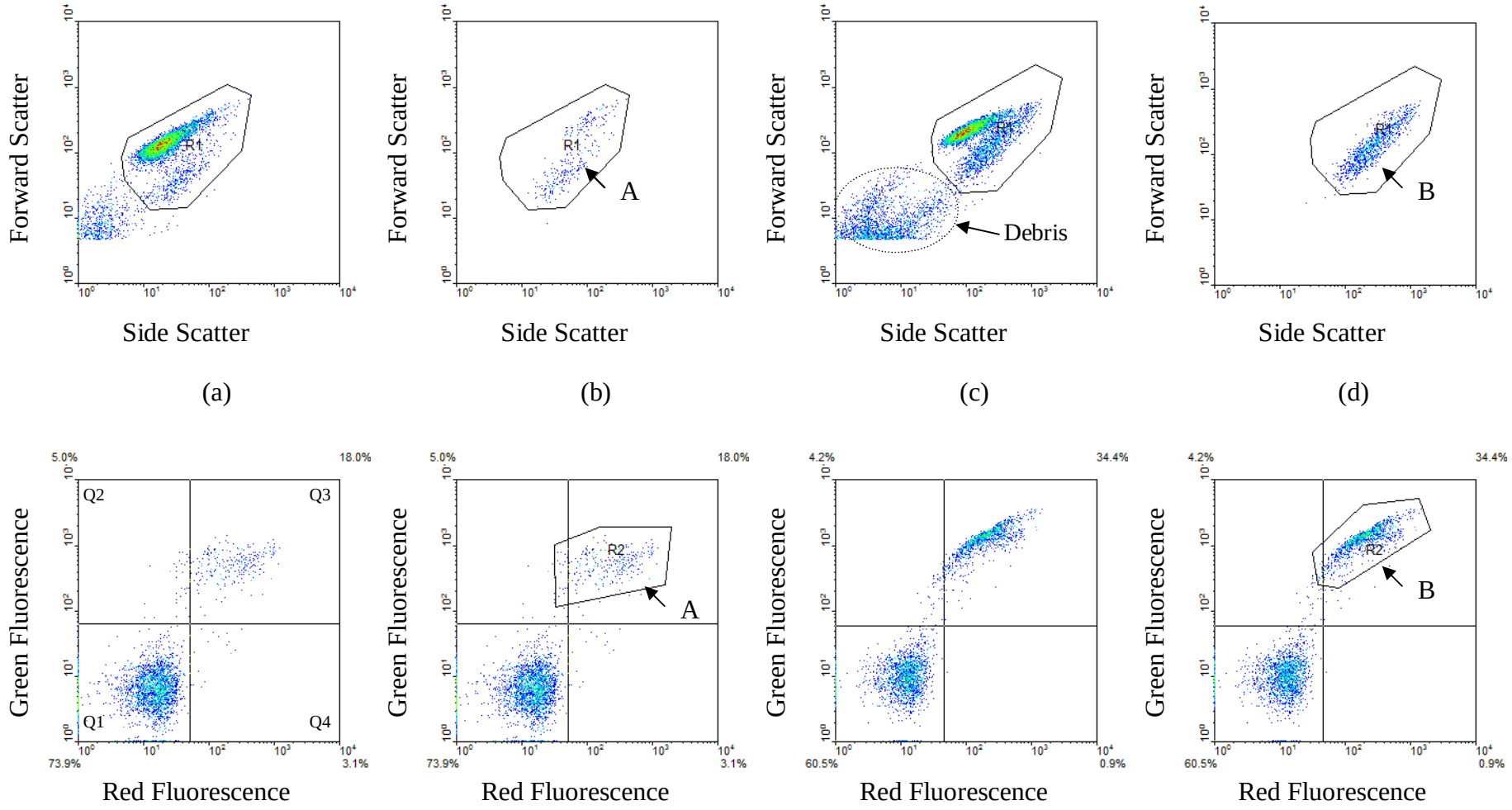

Figure 3-1: Annexin-V (AV) conjugated to phycoerythrin (PE) used with Sytox Green (AV-PE/SG) (1 µg mL^{-1} and 0.01 µM, respectively) stained GS-CHO cells (1 x 10^6 cells mL^{-1}) before and after CCCP treatment (10 µM for 12 h at 36.5°C) (Sections 2.11.6 and 2.5.1). (a) Non-treated AV-PE/SG stained cells; (b) Non-treated AV-PE/SG stained cells back gated on population (A) from green fluorescence v red fluorescence (GF-RF) to forward scatter light v side scatter light (FS-SS) cytograph; (c) CCCP treated AV-PE/SG stained cells; (d) CCCP treated AV-PE/SG stained cells back-gated on population (B) from GF-RF to FS-SS. Quadrant 1 (Q1): Viable Cells; Q2: Early Necrotic Cells; Q3: Late Necrotic Cells; Q4: Apoptotic Cells.

This decrease in cell viability was probably caused by the centrifugation steps necessary to wash the cells in PBS and then re-suspend them in a high Ca^+ binding buffer, which is required for maximum AV binding to PS. The same decrease in viability was observed with Calcein-AM/PI staining after exposing cells to the same washing steps. It is possible that other steps in the sampling and staining method contributed to the decrease in viability (Section 3.3.3).

Since the staining protocol probably injured cells, it is reasonable to suggest that cells were damaged to such an extent that any apoptotic population had its cytoplasmic membrane ruptured during staining and thereafter presented necrotic features, i.e., a permeable cytoplasmic membrane identified by staining with SG. This is unlikely for three good reasons. First, that samples stained with AV-PE/SG without washing and binding buffer steps retained their unstained viability but did not exhibit apoptotic features, showing only a smaller necrotic population; crucially, some PS labelling with AV-PE occurred in the necrotic population, showing that PS labelling of apoptotic cells could have occurred without the binding buffer. Second, that low-level cell damage of the sort experienced during the staining protocol would probably trigger apoptosis in some viable cells. Third, that apoptotic morphology, as detailed for wild-type CHO cells (Arden and Betenbaugh, 2004), was at no point observed by microscopy. Indeed, cells were observed to swell and rupture, as is typical of necrosis (Darzynkiewicz et al., 1996). Note: cell damage during staining implies that there existed a sub-population of viable cells that were more susceptible to damage.

Because apoptotic cell death has been observed in CHO culture, it is sensible to question the efficacy of the staining protocol, but confirmation of the technique's

efficacy as a means for detection of apoptosis is abundant in the literature. AV used in conjunction with a nucleic acid stain, typically PI or EB, is an established method with proven capability to detect apoptosis (Sgonc and Gruber, 1998) and the staining protocol used in this study (using conjugated AV and a nucleic acid stain) is reported to stain apoptotic cells successfully in many relevant flow cytometric studies of cell culture (Koopman et al., 1994; Vermes et al., 1995; Ishaque, 2000). Few reports could be found using SG, but the likely reason is that SG was developed by Molecular Probes after PI and EB, and has yet to be adopted widely. SG has improved nucleic acid binding, superior exclusion from viable cells and a brighter fluorescence (Shapiro, 2003b). Despite the relative scarcity of AV-PE/SG, successful identification of viable, apoptotic and necrotic cells is reported, using the same staining protocol and stain combination outlined in this report (Mukhopadhyay et al., 2007; Varum et al., 2007). In the literature, the method's efficacy is clear.

Thus, there is strong evidence supporting both the efficacy of the apoptosis inducer and the method of apoptosis detection. It is therefore concluded that the GS-CHO strain used in this study died not by apoptosis, as might be expected, but by necrosis. Evidence supporting this conclusion is provided by the absence of morphological indicators and the negative staining for apoptosis after application of the proven apoptosis inducer CCCP. Apoptosis was absent in CHO cells studied by Singh and Al-Rubeai (1994), but was identified in several other studies of CHO cells (Moore et al., 1995; Goswami et al., 1999; Tey et al., 2000; Arden and Betenbaugh, 2006).

These results emphasise the importance of combined staining for identification of multiple, interrelated cell characteristics. Here, cytoplasmic

membrane permeability indicated necrosis, where AV-PE staining alone would have indicated apoptosis. This staining protocol (Section 2.11.6) was also used for stirred tank reactor (STR) experiments (Sections 3.4.3 and 4.4.3), as it was important to monitor, and not presume, the mode of cell death for culture in the STR.

3.2.2 Cell Viability with Calcein-AM and PI: Live or Dead

Dual staining with Calcein acetoxymethyl (Calcein-AM) and Propidium Iodide (PI) (Calcein-AM/PI) (Section 2.11.5) was used to delineate three cell populations: viable cells (Calcein positive, PI negative) identified by bright green fluorescence (GF), dead cells (Calcein negative, PI positive) identified by red fluorescence (RF) and an intermediate sub-group (Calcein positive, PI positive) that have both GF and RF, referred to here as the dual stained population (DSP).

These three populations were back gated to FS-SS cytographs (Figure 3-2). Viable cells corresponded to a distinct population with higher FS and lower SS; dead cells, a distinct population with lower FS and slightly higher SS signal (Figure 3-2, D). The third population, the dual stained population (DSP), had the same SS as the viable cell population, but with considerably elevated FS, placing them on the upper-end of the viable cell population (Calcein positive, PI negative). This was elucidated by back-gating the DSP to a FS-SS cytograph (Figure 3-2, C). The light scattering properties detailed above may be cautiously interpreted to provide an insight into the morphology and physiology of the three populations.

The dead or necrotic cells identified with Calcein-AM/PI (Calcein negative and PI positive) had the same the light scattering properties as necrotic cells identified with AV-PE/SG (AV-PE positive and SG positive) (Section 3.2.1). It is unsurprising to find that the light scattering properties of the populations identified

as necrotic by positive nucleic acid staining were in accordance: PI and SG are both effective nucleic acid stains that should be excluded from viable cells. The light scattering properties of respective viable cell populations were also in accordance.

The DSP exhibited the FS and SS reported for early stage necrotic cells (Darzynkiewicz et al., 1992), which suggests that, like early necrotic cells, they had not yet begun to degrade structurally, implying that their death had not occurred a long time before analysis on the FC. This is consistent with the conclusion made by Isailovic (2007) in a flow cytometric characterisation study of *Spodoptera frugiperda-21* (Sf-21) using Calcein-AM/PI; dual staining was attributed to either the persistence of esterase activity in dead cells or slow leakage of Calcein from recently permeable (dead) cells.

Unlike mitochondrial membrane potential, $\Delta\Psi m$, which is wholly reliant on cytoplasmic membrane integrity, and cannot persist after the cytoplasmic membrane has become permeable to PI or SG, it is perfectly reasonable to expect esterase activity to continue after the cell death: esterase activity is likely to be independent of cellular respiration. Other intracellular enzymes, such as lactate dehydrogenase (LDH) and galactosidase, usually retain activity when released from ruptured cells, and often, incidentally, to the detriment of extracellular product (Goergen et al., 1993; Gramer et al., 1995).

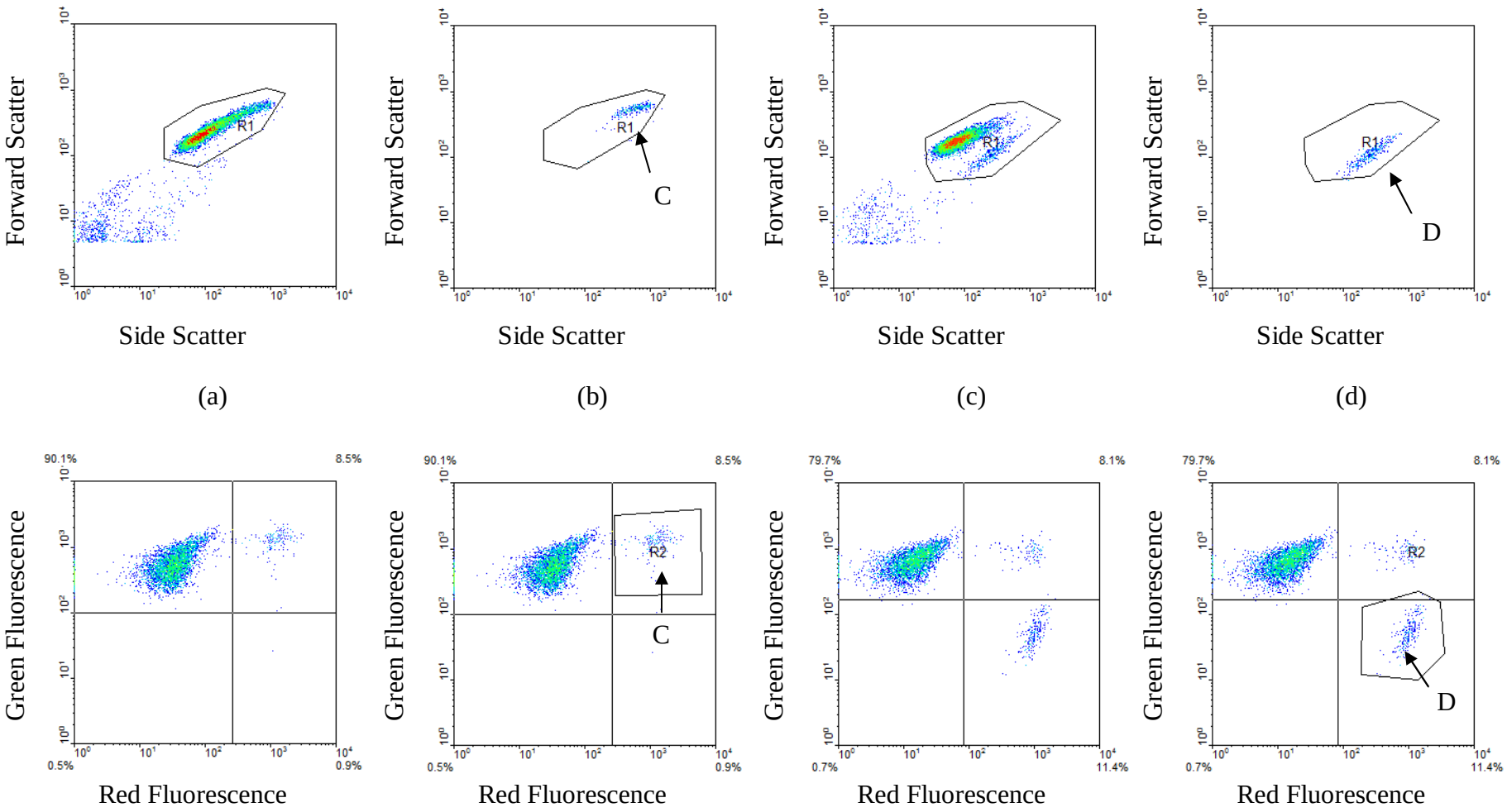

Figure 3-2: Calcein-AM/PI (50 nM and 3.7 µM, respectively) stained GS-CHO (1 x 10^6 cells mL^{-1}) cells before and after CCCP treatment (10 µM for 12 h at 36.5°C) (Sections 2.11.5 and 2.5.1). (a) Non-treated Calcein-AM/PI stained cells; (b) Non-treated Calcein-AM/PI stained cells back gated on population (C) from green fluorescence v red fluorescence (GF-RF) to forward scatter light v side scatter light (FS-SS) plot; (c) CCCP treated Calcein-AM/PI stained cells; (d) CCCP treated Calcein-AM/PI stained cells back-gated on population (D) from GF-RF to FS-SS.

Four hypotheses as to the nature of this dual stained population (DSP), i.e., cells stained with Calcein-AM and PI, are here propounded. Further evidence allowed them to be tested (Sections 3.4.2 and 4.4.2). First hypothesis: if the presumption of continued enzyme activity after death is rejected, then the DSP must have died after addition of Calcein-AM to the sample, to allow Calcein to be formed in the cell before enzyme activity ceased at the time of death. Cell death during staining implies that there existed a sub-population of viable cells that was less robust than the majority of viable cells, which evidently remained viable. For this hypothesis, Calcein would need to have been retained in the dead cell for a minimum of 15 minutes. The time required for sample staining (i.e., addition of the stain and then an incubation period).

Second hypothesis: if it is accepted that enzyme activity did continue after cell death, the clear absence of intermediary levels of green fluorescence implies that a catastrophic drop in esterase activity or retention of Calcein occurred soon after death. Thus, the DSP must have died recently, and, if so, was composed of one or a mixture of two cases: one, cells that had recently perished in the shake flask; two, cells that were viable when taken from the shake flask and were then killed during staining and analysis. Both cases allow testable predictions to be made.

In the first case, the DSP population died in the stirred tank reactor (STR). Cells that had recently died in the STR are, it is suggested, revealed by dual staining when the sample is assayed on the FC. Therefore, when μ is no longer increasing (i.e., when the rapid growth phase ends) its size should be proportional to the rate of cell death (r_d).

In the second case, the DSP population is assumed present as a sub-population in the STR, but is not killed until after sampling (i.e., removal from the STR). The DSP is therefore proportional to the number of less robust viable cells in the STR, i.e., cells that

are especially sensitive to whatever factors could cause death during sampling and staining. Sensitivity might reasonably be expected to increase as 'toxic' metabolites (such as lactate and ammonia) accumulate, as generally occurs in closed vessel cultures (Sections 3.5.3 and 3.5.4). The existence of a sub-population of less robust cells was also necessary for the hypothesis above, proposing that enzyme activity ceased at the time of cell death (indicated here by staining with PI), and this less robust sub-population can therefore be inferred regardless of the presumed cellular enzyme activity. Support for the hypothesis that the DSP represented a sub-population of less robust cells that were killed during staining is provided by the observed increase in necrotic cell death during AV-PE/SG staining (Section 3.2.1). However, the two staining methods do differ: only AV-PE/SG includes a buffer change step (Section 2.11.6), which may be damaging. Thus, between the two methods, cell damage may vary in extent, and possibly type (i.e., lethal or sub-lethal). A third contrary hypothesis is therefore possible.

Third hypothesis: the DSP represented a small percentage of cells that were especially resilient and that after death retained significant enzyme activity or exhibited especially slow leakage of Calcein. In this hypothesis, the dual staining could be entirely unrelated to time since cell death. Perhaps the sub-population of dual stained cells had their cytoplasmic membrane rendered permeable to PI but with sufficient structure maintained to allow for continued enzyme activity and slow leakage of Calcein. Neither recent cell death nor a sub-population of less robust cells are required to explain dual staining if it is assumed that this dead cell population was able to persist in the shake-flask because further degradation did not occur or degradation was at lower rate than the majority of dead cells. If this third hypothesis is correct, this resilient population would be

expected to accumulate and the DSP should therefore be proportional to the dead cell number (*DCN*).

Fourth hypothesis: intercalation with DNA provides PI with hydrophobic conditions required for peak fluorescence (Section 1.10.2.1), but some non-specific binding may occur (Shapiro, 2003a) and has been suggested as a cause for the lower viability observed when staining with PI on the FC, as compared the viability of the same sample when staining with TB on the HC (Al-Rubeai et al., 1996). However, since strongly hydrophobic conditions, such as those occurring during intercalation with DNA, are required for peak fluorescence, non-specific binding of PI should be revealed as a population with diminished red fluorescence (RF). The DSP did not appear to have lower RF and this hypothesis should be dismissed here without further evidence.

These results re-emphasise the importance and utility of dual staining: by using both Calcein-AM and PI together, a sub-population of cells is revealed that would be mistakenly counted as viable when staining with only Calcein-AM. The DSP population was observed in the STR and these hypotheses were revisited (Sections 3.3.1 and 4.4.2).

3.2.3 Mitochondrial Membrane Potential

The maintenance of mitochondrial membrane potential, $\Delta\Psi m$, is essential for energy generation by oxidative phosphorylation and its loss has been shown to be one of the fundamental indicators of apoptotic cell death (Desagher and Martinou, 2000; Ly et al., 2003); loss of $\Delta\Psi m$ is also an indicator of necrosis (Darzynkiewicz et al., 1996), and any $\Delta\Psi m$ assay would, if a definitive mode of cell death were sought, ideally provide simultaneous staining with a membrane impermeable stain.

3.2.3.1 $DIOC_6(3)$ and PI.

Cells were stained with $DiOC_6(3)$ and PI (Section 2.11.7). The intensity of $DiOC_6(3)$ green fluorescence (GF) is expected to be dependent on $\Delta\Psi m$ and cell size (Haugland, 2002). Dual staining with $DiOC_6(3)$/PI is reported in the literature to delineate three cell populations: viable, apoptotic and necrotic (Vermes et al., 2000). Before addition of the decoupling agent CCCP to depolarise mitochondria, over 90% of the cells were viable. Viable cells exhibited high GF and low RF ($DiOC_6(3)$ positive, PI negative); necrotic or late stage apoptotic cells, which have a permeable membrane, as identified by the high red fluorescence (RF) of PI, should have lost $\Delta\Psi m$, but they too exhibited high GF indicative of $DiOC_6(3)$ staining equivalent to untreated viable cells (Figure 3-3). The necrotic population ($DiOC_6(3)$ positive, PI positive) increased after incubation with CCCP (Figure 3-3, E and F). There was no apoptotic population ($DiOC_6(3)$ positive, PI negative), which would exhibit low GF and low RF.

When the stained cell population was back-gated to a FS-SS cytograph, viable cells ($DiOC_6(3)$ positive, PI negative) corresponded to a distinct population with higher FS and lower SS; necrotic cells ($DiOC_6(3)$ positive, PI positive) corresponded to a distinct population with low FS and higher SS. The light scattering properties of live and dead cells identified using $DiOC_6(3)$/PI dual staining were consistent with those of live and dead cell populations back-gated from the Calcein-AM/PI and AV-PE/SG staining.

There are several reports of $DiOC_6(3)$ being used with success to indicate $\Delta\Psi m$ (Petit et al., 1995; Zamzami et al., 1995; Metivier et al., 1998). However, the results obtained here are consistent with those studies suggesting that $DiOC_6(3)$ is an ineffective indicator of $\Delta\Psi m$ (Salvioli et al., 1997; Zuliani et al., 2003). Dead cells (PI positive) are incapable of maintaining a polarised mitochondria, but exhibited the same degree of

$DiOC_6(3)$ staining, as indicated by GF, as did viable cells, stained with $DiOC_6(3)$ alone. Indeed, the results of this study also indicated that $DiOC_6(3)$ is insensitive to cytoplasmic membrane potential ($\Delta\Psi$), which is lost when the cytoplasmic membrane is ruptured.

Binding of the stain in a charge independent manner suggests that the lipophilic properties of the stain allowed non-specific cytoplasmic and cell organelle staining. Salvioli et al. (1997) support this presumption in their similar study that provides a germane comparison with the results in this report. They also induced mitochondrial depolarisation using a decoupler that is analogous to CCCP, FCCP (carbonyl cyanide p-(trifluoromethoxy) phenylhydrazone), and in accordance with this study, observed little change to $DiOC_6(3)$ fluorescence.

Furthermore, no response was observed after treatment of the leukemic cells with the K^+ ionophore, valinomycin. Contrary to this study, a marked fluorescence decrease was observed when $\Delta\Psi$ was dissipated by treatment with KCL-rich medium or Na^+/K^+ ATPase inhibitor ouabain (Salvioli et al., 1997).

Terasaki et al. (1984), Haugland (2002) and Shapiro (2003a) all found that at low concentrations the stain was effectively localised in the mitochondria, and Rottenberg and Wu (1998) suggest that by maintaining the stain concentration below 1 nm cytoplasmic binding can be minimised by decreasing accumulation of the cation from the medium in the cytoplasm; this approach seeks to decrease the sensitivity of the stain to the cytoplasmic membrane potential ($\Delta\Psi$). However, in this study $DiOC_6(3)$ at a concentration of 0.9 nm (chosen specifically to minimise cytoplasmic binding) was insensitive to the $\Delta\Psi$ and $\Delta\Psi m$ of CHO cells. Further decrease in the stain concentration is therefore likely to be ineffective.

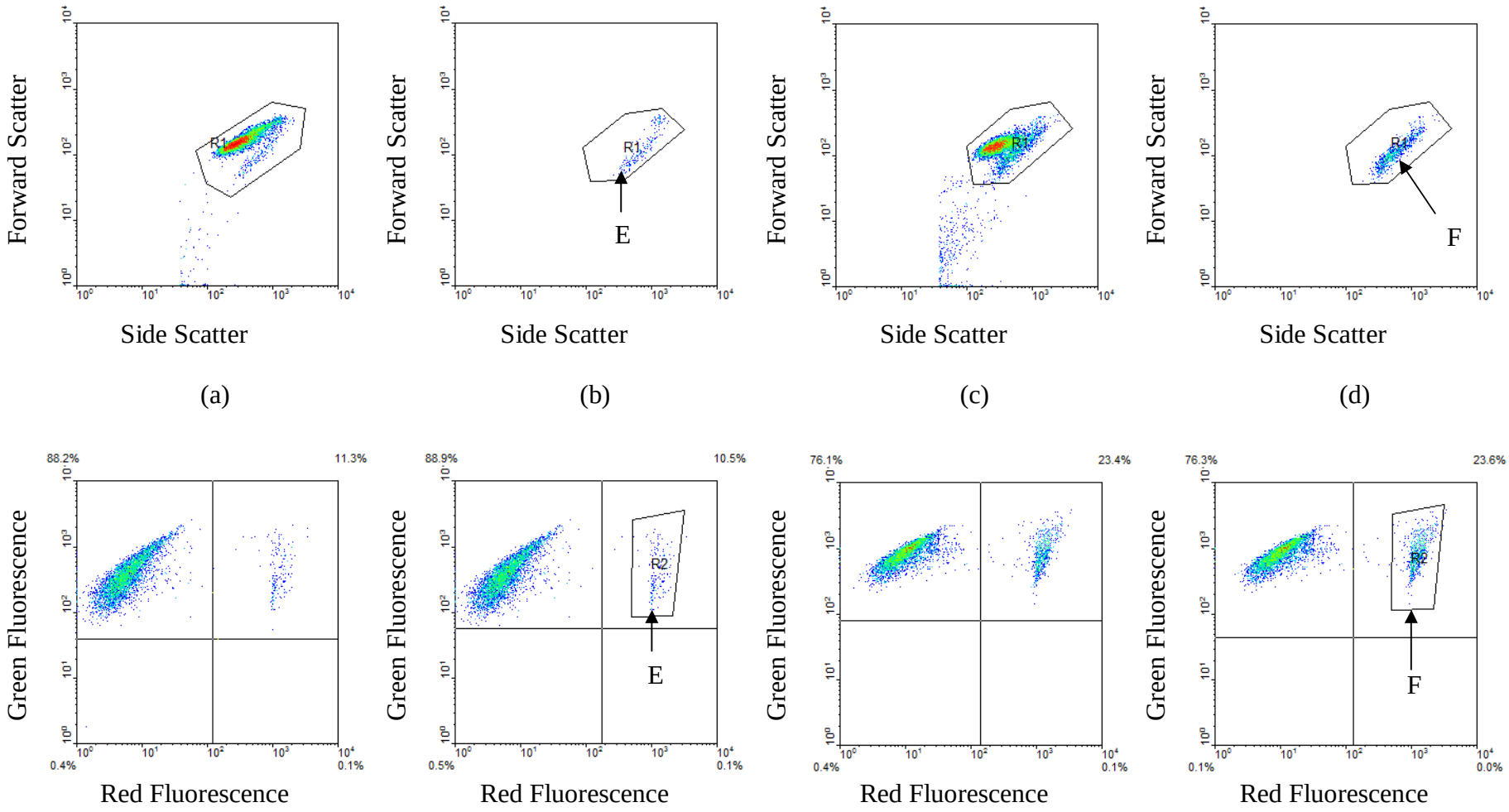

Figure 3-3: $DiOC_6(3)$/PI stained (0.9 µM and 3.7 µM, respectively) GS-CHO cells (1 x 10^6 cells mL^{-1}) before and after CCCP treatment (10 µM for 12 h at 36.5°C) (Sections 2.11.7 and 2.5.1). (a) Non-treated $DiOC_6(3)$/PI stained cells; (b) Non-treated $DiOC_6(3)$/PI stained cells back gated on population (E) from green fluorescence v red fluorescence (GF-RF) to forward scatter light v side scatter light (FS-SS) plot; (c) CCCP treated $DiOC_6(3)$/PI stained cells; (d) CCCP treated $DiOC_6(3)$/PI stained cells back-gated on population (F) from GF-RF to FS-SS.

This was demonstrated by a concentration ranging study (Isailovic, 2007): dual staining with both $DiOC_6(3)$ and PI was observed at $DiOC_6(3)$ concentrations ranging from 0.2 nm to 18 nm. Isailovic (2007) found that dual staining with $DiOC_6(3)$ and PI occurred regardless of the concentration, and concluded, as this report does, that $DiOC_6(3)$ is an unreliable indicator of $\Delta\Psi m$.

3.2.3.2 JC-1

$DiOC_6(3)$ proved to be an ineffective monitor of $\Delta\Psi m$, as was feared on the basis of previous studies found in the literature (Section 1.10.4.1). Salvioli et al. (1997) conducted a similar study with a decoupling toxin (FCCP) and suggested JC-1 as an effective alternative to $DiOC_6(3)$. JC-1 exists either as a green fluorescent (527 nm) monomer at depolarized membrane potential (J-monomer) or as an orange fluorescent (590 nm) aggregate (J-aggregate) at hyperpolarised membrane potential (Haugland, 2002), as present in normally functioning mitochondria.

Cells were stained with JC-1 (Section 2.11.7) and before addition of CCCP two populations were clearly visible: a large population corresponding to 90% of the cells exhibited relatively low green fluorescence (GF) and red fluorescence (RF) and a small population, the remaining 10% of the cells, exhibited elevated GF and RF (Figure 3-4, a). After incubation with CCCP, the population of elevated green and red fluorescent cells remained unaltered, (Figure 3-4, b). The large population with low GF and low RF corresponded to a distinct population with higher FS and lower SS; these light scattering properties matched those of cells identified as viable by dual staining with AV-PE/SG and with Calcein-AM/PI (Figure 3-1 and Figure 3-2). The small population with high GF and high RF corresponded to a distinct population with lower FS and slightly higher SS (Figure 3-4, G and H); these light

scattering properties matched those of cells identified as dead or necrotic by staining with Calcein-AM/PI and AV-PE/SG. A small sub-population of cells with low GF and high RF was also identified (Figure 3-4, I); after staining with CCCP these corresponded to the middle of the viable cell population, when back gated to a FS-SS cytograph (not shown). Fluorescent microscopy showed that the RF from JC-1 was localised in the mitochondria and the GF was diffuse throughout the cytoplasm (Figure 3-6, c).

Viable (i.e., respiring cells) are expected to maintain ΔΨm and therefore to exhibit higher RF and lower GF than dead cells, which lose ΔΨm when they cease respiring, so it was surprising to find that the majority of viable cells have lower GF and lower RF than dead cells. When the cells were incubated with CCCP the proportion of cells with elevated GF and RF was found to increase, compare population G with H (Figure 3-4). This is again in accordance with the increase in dead cells observed when staining with Calcein-AM/PI and AV-PE/SG, and lends further support to the conclusion that this population was dead.

Although it is surprising, the concurrent increase in GF and RF does not imply that the mitochondrial membrane potential (ΔΨm) had increased in this population: the ratio of RF to GF is used to indicate ΔΨm, and it is clear that the ratio of J-monomers and J-aggregates was constant during cell death (Figure 3-4). Indeed, the use of a ratio of the two colours (527 nm J-monomers and 590 nm J-aggregates) is intended to discount factors that may increase stain total uptake, such as mitochondrial size, shape and density, and is one of the vaunted benefits of JC-1 (Haugland, 2002). Evidently, the concurrent increase in GF and RF was caused by some factor that increased the total stain uptake.

When cells die by necrosis they exhibit osmotic swelling and their mitochondria dilate (Desagher and Martinou, 2000); note that this swelling and dilation is caused by the influx which accompanies cytoplasmic membrane rupture, and when it occurs both ΔΨm and ΔΨ are lost. The increased cell volume that typically accompanies necrotic death could certainly account for the increase in GF from J-monomers, but for mitochondrial dilation to increase the numbers of J-aggregates would mean that J-aggregates could be formed and persist when ΔΨm was lost. J-aggregates form at high concentration densities of J-monomer (Haugland, 2002) so if conditions prevailed that allowed J-monomers to persist and accumulate in the mitochondria then J-aggregates could well have formed. Such conditions are improbable, once ΔΨm has dissipated.

Nevertheless, J-aggregates have been observed to form spontaneously in solution when JC-1 was used to stain bacteria, providing evidence of spontaneous aggregation that does not necessarily require hyper-polarity (Shapiro, 2003a). There are, however, no reports in the literature of increased J-monomer and J-aggregate concentrations within dead cells. Although the efficacy of the stain as an indicator of ΔΨm is cast into doubt by the staining observed for necrotic cells, the presence of a viable cell population with elevated J-aggregates (Figure 3-4, I), could indicate that CCCP treatment created a sub-population of viable cells with elevated ΔΨm.

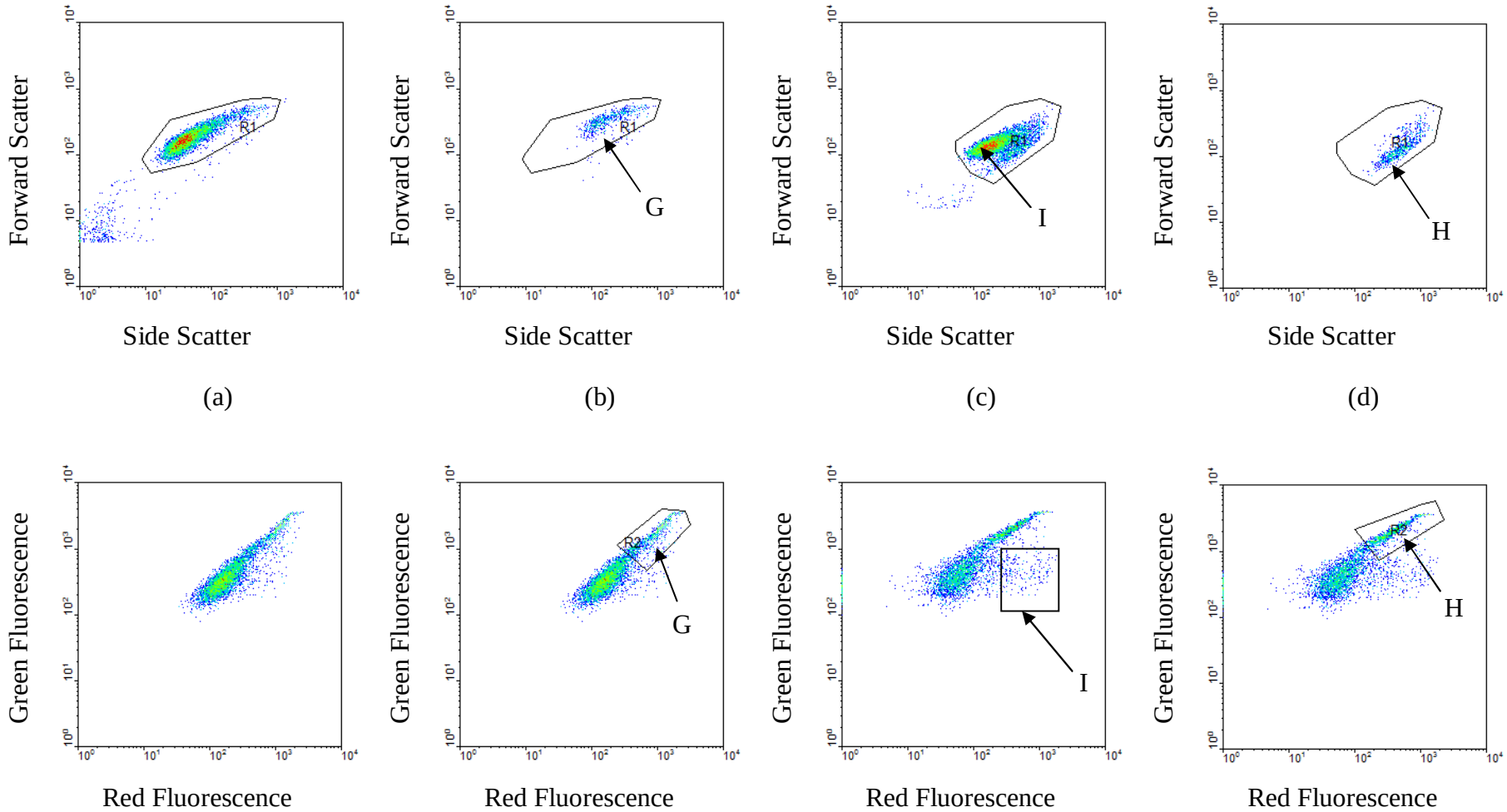

Figure 3-4: JC-1 stained (1 µM) GS-CHO cells (1 x 10^6 cells mL^{-1}) before and after CCCP treatment (10 µM for 12 h at 36.5°C) (Sections 2.11.7 and 2.5.1). (a) Non-treated JC-1 stained cells; (b) Non-treated JC-1 stained cells back gated on population (G) from green fluorescence v red fluorescence (GF-RF) to forward scatter light v side scatter light (FS-SS) cytograph; (c) CCCP treated JC-1 stained cells with population (I) from GF-RF identified on FS-SS; (d) CCCP treated JC-1 stained cells back-gated on population (H) from GF-RF to FS-SS.

The mitochondrial decoupling that CCCP causes has been found to increase respiration rate (Rottenberg and Wu, 1998), and may well have been responsible for this population.

From the ambiguous results observed, it is concluded that JC-1 is an unreliable indicator of $\Delta\Psi m$. Hence, JC-1 was not used for STR analysis (Sections 3.4 and 4.4).

3.2.3.3 CM-H_2XRos

CM-H_2XRos does not fluoresce until it enters a respiring cell, where it is oxidized to the fluorescent mitochondrion-selective stain and sequestered by the mitochondria (Haugland, 2002). The untreated population of mid-rapid growth phase cells stained with CM-H_2XRos (Section 2.11.7) was homogenous with regard to magnitude of CM-H_2XRos oxidation, as indicated by the intensity of the red fluorescence (RF) (Figure 3-5). After incubation with CCCP, two populations are clearly visible, one with elevated RF (Figure 3-5, J). Increased RF has been observed by several other studies using toxic substances to induce cells' death; and is often attributed to one of two different mechanisms.

CM-H_2XRos fluorescence increases with respiration activity, which CCCP has been shown to stimulate above the basal rate (Rottenberg and Wu, 1998). This assertion is supported by Poot and Pierce (1999): fluorescence was strongly linked to oxidative turnover when it decreased as cells were exposed to the respiration complex III inhibitor antimycin A. However, in the same study, fluorescence in late-stage apoptotic cells, as identified by loss of mitochondrial membrane potential (Poot et al., 1997), did not respond to antimycin A, and was thought to be caused by oxidative degradation of lipids (lipid peroxidation), such as the mitochondrial

membrane, occurring by release of reactive oxidative species (ROS), e.g., O^{2-} and OH^{-}. CM-H_2XRos has been successfully used to monitor the ROS (Kim et al., 2002; Shanker et al., 2004; Shanker et al., 2005; Park et al., 2006) that are expected to be released during mitochondrial degeneration (Batandier et al., 2002). In this literature, induced ROS release was reported to increase CM-H_2XRos fluorescence. The literature suggests that CM-H_2XRos can reveal differences in respiration and that it is also influenced by ROS— two factors that may not be mutually exclusive.

Thus, two mechanisms could have resulted in the increased red fluorescence: first, increased respiration rate that resulted from some degree of mitochondrial decoupling, which allowed greater movement of protons; second, increased generation of ROS that accompanied mitochondrial degeneration (Batandier et al., 2002). Light scattering properties could be used to help discriminate between the two.

Unfortunately, the staining method used for CM-H_2XRos required fixing the cells in paraformaldehyde, and fixing altered their light scattering properties, making analysis difficult. Nevertheless, back gating to the FS-SS clearly showed that the cell population with elevated RF corresponded to a population with elevated FS and SS (Figure 3-5, J); these light scattering properties were identified as those of dead cells when staining with AV-PE/SG and Calcein-AM/PI (Section 3.2.1 and Section 3.2.2). Based on the light-scattering properties of necrotic or dead GS-CHO populations, which have been established with confidence in this report by back-gating from stained cell populations, it is concluded that increased RF was generated by ROS released during mitochondrial degradation.

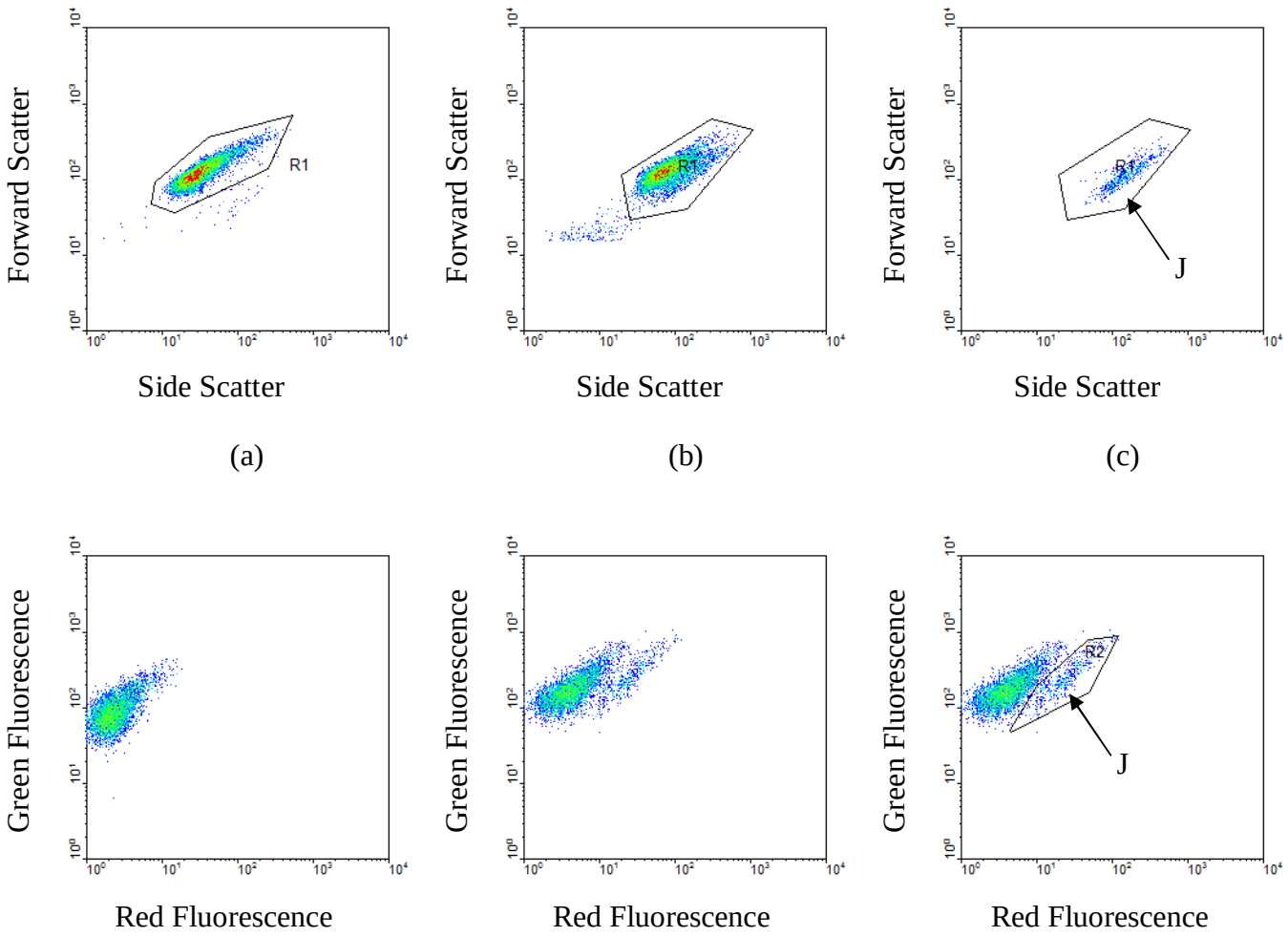

Figure 3-5: CM-H_2XRos (500 nM) stained GS-CHO (1 x 10^6 cells mL^{-1}) cells before and after CCCP treatment (10 µM for 12 h at 36.5°C) (Sections 2.11.7 and 2.5.1). (a) Non-treated CM-H_2XRos stained cells; (b) CCCP treated CM-H_2XRos stained cells; (c) CCCP treated CM-H_2XRos stained cells back-gated on population (J) from green fluorescence v red fluorescence (GF-RF) to forward scatter light v side scatter light (FS-SS).

CM-H_2XRos was not used for STR analysis (Sections 3.4 and 4.4) because suitable nitrogen storage conditions were not available. Without the nitrogen storage recommended by the stain manufacturer (Molecular Probes), oxidation of the stain is known to occur. It is unlikely that significant oxidation occurred in the 12 hours between staining of untreated and CCCP treated cells, but recent research (Isailovic, 2007) has shown that for a 20 day study, as required to characterise growth in a typical fed-bath STR, oxidation of the stain during improper storage renders it useless.

3.3 Culture Growth in Shake Flasks: Cell Count and Viability

Shake flask culture is widely used for the early stages of process development, as well as for cell clone screening studies. Shake flasks are the most widely used reaction vessel in biotechnology and have been for many decades (Maier et al., 2004). Despite its prevalence and importance as a culture vessel, a review of the literature found that characterisation of animal cell physiology during shake flask culture is rare.

3.3.1 A Comparison of Haemocytometry and Flow Cytometry

GS-CHO cell culture growth in a 2 L shake flask was monitored over a 280 h period. 2 mL samples were taken every 24 h from each flask for immediate analysis by flow cytometry (FC) and haemocytometry (HC). FC live/dead cell counts were made using dual staining with Calcein-AM and Propidium Iodide (PI) (Section 2.11.5), and HC live/dead cell counts were made using Trypan Blue (TB) exclusion (Section 2.10).

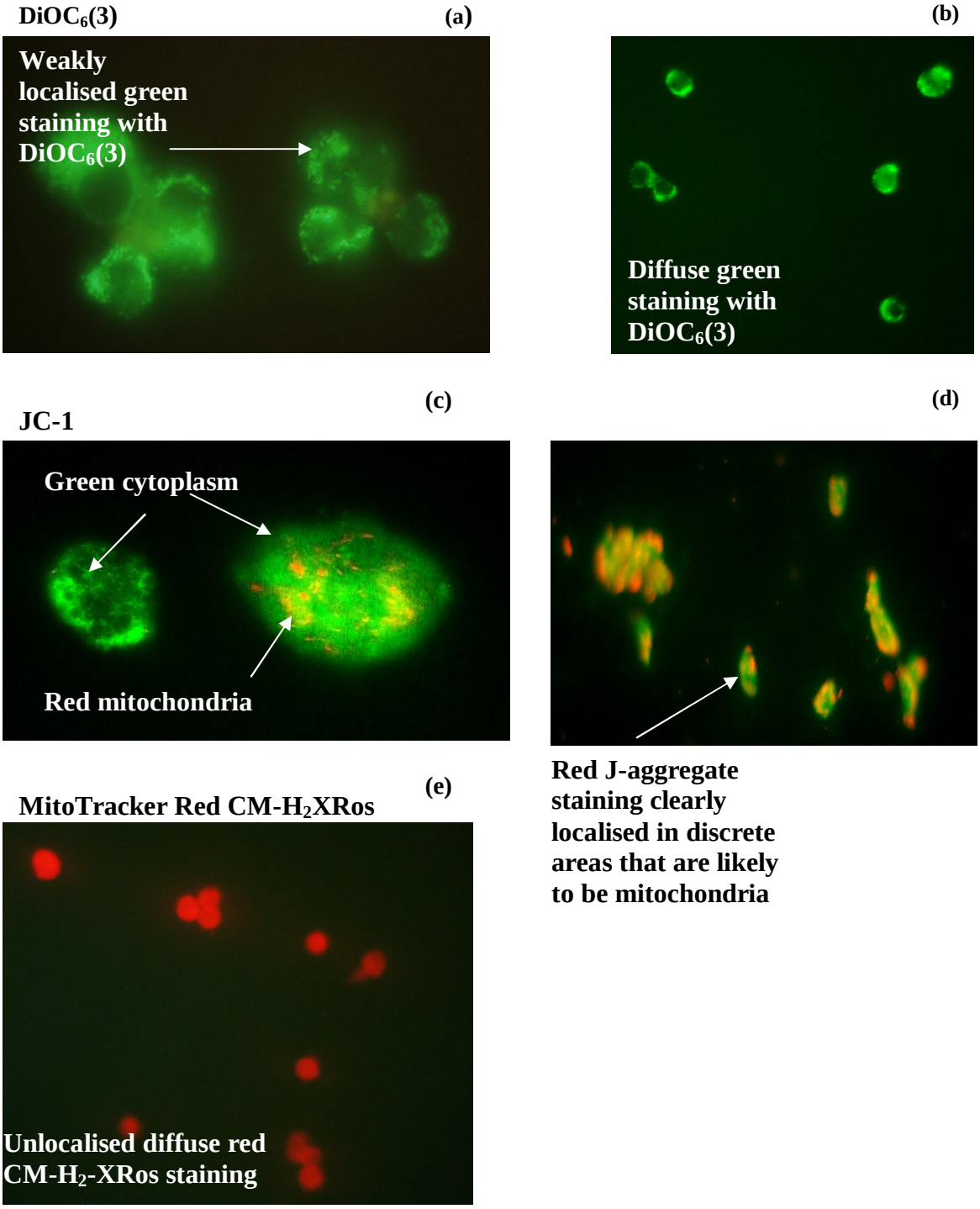

Figure 3-6: Photograph of CCCP treated (10 µM for 12 h at 36.5°C and fluorescent stained GS-CHO cells under fluorescent microscope (Section 2.5.1). (a) and (b) $DiOC_6(3)$ stained (0.9 µM) at 100x and 20x magnification, showing non-localised green staining; (c) and (d) JC-1 stained (1 µM) at 100x and 20x magnification, showing highly localised staining, with red mitochondria and green cytoplasm; (e) $CM\text{-}H_2XRos$ stained (500 nM) at 20x magnification, showing non-localised red staining.

PI and TB are probably similar enough for a useful comparison to be made: both are used on the principle that viable cells will exclude the stain, providing a simple viability assessment. Calcein-AM should stain viable cells green and was used to provide a positive control for dead cell staining by PI on the FC. The common HC method lacks a corresponding positive control.

TB exclusion is widely used for live/dead cell counting in the biopharmaceutical industry, where viable cell counts are important for process optimisation and calculation of nutrient feed rates in fed-batch STR cultures; thus, HC was justifiably used throughout this research to provide a ready comparison with commercial data. The purpose of this study was to explore and define the relative efficacy of the two methods that were used to monitor viable cell number during the fed-batch experiment (Section 3.4) and scale-down experiments (Chapter 4). By using Calcein-AM as a positive control with PI, this study built on the work of Al-Rubeai et al. (1996) who compared TB exclusion on the HC with PI exclusion on the FC as methods for evaluation of cell number and viability in CHO culture. Comparative studies of the HC and the FC using simultaneous staining with PI and a positive control have been conducted: fluorescein diacetate has been employed for hybridoma cell culture (Altman et al., 1993) and Calcein-AM for insect cell culture (Isailovic, 2007); the compelling findings of their research provide further impetus for a comparison of the two methods on this industrially relevant GS-CHO cell line (proprietary to Lonza).

To determine viability and draw a viability curve for analysis by FC one must inspect the forward scatter light v side scatter light (FS-SS) cytographs and their corresponding green fluorescence v red fluorescence (GF-RF) cytographs

(Figure 3-9 and Figure 3-10). Cells stained with Calcein-AM/PI revealed the three populations present and detailed for CCCP induced cell death (Section 3.2.2); accordingly, the same relationship between the cells' light scattering and their staining is revealed by back-gating from GF-RF cytographs to FS-SS cytographs (Figure 3-9 and Figure 3-10, A and B).

Viable cell curves were drawn for counts using each method (Figure 3-7). A comparison of the two curves finds them alike, particularly so when plotted on a logarithmic axis (Figure 3-8), revealing three broad phases that correlate with a rapid growth phase, stationary phase and death phase, as is typical of cell culture growth in any closed vessel. Cells grew from the seeding concentration of ~2 x 10^5 cells mL^{-1} to a maximum viable cell number (*VCNmax*) of 44 ± 2 x 10^5 cells mL^{-1} (mean ± range of data, until otherwise stated) determined by FC and, correspondingly, 47 ± 2 x 10^5 cells mL^{-1} determined by the HC (Figure 3-7). This cell culture performance exceeded expectations for batch culture, which is expected to be limited to 20-30 x 10^5 cells mL^{-1} (Al-Rubeai et al., 1992).

An initial peak viable cell number (*VCN*) was reached after ~ 72 h, shown by both methods, marking the end of rapid growth phase, at cell viability of 36 ± 3 x 10^5 cells mL^{-1} determined by FC and 29 ± 1 x 10^5 cells mL^{-1} by HC; this correlates to a steeper gradient on the curve of *VCN* determined by FC. Accordingly, the mean specific growth rate (μ) during the rapid growth phase was slightly greater for FC, at 0.027 h^{-1} compared to 0.026 h^{-1} by HC, with corresponding doubling times of 25 h and 27 h respectively. No great difference.

At this stage, the number of experiments was insufficient for a statistically meaningful test of the difference between *VCN* counts made with two methods

(*ΔVCN*). However, further studies with continued combined analysis by FC and HC provided the opportunity for a statistical test of the difference between counts made by the flow cytometer (FC) and haemocytometer (HC) of both viable cell number (*VCN*) and dead cell number (*DCN*) (Section 4.4.1). A similarly rigorous comparison could not be found in the literature.

3.3.2 Cell Viability with Calcein-AM and PI: Live or Dead

Samples were taken approximately every 24 h from the shake flask culture (Section 3.3.1) and stained with Calcein-AM/PI for analysis on the flow cytometer (FC) (Section 2.11.5). Three populations were revealed in each sample, stained with Calcein-AM, PI, or both stains (i.e., the dual stained population, DSP). This finding is entirely consistent with the findings of the control study in which cell death was induced by the toxin CCCP (Section 3.2.2), and shows that the light scattering and staining exhibited in that study is not restricted to induced cell death. Based on the results of CCCP induced cell death and staining with Calcein-AM/PI (Section 3.2.2), a preliminary conclusion was made that the DSP was very probably dead, perhaps recently so. Since this population also appeared in the shake flask culture it merits further discussion.

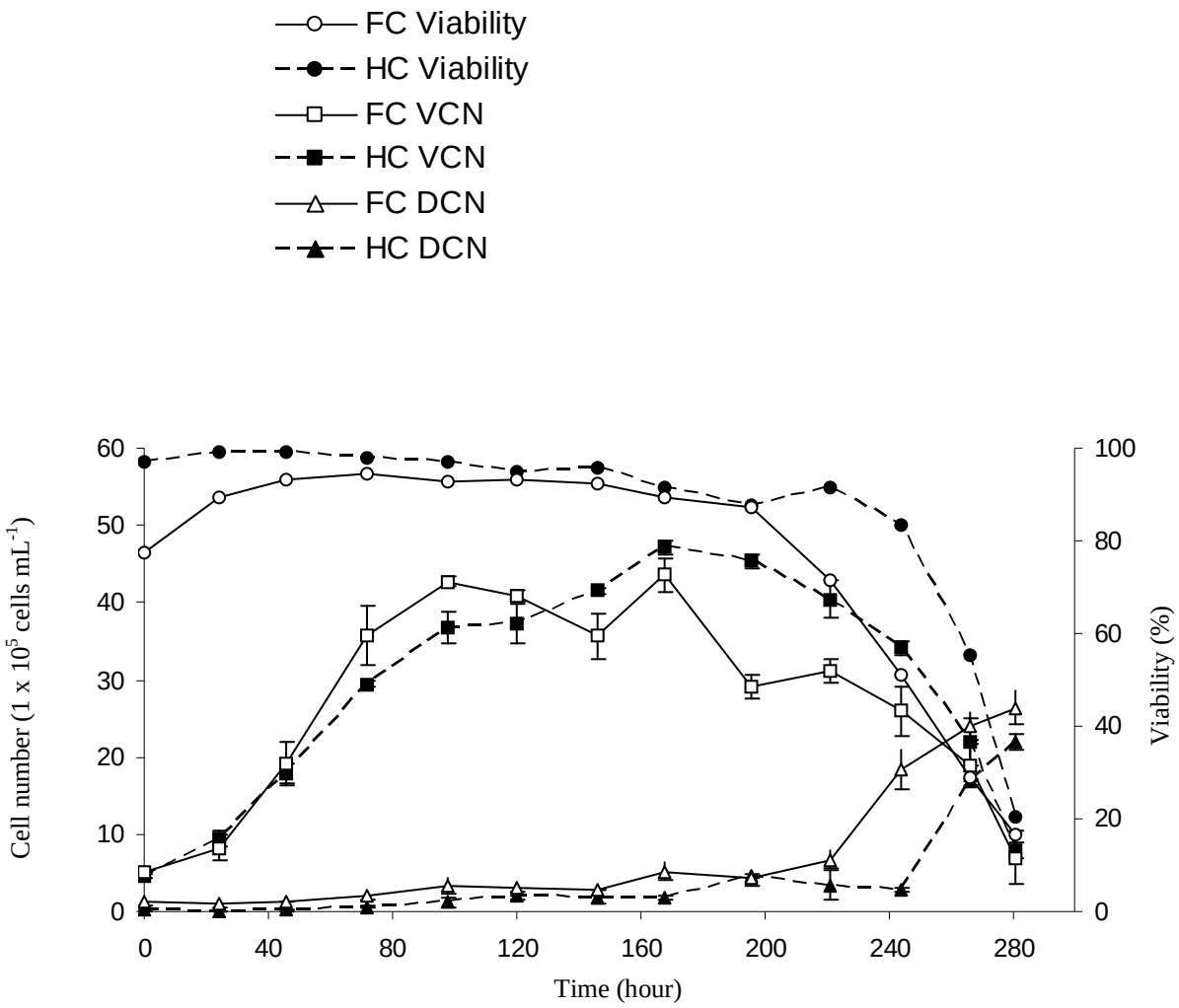

Figure 3-7: Growth curves of GS-CHO cell culture in a 2 L shake flask inoculated at 2 x 10^5 cells mL^{-1}. Comparison of flow cytometric (FC) ratiometric count method (Sections 2.11.4) with Calcein-AM/PI staining (Section 2.11.5) (solid line, open points) and haemocytometric (HC) Trypan Blue (TB) exclusion method (Section 2.10) (dashed line, closed points) for cell count and viability assessment: viable cell number (square), dead cell number (triangle) and viability (circle). Each time point is the average of two counts, error bars represent the data range of the duplicate samples.

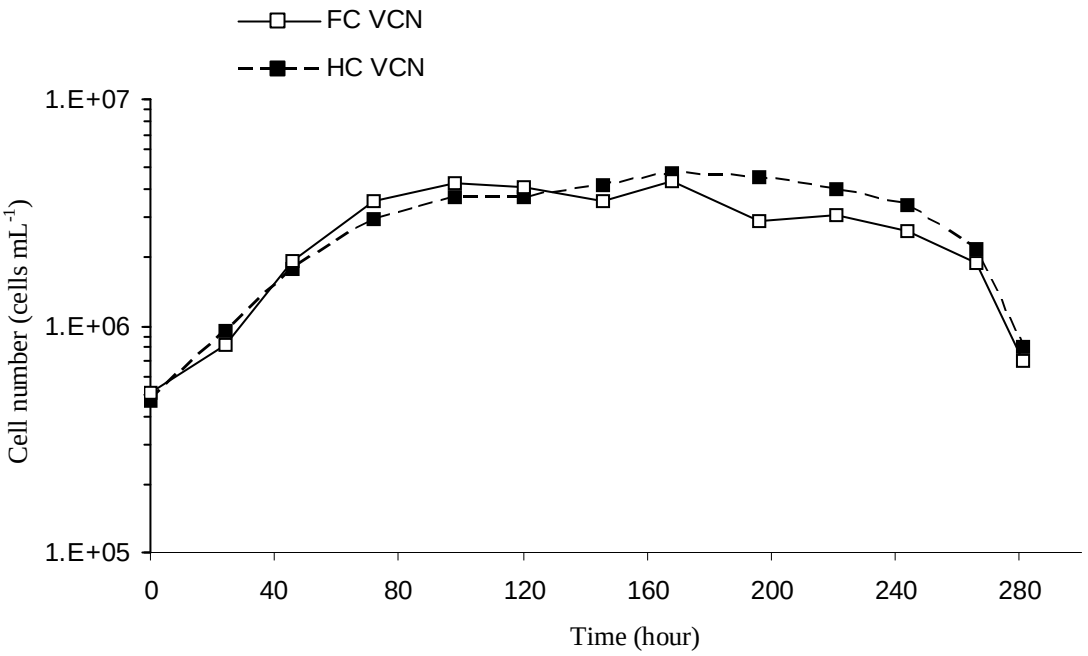

Figure 3-8: A logarithmic growth curve of GS-CHO cell culture in a 2 L shake flask inoculated at 2 x 10^5 cells mL^{-1}. Comparison of flow cytometric (FC) ratiometric count method (Section 2.11.4) with Calcein-AM/PI staining (Section 2.11.5) (solid line, open points) and haemocytometric (HC) Trypan Blue (TB) exclusion method (Section 2.10) (dashed line, closed points) for cell count and viability assessment, plotted with a logarithmic y-axis: viable cell number (square).

It is clear that the DSP, as a percentage of the combined *VCN* and *DCN*, the total cell number (*TCN*), did not increase significantly as the culture declined (Figure 3-10), but instead showed little variation throughout the culture, varying randomly around 4% ± 2% (mean ± standard deviation, N = 13). (Note: N is the number of independent samples). Three hypotheses conceivably explained the origins of this population (Section 3.2.2); allowing predictions of the expected variation of the DSP in a typical batch or fed-batch shake flask or STR culture. These predictions can now be tested.

If dual staining was the result of recent cell death in the STR then the percentage size of the DSP should have been almost zero in the early stages of the culture, when rate of death was very low. It should then have increased as the rate of cell death (r_d) increased from the stationary phase to the death phase. If a proportion of viable cells were more robust and maintained enzyme activity and slow Calcein leakage after death then the percentage size of the sub-population should have increased as the number of cell deaths increased. Since the sub-population was constant, these two hypotheses should be dismissed. Can it therefore be concluded that the DSP was composed of a sub-population of less robust viable cells that died during staining?

If the DSP represented a less robust proportion of viable cells that were present in the STR before sampling, staining and analysis, the proportion must have increased as viability decreased. Indeed, since the DSP, as a proportion of the total population size, exhibited little variation in spite of the decreased viable population (from which it would be drawn), the proportion of less robust cells would have to

have increased to a degree that matched the decrease in viability – this might reasonably be expected.

In a batch culture, viability typically decreases with culture duration, as accumulation of metabolites (Sections 3.5.3 and 3.5.4), primarily ammonia and lactate, and substrate limitation (e.g., glucose or glutamine limitation) increasingly inhibit cell growth and alter cell protein production (Rearick et al., 1981; Lao and Toth, 1997; Sun and Zhang, 2004; Chen and Harcum, 2005). It is entirely reasonable to propose that the same deleterious factors responsible for decreased percentage viability could have increased the proportion of less robust cells in those viable cells that remained. In this way, the DSP would remain constant.

In conclusion, sensitivity to factors that might cause cell death appears to be a variant amongst the viable cell population. Furthermore, the proportion of cells that exhibit such sensitivity can be expected to increase as conditions in the STR became increasingly deleterious for cell culture. Deleterious conditions are indicated by falling viability. The sensitivity of this sub-population was such that it was killed at some point during staining with Calcein-AM/PI and analysis with FC. If enzyme activity is assumed to have ceased immediately at the point of cell death, then the DSP must have been created after staining, to allow Calcein formation. If activity is assumed to have continued, then the DSP could have been created at any point after the sample was taken from the STR. In either case, FC analysis may be implicated in cell-death.

3.3.3 Cell Damage during Staining and Flow Cytometry

Flow cytometry (FC) could have resulted in the death of less robust viable cells in four ways: incubation, stain toxicity, stain's solvent toxicity and direct hydrodynamic or mechanical damage ('shear'); these will be discussed in turn.

As noted (Section 2.11.5), a 15 minute incubation period at 36.5^{o}C was recommended for optimal staining with the FC stains used in this study (Haugland, 2002). No such incubation was required for haemocytometry (HC). It is possible that during this incubation period a deleterious change in pH occurred. A deliberate shift in pH from 7.3 to above 8.5 decreased viability of GS-NS0 culture after 10 minutes (Osman et al., 2001). Note that alkali addition or CO_2 stripping by sparging the STR with an inert gas was very likely required to achieve such a high pH in their sodium bicarbonate buffered medium. A shift of this magnitude was unlikely in the incubated samples. In Osman et al. (2001), a shift to pH 6.5 decreased viability, but only after more than 600 minute. Since the pH in the culture studied here was already low (pH 6.8) from day 4, any shift in pH that accompanied transfer to the incubator would likely have been to increase pH, as some CO_2 may have been lost.

PI is a toxic mutagen, so too, for that matter, is TB (Haugland, 2002). These toxins are unlikely to have decreased *VCN*: nucleic stains are most harmful only when they enter the cell and interact with nucleic acid or nucleic acid metabolism (Pin et al., 2006), and the utility of PI and TB, of course, depends on their short-term inability to interact with and enter live cells. Calcein-AM has very low levels of toxicity (Jacopo et al., 2000; Haugland, 2002). Of course, the indicator for cell death is permeablisation of the cytoplasmic membrane to PI or TB, but at this point the

cell is no longer able to maintain an active metabolism and should not be induced to further degradation by toxins.

PI and TB were dissolved in phosphate buffer solution (PBS), which was likely benign, but Calcein-AM must be dissolved in an aprotic solvent, such as dimethyl sulfoxide (DMSO), which may be deleterious. To mitigate solvent toxicity, in this study less than 0.1% DMSO was used, as recommended (Haugland, 2002) and supported by the literature. Qi et al. (2008) found cell cultures were unharmed by 0.1-0.25% DMSO over 24 h, and Fiore and Degrassi (1999) actually used 1.5% DMSO to inhibit cell concentration dependent apoptosis in CHO cells. Furthermore, a review reports several studies in which DMSO concentrations below 1.0% did not interfere with results (Santos et al., 2003).

Cells are probably exposed to greater hydrodynamic forces during FC than HC: in FC, cells must be hydrodyamically focused for accurate arrival at the focal point of the laser; HC requires only pipette manipulation. Nevertheless, no reports of hydrodynamic damage caused by FC cell analysis could be found in the literature; damage attributed to FC is restricted to fluorescence activated cell sorting (FACS). Reportedly, during sorting (using a Becton, Dickinson and Company (BD) FACSVantage) cell viability was decreased by extensional forces created by the large pressure drop across the exit nozzle (Mollet et al., 2008). In this the study here, cells were analysed by light scattering from within the flow-cell: any hydrodynamic forces associated with the exit nozzle likely occurred downstream of assessment of viability. In conclusion, stain toxicity and hydrodynamic forces are unlikely to have created the DSP by killing less robust viable cells, but a pH change during incubation may have.

3.4 Culture Growth in a Fed-batch STR

The predominant means for the large-scale production of recombinant protein is the stirred tank reactor (STR) (Birch and Racher, 2006). For late stage process development, laboratory-scale and pilot-scale STR are required to create conditions that resemble those expected during production in a large-scale (~20 m^3) STR. Nevertheless, when biopharmaceutical companies develop a protein production process for transfer to large-scale, shake flask culture, because of its simplicity and low cost, is often used to conduct preliminary studies and to escalate cell numbers.

3.4.1 Comparison of STR and Shake Flask Cell Culture

Glutamine synthetase Chinese hamster ovary (GS-CHO) cell culture growth in duplicate 5 L fed-batch stirred tank bioreactors, STR, (Section 2.6) was monitored over a 20-day period. 2 mL samples were taken from each STR for immediate analysis on the flow cytometer (FC) and haemocytometer (HC) on average every 24 hours (h). FC and HC analysis methods were the same as those used for the shake flask (Section 3.3).

As earlier (Section 3.3.1), a comparison of FC and HC is concurrent to analysis of culture performance. Here culture performance in the shake flask and the STR are compared. Note two important differences between the culture methods: first, methionine sulfoximine (MSX) inhibition of the glutamine synthetase (GS) gene was not present in the STR, permitting antibody production, which did not occur in the shake flask, because MSX was present; second, the STR received a substrate feed to maintain glucose at between 3 and 6 gL^{-1}.

Viable cell number (*VCN*), dead cell number (*DCN*) and viability from FC and HC cell counts were very similar (Figure 3-11 and Figure 3-12). As in the shake

flask culture, there did not appear to be a significant difference between the two cell count methods. Nevertheless, cell counts from the two methods were compared using sufficient experiments for acceptable statistical analysis (Section 4.4.1). Growth followed three distinct phases, typical of cell culture: rapid growth, stationary phase and death phase (Figure 3-12). As in the shake flask, there was no obvious lag phase in cell growth.

Cells grew from the inoculation *VCN* of 2 x 10^5 cells mL^{-1} to a maximum viable cell number (*VCNmax*) of 93 ± 5 x 10^5 cells mL^{-1} (mean ± range of data, until otherwise stated) determined by FC (Figure 3-12) and correspondingly 80 ± 8 x 10^5 cells mL^{-1} determined by HC. This *VCNmax* is in accordance the expected growth of the GS-CHO cell line (Birch and Racher, 2006). *VCNmax* in the STR was ~50% greater than in the shake flask, and likely reflects the combined benefits of substrate feeding and effective control of the culture environment.

Culture duration, measured from inoculation until viability fell below 30%, increased from 280 h in the shake flask cultures to 480 h in the STR. Furthermore, rapid growth in the STR continued for 234 h, 160 h longer than in the shake flask, albeit at one third of the mean specific growth rate, μ. Much of the increased culture duration in the STR could be accounted for by the protracted rapid growth phase. In the rapid growth phase μ was 0.0144 h^{-1} by FC and 0.0147 h^{-1} by HC; doubling times, *td*, were 47 h and 48 h, respectively. These values are essentially the same for FC and HC. Thus, *td* in the rapid growth phase of the STR was almost twice the *td* in the rapid growth phase of the shake flask culture (25 h and 28 h) (Section 3.3.1).

Butler (2004a) state that *td* in animal cell culture is typically 24 h. In the literature, reported *td* for CHO and hybridoma cell culture could be found ranging

from 11 h to 39 h (Kurano et al., 1990a; Hayter et al., 1991; Hayter et al., 1992a; Ozturk et al., 1992; Godoy-Silva et al., 2009b). The almost halving of μ from the shake flask to the STR is likely to be explained by a crucial difference between the two experiments: methionine sulfoximine (MSX) was present only in the shake flask culture (Section 2.2). MSX inhibits the GS gene, which is responsible for antibody production as well as regulating glutamate synthesis. In the shake flask, antibody production was inhibited by MSX; in the STR, antibody production was considerable (Figure 3-20).

Thus, the low μ in the STR usefully demonstrates the significant burden of antibody production. Nevertheless, the influence of the substrate feed should also be considered. At the concentration range maintained in the STR, glucose has been found to decrease μ (Kurano et al., 1990a; Fieder et al., 1995; Takuma et al., 2007). However, the shake flask and STR used the same medium (with MSX added to the shake flask) and they therefore had the same initial glucose concentration (6 g L^{-1}). Furthermore, substrate feeding could not have altered growth until 96 h and in the shake flask *VCNmax* of ~ 40 x 10^5 cells mL^{-1} was reached after only 80 h; whereas in the STR after 80 h *VCN* was ~ 10 x 10^5 cells mL^{-1}.

In the stationary phase the *VCN* oscillated (Figure 3-11) in the same manner observed in the shake flask experiment, although in the STR cell counts using the HC also oscillated, unlike in the shake flask (Figure 3-7). The mean *VCN* during the stationary phase was 77 $\pm$ 9 x 10^5 cells mL^{-1} by FC, and 68 $\pm$ 7 x 10^5 cells mL^{-1} by HC.

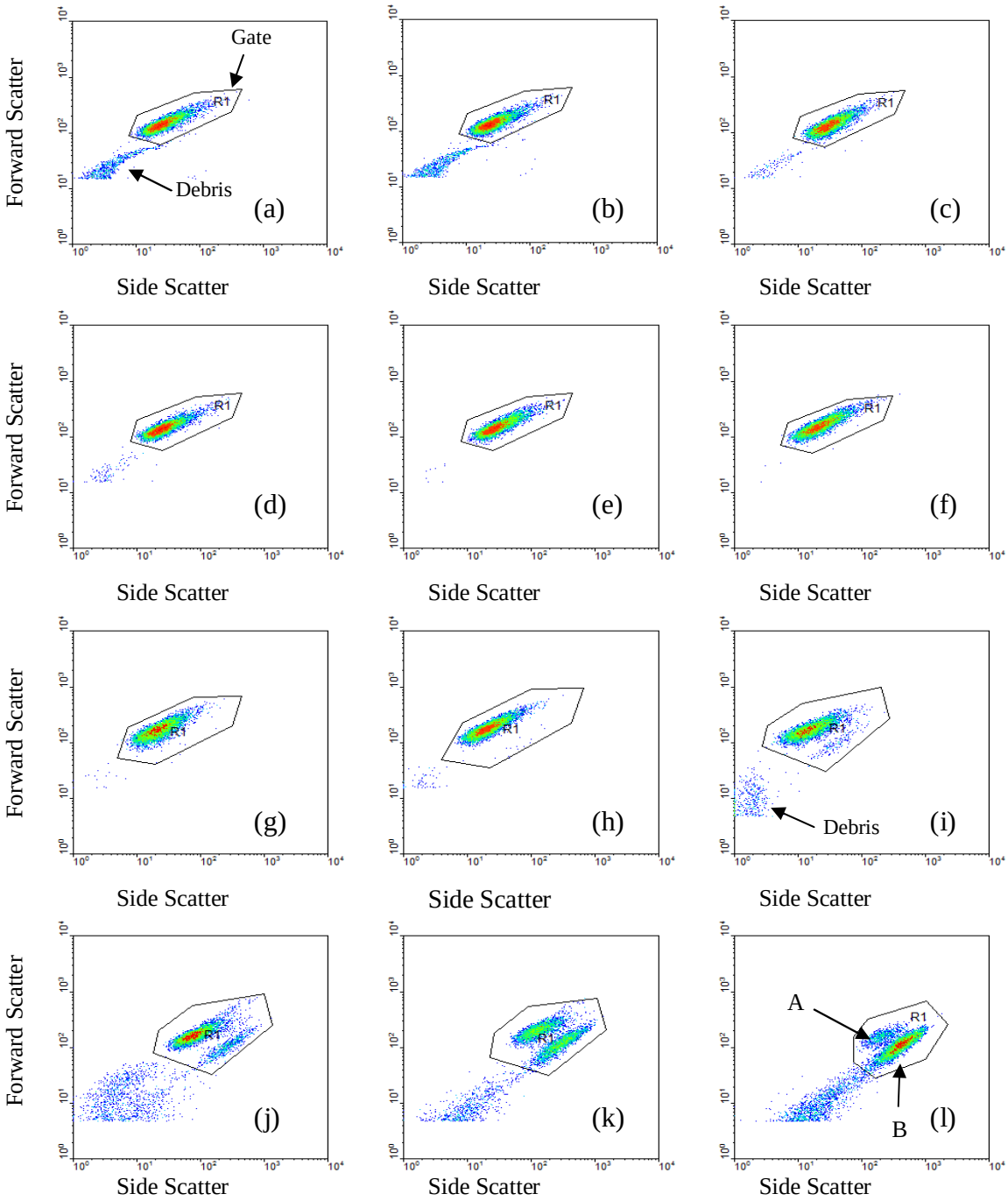

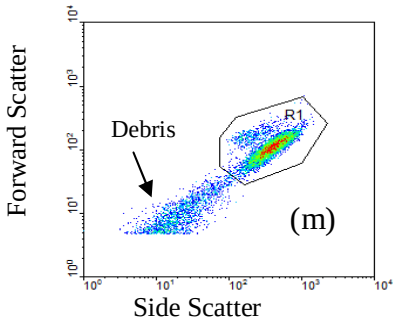

Figure 3-9: Shake flask growth data cytographs for GS-CHO cells stained with Calcein-AM/PI (50 nM and 3.7 µM, respectively) (Section 2.11.5). Forward scatter light v side scatter light (FS-SS): (a) 0 hour (h): inoculation; (b) 24 h; (c) 46 h; (d) 72 h; (e) 98 h; (f) 120 h; (g) 146 h; (h) 168 h; (i) 196 h; (j) 221 h; (k) 244 h; (l) 266 h; (m) 281 h. Population A and B, cytograph (l), are live and dead cell populations, respectively and correspond to populations A and B, cytograph (l), in Figure 3-10, showing Calcein-AM/PI staining.

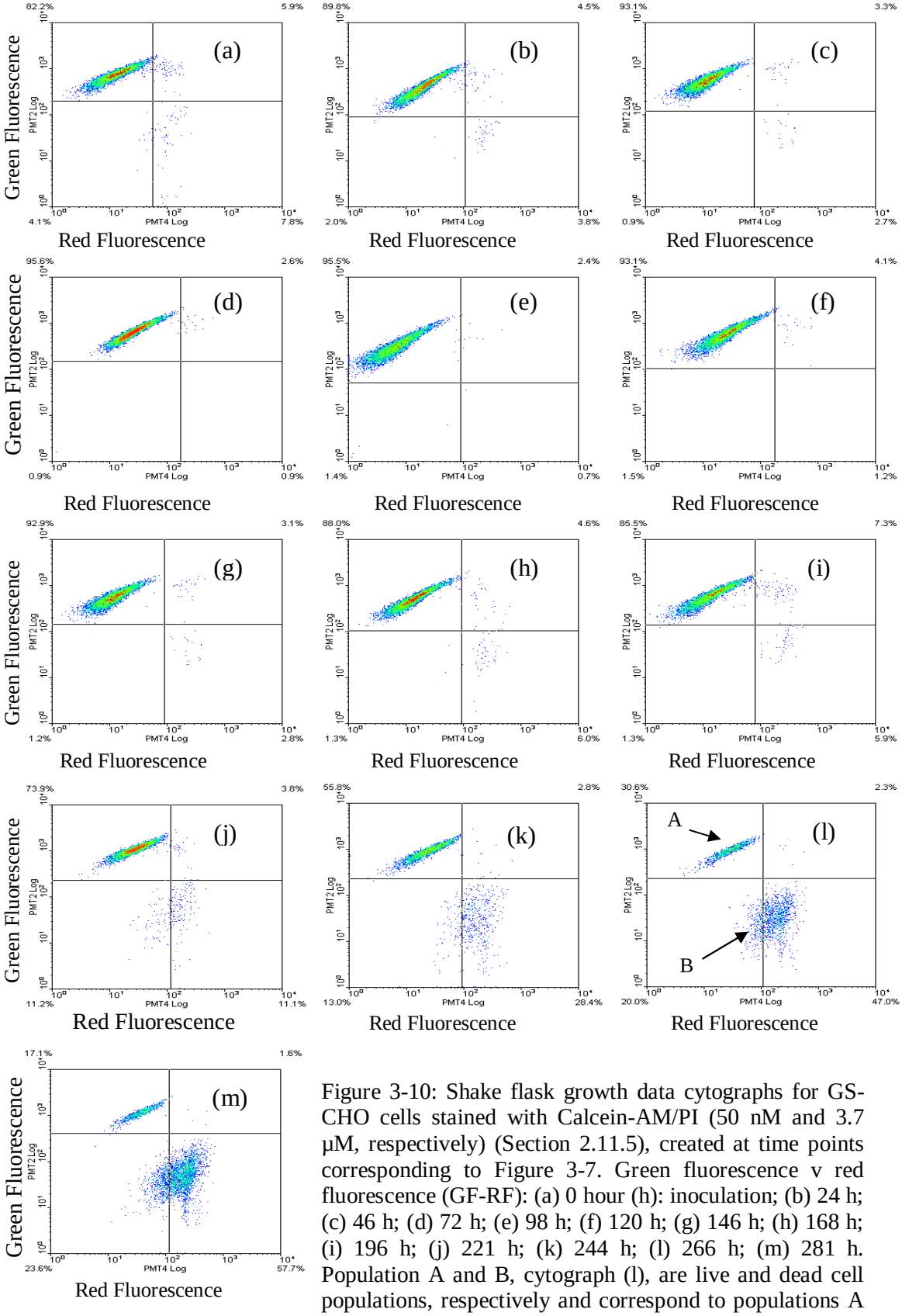

Figure 3-10: Shake flask growth data cytographs for GS-CHO cells stained with Calcein-AM/PI (50 nM and 3.7 µM, respectively) (Section 2.11.5), created at time points corresponding to Figure 3-7. Green fluorescence v red fluorescence (GF-RF): (a) 0 hour (h): inoculation; (b) 24 h; (c) 46 h; (d) 72 h; (e) 98 h; (f) 120 h; (g) 146 h; (h) 168 h; (i) 196 h; (j) 221 h; (k) 244 h; (l) 266 h; (m) 281 h. Population A and B, cytograph (l), are live and dead cell populations, respectively and correspond to populations A and B in Figure 3-9, showing forward scatter light v side scatter light properties of the cells.

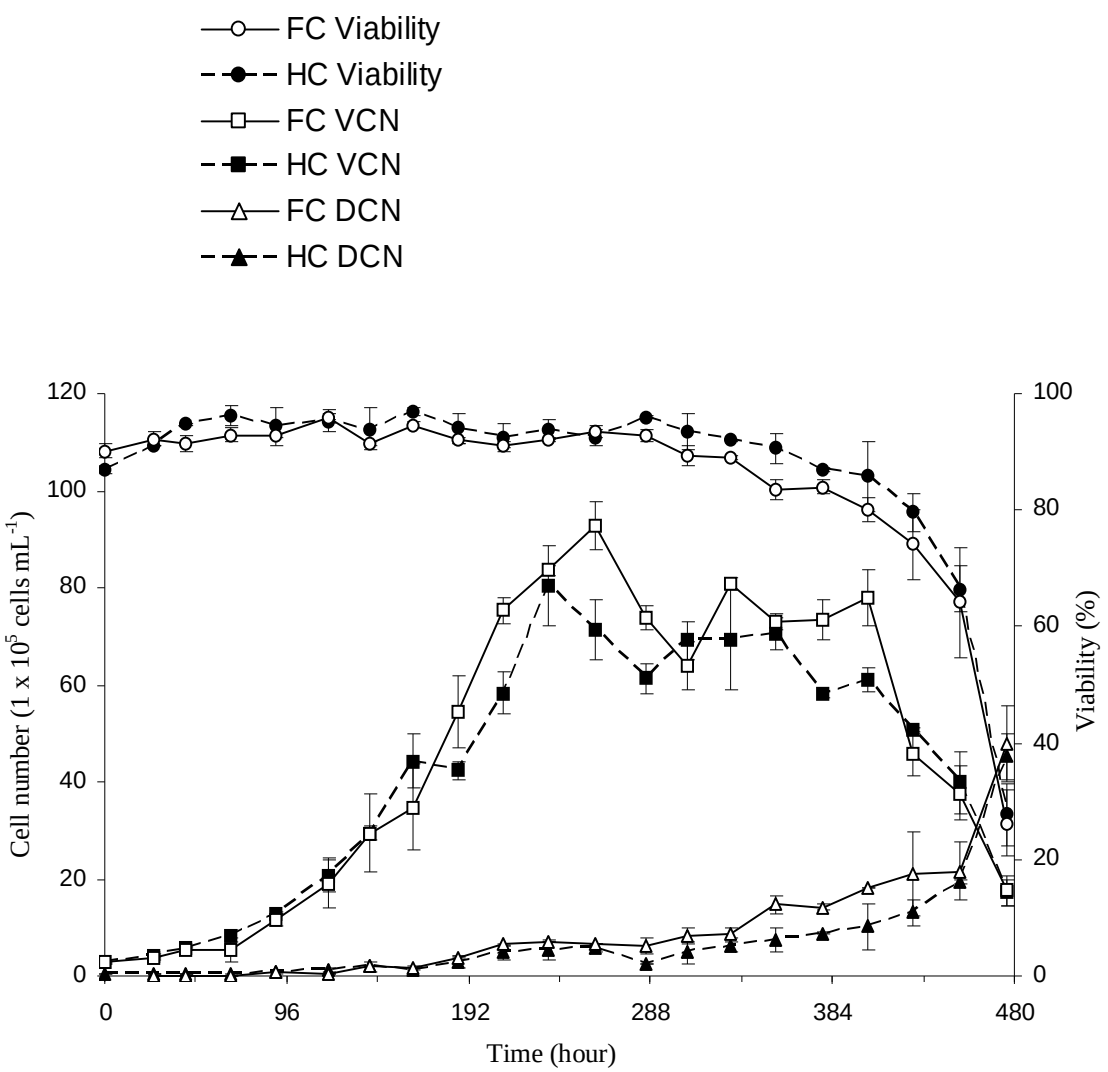

Figure 3-11: Growth curves of GS-CHO cell culture in a 5 L fed-batch stirred tank reactor (STR) with a 3 L medium volume ('working volume') inoculated at 2 x 10^5 cells mL^{-1} (Section 2.6): comparison of cell count and viability assessment by the flow cytometric method (Section 2.11.4) and haemocytometric method (Section 2.10). The flow cytometric method used the ratio of a standard concentration (1 x 10^6 beads mL^{-1}) of fluorescent beads to cells to provide a total cell number (*TCN*) (Section 2.11.4), and Calcein-AM/PI staining (50 nM and 3.7 µM, respectively) as a viability indicator (Section 2.11.5). Haemocytometry was conducted as a typical Trypan Blue (TB) exclusion method (Section 2.10). Flow cytometry: solid line, open points. Haemocytometry: dashed line, closed points. Viable cell number (*VCN*) (square), dead cell number (*DCN*) (triangle) and viability (circle). Each time point is the average of duplicate experiments, error bars represent the data range of the duplicate experiments.

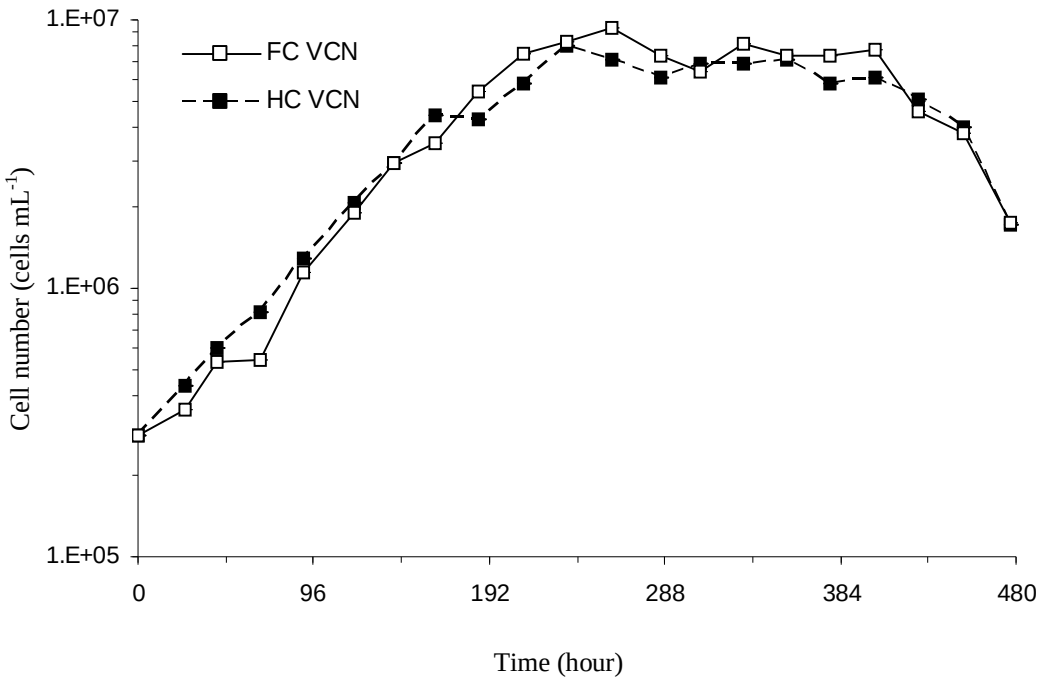

Figure 3-12: A comparison of viable cell number (*VCN*) (square) found by the flow cytometric method (solid line, open point) (Sections 2.11.4 and 2.11.5) and the haemocytometric method (dashed line) (Section 2.10). Refer to Figure 3-11, for original growth curves.

Clearly, both methods revealed a considerable fluctuation in *VCN* throughout the stationary phase. For the shake flask culture it was reasoned that cell death released nutrients into the medium, providing a stimulus and renewed growth to nutrient deprived cells. During a fed-batch culture, however, it is much less likely that cells became nutrient limited: typically, the limiting substrate is glucose, and by feeding this was continuously abundant (6 g L^{-1}). Nevertheless, is still possible that some nutrient deprivation was occurring. Note that perturbations in the *VCN* of a GS-CHO culture were recorded, but not explained, in the growth curve provided by Lonza (Birch, 2005), who own the rights to the cell line.

In accordance with the shake flask study, the percentage viability was, on average, lower when measured by FC than by HC: in the shake flask by 2 ± 4% (mean ± standard deviation, until otherwise stated) and in the STR by 3 ± 2% (Figure 3-11). The viability in the STR dropped below 90% after (by the FC method) 307 h, while in the shake flask this point is reached after 168 h. Almost all of this 139 h protraction is accounted for by extension of the rapid growth phase in the STR.

In conclusion, cell culture performance in the fed-batch STR was a considerable improvement on the performance in the batch shake flask. Transfer from shake flask to STR is not always associated with improved *VCN*, viability and antibody titre (Buchs and Zoels, 2001; Reyes et al., 2003), but the fundamental differences between the two vessels favour the attainment of optimal culture conditions in the STR.

3.4.2 Cell Viability with Calcein-AM and PI: Live or Dead

The FS-SS and corresponding GF-RF cytographs for analysis of the STR culture (Figure 3-13 and Figure 3-14) closely resemble those for the shake flask culture (Figure 3-9 and Figure 3-10). Throughout much of the culture, the GF-RF cytographs show that the cell population could be split into three populations: viable (Calcein positive, PI negative), dead (Calcein negative, PI positive) and dual stained (Calcein positive, PI positive). This reflects the same split as CCCP induced death (Section 3.2.2) and the shake flask (Section 3.3.1).

The DSP (as a percentage of the total population) remained constant at 3.5 ± 0.8% (mean ± standard deviation, N = 40) and was similar to the DSP found (4 ± 2) in the shake flask study (Section 3.3.2). Unlike that study, the number of independent samples, N, was greater than 30 and the 95% confidence interval could be found with acceptable reliability, giving a DSP of 3.5 ± 0.2% (mean ± 95% confidence interval). Thus, the DSP found in the STR supports the conclusions of that study (Section 3.3.2). Factors that could have caused less robust cells to stain during sampling and staining have been discussed (Section 3.3.3).

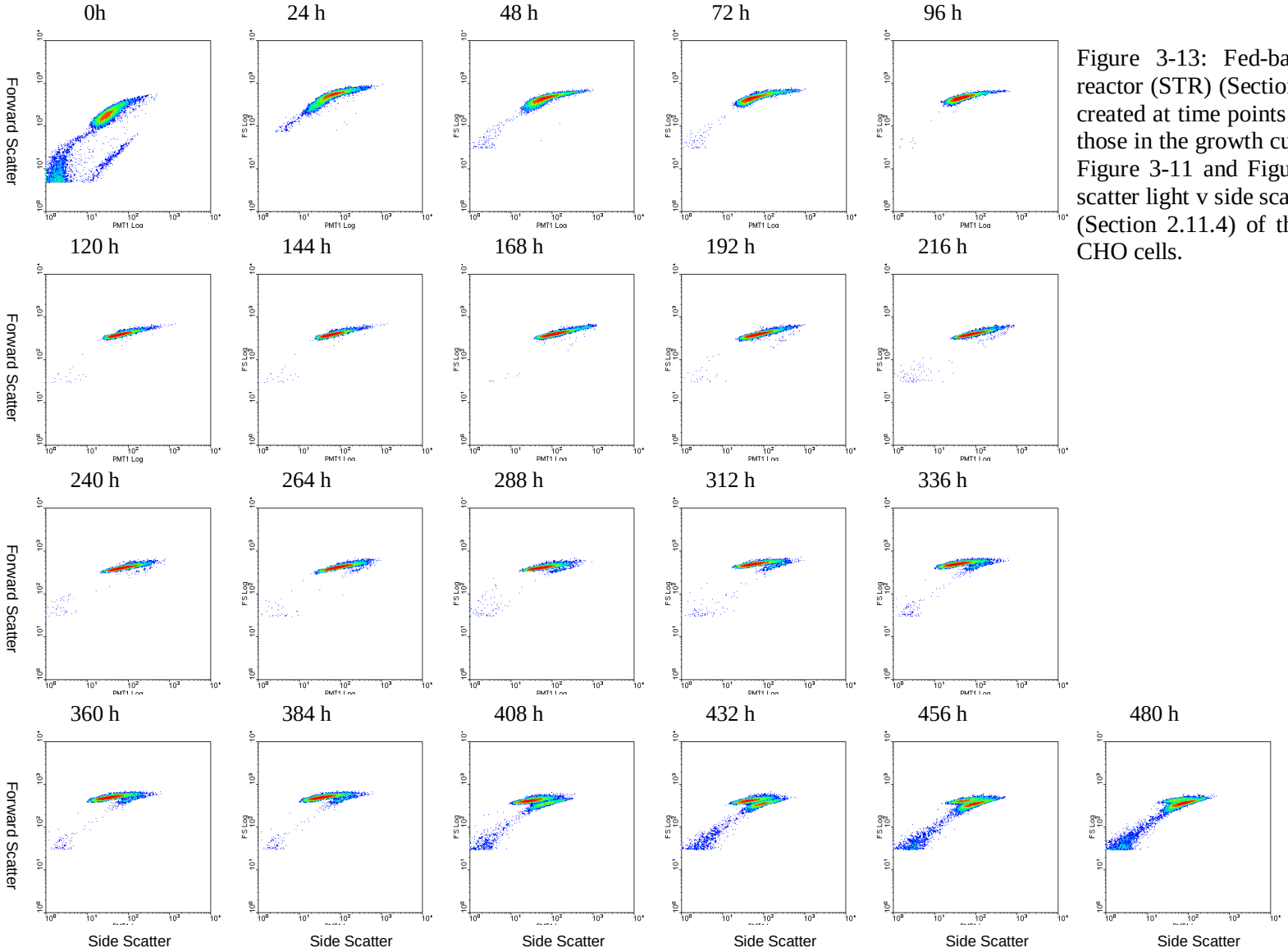

Figure 3-13: Fed-batch stirred tank reactor (STR) (Section 3.4) cytographs created at time points corresponding to those in the growth curves presented in Figure 3-11 and Figure 3-12: forward scatter light v side scatter light (FS-SS) (Section 2.11.4) of the unstained GS-CHO cells.

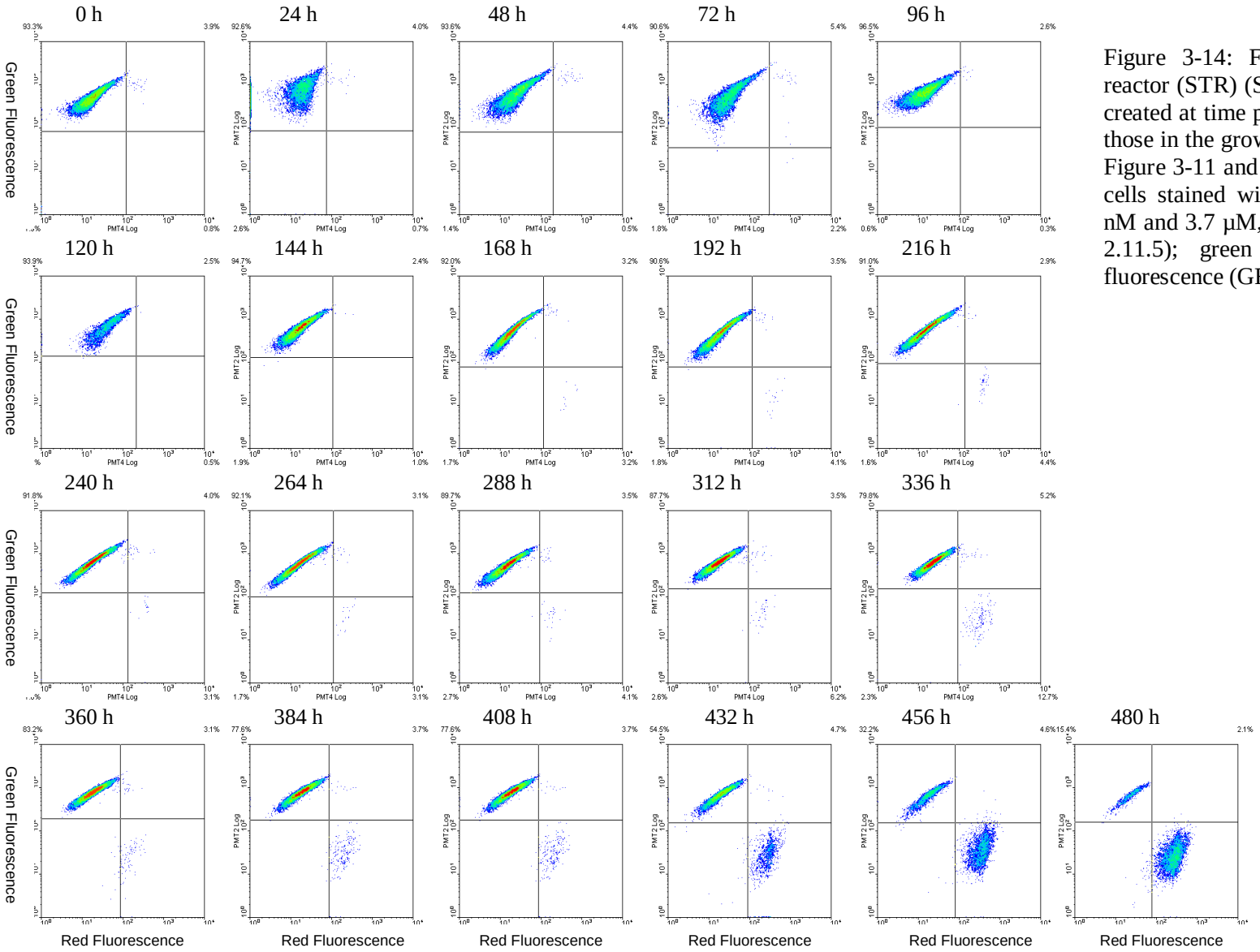

Figure 3-14: Fed-batch stirred tank reactor (STR) (Section 3.4) cytographs created at time points corresponding to those in the growth curves presented in Figure 3-11 and Figure 3-12: GS-CHO cells stained with Calcein-AM/PI (50 nM and 3.7 µM, respectively) (Section 2.11.5); green fluorescence v red fluorescence (GF- RF).

3.4.3 Mode of Cell Death with AV-PE/SG: Apoptosis or Necrosis

As in CCCP induced death (Section 3.2), no apoptotic population was present; cell death was by necrosis (Figure 3-15). This strongly supports a conclusion that cell death in this cell line is by necrosis alone (Section 3.2.1). The necrotic cell count was consistently higher than the *DCN* identified by HC and the Live/Dead FC method (Calcein-AM/PI); this was true of the control study and was discussed (Section 3.2.1), the same reasoning applies.

Unlike the control study, a significant second necrotic population was clearly visible from 120 h to 288 h (Figure 3-15, G). This population showed elevated red fluorescence (RF). RF should correlate with extent of staining with Annexin-V conjugated to Phycoerythrin (AV-PE). Note the transposition of phosphatidylserine (PS) from the cytoplasmic interior to the exterior of the intact cytoplasmic membrane is a key indicator of the apoptotic process, and is not thought to occur in necrotic cells (Darzynkiewicz et al., 1996; Ishaque, 2000). In necrotic cells, PS staining likely occurs when degradation of the cytoplasmic membrane allows the stain access to interior PS; further, severe degradation could feasibly displace sections of the cytoplasmic membrane to face the cell exterior. Therefore, greater AV-PE staining may indicate increased extent of cytoplasmic membrane rupture that allowed greater access of the stain AV-PE to PS. However, this need not be so: greater AV-PE staining could also occur in larger cells with more surface area of cytoplasmic membrane and (assuming constant density of PS per unit area of cytoplasmic membrane), therefore, more PS that would permit such larger cells to bind more AV-PE.

To differentiate between the two necrotic populations the lower RF population is referred to as ‘early necrotic’ and the higher RF as ‘late necrotic’, with RF indicative of PE-AV staining increasing from early to late necrotic.

Light scattering can be used as an indicator of cell size and internal ‘granularity’. Larger cells might exhibit greater FS. Heavily degraded cells might exhibit lower SS, having lost intracellular constituents from the disrupted cytoplasmic membrane. Light scattering properties of viable and necrotic cells have been discussed (Section 3.2.1).

When the late necrotic population was back gated to a FS-SS cytograph it exhibited the same light scattering characteristics as the cells with lower AV-PE staining (not shown). The equivalence of FS and SS between the two necrotic populations with differing levels of AV-PE staining does not provide evidence for a difference in cell membrane integrity or cell size that might explicate AV-PE between the two populations. However, light scattering properties have been shown to be an imprecise indicator of cells’ morphology (Section 3.2.1). It is certainly possible that further cytoplasmic membrane degradation did not result in any further change to the cells’ internal milieu, and, equally, that cell size was not accurately indicated by light scattering. In summary, elevated RF, as an indicator of elevated AV-PE staining, could be attributed to elevated cytoplasmic membrane degradation or larger cell size. Consideration should therefore be given to the mechanisms underlying the extent of cytoplasmic degradation and the size of cells. The culture environment could influence both.

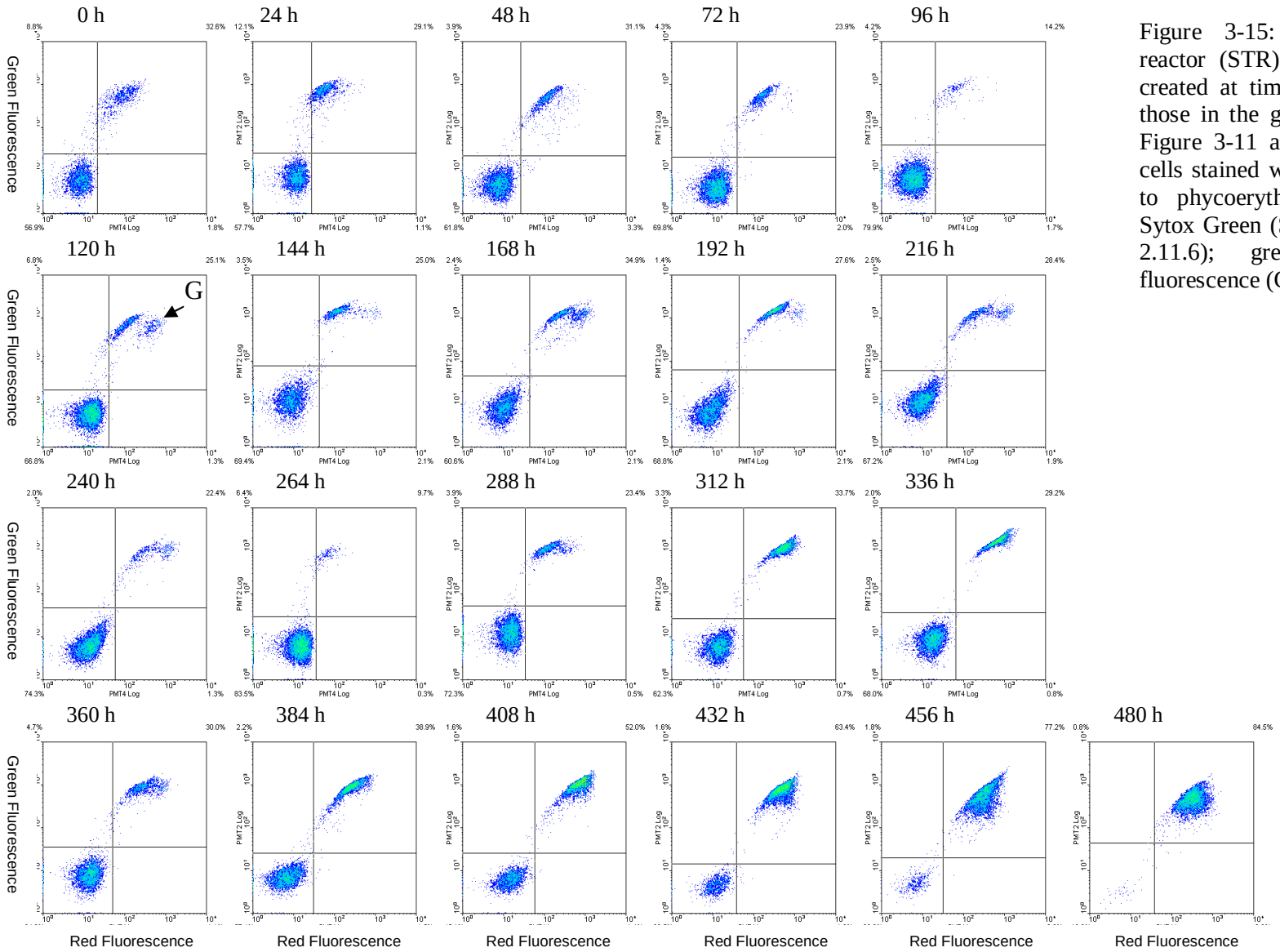

Figure 3-15: Fed-batch stirred tank reactor (STR) (Section 3.4) cytographs created at time points corresponding to those in the growth curves presented in Figure 3-11 and Figure 3-12: GS-CHO cells stained with Annexin V conjugated to phycoerythrin (AV-PE) used with Sytox Green (SG), (AV-PE/SG) (Section 2.11.6); green fluoresce v red fluorescence (GF-RF).

The late necrotic population was observed in the first sample taken from the STR after substrate feeding began at 96 h. This also coincided with the drop in pH from 7.1 to 6.8. (Note: pH was deliberately allowed to fall from 7.1 to 6.8 and was successfully controlled at 6.8 ± 0.1, Section 2.6). From 96 h to 120 h, the osmolality had also risen sharply from 325 mOsm kg^{-1} to 350 mOsm kg^{-1}, reaching a plateau of 375 mOsm kg^{-1} at 160 h. The population of dead cells revealed by Live/Dead cell count on the FC and HC was negligible at 120 h, when the 'late necrotic' sub-population first appeared. The disappearance of the 'early necrotic' population at 312 h corresponded to the beginning of a rapid decline in culture viability (Figure 3-12), at that point the necrotic population was singularly 'late necrotic'.

Since a sub-population of viable cells can be severely ruptured by the staining method, one might reasonably expect gross damage to occur to necrotic cells, which already exhibit membrane degradation; this process may explain the replacement of the 'early necrotic' with the 'late necrotic' population. The 'late necrotic' population could therefore provide an indicator of culture stress.

3.5 Cell Culture Data

3.5.1 Glucose and Glutamate

Glucose, as the primary carbon source for cell growth, and glutamate, the primary nitrogen source (Xie and Wang, 1994), were provided by a substrate feed. Feeding rate was controlled to maintain glucose between 3 and 6 g L^{-1}.

GS-CHO cells are able to utilise glutamate to produce their own glutamine (Zhang et al., 2006), and the substrate feed was glutamine free. Glutamine was not provided for two good reasons. First, cells without the strong expression of the GS transcript, which confers antibody production, will, it is hoped, be nitrogen limited when glutamine concentration is low; this should provide a selection pressure for productive cells even in absence of MSX, which is used to suppress endogenous glutamine synthetase activity during producer-cell selection. Second, glutamate feeding generally results in a lower ammonia concentration in the culture than glutamine feeding (Zhang et al., 2006). In cells without GS, glutamate is unlikely to support such high levels of growth (Capiaumont et al., 1995) and the GS transcript should confer a growth advantage in glutamine free medium.

Surplus glutamine was found to accumulate (Figure 3-16), in accordance with (Zhang et al., 2006). Although this removed selection bias for GS cells, it did not appear to be accompanied by loss of the GS transcript and proliferation of cells unburdened with antibody production, which would have been indicated by a fall in specific antibody production (*qIgG*) that was accompanied by increased μ. Thus, it is inferred that the cell line was stable, in accordance with a comprehensive study of GS-CHO stability by Porter et al. (2007).

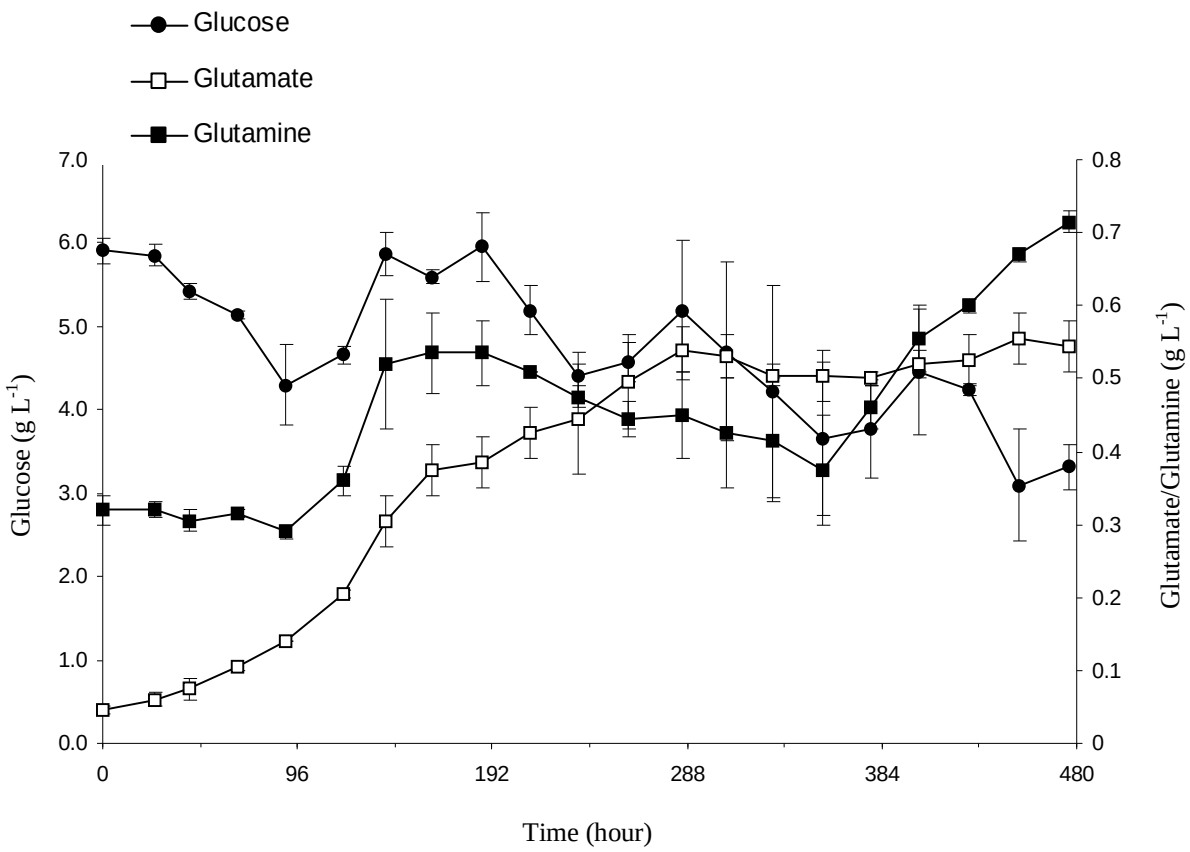

Figure 3-16: Glucose (solid circle) and Glutamate (solid square) were provided by a continuous nutrient feed to the fed-batch stirred tank reactor (STR) (Section 3.4) begun ~96 hours (h) after inoculation. Feed rate was based on the cell culture's specific growth rate (Figure 3-21). Glutamine (open square) is produced by GS-CHO. Each value is the average of duplicate experiments (Figure 3-11); error bars represent the data range of the duplicate experiments.

Feeding began after 96 h or when the viable cell number (*VCN*) reached 10 x 10^5 cells mL^{-1}, whichever was sooner. In this culture, feed was initiated at 96 h, which coincided with the *VCN* exceeding 10 x 10^5 cells mL^{-1}. When feeding began, it created an immediate rise in the levels of glucose and glutamate (Figure 3-16). Glucose consumption could not be measured during these STR runs because of equipment limitations. Glucose consumption has been found to correlate well with lactate production in mammalian cell culture (Hu et al., 1987). However, the lactate profile of this culture included a significant period of lactate consumption (Figure 3-17; Section 3.5.3); this type of metabolic behaviour remains to be elucidated and precludes an inferred estimate of glucose consumption.

As antibody production is allied to growth and is greatly decreased when the rapid growth phase ends (Section 3.6), glucose that was consumed in the stationary phase must have been required almost entirely for maintenance of cell homeostasis (Bailey and Ollis, 1986), referred to as maintenance energy. The increase in maintenance energy throughout the stationary phase likely reflects the increasing burden placed on the cell population by rising lactate, ammonia, and osmolality. Note that the change in glucose and glutamine concentration (Figure 3-16) is not a good indicator of consumption rate, because feed rate was altered every 24 h to maintain glucose at 3-6 g L^{-1}.

3.5.2 pH

The pH of the culture was controlled by the addition of a bicarbonate alkali (Section 2.6). The STR began at pH 7.1 and pH was allowed to gradually fall until it had reached pH 6.8, after ~100 h. For the remainder of the culture period the STR was controlled with alkali and CO_2 at pH 6.8 ± 0.1. There was no observed difficulty

controlling the culture within this dead-band (i.e., the pH did not oscillate markedly around the setpoint). The pH began to drop from 7.1 soon after the substrate feed commenced at 90.5 h, and by 120 h had reached pH 6.8. Being highly acidic (pH 2.5), the substrate feed was almost certainly implicated in the pH drop; it is likely that lactate accumulation until ~192 h also contributed greatly (Figure 3-17). It was noted that alkali was required to prevent the culture falling below pH 6.79; unfortunately, because of equipment limitations this could not be quantitatively recorded, substrate feed, lactate and alkali contributed to an increased medium osmolality (Figure 3-19).

A pH shift was created to optimise conditions for product titre and product quality. No obvious decrease in viable cell number (*VCN*) and viability were associated with the pH shift, implying that the rate at which pH fell was slow enough for cells to acclimatize. pH perturbations, such as a rapid drop (order of seconds or minutes) from pH 7.1 to pH 6.8, have been shown to decrease viability (Osman et al., 2001)

3.5.3 Lactate

Lactate and ammonia are the predominant metabolites of animal cell culture (Section 1.7.4.2). Lactate is a by-product of glycolytic glucose metabolism (Tsao et al., 2005). Lactate accumulation occurred from the beginning of the culture, rising to an initial peak value of ~2.5 g L^{-1} mid-way through the rapid growth phase (Figure 3-17). The specific rate of lactate production, *qLactate*, continued to fall throughout the rapid growth phase and was unaffected by the start of feeding from 96 h (Figure 3-18).

From about 200 h, 48 h before the end of the rapid growth, lactate concentration began to fall, falling rapidly less than 24 h before the stationary phase began, and reaching its lowest point of 0.0 g L^{-1} 48 h after the cell culture finished its rapid growth phase. Much of the lactate consumption period was accompanied by a stable ammonia concentration: either ammonia production had ceased or production and consumption were balanced (Figure 3-17).

After reaching a minimum at the end of the rapid growth phase, the lactate concentration then rose throughout the stationary and death phases, reaching a maximum stable value in the last 48 h of culture, 3.0 g L^{-1}, which corresponded to a period of rapid decline in cell viability and indicates that metabolism had ceased (accepting the unlikely possibility of increased metabolic efficiency at this stage). In CHO cell culture, lactate concentration has been observed to inhibit cell growth when above 5.22 g L^{-1} (58 mM) (Xing et al., 2008) and 5.4 g L^{-1} (60 mM) (Lao and Toth, 1997). The relatively modest lactate values reached (3.0 g L^{-1}) here were unlikely to have greatly inhibited cell growth directly, but by increasing osmolality may well have indirectly, as reported (Kurano et al., 1990a; Lao and Toth, 1997). Osmolality is discussed (Section 3.5.5).

qLactate was greatest at the beginning of the culture (~35 pg lactate $cell^{-1}$ h^{-1}) decreasing with time to a minimum at the start of the stationary phase (Figure 3-18); It then rose slowly by less than 10 pg lactate $cell^{-1}$ h^{-1} over the duration of the culture period. This trend is in accordance with CHO cell and hybridoma cell cultures found in the literature, as is the maximum and minimum *qLactate* (Kurano et al., 1990a; Hayter et al., 1991; Ljunggren and Haggstrom, 1994; Godoy-Silva et al., 2009b). Godoy-Silva et al. (2009b) observed a drop in *qLactate* throughout the

growth phase from a maximum value of 60 to a minimum of 30 in STR culture; Hayter et al. (1991), from 45 to 0 in shake flask culture. Similar values are reported for hybridoma culture (Ljunggren and Haggstrom, 1994).

In this culture, lactate accumulation was followed by a significant period of lactate consumption (Figure 3-17), similar to that observed by Tsao et al., 2005, although, unlike here, they did not not observe a significant resumption of lactate production after consumption. Tsao et al., 2005 observed that pH had a profound effect on lactate consumption in CHO cell culture experiments conducted at pH 7.4, 7.1 and 6.8. Lactate consumption was much at greater pH 6.8.

Here the lactate consumption period was concurrent with the transition from rapid growth phase to the stationary phase (Figure 3-12) and is shows astonishing congruence with the decline in specific antibody production rate (*qIgG*) and specific growth rate (μ) (Figure 3-20 and Figure 3-21). Lactate production resumed in the stationary phase and continued as viability fell.

Published reports of lactate consumption are few; nevertheless, it has been reported that consumption of lactate is an attribute of 'well performing industrial cell culture' (Mulukutla et al., 2010). This may be true, but, in accordance with the results seen here, Li et al., 2010 reported (in an oral paper) that a strong correlation is often seen between lactate depletion (later in culture duration) and acceleration of viability decline and productivity plateau and speculate that lactate feeding may benefit cultures where lactate is consumed after initial accumulation. Neither of these two groups attempt to explicate lactate consumption.

Lactate production, in industrial, glucose fed, cell culture, typically results from the high flux of glucose to pyruvate and supposed inefficient coupling between

glycolysis and the TCA cycle (Tsao et al., 2005). Aerobic lactate production is atypical for normal diploid cell strains; here it likely to be an attribute of the highly proliferative CHO cell strain, and is therefore akin to the Warburg effect reported in similarly rapacious cancer cells (Vaquez et al., 2010; Dang and Semenza, 1999; Warburg, 1930). Recent evidence that lactate is remetabolised as a prominent substrate for oxidative tumour growth invites further comparison with cancer cells (Sonveaux et al., 2008; Feron, 2009). Lactate consumption in industrial cell culture has received less attention and has generally been associated with depletion of the limiting substrate (usually, glucose) (Ozturk et al., 1992). If not to enable its consumption, glucose limitation is typically observed to decrease lactate production (Ljunggren and Haggstrom, 1994; Zhou et al., 1995; Europe et al., 2000). Altamirano et al. (2006) reported significant co-metabolism of lactate and galactose at limited levels of glucose.

In this study, however, glucose was maintained at between 3 and 6 g L^{-1}. A concentration considered amply sufficient. Limiting values in the literature are somewhat lower, reported for CHO at 0.22 g L^{-1} (1.22 mM) (Lu et al., 2005) and recombinant CHO (rCHO) at 1.08 g L^{-1} (6 mM) (Sun and Zhang, 2004); the elevated substrate consumption of rCHO is attributed to requirements of recombinant protein production. Efficient metabolism of glucose uses pyruvate for oxidative metabolism instead of inefficient glycolysis. If glucose limitation often results in its efficient utilisation and low lactate production, perhaps, in this case, an artificial glucose limitation occurred.

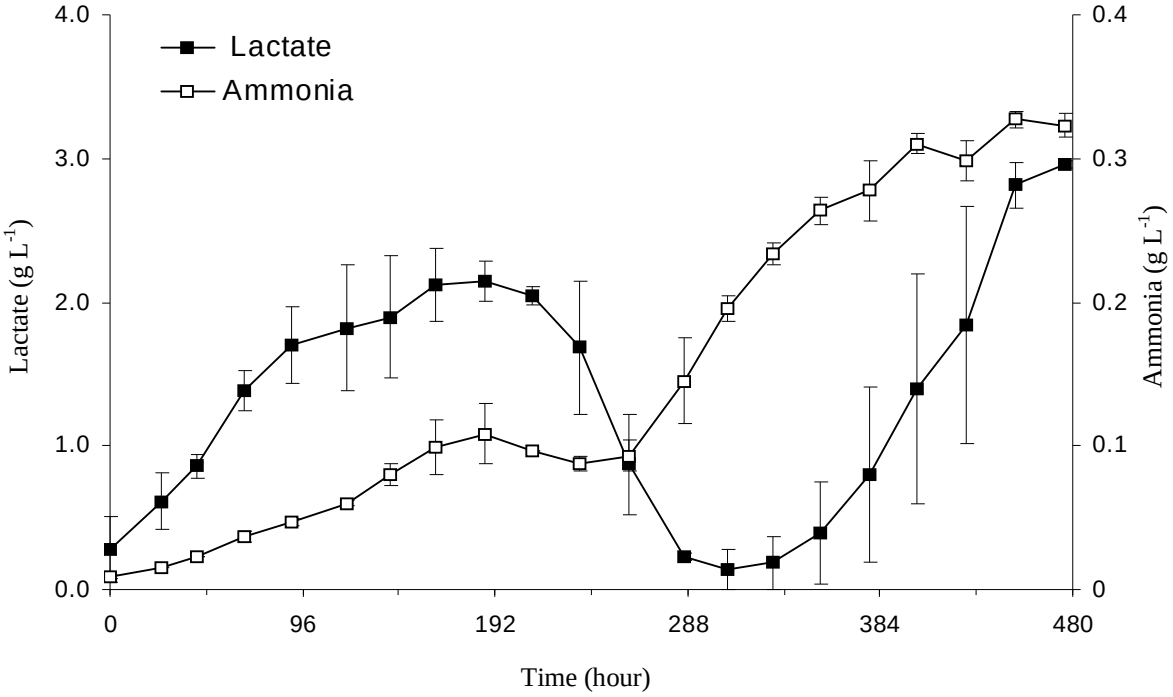

Figure 3-17: Concentrations of lactate (solid line, closed square) and ammonia (solid line, open square) in the fed-batch stirred tank reactor (STR) (Section 3.4) were found using a Bioprofile analyser (Section 2.12) . Each value is the average of duplicate experiments (Figure 3-11); error bars represent the data range of the duplicate experiments.

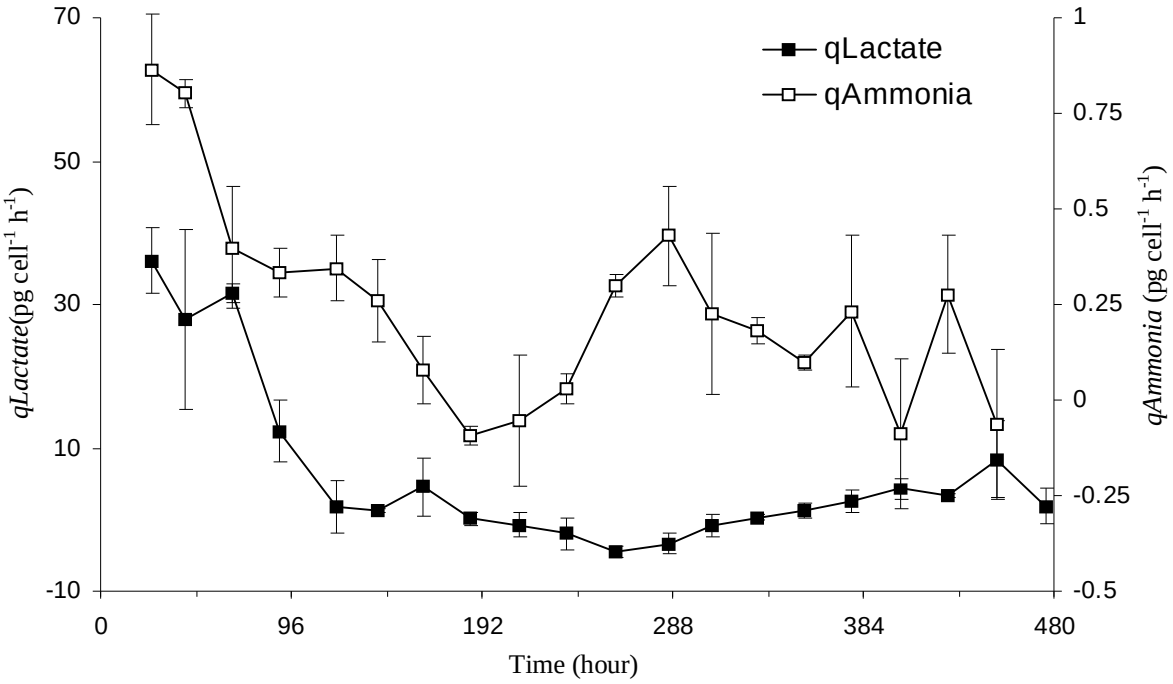

Figure 3-18: Specific rate of production for lactate, *qLactate*, (solid line, closed square) and ammonia, *qAmmonia*, (solid line, open square) in the fed-batch stirred tank reactor (STR). Each value is the average of duplicate experiments (Figure 3-11); error bars represent the data range of the duplicate experiments.

The maximum feasible rate of glucose transport into the cell or into the cell's mitochondria may have been insufficient to meet energy demand. Lactate consumption may thus have provided rapidly growing cells with an additional source of pyruvate for efficient oxidative generation of energy.

Lactate consumption may also have provided a means to increase NADH concentration towards a desired cytosolic $NADH/NAD^+$ redox state. Increased NADH is unlikely to have directly benefited proliferation, as its main role is a reducing agent for biosynthesis. The reported influence of extracellular pH (pHe) on cellular control of redox state (Shafer and Buettner, 2001) may help to explain the influence of pHe on lactate consumption, as observed by Tsao et al. (2005).

According to Le Chatelier's principle, low pH should have favoured the influx of weak acids, such as lactate. Thus, low culture pH may have provided a sufficient proton gradient across the cell membrane for the energetically favourable consumption of lactate. It is conceivable that glucose consumption was constrained by a fundamental thermodynamic limit on the maximum possible proton gradient across the mitochondrial membrane (Antinozzi et al., 2002). If this were the case, lactate consumption could have provided the reducing equivalents needed to restore or maintain a favourable redox environment at high rates of glucose oxidation.

On the one hand, lactate consumption may be indicative of the unmet nutrient demands. On the other hand, glycolytic activity, and lactate production, may be a prerequisite for a highly proliferative state of the cell culture, as is thought generally to be the case in cancer cells (Xu et al., 2005;Vazquez et al., 2010), which exhibit aerobic production of lactate (Warburg effect). Lactate consumption may therefore reflect, and have at its origin, the concomitant change from rapid growth to

a stationary phase – this is supported by the utility of lactate-derived NADH for biosynthesis and not growth. This could imply that insufficient reducing agents are available for biosynthesis. In both cases, the concurrent decline in *qIgG* and μ (Figure 3-21) may be remedied by lactate feeding, as suggested by Li et al., 2010.

Considering the possible importance of metabolism on product titre, a useful further study might investigate the influence of dichloroacetate (DCA) on such cell culture. As a treatment for lactic acidosis, DCA is reported to increase pyruvate dehydrogenase activity, improve glucose utilisation, and lactate oxidation (Stacpoole, 1983; Toth et al., 1993; Krishna et al., 1994). It is unknown how manipulation of the lactate metabolism would influence ammonia production, which ceased during the lactate consumption phase, implying a shift to glutamine metabolism.

3.5.4 Ammonia

Ammonia (NH_3) is a by-product, or metabolite, (Section 1.7.4.4) of the glutamate and glutamine metabolism (glutaminolysis), and is also produced by the thermal degradation of glutamine (Butler, 2004a). Throughout the growth phase of the culture, ammonia accumulated at a low rate until, after 160 h, it reached 0.09 g L^{-1} (5 mM). This ammonia concentration is reported to inhibit cell growth in CHO culture (Hayter et al., 1991; Yang and Butler, 2000; Xing et al., 2008), and is more than double a value reported to decrease cell viability and antibody productivity in, clearly less robust, hybridoma cells (Reuveny et al., 1986). Contrary to the literature, 0.09 g L^{-1} was attained halfway through the rapid growth phase and viability and μ remained stable.

It was probably a coincidence then that when the ammonia concentration reached an initial maximum and plateau at 0.09 g L^{-1} it then remained stable, with a slight decline, until the end of the rapid growth phase. At the beginning of the stationary phase, *VCN* began to oscillate (Figure 3-11) and the ammonia concentration once again began to increase (Figure 3-17). The ammonia concentration of 0.25 g L^{-1} at 360 h coincided with an abrupt decline in viability (Figure 3-11) and increase in osmolality (Figure 3-19). Before 360 h osmolality was stable and low, while lactate was rising but low. Thus, only ammonia was at a deleterious concentration when viability began to decline significantly. In the absence of other obvious deleterious factors, this drop in viability strongly suggests that ammonia accumulation was a key factor in the eventual rapid decline of the culture.

As noted (Section 3.5.3), the plateau and slight decline in ammonia concentration coincided with lactate consumption (Figure 3-17), beginning at approximately the same time (~192 h), but ending ~24 h earlier (~264 h). In GS-CHO cells, glutamine synthetase (GS) catalyses the condensation of ammonia and glutamate to form glutamine (Barnes et al., 2000) and the majority of ammonia was likely generated by metabolic hydrolysis of glutamine. Thus, the shift from ammonia production to a steady-state in this period implies either that glutamine hydrolysis to glutamate, and associated release of ammonia, did not occur or that hydrolysis continued and the ammonia was stored or metabolised. Glutamine is a valuable nitrogen and energy source (Newsholme et al., 2003a; Newsholme et al., 2003b) and its hydrolysis is likely to have continued even as μ and *qIgG* fell. Thus, the metabolism of ammonia, for elevated glutamine synthesis is in accordance with

the nutrient deprivation hypothesis mooted for lactate consumption, but because glutamine is often a source of carbon for the tricarboxylic acid cycle (TCA) and nitrogen for biosynthesis, such speculation does not clarify the utility of the metabolic shift for the cells in culture. It is clear that a potentially desirable shift in cell metabolism is concomitant with certainly undesirable shift in cell growth and productivity kinetics; the order of cause and effect remains to be elucidated.

3.5.5 Osmolality

Compared to levels of metabolites (Sections 3.5.3 and 3.5.4), osmolality (Section 1.7.2) was relatively stable until 360 h (Figure 3-19). It rose from 300 mOsm kg^{-1} at inoculation to an initial peak of 400 mOsm kg^{-1} at 160 h. The osmolality first began to rise markedly at about 96 h, in parallel with substrate feeding to maintain glucose and a requirement for alkali to maintain pH at the new setpoint of 6.8 (from 7.1). Rising lactate production associated with glucose consumption probably provided a significant contribution to osmolality, as indicated by the simultaneous peak in lactate concentration and osmolality. The osmolality then fell, as lactate fell, to ~375 mOsm kg^{-1}, remaining stable at ~375 mOsm kg^{-1} until the death phase. After 360 h, as the culture entered the death phase, the osmolality was likely elevated by rising metabolites (lactate, ammonia and glutamine), substrate concentrations, and the alkali required to control the culture's pH.

Osmolality is reported both to have inhibited cell growth and increased specific antibody production (Ozturk and Palsson, 1990; Ozturk et al., 1992; Kimura and Miller, 1996; Kim and Lee, 2002; Schmelzer and Miller, 2002; de Zengotia et al., 2002). A large study on inhibitory threshold values reported that inhibition of CHO cell growth did not begin until 382 mOsm kg^{-1} (Xing et al., 2008). Therefore,

the osmolality reached before the death phase may have shortened the rapid growth phase, but was unlikely to have significantly decreased cell viability.

Elevation in osmolality from 316 to 450 mOsm kg^{-1} has been found to decrease μ by 60% (Kimura and Miller, 1996; Zhu et al., 2005). Similarly, a 50% decrease in viability was found when osmolality was increased from 320 to 450 mOsm kg^{-1} (de Zengotia et al., 2002). Thus, the increase in osmolality from 375 at 360 h to over 500 mOsm kg^{-1} at the end of this culture is likely to have contributed greatly to rapid culture decline. In summary, osmolality did not appear to precipitate decline of the culture; rather, it closely followed decline and likely eventually attributed to the demise.

3.6 Fed-Batch STR Productivity: IgG Antibody Production

The specific immunoglobulin G antibody productivity (*qIgG*) rose to a peak of ~1.5 pg $cell^{-1}$ h^{-1} at ~119 h (Figure 3-21), in the middle of the rapid growth phase. This lag in production was probably the result of the cells' adjustment to antibody production: MSX, which inhibited GS transcription in the shake flask (Section 3.4.2) and STR inoculum cultures, was no longer present in the STR culture. At the end of the rapid growth phase, the culture had reached a peak of 820 mg mL^{-1} (rounded to 3 significant figures, 3.s.f., here and elsewhere). Antibody titre slowly increased throughout the stationary phase to a maximum of 1020 mg mL^{-1} by the beginning of the death phase. Antibody production ceased when the death phase began.

The specific rate of antibody production, *qIgG*, and the maximum antibody titre (Figure 3-20 and Figure 3-21) were in accordance with those values provided by Lonza for GS-CHO (Birch and Racher, 2006). Here, it is clear that *qIgG* was associated with μ (Figure 3-21). Indeed ~80% of antibody production occurred in

the first 160 h. The decline in *qIgG* and μ was matched by a decline in metabolic activity, as indicated by diminished *qLactate* and *qAmmonia* (Figure 3-18). Growth associated antibody production, seen here, correlates well with the literature for antibody production in CHO cell culture (Hayter et al., 1991; Chen et al., 2001; Godoy-Silva et al., 2009b).

Nevertheless, the abrupt decline in *qIgG* that occurred at the end of the rapid growth phase was not in accordance with the growth and antibody productivity reported for GS-CHO by Birch and Racher (2006). They observed a continuous linear increase in antibody titre from the beginning of the rapid growth phase and continuing throughout much of the stationary phase. However, it is evident from the contradictory reports in the literature that antibody production and its relationship to cell growth can vary with cell line. For example, there are several reports of antibody production – in hybridoma cells, at least – asserting that production was restricted to the G1 and S phases of the cell cycle (Mccormick et al., 1984; Al-Rubeai and Emery, 1990; Amos et al., 1992; Kromenaker and Srienc, 1994), yet this restriction was not universally observed (Hayter et al., 1992b), and was clearly not present in this GS-CHO cell line. It is concluded that antibody production of this GS-CHO cell line was strongly allied to cell growth, following classic Luedeking-Piret (Luedeking and Piret, 1959) production kinetics. There is insufficient evidence to conclude that the decline in cell growth and commensurate decline in productivity were precipitated by a metabolic shift (perhaps caused by unmet nutrient demands) that resulted in lactate consumption (Section 3.5.3) and quiescence of ammonia production (Section 3.5.4).

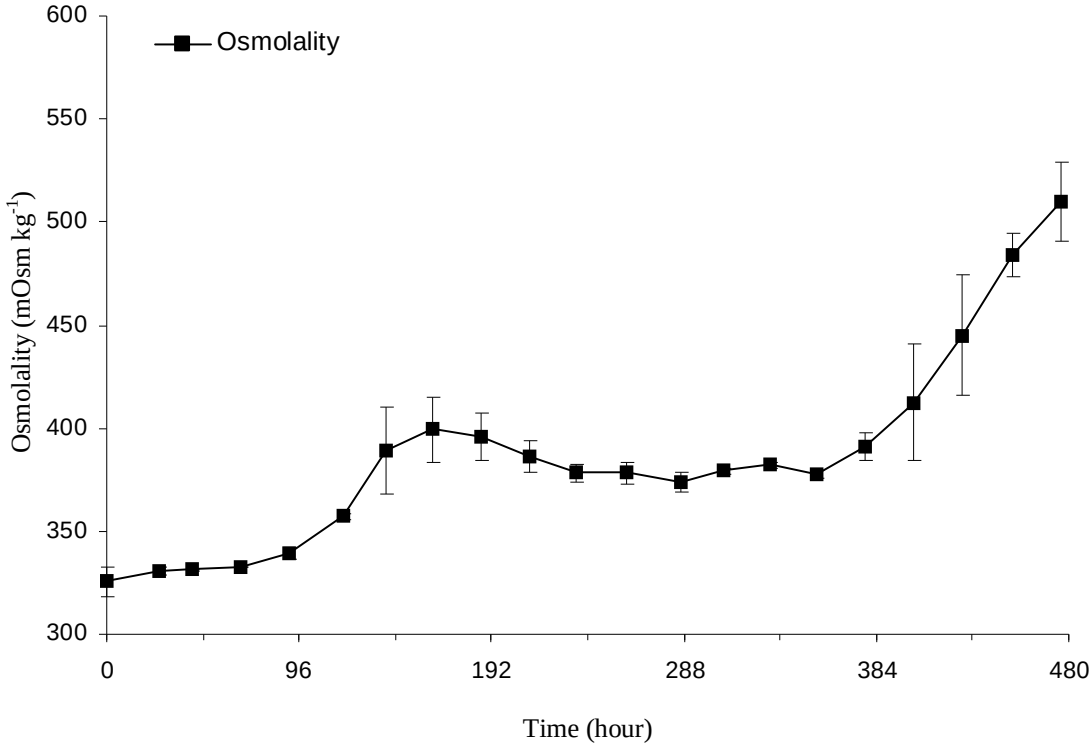

Figure 3-19: Medium osmolality in the fed-batch stirred tank reactor (STR) (Section 3.4) was found using a Bioprofile analyser (Section 2.12). Each value is the average of duplicate experiments (Figure 3-11); error bars represent the data range of the duplicate experiments.

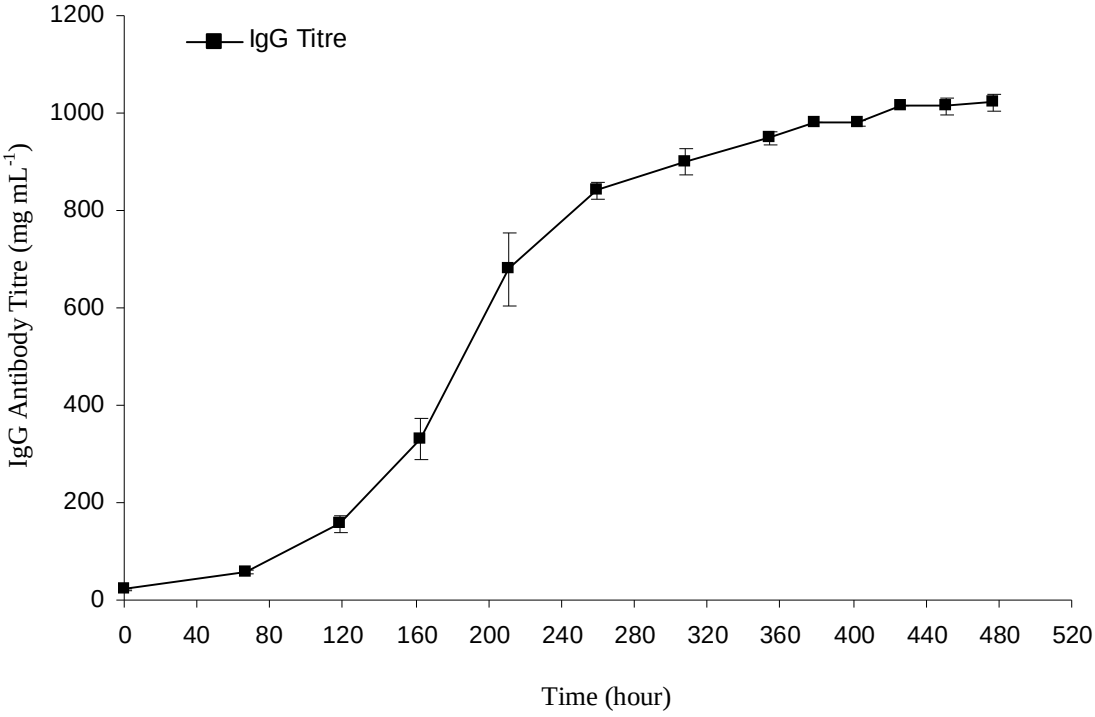

Figure 3-20: IgG antibody titre (Section 2.13) for in the fed-batch stirred tank reactor (STR) (Section 3.4). Each value is the average of duplicate experiments (Figure 3-11); error bars represent the data range of the duplicate experiments.

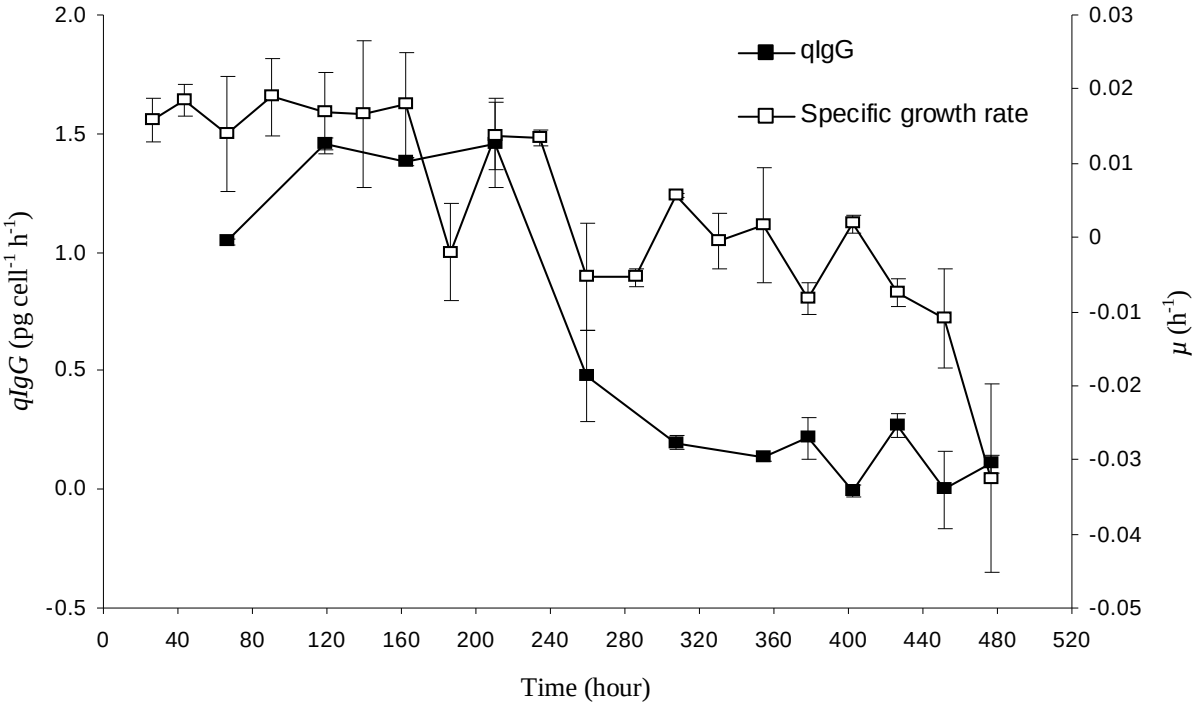

Figure 3-21: Specific rate of antibody production, *qIgG*, (solid line, closed square) and specific growth rate, μ, (dashed line, open square) for GS-CHO culture in a fed-batch bioreactor. Each value is the average of duplicate experiments (Figure 3-11); error bars represent the data range of the duplicate experiments.

Chapter 4: Results and Discussion of Scale-Down

4.1 Introduction

By seeking to create perturbations that were of similar magnitude and frequency to those in a large-scale vessel, this study differs in two important aspects from the only other known study of mammalian cell culture using a two-compartment scale-down system (Osman et al., 2002). Firstly, it differs in the volume of the second compartment, representative of the feed zone. In this study, the volume of the plug flow reactor (PFR) was chosen as 5% of the volume of the laboratory-scale stirred tank reactor (STR). Five percent represents the expected relative volume of the feed zone in a large-scale stirred tank reactor STR. Osman et al. (2002) chose a seemingly arbitrary 17% of the STR volume. They do not specify why this percentage was chosen. The inflexibility of the STR+STR model (because glass STR are made in standard sizes, and are expensive to have made bespoke) suggests that 17% was fixed by vessel constraints, and not entirely by consideration of large-scale heterogeneity. Secondly, it differs in the timing of perturbations: Osman et al. (2002) created perturbations with a predefined regularity. Whereas in this study, perturbations in pH were possible every time that alkali was required for pH control, like the addition zone of a large-scale STR (Section 1.5).

4.2 Design of Scale-Down Experiments

In such a model, PFR volume, *V*, is selected to be proportional to the approximate size of the concentration plume when an addition to the large-scale reactor is first made. The volumetric flow rate, *Q*, is then manipulated so that the mean residence time, *RT*, within the PFR is equal to the large-scale mixing time, θ_m. Assuming plug flow, the PFR is designed thus:

$$\theta_{\mathrm{m}} = 5.9\left(\varepsilon_T\right)^{-1/3}\left(D/T\right)^{-1/3}T^{2/3} \qquad \textbf{4-1}$$

$$RT = \theta_{\mathrm{m}} \qquad \textbf{4-2}$$

$$RT = \frac{V}{Q_R} \qquad \textbf{4-3}$$

Based on earlier estimates of the volume of the region of elevated concentration after feeding (feed zone) in a large-scale STR, the volume of the PFR used for this study was 5% of the laboratory-scale STR volume (Namdev and Thompson, 1992; Bylund et al., 1999; Amanullah et al., 2001; Hewitt and Nebe-Von-Caron, 2001). The PFR was therefore 150 mL for the 3 L STR (Section 2.7).

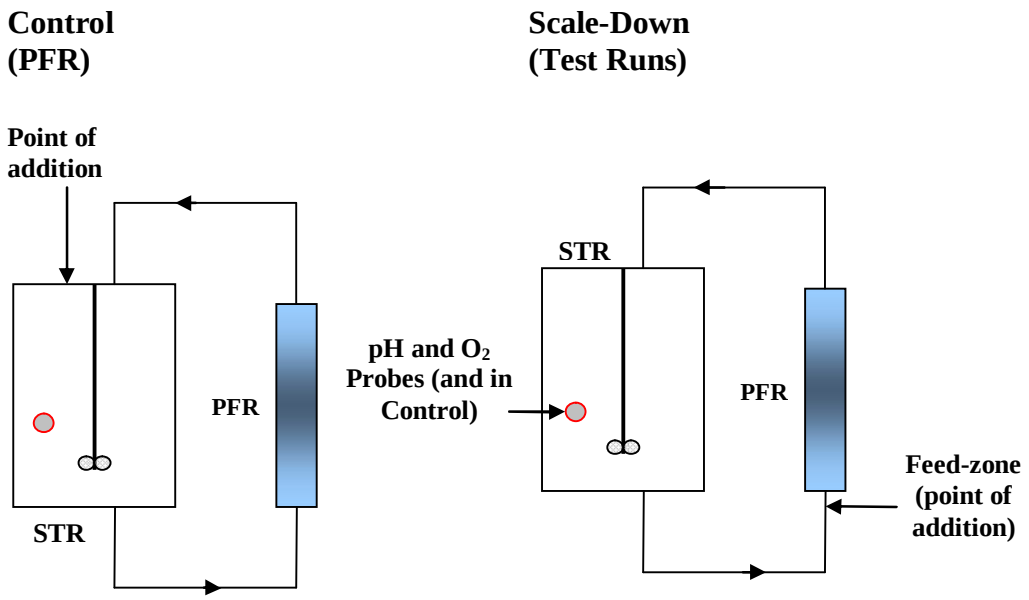

Figure 4-1: Schematic of the control experiment and test case experiments. Showing a 150 mL plug flow reactor (PFR) made from a length of platinum cured silicone tubing (1.98 m length, 9.8 mm internal diameter and 1.6 mm wall thickness). In the control, additions were made only to the 5L stirred tank reactor (STR) (3 L working volume) (Section 2.7.1). In the test case, additions were made only to the entry point of the PFR (Section 2.7). For both control and test cases, recirculation from the STR through the PFR was continuous from day 0 and at a fixed flow-rate of either 150 or 75 mL min^{-1}, creating a mean residence time in the PFR (*RT*) of 60 or 120 seconds (s).

4.3 Characterisation of PFR

RT s	Q mL min^{-1}	Maximum estimated drop in *DOT*[a] %	Maximum estimated drop in glucose[b] %	ε_{max} in PFR tubing[c] W kg^{-1}	ε_{max} in the STR[d] W kg^{-1}
60	150	17	0.3	0.04	1
120	75	35	0.15	0.009	1

Table 4-1: Flow characteristics of the plug flow reactor (PFR). Sample calculations are provided (Sections 4.3.1– 4.3.4).

4.3.1 Maximum estimated drop in *DOT*

Based on the assumption of plug flow (radial mixing, but not axial mixing), the maximum drop in *DOT* (*ΔDOT*) created by cellular consumption of oxygen in the PFR is calculated thus:

$$Oxygen\,Consumption = \left(OUR \times VCN\max \times RT\right) \qquad \textbf{4-4}$$

$$\Delta DOT = \left(\frac{Oxygen\,Consumed}{DOT\ saturation}\right) \times 100 \qquad \textbf{4-5}$$

Where *OUR*, specific oxygen uptake rate, is assumed to be 3 x 10^{-13} mol O_2 cells^{-1} h^{-1} (Nienow and Langheinrich, 1996), tubing is assumed to be impermeable to oxygen, *VCNmax*, the maximum viable cell number, is assumed to be 100 x 10^5 cells mL^{-1} and *RT* is equal to 60 s.

$$Oxygen\,Consumption = \left(\left(\frac{3\times10^{-13}}{3600}\right)\times100\times10^{5}\times60\right)$$

$$Oxygen\,Consumption = 5\,x10^{-8}\ mol\ O_2$$

$$\Delta DOT = \left(\frac{5\times10^{-8}}{2.9\times10^{-7}}\right)\times100$$

$$\Delta DOT = 17\%\ saturation$$

The *ΔDOT* is calculated using the *DOT* of water at 37°C saturated with O_2 from air sparged into the STR at atmospheric pressure. In all experiments in this study, the *DOT* in the STR was 30% of air saturation (%); thus, the initial *DOT* of medium entering the PFR was assumed to be at 30%, and a *ΔDOT* greater than 30% might be expected to result in oxygen limitation.

4.3.2 Maximum estimated drop in Glucose

Using the same assumption of plug flow, the maximum estimated percentage drop in glucose in the PFR (*ΔGluc*) can, likewise, be calculated:

$$Glucose\,Consumption = \left(GUR \times VCN \times RT\right) \qquad \textbf{4-6}$$

$$\Delta Gluc = \left(\frac{Glucose\,Consumption}{Glucose\,Feed\,Concentration}\right) \times 100 \qquad \textbf{4-7}$$

Where *GUR*, glucose uptake rate, is assumed to be 54 pg glucose $cell^{-1}$ h^{-1} (Hayter et al., 1991), *VCNmax* is the assumed to be 100 x 10^5 cells mL^{-1} and *RT* is the expected mean *RT* for cells in PFR.

$$Glucose\,Consumption = \left(\left(\frac{5.4 \times 10^{-11}}{3600}\right) \times 100 \times 10^5 \times 60\right)$$

$$Glucose\,Consumption = 9 \times 10^{-6}\ g\ mL^{-1}$$

The percentage drop in glucose concentration, *ΔGluc*, is calculated using the glucose concentration of the medium, which was maintained at 0.006 g mL^{-1} (6 g L^{-1}) by feeding (Section 2.6).

$$\Delta Gluc = \left(\frac{9 \times 10^{-6}}{6 \times 10^{-3}}\right) \times 100$$

$$\Delta Gluc = 0.15\%$$

4.3.3 Maximum Energy Dissipation Rate in the PFR

Flow is the PFR and connecting tubing was found to be in the laminar flow regime (Section 4.3) and $E_{\max,pipe}$, W m^{-3}, which occurs at the walls of the tubing, can therefore be calculated according to Equation (8) in Mollet et al. (2004):

$$E_{\max,pipe} = \mu\left(\frac{16Q^2}{\pi^2 R^6}\right) \qquad \textbf{4-8}$$

Division by density, ρ, (1000 kg m^{-3}) changes the units from W m^{-3} to W kg^{-1}, giving the following equation:

$$\varepsilon_{\max,pipe} = \nu\left(\frac{16Q^2}{\pi^2 R^6}\right) \qquad \textbf{4-9}$$

where ν, kinematic viscosity of the medium, was 1 x 10^{-6} m^{2}s^{-1} (assumed to equal to water). Q (m^3 s^{-1}) in the PFR was 150 mL min^{-1} (2.5 x 10^{-6} m^3 s^{-1}) and 75 mL min^{-1} (1.25 x 10^{-6} m^3 s^{-1}) for retention times of 60 s and 120 s, respectively. R, radius of the pipe, was 3.2 mm for connection tubing, and 4.8 mm for the PFR. $\varepsilon_{\max,pipe}$ was generated in the connection tubing, as it had the smaller radius.

$$\varepsilon_{\max,pipe} = 1\times10^{-6}\left(\frac{16\times\left(\frac{150}{60}\times10^{-6}\right)^2}{3.141^2\left(3.2\times10^{-3}\right)^6}\right)$$

$$\varepsilon_{\max,pipe} = 1\times10^{-6}\left(\frac{1\times10^{-10}}{1.06\times10^{-14}}\right)$$

$$\varepsilon_{\max,pipe} = 0.009\ W\ kg^{-1}$$

4.3.4 Maximum Energy Dissipation Rate in the STR

Calculated according to equations for power input, *P*, and energy dissipation in a STR (Equations 1-3 and 1-4 in Section 1.7), using the impeller diameter, *D*, and agitation rate, *N* (Section 2.6).

$$P = Po\rho N^3 D^5 \qquad \textbf{4-10}$$

$$P = 1.8 \times 1000 \times \left(\frac{200}{60}\right)^3 0.055^5$$

$$P = 0.034\ W$$

$$\left(\bar{\varepsilon}_T\right)_{bulk} = \frac{P}{\rho V} \qquad \textbf{4-11}$$

$$\left(\bar{\varepsilon}_T\right)_{bulk} = \frac{0.034}{1000 \times 0.003}$$

$$\left(\bar{\varepsilon}_T\right)_{bulk} = 0.011 Wkg^{-1}$$

$(\varepsilon_T)_{\mathrm{Im}ax}$ is based on the assumption that $(\varepsilon_T)_{\mathrm{Im}ax}$ = 100 x $(\bar{\varepsilon}_T)_{bulk}$ (Section 1.5). This is one of the larger estimates reported in the literature (Section 1.5) and the resulting $\left(\varepsilon_T\right)_{\mathrm{Im}ax}$ should not be considered conservative. In any case, these factors are generally unreliable as they critically depend on the volume chosen for the 'impeller region' (Section 1.5).

$$\left(\varepsilon_T\right)_{\mathrm{Im}ax} \approx \left(\bar{\varepsilon}_T\right)_{bulk} \times 100 \qquad \textbf{4-12}$$

$$\left(\varepsilon_T\right)_{\mathrm{Im}ax} \approx 1 Wkg^{-1}$$

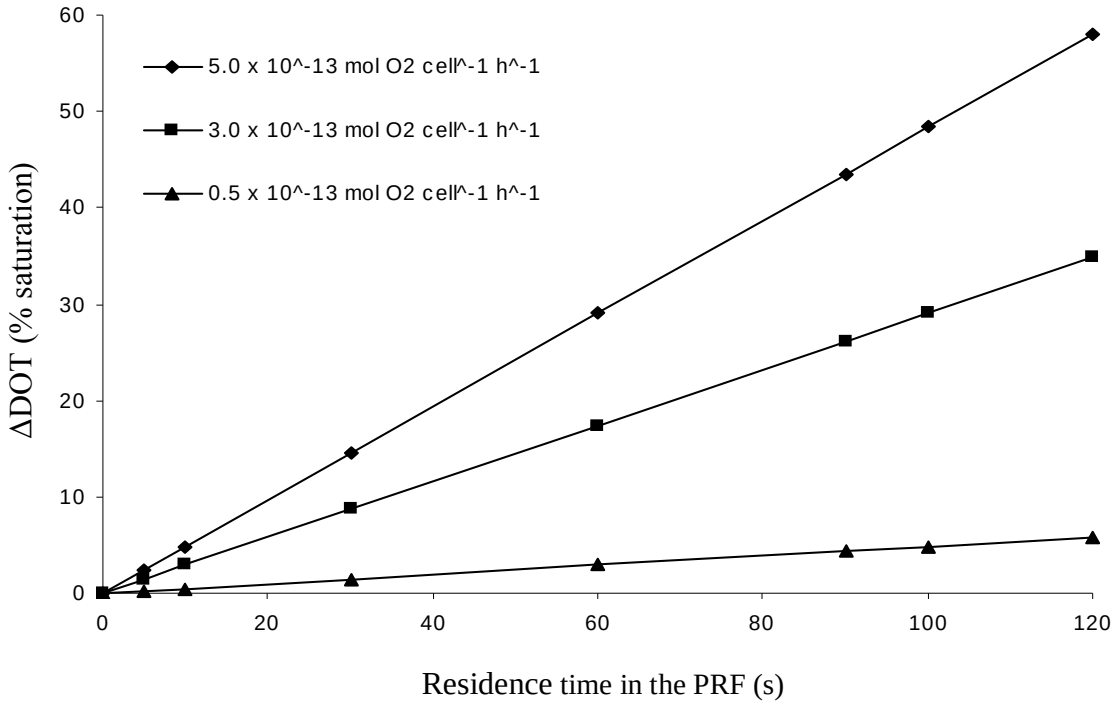

Figure 4-2: Δ*DOT* v *RT* (drop in dissolved oxygen tension v mean residence time in the plug flow reactor). The three curves represent the range of oxygen uptake rate (*OUR)* values found in the literature: 0.5 x 10^{-13} mol O_2 $cells^{-1}$ h^{-1} (triangle) (Fleischaker and Sinskey, 1981), 3 x 10^{-13} mol O_2 $cell^{-1}$ h^{-1} (square) (Nienow and Langheinrich, 1996; Ducommun et al., 2000; Deshpande and Heinzle, 2004) and 5 x 10^{-13} mol O_2 $cells^{-1}$ h^{-1} (diamond) (Fleischaker and Sinskey, 1981). Δ*DOT* was calculated assuming a viable cell number (*VCN*) of 100 x 10^5 cells mL^{-1} (*VCNmax* observed in this study was 93.5 x 10^5 cells mL^{-1}).

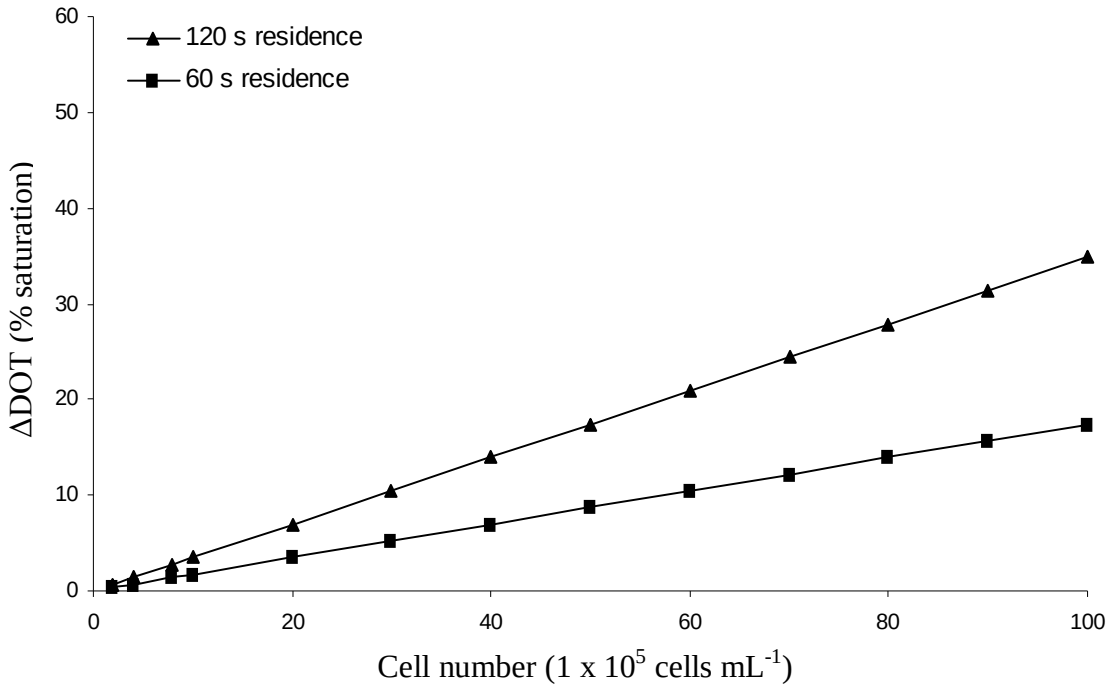

Figure 4-3: Δ*DOT* v *VCN* (drop in dissolved oxygen tension v viable cell number). 60 second (s) mean residence time (*RT*) in the plug flow reactor (PFR) (square); 120 s residence (triangle). *DOT* was calculated assuming an oxygen uptake rate (*OUR)* of 5 x 10^{-13} mol O_2 $cells^{-1}$ h^{-1}, the highest value found in the literature (Fleischaker and Sinskey, 1981). O_2 depletion (Δ*DOT* of 30% saturation) may occur at *VCN* above 170 x 10^5 cells mL^{-1} after a 60 s residence and *VCN* above 86 x 10^5 cells mL^{-1} after a 120 s residence**.**

4.4 Results and Discussion

4.4.1 Comparison of Flow Cytometer and Haemocytometer

12 stirred tank reactor (STR) experiments (6 duplicates) were conducted (Section 2.7); haemocytometry (HC) and flow cytometry (FC) were both used to count viable, dead and total cell number (*VCN*, *DCN* and *TCN*) (Sections 2.10 and 2.11). To compare the two count methods, the difference between the *VCN*, *DCN*, *TCN* and Viability for each time point in each STR was calculated by taking the HC value from the FC value (e.g., $\Delta VCN = VCN$ FC - VCN HC); this gave 229 values for the difference in *VCN* and *DCN* between the two methods. A statistical test (Shapiro Wilk W test) for goodness of fit to the normal distribution showed that the values for ΔVCN, ΔDCN, ΔTCN (ΔTCN = $\Delta VCN + \Delta DCN$) and $\Delta Viability$ were insufficiently normal to allow usage of a t-test for hypothesis testing. For data that are not normally distributed non-parametric methods such as the Wilcoxon signed rank test used here can provide a valid hypothesis test. With a null hypothesis that the mean difference (Δ) between the two count methods was zero (Ho = 0), the results of the test strongly support the following assertions: that, on average, throughout all of the experiments, the *TCN* was significantly greater when measured by flow cytometry ($p < 0.05$); that no significant difference between the two methods existed for *VCN* ($p > 0.05$); that the *DCN* was significantly greater when measured by flow cytometry ($p < 0.05$) (Table 4-2). The equivalence of the mean ΔTCN (9 ± 12) (expressed as mean ± standard deviation, unless otherwise stated) and the mean ΔDNC (7 ± 9) and the low mean ΔVCN (1 ± 10) strongly supports the conclusion that an elevated count of dead cells is responsible for the greater *TCN* given by flow cytometry.

	Δ*VCN*	Δ*DCN*	ΔTCN	ΔViability
	(1 x 10^5 cells mL^{-1})			(%)
Mean	1	7	9	-7
Std Dev	10	9	12	10
Std Err Mean	1	1	1	1
Upper 95% Mean	2	8	10	-6
Lower 95% Mean	0	6	7	-8
Number of values (N)	229	229	224	229
Hypothesized Value (Ho)	0	0	0	0
Actual Estimate (Ha)	1	7	9	-7
Degrees of Freedom	228	228	223	228
Test Statistic (Rank)	1463	11176	9171	-11307
Prob > |t|	0.1402	0.0001	0.0001	0.0001
Prob > t	0.0701	0.0001	0.0001	1
Prob < t	0.9299	1	1	0.0001

Table 4-2: Calculation of the mean difference between cell counts made using flow cytometry (FC) and haemocytometry (HC), showing the difference between counts of the viable cell number (*VCN*), dead cell number (*DCN*) and total cell number (*TCN*). Δ*VCN* = *VCN* FC – *VCN* HC. Non-parametric statistical analysis (Wilcoxon Signed Rank Test) was required because the distribution was not sufficiently normal for the familiar t-test. Rejection of null hypothesis (Ho) at $P > 0.05$; therefore, the mean Δ*DCN*, ΔTCN and Viability is statistically significant and the Δ*VCN* is insignificant. Cell number values rounded to the nearest 1 x 10^5 cells mL^{-1}.

Inspection of the data when plotted (Figure 4-4) suggests that the Δ*DCN* was significant only in those experiments with recirculation and that, since Δ*VCN* was insignificant in *all* experimental cases, ΔTCN too was significant only in experiments with recirculation.

Equal variances are required for a comparison of means using the analysis of variance (ANOVA) method to determine if a statistical difference exists between means, and, if it does, whether any of the means are significantly larger or smaller than the rest of the set of means. Unfortunately, the variances were found to be unequal and ANOVA would not provide a useful result. However, it is still possible to perform a non-parametric matched-pair test to establish the significance of the difference. This test establishes if the difference between two means is statistically significant.

Comparison of the mean Δ*DCN* was made between three experimental cases: fed-batch STR (STR) without recirculation in the PFR (Experiment 1), Control STR with recirculation in the PFR at a 60 s mean residence time, but with feeding to the STR (Experiment 2) and test cases with recirculation and feeding to the PFR (Experiments 3, 4, 5 and 6 combined).

Before comparison of the three cases, the mean Δ*DCN* for each of the three cases was tested separately against the null hypothesis, Ho, that the mean Δ*DCN*, was zero, i.e., Ho=0. This test indicated that in all of the three cases, with and without recirculation, there was a statistically significant difference between the *DCN* found by HC and FC, Δ*DCN* (Table 4-3); furthermore, Δ*DCN* was almost fivefold greater for both experimental cases with recirculation than without (Table 4-3). Thus, it may reasonably be inferred that some aspect of recirculation greatly

increased the count difference between HC and FC so that the *DCN* was significantly greater when measured by FC than by HC.

The following comparison of means establishes if there was a statistically significant difference in the Δ*DCN* between the above three experimental cases: without recirculation, with recirculation but feeding to the STR, and with recirculation and feeding to the PFR. The difference between the mean Δ*DCN* was found by subtracting the mean Δ*DCN* for each case (e.g., mean Δ*DCN* of Experiments 3, 4, 5 and 6 – mean Δ*DCN* of Experiment 1). These values were then tested against the null hypothesis that there was zero difference, on average, between the Δ*DCN* found in each of the three experimental cases, i.e., Δ*DCN* was equal for the three cases, Ho = 0.

As implied by the roughly fivefold greater Δ*DCN* found for experiments with recirculation, recirculation cases had a significantly greater Δ*DCN* than cases without recirculation. There was no significant difference between Δ*DCN* for cases with recirculation. (Table 4-4). In summary, the *DCN* found by FC was significantly higher than the *DCN* found by HC for all experimental cases. However, the degree to which the *DCN* found by FC exceeded the *DCN* found by HC, Δ*DCN*, was itself significantly greater for experimental cases with recirculation than cases without recirculation. There was no significant difference between Δ*DCN* for all cases with recirculation. There was no significant difference in *VCN* given by both counting methods, Δ*VCN*, for all experimental cases. Since there was no significant difference between *VCN* for both count methods, but *DCN* was found to be significantly greater by FC, then the *TCN* must be significantly greater by FC.

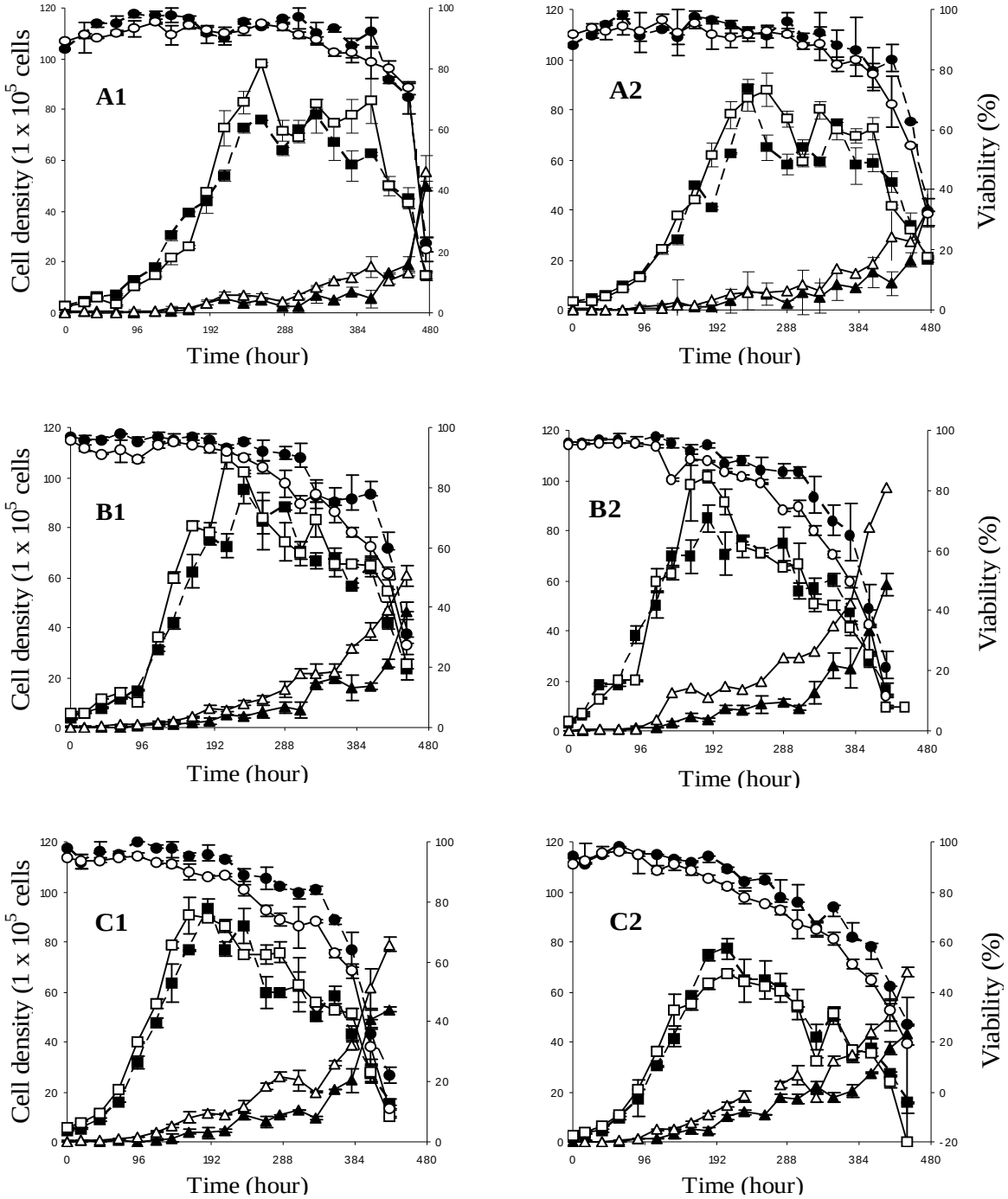

Figure 5-4: Comparison of cell counts made using the haemocytometer (HC) (closed points) and flow cytometer (FC) (open points). Viable cell number, *VCN*, (square), dead cell number, *DCN*, (triangle) and viability (circle). A: Fed-batch stirred tank reactor (STR). B: Fed-batch STR with recirculation through the plug flow reactor (PFR) (Control Experiment for recirculation). C: pH control to the PFR (60 seconds (s) mean residence time (*RT*) in the PFR). D: pH & substrate to the PFR (60 s). E: pH & sub (120 s). F: pH(100x) & sub (120 s). Numbers 1 and 2 are duplicate experiments. Each time point is the average of two cell counts, error bars represent the data range.

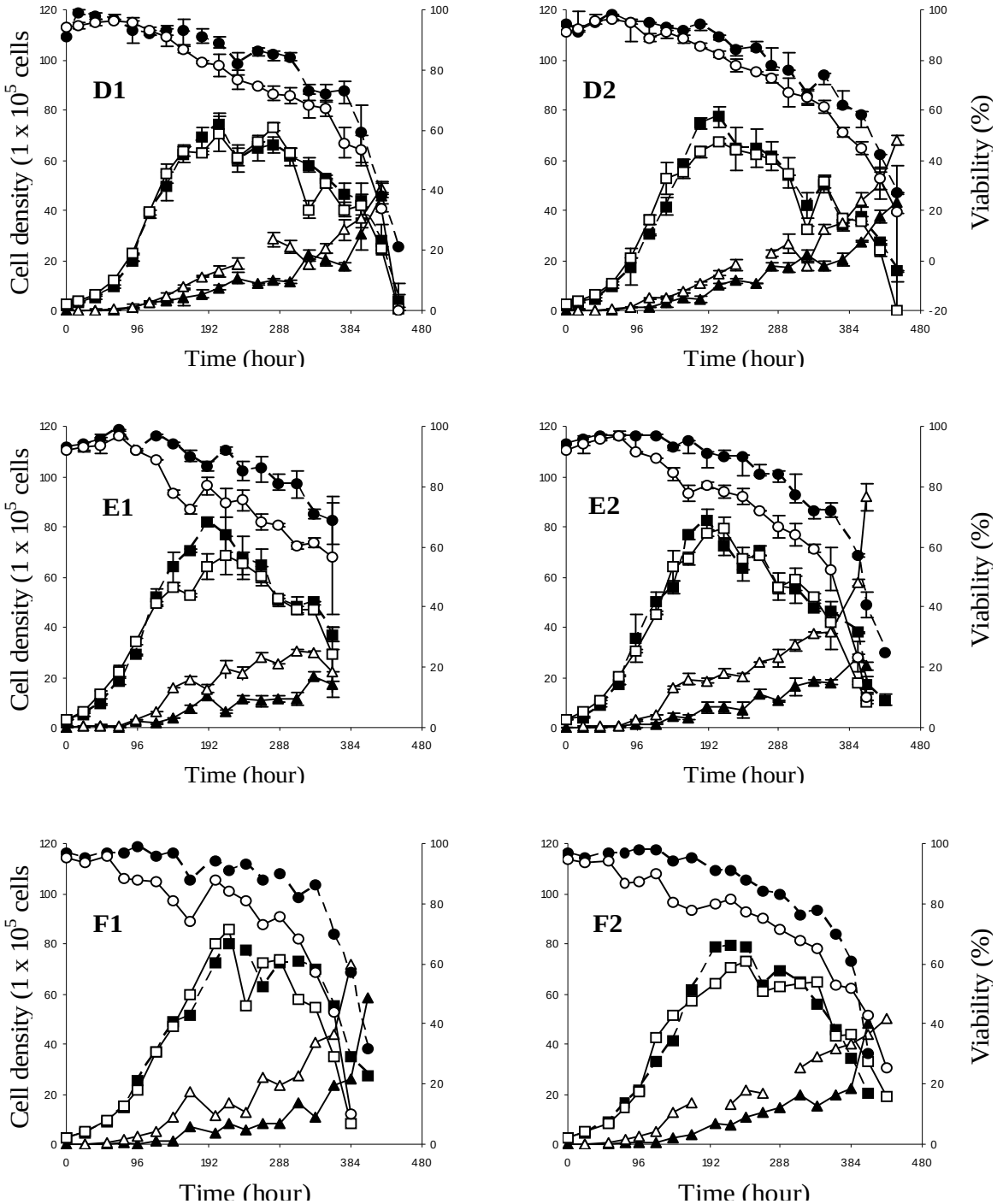

Figure 5-4: Comparison of cell counts made using the haemocytometer (HC) (closed points) and flow cytometer (FC) (open points). Viable cell number (square), dead cell number (triangle) and viability (circle). A: Fed-batch stirred tank reactor (STR). B: Fed-batch STR with recirculation through the plug flow reactor (PFR) (Control experiment for recirculation). C: pH control to the PFR (60 seconds (*s*) mean residence time (*RT*) in the PFR, s). D: pH & substrate to the PFR (60 s). E: pH & sub (120 s). F: pH(100x) & sub (120 s). Numbers 1 and 2 are duplicate experiments. Each time point is the average of two cell counts, error bars represent the data range.

	Δ*DCN* Control No Recirculation Experiment 1	**Δ*DCN* Recirculation Control Experiment 2 (1 x 10^5 cells mL^{-1})**	**Δ*DCN* Recirculation Perturbation Experiments 3 to 6**
Mean	2	9	8
Std Dev	4	10	9
Std Err Mean	1	2	1
Upper 95% Mean	1	6	7
Lower 95% Mean	4	13	10
Number of Values (N)	41	39	139
Hypothesized Value (Ho)	0	0	0
Actual Estimate (Ha)	2	9	9
Degrees of Freedom	40	38	138
Test Statistic (Rank)	238	382	4316
Prob > |t|	0.001	0.0001	0.0001
Prob > t	0.000	0.0001	0.0001
Prob < t	1	1	1

Table 4-3: Calculation of the mean difference between cell counts made using flow cytometry (FC) and haemocytometry (HC), as Table 4-2. Δ*DCN* are grouped into the three broad experimental cases: control without recirculation and feeding to the stirred tank reactor (STR) (Experiment 1); control with recirculation through the plug flow reactor (PFR) and feeding to the STR, as in Experiment 1 (Experiment 2); recirculation through the PFR with feeding to the PFR (Experiments 3 to 6). Statistical analysis performed as Table 4-2. Cell number values rounded to the nearest 1 x 10^5 cells mL^{-1}.

	Recirculation Control - Control No Recirculation	Recirculation Perturbation - Control No Recirculation	Recirculation Perturbation - Recirculation Control
Experiments	**(2) - (1)**	**(3 to 6) - (1)**	**(3 to 6) - (2)**
Rank	328	317	57.5
Prob > |z|	0.0001	0.0001	0.43
Prob > z	0.0001	0.0001	0.21
Prob < z	1	1	1

Table 4-4: Calculation of the mean difference between cell counts made using flow cytometry (FC) and haemocytometry (HC), as Table 4-2. ΔDCN are grouped into the three broad experimental cases: control without recirculation and feeding to the stirred tank reactor (STR) (Experiment 1); control with recirculation through the plug flow reactor (PFR) and feeding to the STR, as in Experiment 1 (Experiment 2); recirculation through the PFR with feeding to the PFR (Experiments 3 to 6). Statistical analysis performed as Table 4-2. Cell number values rounded to the nearest 1 x 10^5 cells mL^{-1}.

As noted, Δ*VCN* was statically insignificant and *VCN* was therefore equivalent for both analysis methods during all experiments. Based on the good accordance in *VCN* between the two different methods, one should be confident that its value was correct, accepting, of course, that *VCN* could have been equally incorrect for both count methods. The same confidence cannot be extended to *DCN*. The large and statistically significant Δ*DCN* found in experiments with recirculation and the small and insignificant difference found in experiments without recirculation clearly implies that the recirculation altered the cell culture in a way that led to an erroneous *DCN* in at least one of the two counting methods. Bearing in mind that the FC *DCN* was on average greater that the HC *DCN*, to determine where the fault lies, one should consider the causes of an artificially low cell count from the HC and of an artificially high cell count from the FC.

There is only one plausible cause for an artificially low *DCN* found by HC: the extra dead cells were consistently ignored during the cell count. As discussed (Section 1.10), HC is subjective, and relies of the user's judgement to discriminate between viable and dead cells (with the aid of TB to stain dead cells) and to count them accurately while ignoring cell debris, such as fragments of cell wall and cell nuclei that are released from lysed cells. Since the same person made all counts with the HC, it might be expected that any error in the count method would have occurred for all experiments, and not just those with recirculation. One of the duplicate STR for experiment 1 (no recirculation control case) was performed after Experiment 2 and 3 (recirculation cases), and any change in technique after conducting the first experiment can therefore be discounted. Thus, it is likely that the HC count was consistent. The FC is somewhat more complicated than the HC and, in turn,

counting can be subject to more complications. Error can be introduced by several means: poor alignment, poor choice of gate and enumeration of particles that closely resemble cells. Alignment and gating rely partly on judgement (although methods for alignment minimise error, Section 2.11.3); cell enumeration is performed solely by the instrument, but the final ratiometric count does rely on gating of fluorescent spheres of know concentration (Section 2.11.4). Each will be discussed in turn.

Poor alignment is unlikely to have occurred, thanks to measures used to test the alignment before each sample run (Section 2.11.3). Nevertheless, had it occurred, it is unlikely to have persisted for more than one sample date because the FC was aligned before each sample and had multiple users known to conduct regular alignment. Furthermore, poor alignment would probably have also altered *VCN* and not *DCN* alone. One can be confident that poor alignment did not create a consistent elevation of the *DCN*.

Gating was applied at two levels: first, a forward scatter light v side scatter light (FS-SS) gate to select the cells, instead of debris or other particulates, on the basis of their refractive index and light scattering (Section 1.10.3); second, a green fluorescence v red fluorescence (GF-RF) gate (or quadrant) to group this selection into live and dead cells based on their staining with Calcein-AM/PI (Section 2.11.5). Thus, improper choice of gate could result in the selection of particles other than cells, such as debris, and subsequent incorrect apportioning of the percentage live and dead cells. As with poor alignment, any problem with gate selection was unlikely to have persisted and would probably have altered the *VCN*.

Nevertheless, if cell debris sufficiently resembled the CHO cells in size, shape and refractive index it could have been included in the first gate. To increase

the *DCN*, subsequent placement in the dead cell quadrant would be required, indicating that the debris was stained with Propidium Iodide (PI) and thereby suggesting, though not confirming, the presence of DNA. Intercalation with DNA provides PI with hydrophobic conditions required for peak fluorescence (Section 1.10.2.1), but some non-specific binding may also occur (Shapiro, 2003a) and has been suggested as a cause for the lower viability observed in a comparison of TB and PI (Al-Rubeai et al., 1996). In this case, non-specific binding of PI to viable cells cannot alone account for the greater DNC, since it would not have increased the *TCN*, and would, by staining live cells, presumably have also decreased *VCN*. Furthermore, as discussed (Section 3.2.2), non-specific binding of PI to cell debris, or viable cells, should be revealed as a population with decreased red fluorescence (RF).

If cell debris can be shown to be greater for experiments with recirculation, then admission of cell debris by the first gate, and subsequent placement of that debris in the dead cell quadrant provides a probable cause for the increase in *DCN*. The FS-SS plots do indeed reveal that a considerable increase in cell debris was present from about 120 h of culture in all of the experiments with recirculation (Figure 4-4, Debris). Alternatively, the count found by HC was low for all experiments with recirculation,

Thus, it is concluded that some aspect of experiments with recirculation resulted in an elevated *DCN* and that cell debris, which is seen to be considerably greater in experiments with recirculation, was probably responsible. It is thought that a proportion of the cell debris present in experiments with recirculation (Figure 4-4, 2 – 6) was unavoidably included in the FS-SS gate for cells because the light

scattering properties of the cell debris were very similar to those of intact cells at that stage in the culture. Light scattering and staining characteristics of the cell debris candidate are considered below (Section 4.4.2 and Section 4.4.3). The inclusion of cell debris in the cell count artificially increased the *TCN*. Cell debris stained with PI appeared in the dead cell quadrant, increasing *DCN* and causing viability (*VCN*/ (*VCN*+*DCN*)) to appear lower. The equivalence of *TCN* and *DCN* suggests that all of the cell debris stained with PI. It should now be considered if the cell debris that increased the *DCN* and *TCN* was already present in the STR or if it was created by destruction of dead cells in the FC.

4.4.1.1 Creation of Cell Debris

Cell death in the STR often ends in lysis and disintegration of the cell (Goergen et al., 1993), which very likely created the debris in the FS-SS plots; cell debris was not observed in the fed-batch without recirculation experiment until a significant decline in viability occurred in the final 48 h of the culture duration. In test cases (experimental cases with recirculation), however, cell debris was present from 200 h and was severe by 330 h, in accordance with the greater decline in viability from the end of exponential growth (Figure 4-4). The quantity of cell debris in experiments with recirculation appears to be so great that it suggests recirculation accelerated the degradation of dead cells. Mechanisms by which recirculation could have generated cell debris are discussed (Section 4.5).

If cell debris was not already present in the STR at the time of sampling, then it would clearly have to have been created at some point during the sampling, staining and analysis by FC. Mechanisms by which FC could result in cell death and cell degradation have been discussed (Section 3.3.3), it was concluded that FC itself

was unlikely to have damaged cells, but that incubation and staining period may have lowered viability. However, significant destruction of viable cells is effectively ruled out by the equal *VCN* found for both count methods. Destruction of dead cells by the FC would imply that dead cells from recirculation experiments had greater susceptibility to catastrophic damage during the FC count; recirculation may well have altered the physiology of the cells, and increased susceptibility to damage cannot be ruled out. Possible aspects of recirculation that might alter cell physiology are discussed (Section 4.5).

4.4.2 Cell Viability with Calcein-AM and PI: Live or Dead

The forward scatter light v side scatter light (FS-SS) cytographs (Figure 4-4) and the green fluorescence v red fluorescence (GF-RF) cytographs (Figure 4-5) obtained for viability assessment of experiments with recirculation were all equivalent. The amount of debris was considerable higher in the recirculation experiments (from experiments 2 to 6) (Figure 4-4, Debris); this was associated with considerably lower viability and higher cell death and may therefore be attributed to high levels of cell lysis and cell disintegration. Unlike the fed-batch STR experiment 1, the amount of cell debris in the recirculation experiments from 2 to 6 was so great, and likely of similar size to the cell population, that it was probably not fully excluded by gating of the viable cell population. Cell debris was probably responsible for population A in Figure 4-5.

Throughout much of the culture, the GF-RF cytographs (Figure 4-5) showed that the cell population could be split into three populations, in accordance with GF-RF cytographs for the fed-batch STR. However, in the recirculation experiments a fourth population was present, characterised by high red fluorescence (RF),

indicative of PI staining and green fluorescence (GF) that was even lower than in dead cells. PI staining strongly indicates that nucleic acid (DNA and/or RNA) was present in this subpopulation. Decrease to GF has a less certain cause.

Since these cells are most certainly dead, it is reasonably assumed that they are no longer stained with Calcein. Dead cells that do show the obvious high GF indicative of staining with Calcein have been indentified (Figure 4-5. C). The absence of a clear transition population with intermediary levels of GF indicates that staining of the dead cells with Calcein was binary: cells were either stained with Calcein and exhibited high GF or were not stained with Calcein and exhibited low GF. Nevertheless, for conditions to become even less propitious for Calcein staining would require further degradation of the dead cell. At some point in this process, the dead cell would have very little structural integrity and would be classified as cell debris.

Similarly, a decrease in the cells' green auto-fluorescence could occur if green flavins nucleotides (FMN, FAD), which appear to be responsible for 488 nm-excited green (500-600 nm) auto-fluorescence (Aubin, 1979; Benson et al., 1979), were lost with the material released from the heavily ruptured cells becoming cell debris. In either case, the further decrease in GF was likely caused by catastrophic disruption of the cell. This population was present only in experiments with recirculation, all of which exhibit high levels of cell debris; furthermore, its appearance coincides with the great increase in cell debris after 360 h (Figure 4-4 and Figure 4-5). It is therefore concluded that this sub-population with lower GF was cell debris.

The dual stained population (DSP), a population of cells stained with Calcein-AM and PI, was 4.4 ± 0.3% (mean ± 95% confidence interval, N = 177) in the experiments with recirculation and 3.5 ± 0.2% (N = 40) in the experiment without. A hypothesis test (Wilcoxon Sign Rank Test) for Ho = 0 found the difference between the two means insignificant ($P > 0.05$). Therefore, it cannot be said that the DSP, perhaps representative of the proportion of less robust viable cells in the culture, was greater in experiments with recirculation. Perhaps such cells did not remain viable in the STR for long, and instead rapidly contributed to the *DCN* or quantity of cell debris. The DSP was equivalent for all experiments with recirculation, providing evidence that perturbations made in these scale-down experiments had little effect on the culture viability.

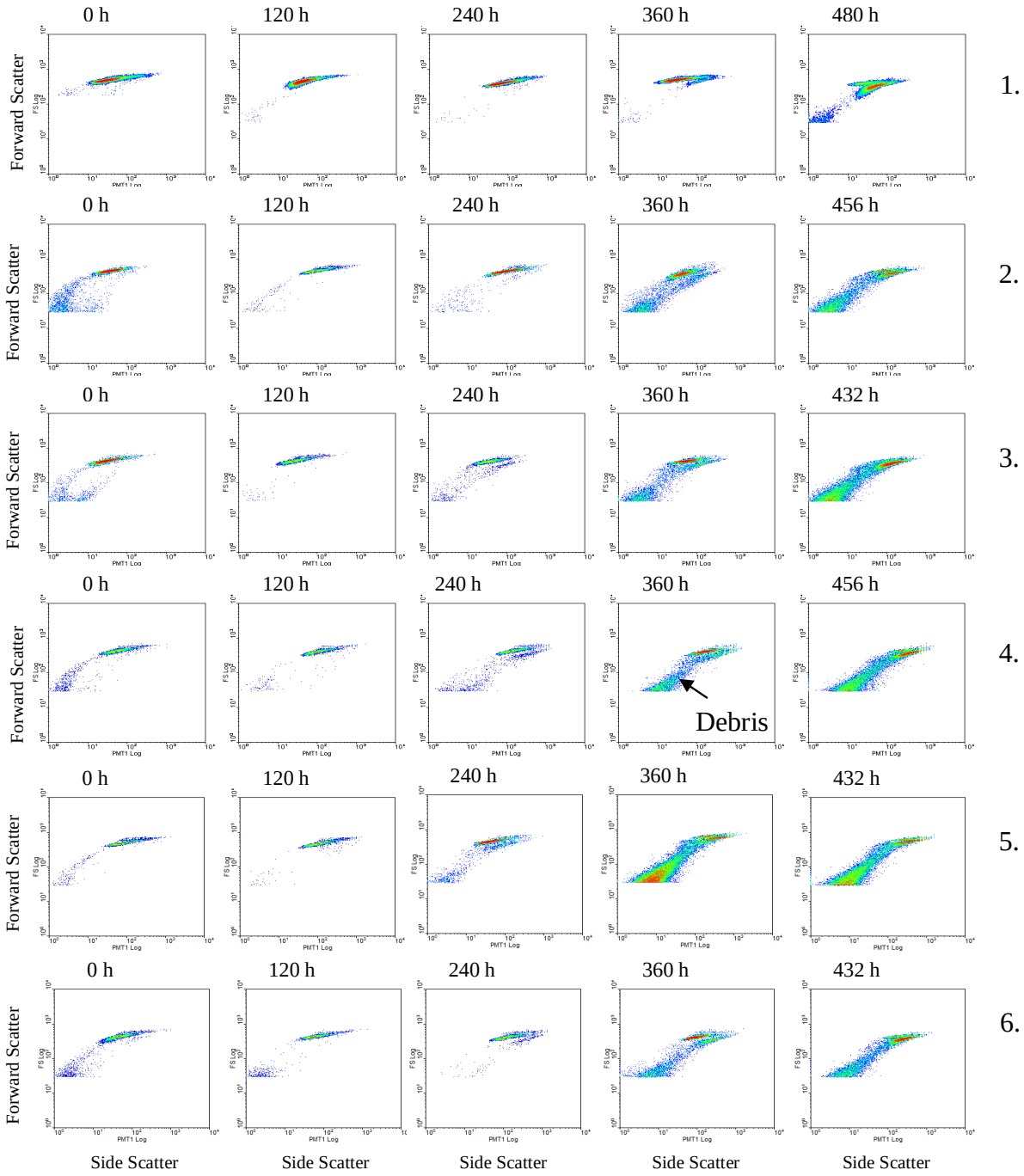

Figure 4-4: Comparison of cytographs: forward scatter light v side scatter light (FS-SS) of unstained GS-CHO cells from all stirred tank reactor (STR) experiment, with and without recirculation through the plug flow reactor (PFR). Numbers 1 to 6 refer to experiments 1 to 6. Suspected cell debris is labelled as 'Debris'.

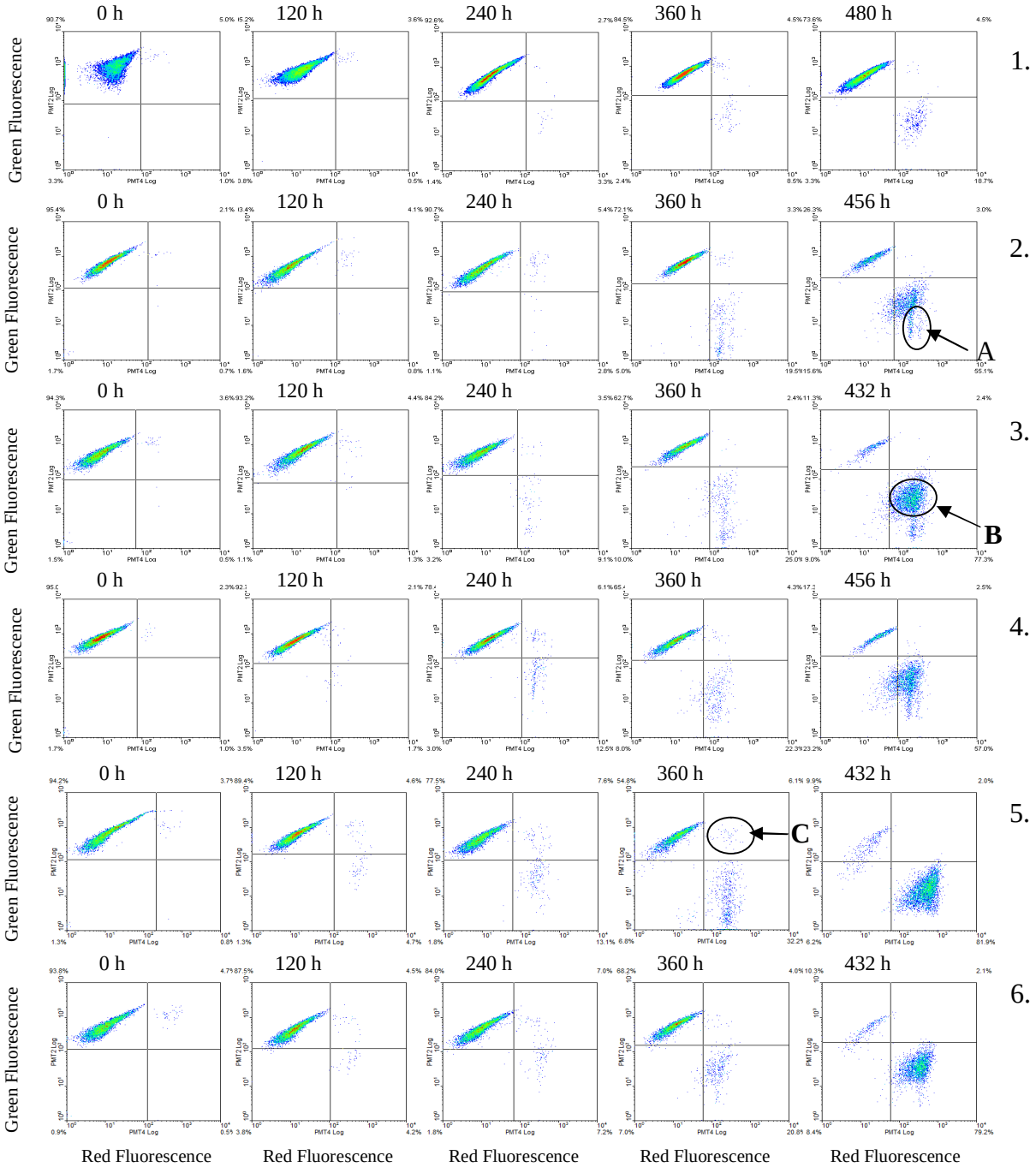

Figure 4-5: Comparison of cytographs: Calcein-AM/PI stained GS-CHO cells; green fluorescence v red fluorescence (GF-RF). Numbers 1 to 6 refer to experiments 1 to 6. A labels what is likely to be cell debris that could not be gated out of the sample; B labels dead cells, stained with PI; C labels cells thought to have died recently, stained with both Calcein-AM and PI.

4.4.3 Mode of Cell Death with Annexin-V/PE and SG: Apoptosis or Necrosis

Cell death was, for all experiments, found to occur by necrosis (AV-PE positive, SG positive), not by apoptosis (AV-PE positive, SG negative) (Figure 4-6), as was observed in experiments using CCCP to induce cell death (Section 3.2.1), cell culture in a shake flask (Section 3.3) and cell culture in a fed-batch STR (Section 3.4). Recirculation through the PFR, though observed to increase cell death, did not alter the mode by which it occurred, nor did the introduction of pH and substrate heterogeneity via the scale-down experiments.

This transition region (Figure 4-6, Transition) implies that staining sometimes may not provide exact delineation of discrete population sub-groups. Further, that the cells' transition from viable to necrotic is unlikely to be instantaneous and may instead be a continuum in which dying cells briefly share staining characteristics of the more discrete viable and necrotic populations.

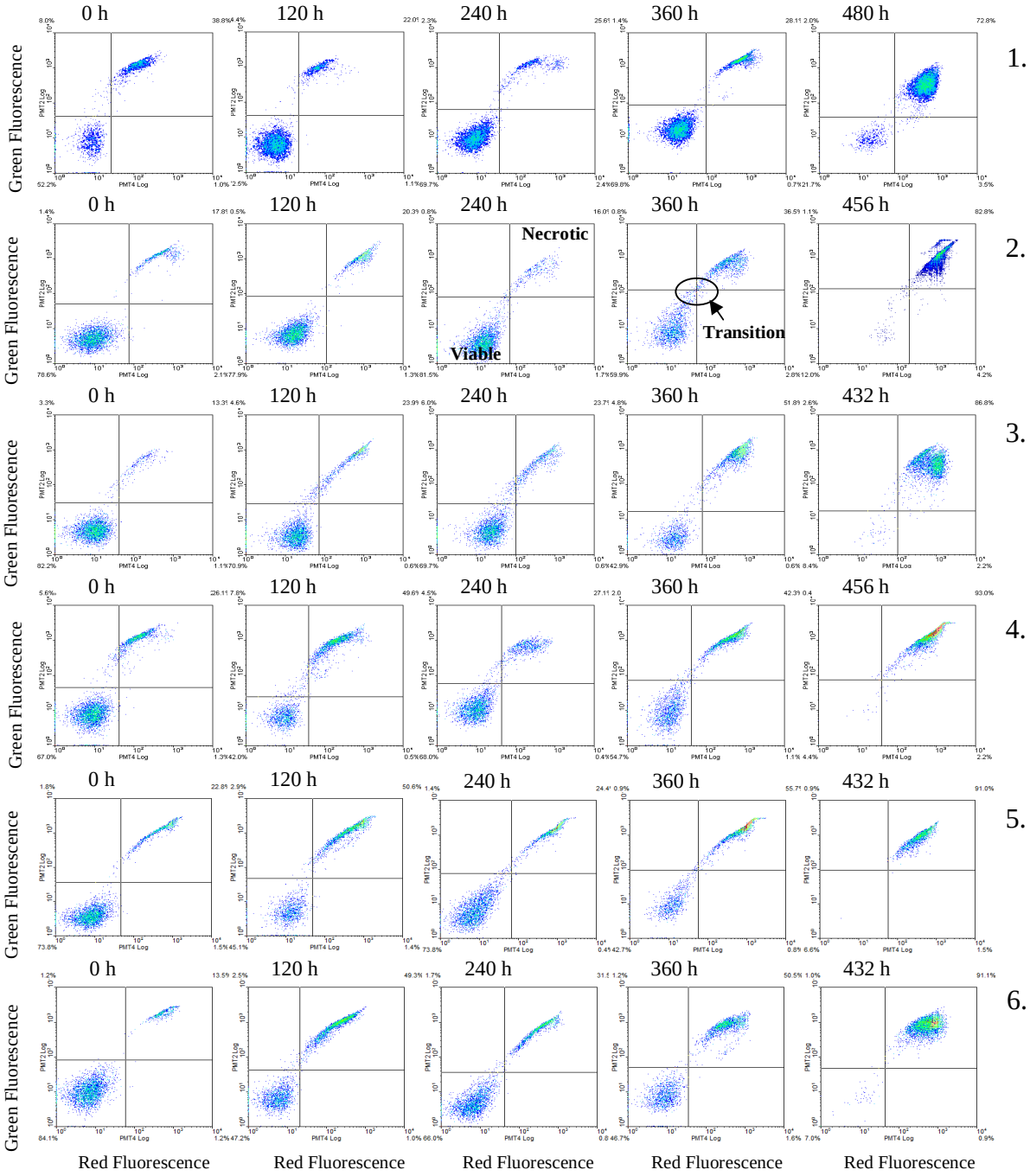

Figure 4-6: Comparison of cytographs: Annexin-V (AV) conjugated to phycoerythrin (PE) used with Sytox Green (SG) (AV-PE/SG) stained GS-CHO cells; green fluorescence v red fluorescence (GF-RF). Numbers 1 to 6 refer to experiments 1 to 6. Viable and Necrotic quadrants are labelled as such. The transition region between their full and clear presence in either the viable or the necrotic quadrant is labelled 'Transition'.

4.4.4 Cell Growth and Antibody Production

The productivity and growth of all 12 experiments is summarised (Table 4-5). *VCN*, viability, antibody titre and *qIgG* for each experiment are presented with a comparison to the control STR with recirculation through the PFR (Figure 4-7, Figure 4-8 and Figure 4-9). Calcein-AM and PI plots (Figure 4-5) were not used to plot viability curves because it has been established that there is no significant difference between *VCN* made by the two methods, and the *DCN* that was given by FC was probably inflated for all experiments with recirculation (Section 4.4.1). What's more, Calcein-AM and PI plots did not provide any useful additional information for the purposes of comparing *VCN* between experiments.

It is clear from graphs of individual experiments (Figure 4-7, Figure 4-8 and Figure 4-9) that all cases with test conditions showed considerably lower performance than the control without recirculation case. All cases with recirculation, including the recirculation control case without perturbations, showed equivalent performance. *VCN*, viability, product titre and *qIgG* in the recirculation experiments were all comparable, and it is likely that any differences from the control are insignificant. This is elucidated by plotting the mean ± standard deviation at each time point for each case of experiments (with and without recirculation) (Figure 4-10, Figure 4-11 and Figure 4-12). Testing for the statistical significance of any differences between specific time points was not possible because the number of experiments was insufficient for a confidence interval to be established.

The comparability of all experiments with recirculation, regardless of whether feeding was made to the PFR or STR, strongly indicates that heterogeneity

in pH and substrate had little effect on important culture parameters: the predominant influence on cell culture was recirculation through the PFR.

A 0.15% drop in glucose concentration (*ΔGluc*) in the PFR of was predicted at 100 x 10^5 (Section 4.3.2). Since the VCN_{max} found in this study were less than 100 x 10^5 cells mL^{-1}, glucose consumption in the PFR is unlikely to have influenced performance of the cell culture (Table 4-1). At VCN_{max}, *DOT* in the PFR may have dropped from 30% to close to 0% in experiments 5 and 6 (120 s residence), but is unlikely to have dropped below 15% in experiments 2, 3, and 4 (60 s residence) (Figure 4-2 and Figure 4-3).

For all recirculation experiments, at the end of the rapid growth phase, viability began to drop significantly 24 hours (h) after the VCN_{max} was attained. All the recirculation experiments were characterised by a shallow but clear decline in cell viability from the end of their rapid growth phase; this contrasted with the fed-batch STR, which exhibited an abrupt decline in cell viability after a stationary phase in which viability was above 80% for approximately 192 h (Figure 4-10). This difference indicates a differing cause for cell death.

In test experiments, the duration of the culture with recirculation was 428 ± 18 h (mean ± standard deviation, N = 10) compared to 508 ± 45 h (mean ± standard deviation, N = 2) for the experiment without recirculation. Note: culture duration measures the point until viability fell below 30%; often 30% viability was reached between samples taken every 24 h, meaning that the culture was sometimes terminated below 30%, adding to the culture duration by a theoretical maximum of 24 h.

In all experimental cases, protein production occurred predominantly during rapid cell growth (Figure 4-9 and Section 3.6). Increased μ in all of the recirculation experiments was not accompanied by elevated antibody titre (Figure 4-9), and antibody titre was lower for experiments with recirculation (Figure 4-12). *qIgG* was equivalently lower for experiments with recirculation (Figure 4-11). In all experiments, approximately 20% of the antibody titre was produced in the stationary phase. Thus, antibody titre was likely decreased by a combination of the shorter duration of the productive rapid growth phase and the lower *qIgG*. It is possible that recirculation placed a burden on the cells that meant some of their resources that would have been directed towards antibody production were instead used to maintain cellular integrity. The probable nature of any burden created by recirculation is discussed (Section 4.5).

Experimental Case	μ_{max} (h^{-1})	VCN_{max} 10^5 cells mL^{-1}	$qIgG_{max}$ pg $cell^{-1}$ h^{-1}	Titre (mg L^{-1})
Fed-batch STR	0.026	78	1.48	1003
Fed-batch STR	0.025	89	1.65	1031
Control (PFR)	0.027	86	1.04	786
Control (PFR)	0.047	84	1.18	811
pH (60 s)	0.026	94	1.14	776
pH (60 s)	0.031	81	1.44	752
pH & sub (60 s)	0.028	75	1.02	791
pH & sub (60 s)	0.033	77	0.97	729
pH & sub (120 s)	0.027	82	1.26	804
pH & sub 120 s)	0.033	82	1.26	784
pH (100x) & sub (120 s)	0.030	80	1.29	841
pH (100x) & sub (120 s)	0.028	80	1.31	819

Table 4-5: Maximum growth and productivity values for each of the six duplicate stirred tank reactor (STR) experiments: maximum specific growth rate (μ_{max}); maximum viable cell number (VCN_{max}); maximum specific rate of antibody productivity ($qIgG_{max}$); harvest antibody titre (Titre). Values rounded to the nearest 1 x 10^5 cells mL^{-1}.

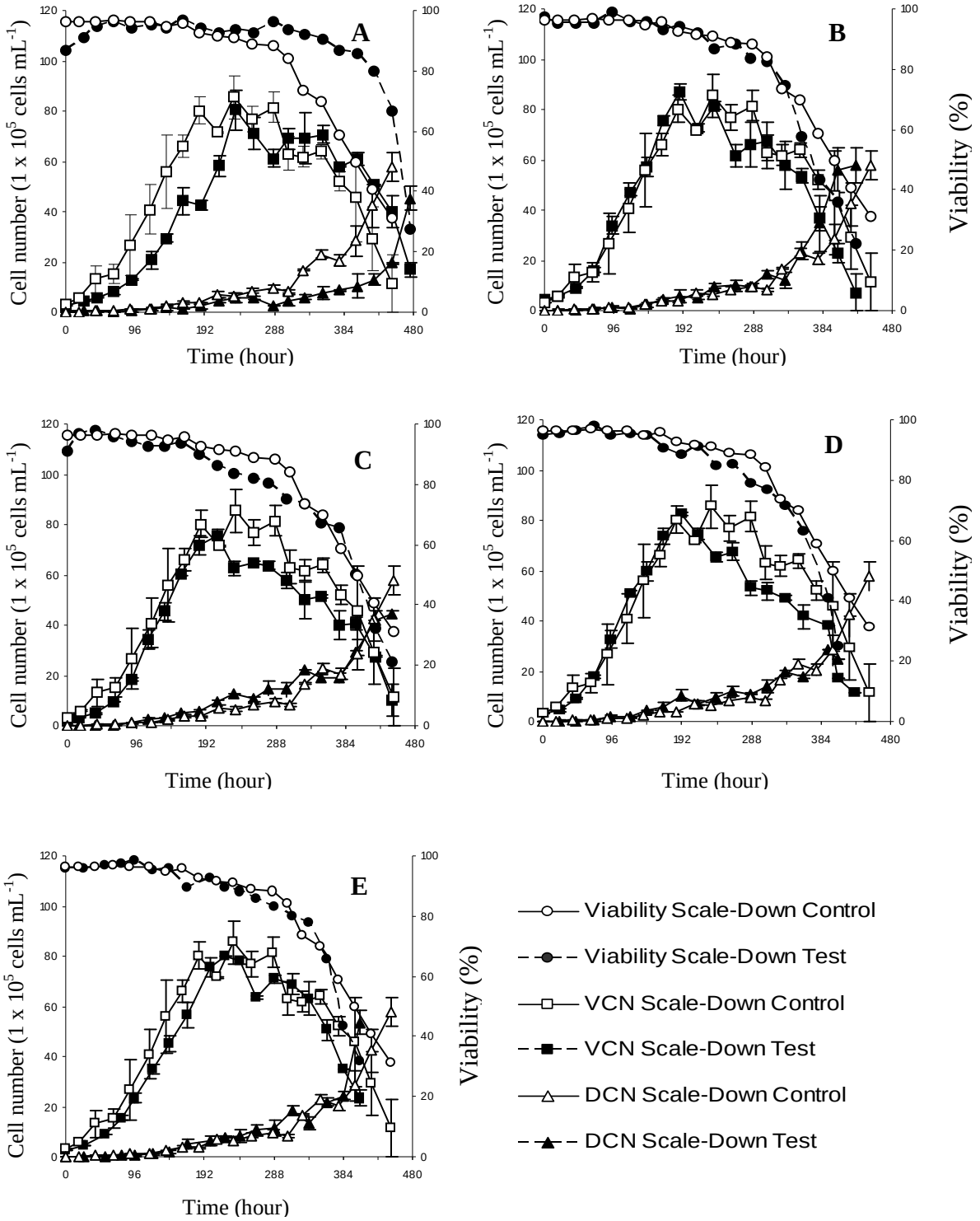

Figure 4-7: Comparison of viable cell number, *VCN*, (square), dead cell number, *DCN*, (triangle) and viability (circle) for the test experiments (solid line, closed points) with the control (PFR) experiment (solid line, open points). A: Fed-batch STR. B: pH (60 s). C: pH & sub (60 s). D: pH & sub (120 s). E: pH (100x) & sub (120 s). Each time point is the average of duplicate experiments, error bars represent the data range of the duplicate experiments.

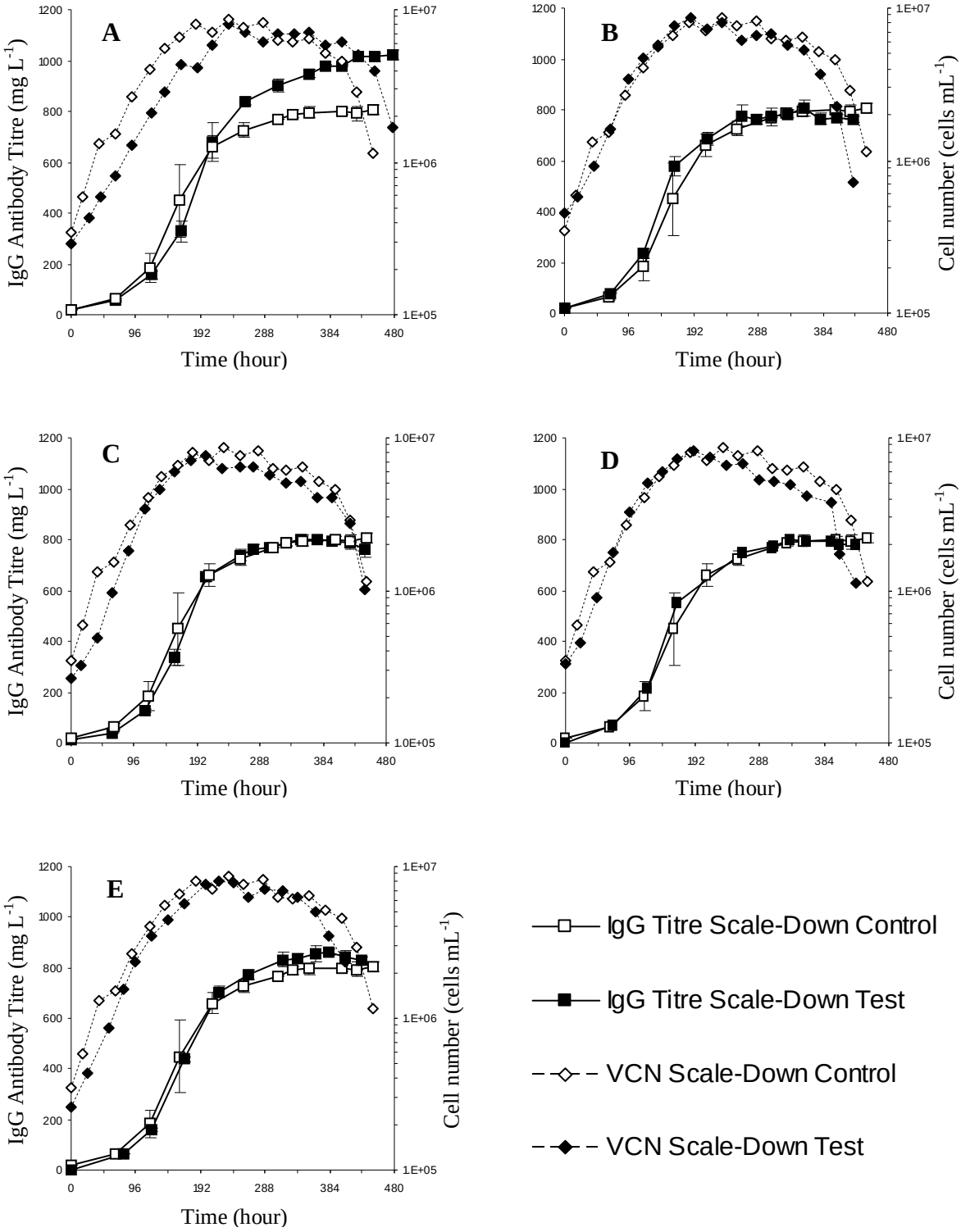

Figure 4-8: Comparison of IgG antibody titre (square) for test experiments (solid line, closed points) with the control (PFR) experiment (solid line, open points). Cell number (dashed line, diamond) plotted on a logarithmic y-axis for growth phase identification. A: Fed-batch STR. B: pH (60 s). C: pH & sub (60 s). D: pH & sub (120 s). E: pH (100x) & sub (120 s). Each time point is the average of duplicate experiments, error bars represent the data range of the duplicate experiments.

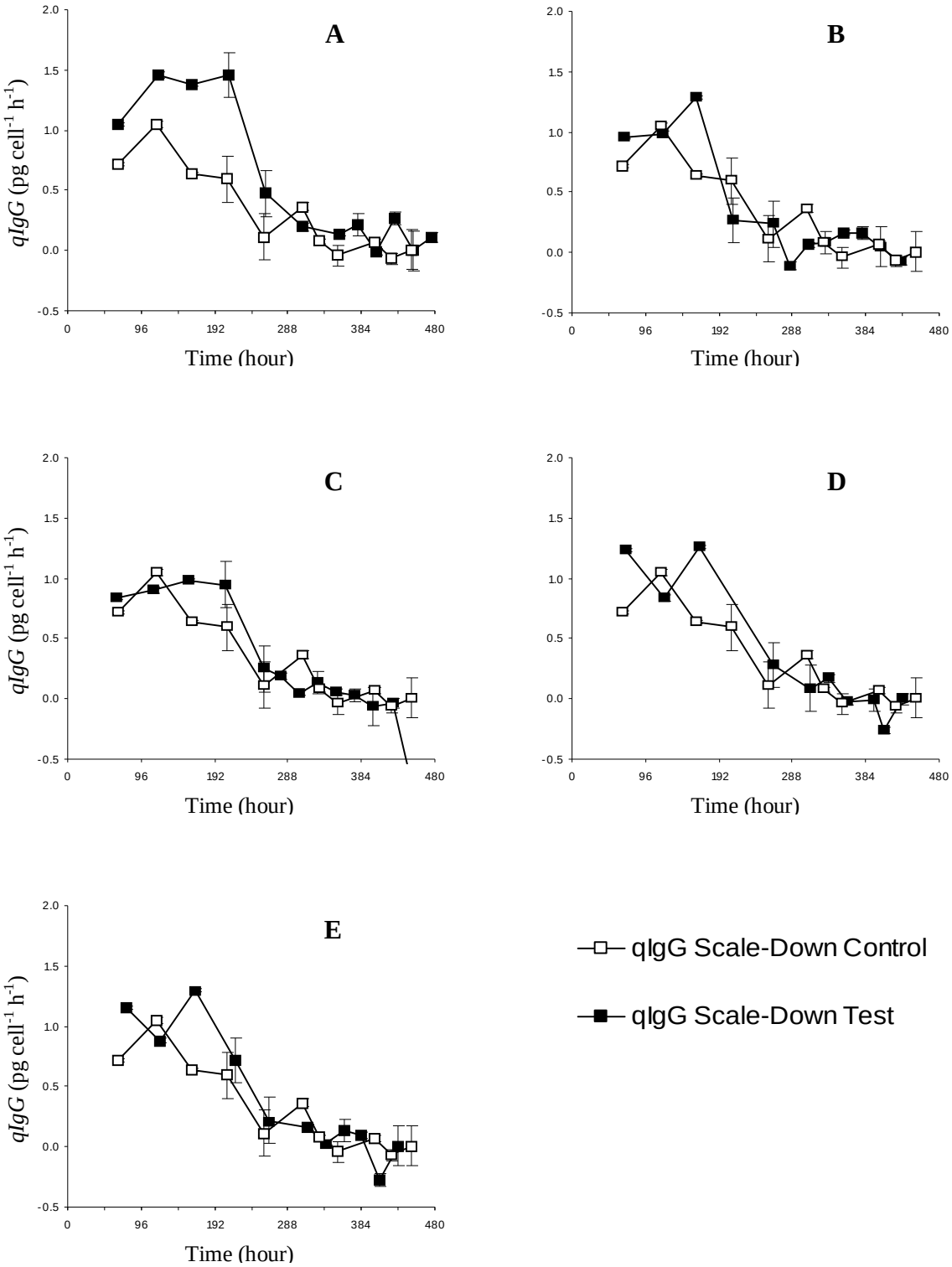

Figure 4-9: Comparison of specific rate of antibody production, *qIgG*, (square) for test experiments (solid line, closed points) with the control (PFR) experiment (solid line, open points). A: Fed-batch STR. B: pH (60 s). C: pH & sub (60 s). D: pH & sub (120 s). E: pH (100x) & sub (120 s). Each time point is the average of duplicate experiments, error bars represent the data range of the duplicate experiments.

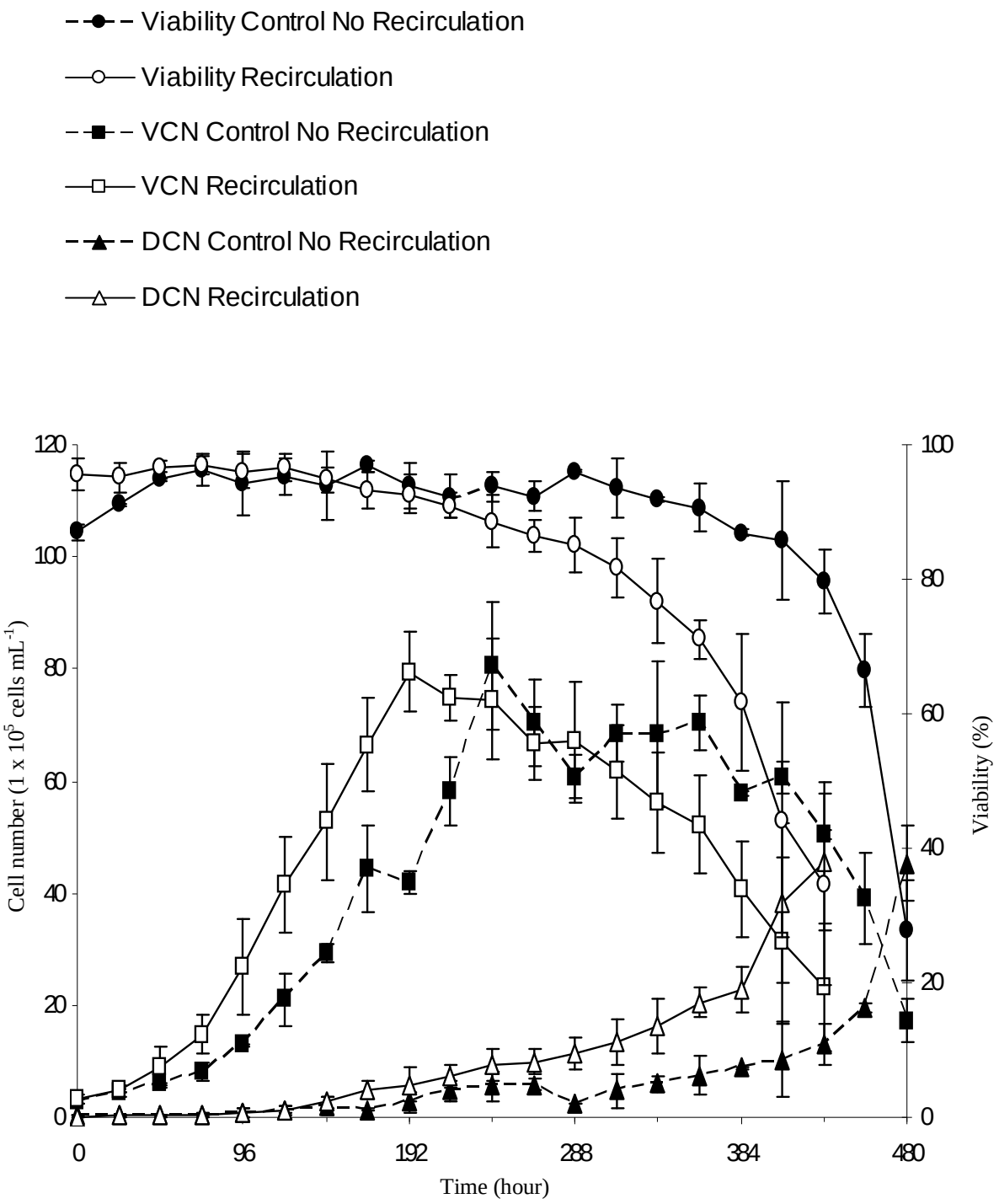

Figure 4-10: Comparison of experiments with continuous recirculation (open points) and without continuous recirculation (closed points) through the PFR. Viable cell number, *VCN*, (square), dead cell number, *DCN*, (triangle) and viability (circle). Each time point is the mean and error bars are 1 standard deviation. (Experiments with recirculation, N = 10. Experiments without recirculation, N = 2).

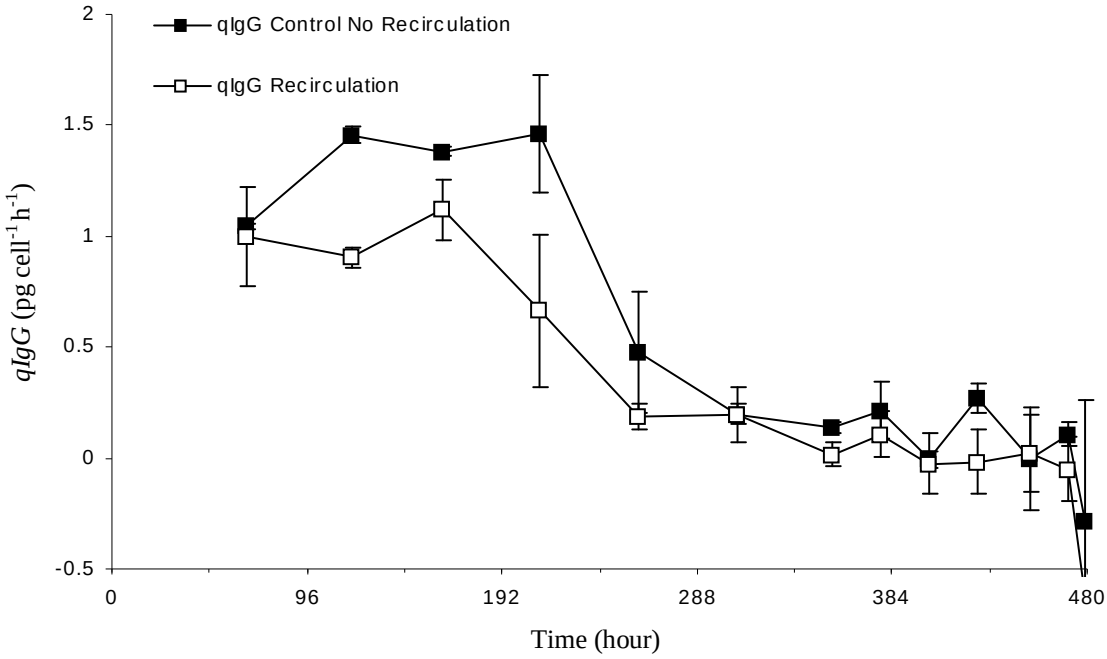

Figure 4-11: Comparison of the specific rate of antibody production (*qIgG*) for experiments with (open square) and without (closed square) continuous recirculation through the PFR. Each time point is the mean and error bars are 1 standard deviation. (Experiments with recirculation, N = 10. Experiments without recirculation, N = 2).

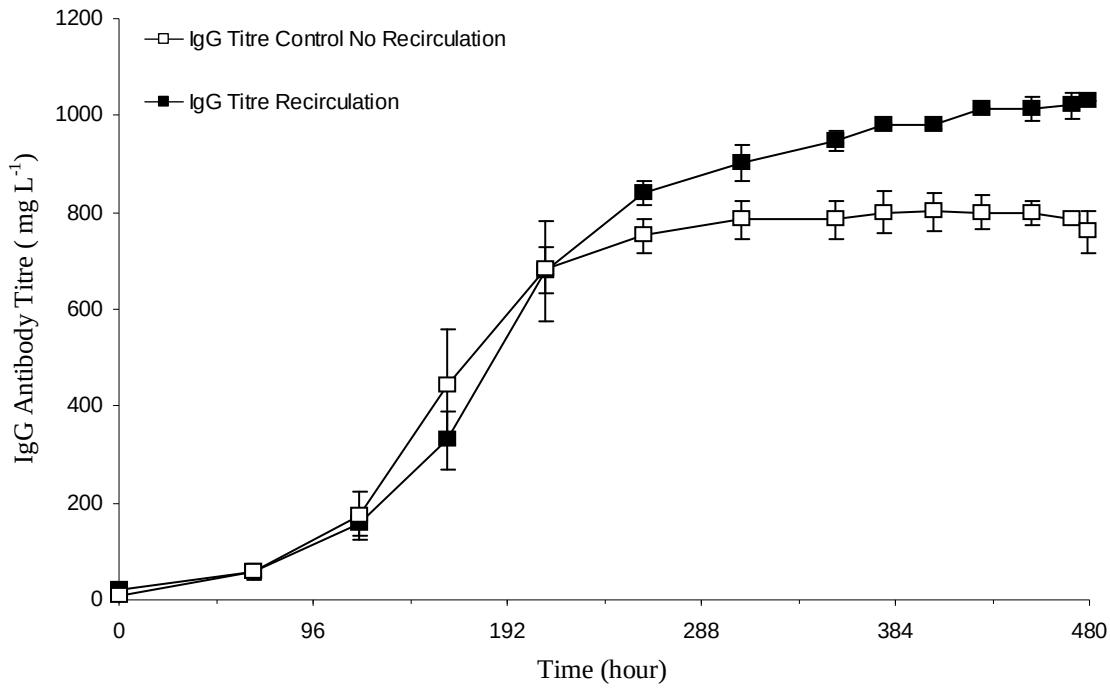

Figure 4-12: Comparison of IgG antibody titre for experiments with (open points) and without (closed points) continuous recirculation through the PFR. Each time point is the mean and error bars are 1 standard deviation. (Experiments with recirculation, N = 10. Experiments without recirculation, N = 2).

4.4.5 Glucose, Lactate and Ammonia

Lactate and ammonia production followed a very similar trend for the control and test experiments: accumulation throughout the rapid growth phase, with a following period of lactate consumption and concurrent low rates of ammonia production as the cell culture transitioned from a rapid growth phase to a stationary phase (Figure 4-13 and Figure 4-14). This provides evidence in support of a hypothesis (Section 3.5.3) that lactate consumption was allied to a physiological change that occurred during the transition between the exponential and stationary phase. The shorter duration of the each culture phase (rapid growth, stationary, death) observed in all experiments with recirculation corresponded to a similarly contracted metabolite profile (Figure 4-16). *qLactate* and *qAmmonia* were comparable for all experiments, with and without recirculation (Figure 4-14 and Figure 4-15), and no clear difference is apparent when the recirculation and non-recirculation cases are compared (Figure 4-18 and Figure 4-19). Metabolites are often considered one of the fundamental causes for deleterious increases in osmolality that can occur in cell culture (Section 3.5.5), and it is therefore reasonable to expect a change in osmolality in accordance with metabolite production (Section 4.4.6).

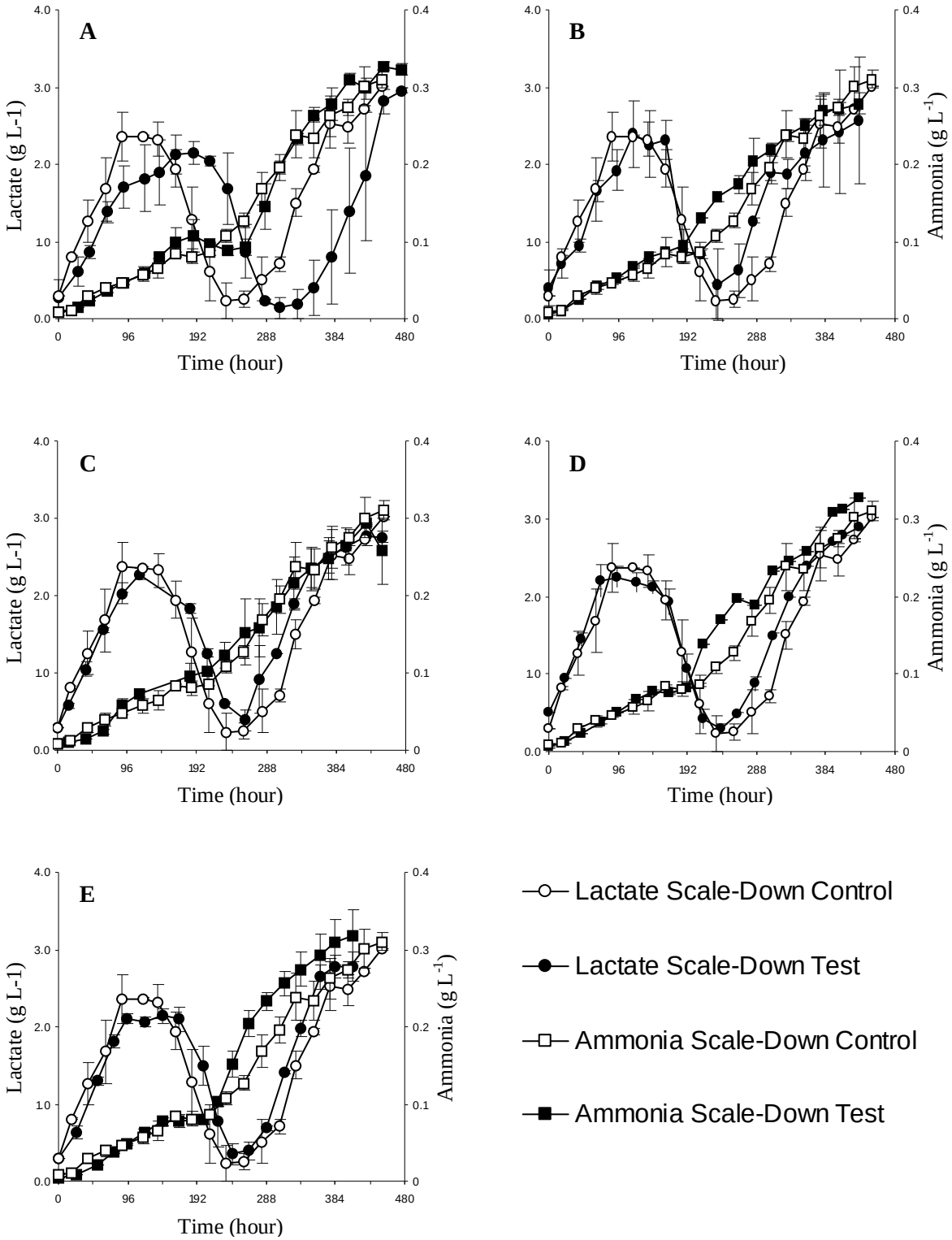

Figure 4-13: Comparison of lactate (circle) and ammonia (square) concentration for test experiments (solid line, closed points) with the control (PFR) experiment (solid line, open points). A: Fed-batch STR. B: pH (60 s). C: pH & sub (60 s). D: pH & sub (120 s). E: pH (100x) & sub (120 s). Each time point is the average of duplicate experiments, error bars represent the data range of the duplicate experiments.

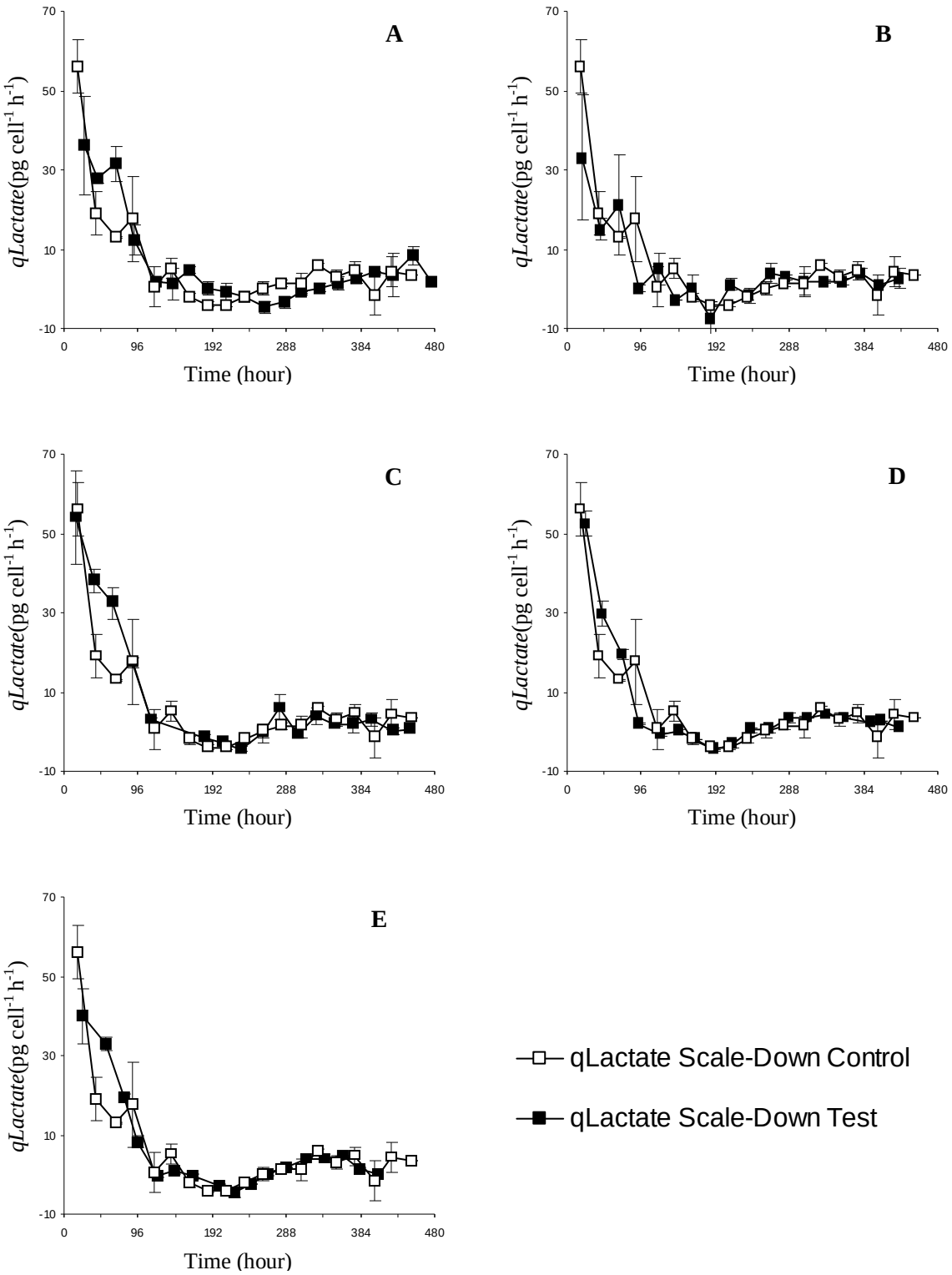

Figure 4-14: Comparison of specific rate of lactate production (*qLactate*) (square) for test experiments (solid line, closed points) with the control (PFR) experiment (solid line, open points). A: Fed-batch STR. B: pH (60 s). C: pH & sub (60 s). D: pH & sub (120 s). E: pH (100x) & sub (120 s). Each time point is the average of duplicate experiments, error bars represent the data range of the duplicate experiments.

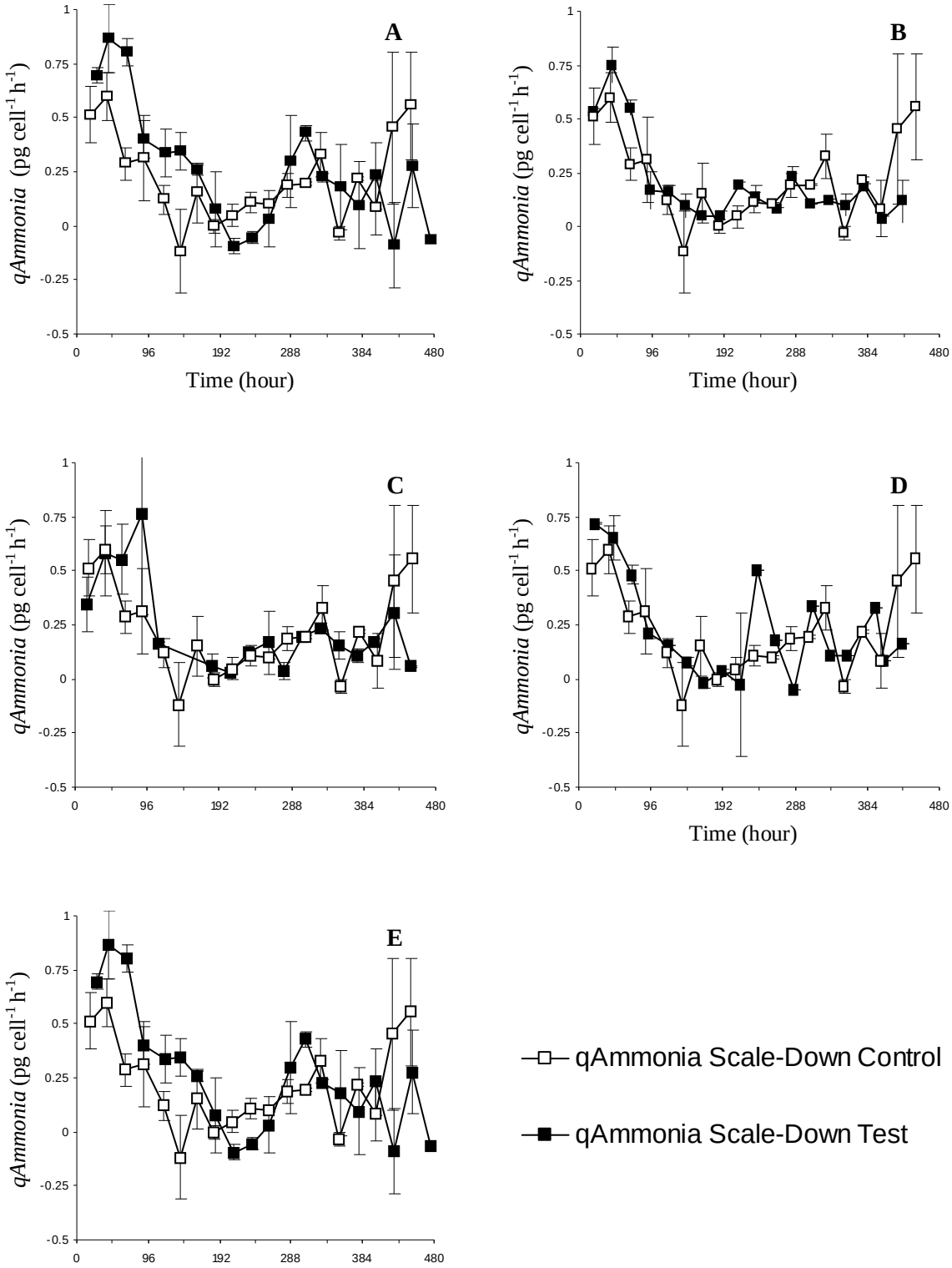

Figure 4-15: Comparison of specific rate of ammonia production, *qAmmonia*, (square) for test experiments (solid line, closed points) with the control (PFR) experiment (solid line, open points). A: Fed-batch STR. B: pH (60 s). C: pH & sub (60 s). D: pH & sub (120 s). E: pH (100x) & sub (120 s). Each time point is the average of duplicate experiments, error bars represent the data range of the duplicate experiments.

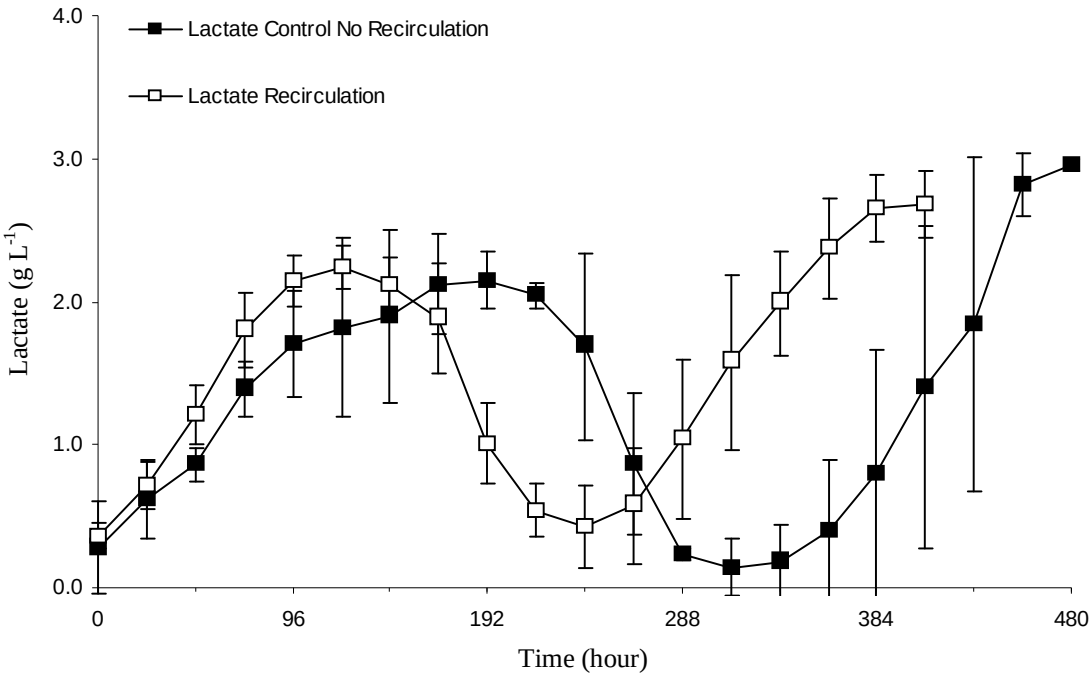

Figure 4-16: Comparison of lactate concentration for experiments with (open points) and without (closed points) continuous recirculation through the PFR. Each time point is the mean and error bars are 1 standard deviation. (Experiments with recirculation, N = 10. Experiments without recirculation, N = 2).

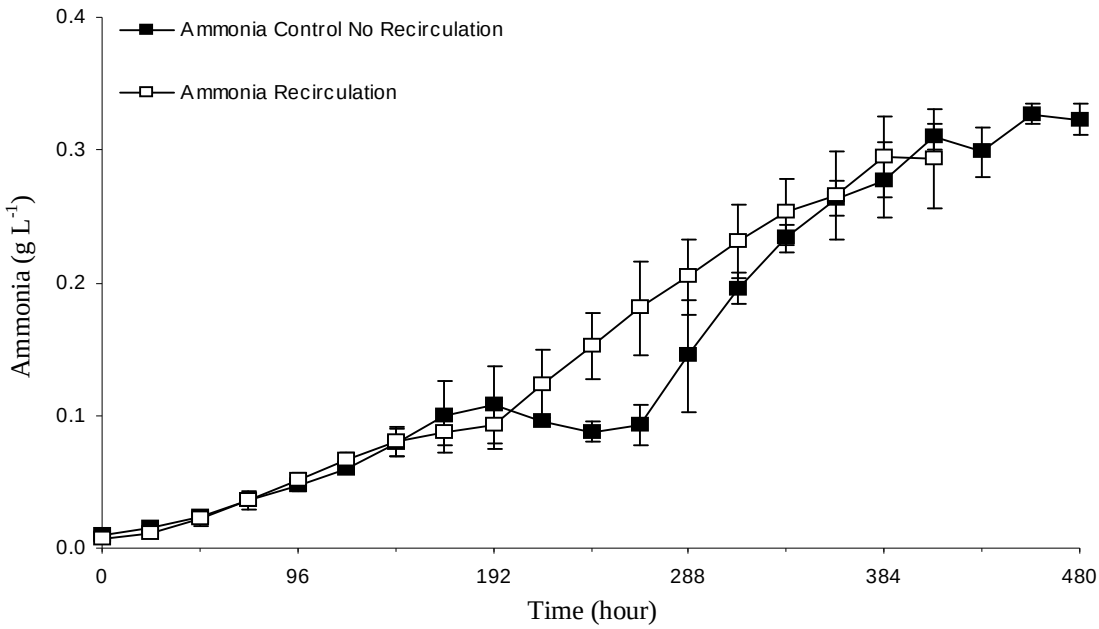

Figure 4-17: Comparison of ammonia concentration for experiments with (open points) and without (closed points) continuous recirculation through the PFR. Each time point is the mean and error bars are 1 standard deviation (Experiments with recirculation, N = 10. Experiments without recirculation, N = 2).

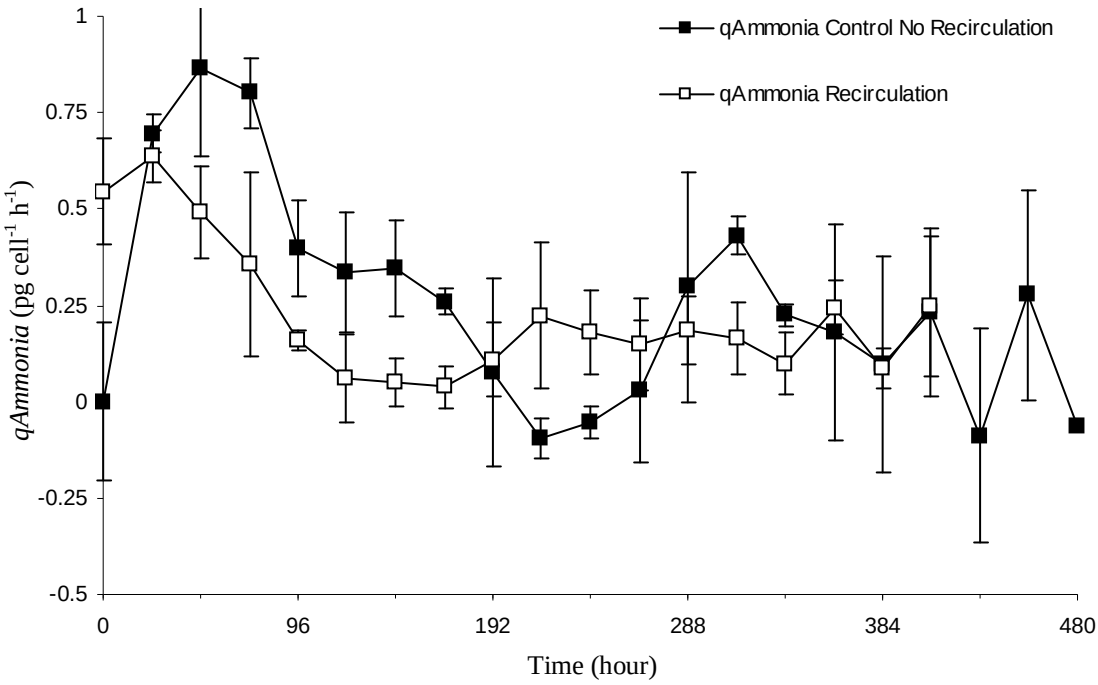

Figure 4-18: Comparison of the specific rate of ammonia production (*qAmmonia*) for experiments with (open points) and without (closed points) continuous recirculation through the PFR. Each time point is the mean and error bars are 1 standard deviation. (Experiments with recirculation, N = 10. Experiments without recirculation, N = 2).

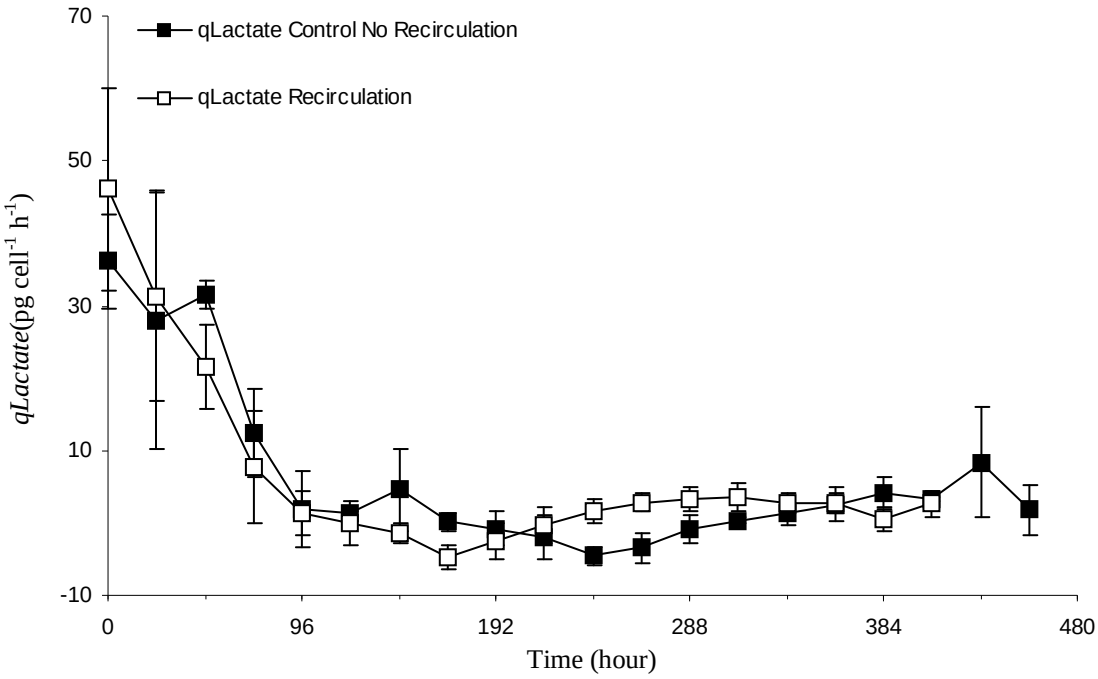

Figure 4-19: Comparison of the specific rate of lactate production (*qLactate*) for experiments with (open points) and without (closed points) continuous recirculation through the PFR. Each time point is the mean and error bars are 1 standard deviation. (Experiments with recirculation, N = 10. Experiments without recirculation, N = 2).

4.4.6 Osmolality

Osmolality was in accordance for all experiments with recirculation (Figure 4-20). In accordance with the earlier production of metabolites that accompanied the greater μ in the rapid growth phase of all experiments with recirculation, a clear difference in osmolality began at ~288 h when lactate and ammonia concentrations began to rise again, having risen with the rapid growth phase and fallen during the stationary phase (Figure 4-11 and Figure 4-13). This indicates that responsibility for the majority of the osmolality increase rested with the quantity of metabolites in the medium. Apart from experiment 6, all experiments with recirculation (Figure 4-20, B – E) had broadly equivalent osmolality; the final osmolality achieved in experiment 6 (Figure 4-20, E) was ~50 mOsm kg^{-1} greater than the control recirculation experiment.

The equivalence of osmolality in all experiments with recirculation regardless of mean residence time (*RT*) in the PFR (60 s and 120 s), apart from experiment 6 (120 s residence in the PFR and 100x alkali), suggests that transfer lag was not great until exacerbated by the 100x stronger alkali. The negligible difference between recirculation experiments up until that point suggests that great quantities of alkali are necessary only in the very late stages of the culture. Elevated osmolality, especially 'hyperosmolality' has been reported to improve antibody titre (Section 1.7.2). In this study, elevated osmolality occurred after antibody production had ceased and could not have greatly influenced antibody titre (Figure 4-8 and Figure 4-9).

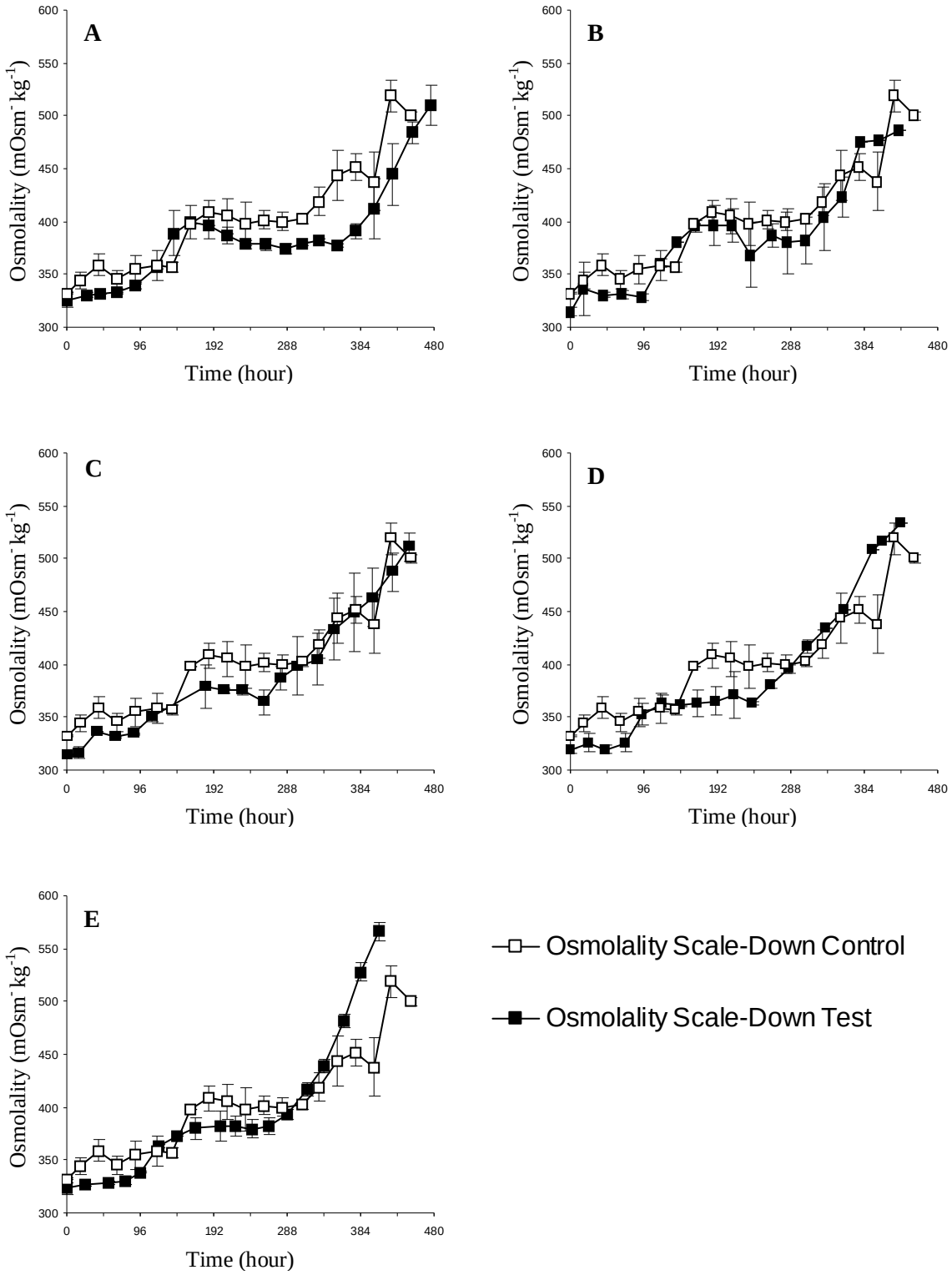

Figure 4-20: Comparison of osmolality (square) for test experiments (solid line, closed points) with the control (PFR) experiment (solid line, open points). A: Fed-batch STR. B: pH (60 s). C: pH & sub (60 s). D: pH & sub (120 s). E: pH (100x) & sub (120 s). Each time point is the average of duplicate experiments, error bars represent the data range of the duplicate experiments.

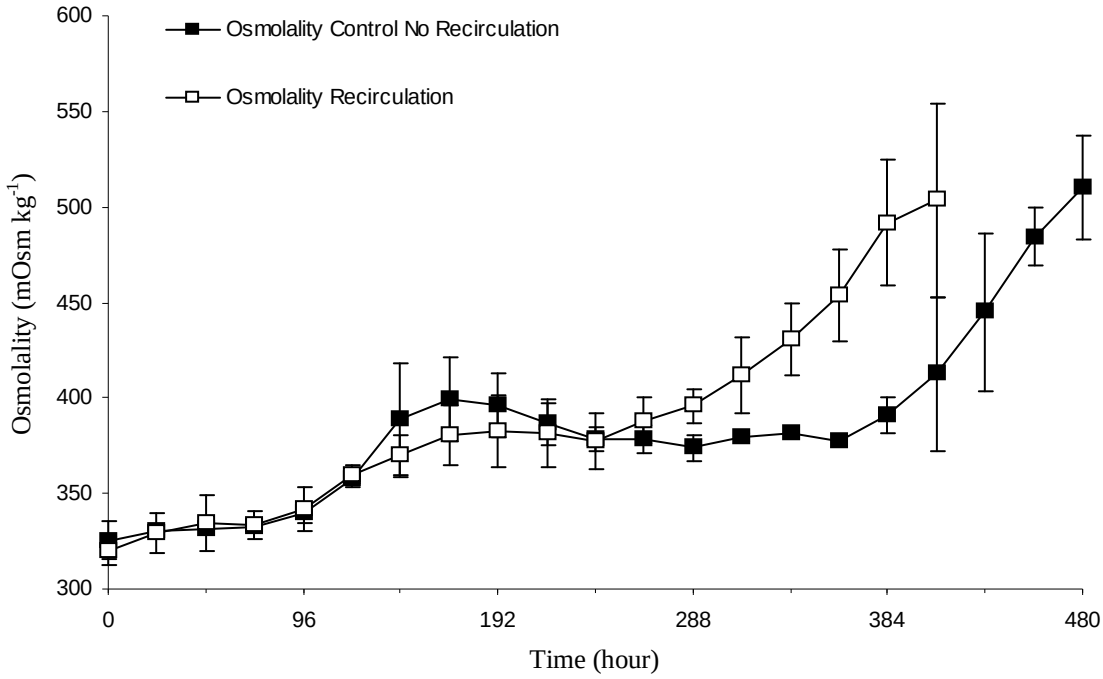

Figure 4-21: Comparison of the osmolality for experiments with (open points) and without (closed points) continuous recirculation through the PFR. Each time point is the mean and error bars are 1 standard deviation. (Experiments with recirculation, N = 10. Experiments without recirculation, N = 2).

4.4.7 Antibody Quality

Product consistency, referred to as antibody quality, can be crucial for the efficacy of the antibody as a drug and has been found to be influenced by process conditions (Section 1.1.1). Several antibody characterisation methods provided a comprehensive analysis of antibody quality (Section 2.14). However, to be sure that there were no minute changes to quality (i.e., efficacy) would have required a complementary set of studies including assessment of *in vitro* and *in vivo* bioactivity and comparative pharmacokinetics and pharmacodynamics studies in relevant species.

4.4.7.1 Mass Heterogeneity

Mass heterogeneity is typically the result of varying degrees of antibody aggregation. Aggregation is sensitive to process conditions and can be indicative of antibody misfolding and degradation by chemical (e.g., pH) or physical processes (e.g., shear) (Section 1.1.1). SDS PAGE (Section 2.14) showed that the molecular mass profiles were comparable for all experimental cases: both band placement and band intensity were comparable (Figure 4-22). Mass spectroscopy showed that the maximum difference between the control and the sample experiments was 6 Da; this is well within the expected ± 100 ppm (parts per million) variation (0.01% of the mass of this Mab) for mass analysis using ESI-Q-TOF (Zhang et al., 2009), and should not therefore be considered as indicative of mass heterogeneity. Thus, it is concluded that the conditions of the scale-down did not result in significant antibody aggregation or degradation.

SDS PAGE (A)

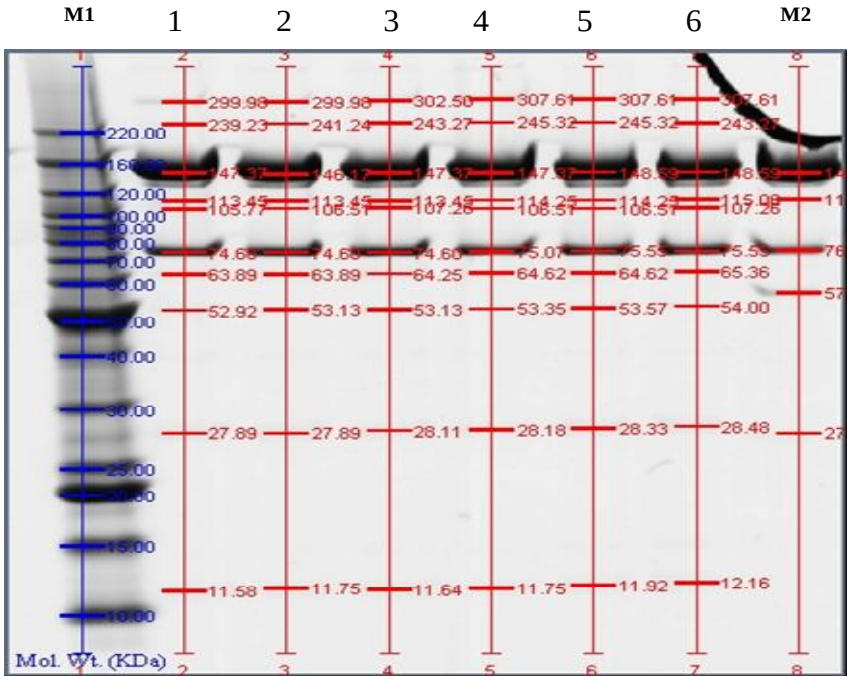

SDS PAGE (B)

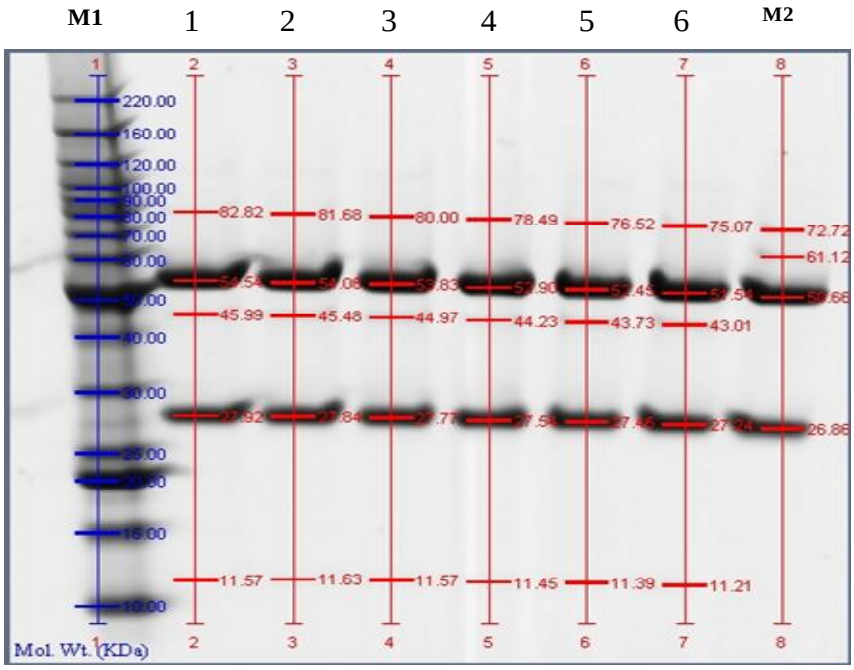

Figure 4-22: SDS PAGE used for comparison of antibody mass (Section 2.14.1). A: non-reducing conditions. B: reducing conditions. Samples shown here were taken from the final time-point (harvest) of each experiment (when % cell viability fell below 30%) and M1 and M2 refer to the molecular weight marker lanes. Lanes 1 to 6 refer to experiments 1 to 6. Experiments (Section 2.7, for details): 1. Fed-Batch STR (Control without recirculation); 2. Recirculation Control (60 s); 3. pH (60 s); 4. pH & sub (60 s); 5. pH & sub (120 s); 6. pH (100x) & sub (120 s).

4.4.7.2 Charge Heterogeneity

Charge heterogeneity is primarily introduced by deamidation and C-terminal lysine micro-heterogeneity (Tsai et al., 1993; Perkins et al., 2000). C-terminal lysine was not present on the antibody studied here and any charge alteration should be attributable to deamidation. Deamidation of asparagine and glutamine introduces an additional negative charge to the antibody and generates acidic species that decrease the protein's isoelectric point (pI) (Liu et al., 2008). These factors have been found sensitive to process condition (Section 1.1.1) and the isoelectric point (Ip) might reasonably be expected to have fallen after repeated exposure to elevated osmolality and pH during alkali addition to the PFR. Isoelectric focusing, IEF, (Section 2.14) showed that the charge profile was comparable for all the experimental cases; both band placement and band intensity were comparable (Table 4-6 and Figure 4-23). The gradual and slight decrease in pH from the left to the right of the gel is attributed to a slight distortion across the gel; this is clear from a comparison of the two standard lanes. The decrease in mean Ip from experiments 1 to 6 is no greater than the variation between the two standards and considered insignificant (Table 4-6).

Experiment	**1**	**2**	**3**	**4**	**5**	**6**
	6.72	6.70	6.66	6.61	6.63	6.61
	6.60	6.57	6.54	6.49	6.49	6.48
	6.50	6.47	6.45	6.42	6.41	6.40
	6.46	6.43	6.40	6.36	6.36	6.35
	6.42	6.38	6.36	6.34	6.30	6.29
	6.37	6.32	6.30	6.26	6.24	6.23
Mean Ip	6.51	6.48	6.45	6.41	6.41	6.39
ΔControl	0.03	Control (PFR)	-0.03	-0.06	-0.07	-0.08

Table 4-6: Comparison of the isoelectric point (Ip) for isoelectric focusing (IEF) analysis (Section 2.14) of purified harvest antibody from experiments 1 to 6 (Section 2.7) - values from a scan of the Gel plate (Figure 5-23). Experiments (Section 2.7, for details): 1. Fed-Batch STR (Control without recirculation); 2. Recirculation Control (60 s); 3. pH (60 s); 4. pH & sub (60 s); 5. pH & sub (120 s); 6. pH (100x) & sub (120 s). The difference between the mean Ip and control mean Ip (ΔControl) is in accordance with the expected error for the IEF method.

Isoelectric Focusing

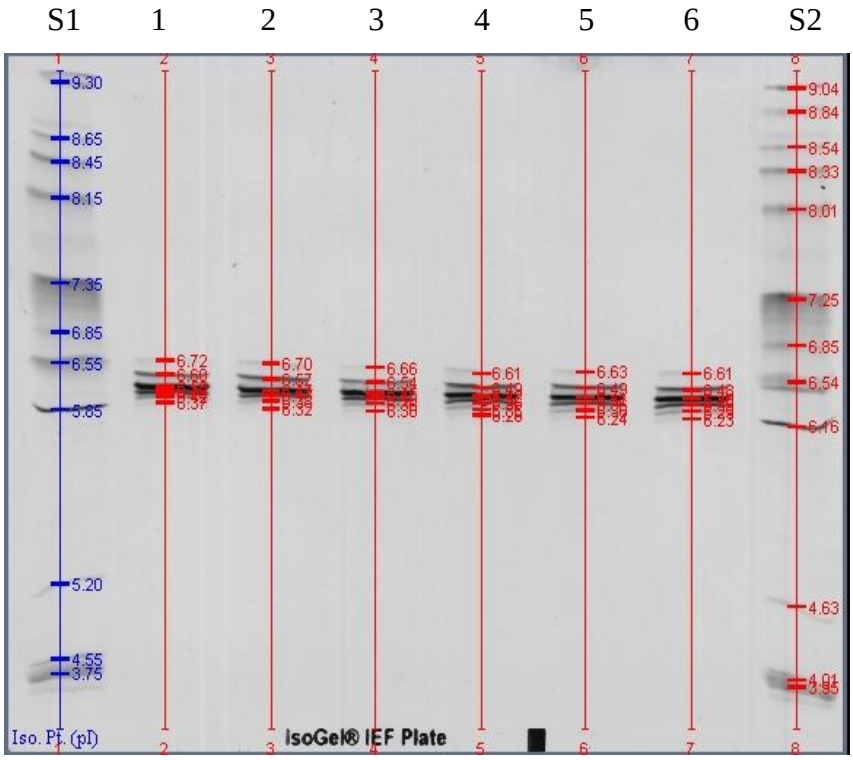

Figure 4-23: Isoelectric focusing for comparison of antibody charge (isoelectric point, Ip). S1 and S2 refer to the standard Ip marker lanes (Section 2.14.3). Lanes 1 to 6 refer to experiments 1 to 6. Experiments (Section 2.7, for details): 1. Fed-Batch STR (Control without recirculation); 2. Recirculation Control (60 s); 3. pH (60 s); 4. pH & sub (60 s); 5. pH & sub (120 s); 6. pH (100x) & sub (120 s).

4.4.7.3 Glycoform Heterogeneity

Glycoform heterogeneity is used here to mean a variation in the oligosaccharides attached to the antibody. As discussed (Section 1.1.1), antibody glycoform can be sensitive to many process parameters in the STR. Since alterations to glycoform have been observed at extremes of pH, at hyperosmolality, substrate limitation and elevated ammonia, it was reasonable to expect that both substrate and alkali perturbations in the PFR might alter the antibody's glycoform profile.

Five glycoforms were identified by NP-HPLC 2-AB: GOF and G1F accounted for the majority of all glycoforms, and G0, G1 and G2F are of low abundance. Note: the NP-HPLC 2-AB used in this study is comparable to glycoform profiling by mass spectroscopy (Thaysen-Andersen et al., 2009). The oligosaccharide structure for each of the above glycoform notations is provided (Figure 4-24). Normalised against the control experiment (experiment 2), some variation in glycoform is evident (Figure 4-25, B). Relative glycoform profiling (Figure 4-25, A) revealed that quantitatively this variation was not considerable and one should take care before attributing it to the scale-down. There are three possible causes for the variation in glycoform: the analytical method, typical variation between duplicate STR experiments, and the conditions of the scale down.

In the literature, only one study could be found to have assessed the accuracy of glycoform analysis by NP-HPLC 2-AB (Thaysen-Andersen et al., 2009); the percentage cumulative variance (*%CV*) calculated from their results and the *%CV* of an interassay control study of a large-scale study are presented for comparison with the results of this study (Table 4-7). Two observations were made: first, the analytical error was greater for low abundance glycoforms; second, the *%CV* was

equivalent for the Thaysen-Andersen et al. (2009) and the large-scale studies, but roughly double for this scale-down study. Thus, the glycoform variation observed in the scale-down was not wholly accounted for by the expected variation in the analytical method. This, however, does not mean that the variation should be attributed to the scale-down method, for such inconsiderable variation between scale-down samples could be attributable to typical variation between multiple identical vessels. Acceptable statistical analysis would require at least 10 (ideally >20) independent replicates.

Comparison with analysis conducted by Thaysen-Andersen et al. (2009) and the large-scale study was made from a single sample from a single vessel, and variation can therefore be clearly identified as being introduced only by the analytical method. In this scale-down study, however, six samples were taken from a series of six different experimental cases that had been conducted in duplicate. The cost and difficulty of thorough antibody quality analysis meant that it was not possible to analyse duplicates from the same experimental case. Sample variation could therefore have been introduced by several factors: the frozen storage period (-80°C), which differed for each sample, the purification process and by the analytical process; furthermore, it is certainly possible that some glycoform variation occurs between practically identical experiments. Unfortunately, the typically glycoform profile variation between identical STR experiments conducted in the large-scale study is unavailable.

Perturbations did not cause significant change to culture performance compared to the control, and all of the other techniques for protein analysis were equivalent. Thus, following cell viability and productivity, one might expect the

glycoform profile in experiments with recirculation through the PFR to be comparable, but different from the control experiment without recirculation. Even this was not so, and the small variation appeared to be arbitrary. Considering the expected variation in the analytical method for a single sample, it is concluded that the glycoform variation between experiments was unlikely to have been significant and should not be attributed to variation in the conditions created by the scale-down.

	Thaysen-Andersen et al., 2009		Large-Scale		Scale-Down	
Glycoform	**mean**	***%CV***	**mean**	***%CV***	**mean**	***%CV***
G0-N	0.90	**16.67**	n/a	n/a	n/a	**n/a**
G0	2.34	**8.55**	5.35	**6.30**	2.24	**17**
G0F	49.97	**2.84**	82.61	**0.53**	68.5	**6.3**
G1	n/a	**n/a**	2.11	**15.97**	1.12	**33**
G1F	40.58	**2.93**	9.57	**4.49**	24.87	**11.1**
G2F	6.22	**8.04**	0.60*	n/a	3.3	**30**

Table 4-7: Accuracy of the NP-HPLC 2-AB method for IgG glycoform profiling. Glycans removed from the antibody by enzymatic deglycosyalion were fluorescently labelled with 2-AB (2-aminobenzamide) and loaded on a Glycosep™ N HPLC for analysis (Section 2.14.2). The mean % relative amount of each glycoform and the % cumulative variance, *%CV*, for the six different experimental cases in this scale-down study (Section 2.7) were analysed once (N = 1) by one operator and compared with accuracy studies conducted using a single sample. The large-scale study analysed the same sample six times (N = 6) using six different operators. Thaysen-Andersen et al., (2009) did not specify number of operators and repeated analysis three times (N = 3). Note: n/a refers to glycoforms that were not present. * *%CV* is not provided for G2F in the large-scale study because G2F was not detected by 4 out of the 6 operators.

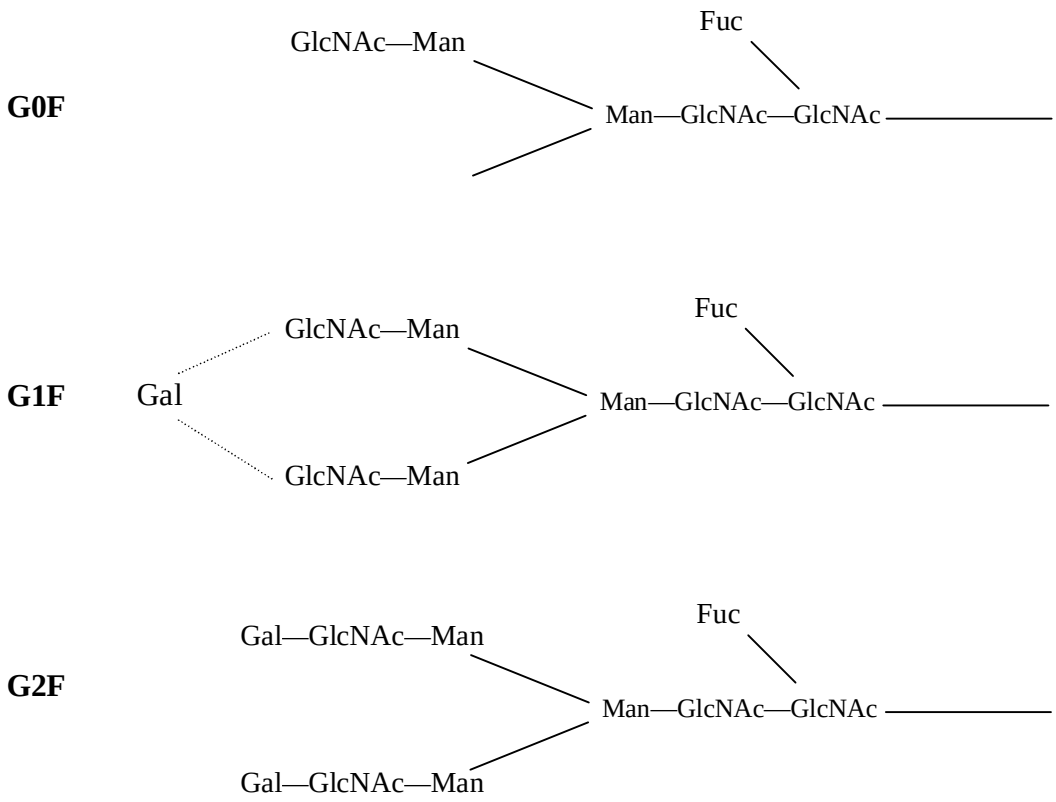

Figure 4-24: The glycoforms of IgG found in this study. Like all N-glycan they have the same core structure: three mannose (Man) and two N-acetyl glucosamine (GlcNac) ($Man_3GlcNac_2$). Therapeutic antibodies generally have 0, 1 or 2 galactose (Gal) terminal residues (G0, G1 and G2) and may have core fucosylation (Fuc). G2 is referred to as complex biantennary and is the common form found in the human immune system, often with terminal Sialic acid groups, not shown.

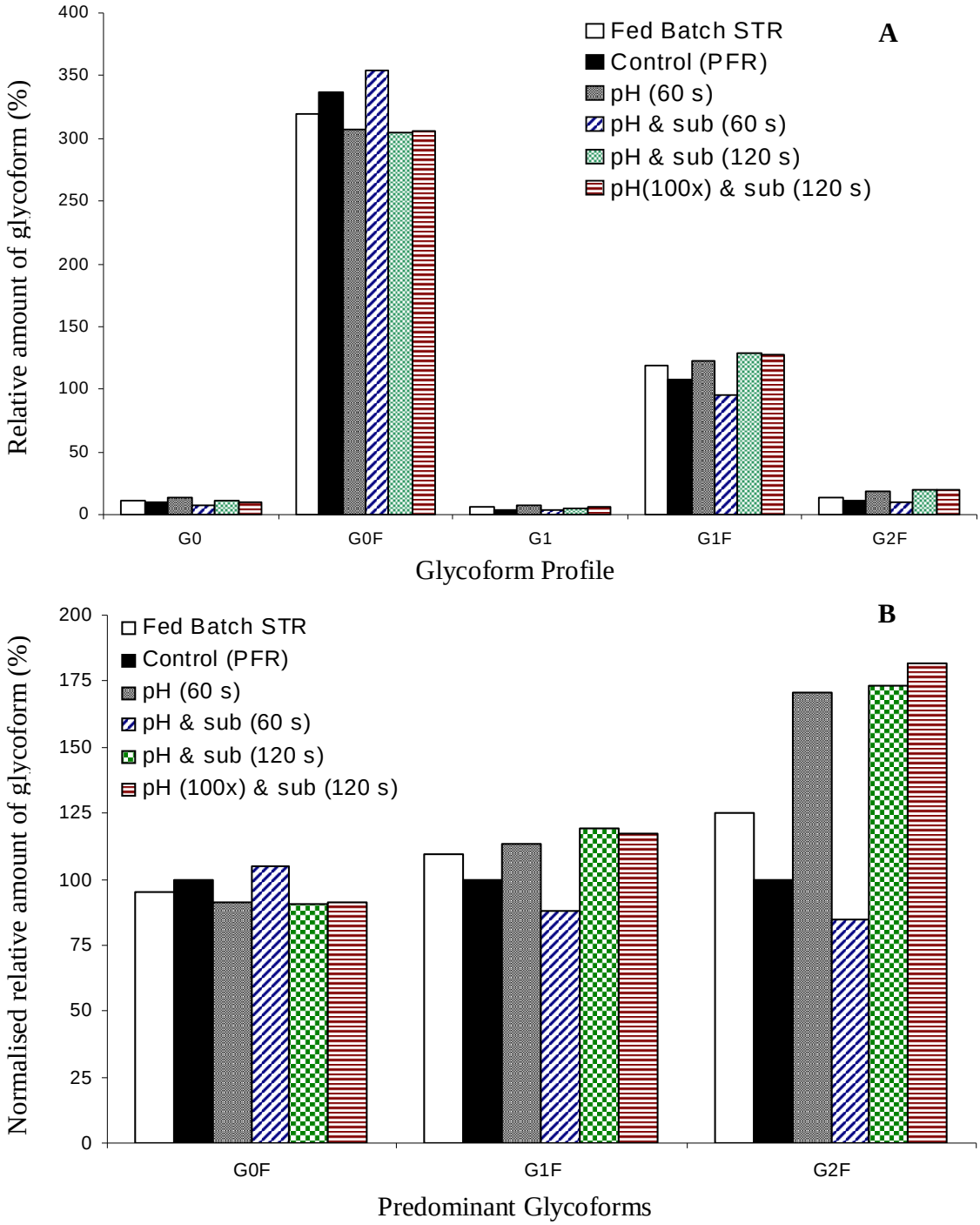

Figure 4-25: Bar chart A: mean relative % of each glycoform on the IgG antibody for each experimental case. Bar chart B: mean relative % of the predominant three glycoforms normalised to the Control (PFR), which is set at 100. Fed-batch STR (white); Control (PFR) (black); pH (60 s) (grey); pH & sub (60 s) (diagonal stripe); pH & sub (120 s) (checked); pH (100x) & sub (120 s) (striped). Using non-parametric ANOVA no significant difference was found in a multiple comparison to the control STR experiment.

4.5 Discussion

It has been consistently found that there was no significant difference between the control experiments and test experiments. A significant difference was observed only between the antibody titre, *VCN*, and viability of the fed-batch experiment without circulation through the PFR and all experiments with recirculation. The notable difference between the fed-batch experiment (1) and recirculation experiments (2 – 6), which are equivalent, leads to the already manifest conclusion: pH and substrate perturbations lasting for 60 s and 120 s had little effect on growth and viability of the GS-CHO cell line used in this study and other perturbations introduced by the PFR had negligible influence. Recirculation itself was the predominant factor.

This clearly demonstrates that, compared to the effects of circulating the culture through the PFR, the exposure of the culture to perturbations in pH and substrate of duration between 60 and 120 s and frequency determined by pH control and glucose requirement had little or no influence on the growth, production and antibody quality of the GS-CHO culture used in this study. The negligible influence of pH perturbations on cell culture is contrary to the findings of the Osman et al. (2002) study of multiple pH perturbations in GS-NS0 cell culture.

Antibody quality was comprehensively addressed and found unaltered by the scale-down. Changes to the glycoform profile were not considered significant and are attributed to typical variation in low abundance glycoforms, introduced by the analysis method. Unlike protein synthesis, antibody glycosylation is not template driven and is purportedly especially sensitive to process conditions (Wold, 1981; Goochee and Monica, 1990; Butler, 2004b). This study, however, showed that

glycosylation was altered neither by the conditions of the scale-down nor by recirculation.

It is surprising that antibody quality, which has been shown to be sensitive to nutrient levels, pH and shear (Section 1.1.1), was not altered by circulation that so manifestly altered cell growth and viability. This might be because the glycosylation of this antibody was in any case limited: in the majority of the literature, the predominant reported influence of process conditions on glycoform profile is to decrease sialylation (Borys et al., 1993; Andersen and Goochee, 1994; Wong et al., 2004; Trummer and Fauland, 2006), yet the CHO cell line used in this study lacks significant levels of sialyltransferase activity and the antibody is therefore expected to have negligible sialylation. Sialylation is the final step in glycoform processing, required for complex biantennary glycoforms that perfectly match the immunogenic qualities of antibodies generated by the human immune system, and it may be that in the animal cells used for therapeutic protein production sialylation is more sensitive to culture environment than steps earlier in the glycosylation pathway. Alternatively, perturbations may simply have been too brief to influence the protein: Werner et al. (1998) found the glycosylation profile of GS-CHO cells to be very stable, and alterations of any sort to immunoglobulins typically required exposure of the entire STR volume to sub-optimal conditions for hours and sometimes days.

Osman et al. (2002) found that the frequency of GS-NS0 exposure significantly altered the affect of pH perturbations (pH 7.3 to pH 8.0) on cell viability, showing that when the frequency of perturbations lasting 200 seconds (s) was increased from every 60 minutes to every 6 minutes cell death increased from ‘3.4% to 28.3%’. However, comparison between this study and their study is

impaired by the differences between the two scale-down models: they created perturbations in 17% of the culture volume that lasted for 200 s, as opposed to the 5% volume and maximum residence of 120 s used here. Between the two studies, frequency of perturbations was also likely to have differed considerably. In their study, perturbations were made with an arbitrarily regularity that was defined by the experimenter. In this study, perturbations occurred only when alkali was required to control pH at the setpoint, as in a large-scale STR. Unfortunately, equipment failures meant it was impossible to record the frequency of alkali additions. Nevertheless, the relatively low pH setpoint for the process used in this study was chosen, in part, to minimise the requirement for alkali.

No studies of the effect of single or multiple glucose perturbations could be found in the literature. The effect of glucose limitation on mammalian cell growth is reasonably well documented: glucose limitation is typically beneficial by decreasing production of metabolites (Europe et al., 2000). Since glucose concentration in the STR was not limiting, substrate perturbations in the PFR were unlikely to increase the production of metabolites greatly. Of greater concern was inhibition caused directly by glucose.

Only a few reports could be found concerning the direct inhibitory affect of elevated glucose concentration (Kurano et al., 1990a; Terada et al., 1998); these studies show that glucose inhibition can occur, but provide no account of the behaviour of animal cells when exposed to glucose elevation for a short duration. Experiments with substrate feeding to the PFR showed no significant difference in *qLactate* or μ compared to the other experiments. Thus, it can be concluded that either the perturbations in substrate created by the almost continuous slow feed of

substrate were insufficient to affect this GS-CHO culture, or that the cells were insensitive to elevated glucose perturbations of the sort created in the PFR. It is probable that both are true: perturbations generated by the substrate were slight and the cells robust.

Glucose perturbations created in two-compartment scale-down studies to generate glucose perturbations like those that occur in large-scale microbial STRs have been shown to alter microbial cell growth and recombinant protein productivity (Bylund et al., 1999; Hewitt et al., 2000; Hewitt and Nebe-Von-Caron, 2001). However, the low cell density, significantly lower rate of cell death, *td*, and correspondingly lower glucose uptake rate (*GUR*) and (*OUR*) of mammalian cell culture again makes a comparison between the two very difficult. For the high *GUR* in high cell concentration microbial culture will certainly result in greater glucose feed requirements and likely create much larger glucose perturbations that can cause O_2 deprivation in the PFR as a result of the cells' high *OUR* during glucose metabolism (Section 1.8.4).

Maintenance of consistent antibody characteristics is in accordance with the findings of Osman et al. (2001) that the antibody charge profile was unaltered (as measured by isoelectric focusing, IEF) when the harvested antibody in cell culture supernatant was incubated at the range of pH values investigated in their pH shift study. Unfortunately, their method accounted only for antibody quality changes that might have occurred in the culture medium after secretion from the cell, neglecting the possible influence of pH shifts on cellular antibody production mechanisms (Section 1.7.1.2). Antibody quality was not reported in their later study of multiple pH perturbations using a two-compartment model (Osman et al., 2002).

Consideration will now be given to what factor or factors created by recirculation through the PFR decrease cell viability in the stationary phase by approximately 20 to 30%, shortened culture duration by 48 h and decreased antibody titre by ~200 mg mL^{-1}, yet did not significantly alter any measured aspect of antibody quality.

What deleterious factors could recirculation through the PFR have introduced? There are at least three: first, heterogeneity introduced by the PFR; second, some sort of shear that was, perhaps, created by the rollers of the pump, air-liquid interfaces, or at the pipe wall; third, 'difficult-to-identify' factors such as leaching of contaminants from polymer connectors for tubing segments, or some deleterious surface interaction with the PFR's silicone and neoprene tubing. The possible combined synergistic effects of multiple factors may have been more damaging than would be expected from their effects alone. Each of these three factors, heterogeneity, shear and difficult-to-identify will be discussed in turn.

First, heterogeneity is inherent in design of the scale-down equipment. Even when alkali and substrate additions were made to the STR, the cell population will inevitably have been exposed to an environment in the PFR that differed from the perfectly mixed and controlled environment of the STR. The absence of pH control in the PFR meant that if significant quantities of metabolites were produced then the pH could be altered to the detriment of cells in the PFR. Nevertheless, it is clear that were the effects of any pH drop in the control recirculation experiment harmful, then pH alterations created by alkali additions to the PFR would surely have been to even greater detriment. The equivalence of all experimental cases with recirculation

implies that any pH perturbation created during recirculation in the PFR was unlikely to have been responsible for the difference created by recirculation.

The absence of an O_2 supply to the PFR could, if the *OUR* were great, have resulted in O_2 limitation within the duration in the PFR, and the same is true for substrate and substrate limitation. Both O_2 limitation and substrate limitation are found in similar two-compartment studies for microbial cells (Section 1.8). Animal cells are much less rapacious. The μ observed in this study was almost 100-fold lower than microbial culture (doubling time of around 24 h, compared to 20 minutes for *E.coli*) with concomitantly lower substrate and O_2 consumption and metabolite production. Calculations (Section 4.3.1) indicate that at 86 x 10^6 cells mL^{-1} and 120 s residence time (*RT*) in the PFR low dissolved oxygen tension (*DOT*) may have occurred. However, cell culture behaviour was equivalent between all recirculation experiments and those conducted with a mean residence time (*RT*) of 60 s in the PFR were unlikely to have experienced a drop in *DOT* of more than 15% even at *VCN*max (Section 4.3.1), such a drop is very unlikely to have altered cell physiology. In the literature for animal cell culture, O_2 limitation has been reported to decrease viability and titre when *DOT* drops below 5 or 10% (Section 1.7.3). Thus, either the small *DOT* perturbations probable in the PFR with 60 s residence decreased cell viability and titre to the same extent as possible larger perturbations at 120 s residence, or perturbations in *DOT* in both cases were insufficient to influence this cell culture. The latter is the more likely, since the oxygen consumption expected in the 60 s PFR is unlikely to have caused a *DOT* to drop that was deleterious.

As cells flowed through the PFR, they were exposed to the hydrodynamic environment created by the interaction of fluid with connecting tubes, ancillary fittings and the contact forces and localised shear in the peristaltic pump (Kieran et al., 1995; Natarajan and Mokhtarzadeh-Dehghan, 2000). Based on shear sensitivity studies (Section 1.6), cell damage in the conventional sense ('pure' shear) would require any shear mechanism in the pump to generate approximately an energy dissipation rate, ε, of at least 1 x 10^2 W kg^{-1}. Calculations show (Sections 5.4.3 and 5.4.4) that the maximum energy dissipation rate, $\varepsilon_{\max,pipe}$, created at the walls of the tubing in the PFR was, at 0.04 W kg^{-1}, far less than the maximum local energy dissipation rate, $(\varepsilon_T)_{\max}$, in the STR (1 W kg^{-1}, assuming $(\varepsilon_T)_{\max}$ = 100 x $(\bar{\varepsilon}_T)_{bulk}$), and at least 3 orders of magnitude lower than the threshold for damage reported in the literature. Therefore, if hydrodynamic 'pump damage' occurred in the PFR circuit, it may only be attributed to one or a combination of uncertain hydrodynamic mechanisms, such as compression or cavitation, such damaging mechanisms are referred to here as shear, even if this term is not strictly applicable in its pure sense.

Pump damage was not reported in any of the previous two-compartment scale-down studies found in the literature. This may be expected for small robust microbial cells, but may be surprising for 'shear sensitive' mammalian cells. However, currently only one group could be found to have attempted a two-compartment scale-down study using mammalian cells (Osman et al., 2002) and it is unclear if their pumping was continuous or only during perturbations.

In studies of the continuous pumping of blood cells for medical purposes such as cardiopulmonary bypass (CPB), peristaltic pumping (sometimes referred to as roller pumping in the blood literature) has been cited as a cause of lysis

(haemolysis) and cumulative sub-lethal damage (Tamari et al., 1993; Morgan et al., 1998; Valeri et al., 2006). It is well established that CPB damages blood (Yarborough et al., 1966; Mulholland et al., 2000; Mulholland et al., 2005), and this damage is attributed to non-physiological forces (Blackshear et al., 1965; Nevaril et al., 1968; Leverette et al., 1972).

In the field of blood perfusion, a great deal of research has focused on ways to decrease this damage; for example, the materials are now exceptionally biocompatible (Mulholland et al., 2005). In addition, there are reports that haemolysis has been decreased by replacement of peristaltic pump with centrifugal pump (Takeda et al., 1984; Morgan et al., 1998); however, contradictory studies have observed no significant difference between haemolysis in peristaltic and centrifugal pumping (Takahama et al., 1985; Hansbro et al., 1999; Valeri et al., 2006). In peristaltic pumping, haemolysis and sometimes sub-lethal impairment has been generally attributed to compression of the tubing and a portion of cells that may become compressed with that section of tubing as the pump rollers rotate (Berstein et al., 1967; Sutera, 1977; Watanabe et al., 2006). Noon et al. (1985) found that blood damage in long-term perfusion was decreased by increasing roller diameter and tubing diameter, and increasing occlusion so that tubing compression was decreased to the point that it was just sufficient to create flow.

Using computational fluid dynamics to model a two-roller pump, Mulholland et al. (2005) reported the existence of ‘a sharp peak in shear stress occurs in roller pumps when the rollers are almost occluding the tube…and because the fluid is incompressible, the pressure between the rollers becomes very high and the fluid is driven through the narrow gaps very fast.’ They state that, as a result, there exists a

very thin boundary layer with high-velocity gradient, thus giving rise to a sharp peak of shear stress, which can reach values of almost 1000 Pa. Haemolysis has also been attributed to 'detrimental flow structures' such as areas of turbulence, stagnation, vortices, high shear-stresses, negative pressure and cavitation (Tsujino et al., 1999; Mulholland et al., 2005; Lee et al., 2009). It is possible that one or a combination of these mechanisms reported to have caused haemolysis resulted in the detrimental affect of recirculation in this study.

The literature provides strong evidence that roller pumps are capable of generating shear that will damage blood cells. How well this translates to GS-CHO cell behaviour during pumping is unknown. Blood cells, like vascular endothelial cells (Malek and Izumo, 1994; Lehoux et al., 2006), may well be physiologically adapted to respond to shear, while GS-CHO have likely been widely adopted for therapeutic production because of their relative insensitivity to shear. Critically, the flow rates of blood pumping studies are typically far greater than used in this study. A flow rate of at least 8000 mL min^{-1} is required for CPB, whereas the maximum flow rate in this study was only 150 mL min^{-1}. Nevertheless, if the mechanism of damage was occlusion by compression of the tubing, flow rate may not have been a key factor in damage. Furthermore, only a small number of cells need be damaged with each rotation of the pump for any of these shear mechanisms to become a significant cause of cell damage during continuous recirculation over the duration of a cell culture, which, needless to say, is many times longer than even the most traumatic operation. Cell damage might take the form of lethal (immediate lysis) or sub-lethal damage; both are thought to occur in the peristaltic pumping of blood.

Osman et al. (2002) do not report pump damage in their two-compartment (STR+STR) study of pH perturbations in GS-NS0 culture, using a recirculation flow rate of 100 mL min^{-1}, provided by a peristaltic pump like the one used in this study (Watson Marlow, 502 S). They do not specify if pumping between the two STR was continuous, or when required to create the pH perturbations. Since perturbations were conducted at specific times, the latter is possible. Neither do they provide a comparison of the recirculation control experiment to a control experiment without recirculation, so it cannot be established whether recirculation itself was deleterious, but to a lesser degree than the pH perturbations.

Perfusion culture of mammalian cells provides another, more frequently studied, example of two-compartment culture. Pump damage was found to decrease the viability of a variety of cell types, including of insect (Merten, 2000; Gorenflo et al., 2004), hybridoma (LaPorte et al., 1996) and CHO cells (Kim et al., 2008). Pump damage was a reported problem in the literature on perfusion culture, but no studies could be found that provided a control study in which cell culture was pumped around the perfusion circuit without perfusion of fresh medium and removal of by-products (e.g., metabolites). In spite of possible pump damage, perfusion culture is also often reported to have greater cell concentration and protein productivity than fed-batch culture (Meuwly et al., 2006; Choo et al., 2007). Pumping effects may be overwhelmed by the benefits generated by the continuous removal of by-products and continuous supply of fresh medium. In support of this premise, perfusion systems that do not circulate a cell suspension, such as depth-filter perfusion systems, are often reported to provide improvements over conventional perfusion (Lee et al., 2005). The rates of pumping in perfusion culture are, in any case, lower

than in this scale-down study, and are therefore likely to be less damaging. This point is illustrated by perfusion rates, which are sometimes reported in STR volumes per day (d^{-1}). Perfusion systems might typically be operated at from 1 to 10 d^{-1}, around 1 to 10 mL min^{-1} for a 2 L laboratory-scale STR (Merten, 2000; Lee et al., 2005; Choo et al., 2007; Kim et al., 2008). Compare this to the scale-down experiments in this study that had a flow rate equivalent to from 108 to 216 d^{-1}, for 120 s and 60 s residence times (*RT*), respectively.

Given that no damage was reported in the Osman et al. (2002) two-compartment (STR+STR) study and that other continuous pumping studies provided a poor comparison (i.e., flow rate is far greater for CPB and far lower for perfusion cell culture), it was reasonable to consider peristaltic pumping as acceptable for recirculation in this two-compartment study.

If it were accepted that pump damage, and therefore probably a shear flow or shear mechanism of some sort (using shear in it loosest sense), were responsible for the difference between the normal fed-batch STR and all of the experiments with recirculation, then recirculation cases might bear some comparison with animal cell culture under conditions of elevated shear. Unfortunately, there are few reliable studies in this area and the mechanism by which shear damage was created would likely differ from this scale-down study. Nevertheless, there is limited evidence that cells' response to shear varies throughout the duration of a typical STR cell culture in accordance with the results of this scale-down study.

In the rapid phase of growth, cells have exhibited decreased susceptibility to 'shear damage' and, in accordance with this study, responded to shear with increased μ (Mardikar and Niranjan, 2000). Furthermore, as in this study, during the

stationary and death phases, 'shear sensitivity' has been reported to increase with a concomitant decrease in viability (Petersen et al., 1988; Zang et al., 1993).

Two relevant studies investigated the effects of 'repetitive hydrodynamic stress' on CHO cells (Godoy-Silva et al., 2009b; Godoy-Silva et al., 2009a): rCHO cells were, for the duration of the culture, circulated through a flow constriction device, referred to as the torture chamber (TC). The TC was used to create a defined energy dissipation rate, (ε_{TC}). The median of a distribution of maximum energy dissipation rates, $(\varepsilon_{TC})_{\max}$, was used to characterise the extent of the hydrodynamic forces, the shear, acting on cells in the TC. A syringe pump was used instead of a peristaltic, purportedly to create relatively pulse free flow; avoidance of 'pump damage' was not reported as a factor in pump selection. The syringe pump was also likely chosen as a reliable means to overcome the pressure drop created by the TC. No 'pump damage' was reported.

Compared to the expected maximum local energy dissipation rate, $(\varepsilon_T)_{I\max}$, in a large-scale STR (less than 0.01 W kg^{-1}) the values generated in their studies are high; nevertheless, the repeated exposure to shear in the TC may be analogous to the repeated exposure to the pump in this study, and it might therefore be instructive to compare the two. Godoy-Silva et al. (2009b) found that repeated exposure to shear ranging from 2.9 x 10^{2} W kg^{-1} to 2.3 x 10^{3} W kg^{-1} increased $\mu_{\max}$ and decreased viability, and culture duration of CHO cells (CHO-6E6), in accordance with this study. However, the group's later study (Godoy-Silva et al., 2009a) using the same shear method on a different industrially relevant rCHO cell line (provided by Pfizer), reported that $(\varepsilon_{TC})_{\max}$ from 60 W kg^{-1} to 6 x 10^{3} W kg^{-1} increased the glycosylation

of an IgG antibody (glycosylation was not measured in their earlier study) and did not significantly alter any other aspect of the culture's performance, including viability, VCN_{max} and antibody titre. Different cell lines were used for their two studies and it is therefore likely that their results were cell line specific, as they noted (Godoy-Silva et al., 2009a). Sensitivity to shear has been found to vary between cell lines (McQueen and Bailey, 1989; Zhang et al., 1993). It is important to note that type and intensity of shear may be important (Tanzeglock et al., 2009), and are certain to have differed between the PFR studied here and the TC.

Shear in the above continuous recirculation study (Godoy-Silva et al., 2009a), was considered to have influenced protein production pathways *in-vivo*. However, once secreted from the cell, the antibody very likely continues to be sensitive to the effects of shear and there are several reports in the literature of elevated protein aggregation and unfolding because of shear. Thus, if the detrimental effects of recirculation on the cell culture were created by shear, then why was the antibody unaffected?

When air-liquid interfaces are carefully removed, laminar shear rates in the order of 1×10^{7} s^{-1} are reportedly required to cause aggregation and/or protein unfolding in concentrated solutions of proteins of viscosity equal to water (Jaspe and Hagen, 2006). Shear stress is perhaps a better measure of the denaturing force acting on the protein; moreover, the shear stress required to disrupt animal cells is well documented in the literature. The typical therapeutic protein formulation used in studies for sensitivity to shear rate is a Newtonian fluid with viscosity similar to water (Jaspe and Hagen, 2006), using viscosity, η (1×10^{-3} Pa s), shear stress, τ (Pa), is simply calculated from shear rate, $\dot{\gamma}$ (s^{-1}), using $\tau = \eta\dot{\gamma}$. Thus, using the

reported antibody damaging shear rate of 1 x 10^7 s^{-1}, antibody damage might be expected at shear stresses above 1 x 10^4 Pa.

Shear stresses reported as causing cell damage vary considerably from 19 x 10^{-3} Pa to 100 Pa with exposure times between 24 h and 10 minutes (Born et al., 1992). Thus, it is clear that the shear stress required to disrupt animal cells is at least two orders of magnitude less than that typically required to aggregate or unfold globular proteins. Therefore, shear in the pump could have been sufficient to decrease cell viability, while being insufficient to alter antibody folding and aggregation.

Other potentially deleterious hydrodynamic factors (shear) such as air-liquid interfaces (Maa and Hsu, 1997; Oliva et al., 2003) pump cavitation and bubble entrainment have also been reported to cause aggregation and/or unfolding of proteins during pumping for cross flow filtration (Narendranathan and Dunhill, 1982; van Reis and Zydney, 2007). The insignificant difference in antibody quality between all experimental cases in this study suggests that such factors were not great or were mitigated. Considering the far greater reported sensitivity of typical animal cells to shear stress than therapeutic proteins, it is certainly possible that the cell damage could have occurred at shear stress levels far below that required to damage the antibody, and, as mentioned above, shear of this type has been found to damage blood cells during continuous pumping. Thus, shear in the pump, such as cavitation and other forms of bubble creation and destruction could have been sufficient to decrease cell viability, while being insufficient to alter antibody folding and aggregation.

In long-duration shear experiments, it has been speculated that the action of damage to proteins attributed to shear might actually be attributable to uncontrolled difficult-to-identify factors. Perhaps this is also the case for the pumping of animal cells. Surface adsorption and associated conformational perturbations has been reported to act synergistically with shear to cause IgG aggregation (Biddlecombe et al., 2007), and during peristaltic pumping of recombinant interleukin-2, exposure to silicone rubber surfaces (and not shear) caused 97% loss in bioactivity (Tzannis et al., 1997). Sub-visible particulates have been shed from stainless steels pumps causing aggregation (Cromwell et al., 2006; Tyagi et al., 2009). In addition, it has been speculated that difficult-to-identify, uncontrolled factors in longer duration shear experiments, like leaching of contaminants, could cause protein aggregation (Bee et al., 2009).

In this study, neoprene particle contamination might have been caused by tube wear at the pump head, and chemicals may leach from tubing or connecting polymers (Hill et al., 2001); no reports were found of chemical leaching from neoprene. In this study, the peristaltic pump created visible tube wear on the exterior of the tubing in the pump head (neoprene was chosen because of its resilience), perhaps some small particles were created by wear of the inner bore of the tubing, such a process is referred to as spallation (Barron et al., 1986; Briceño and Runge, 1992). Particles were not observed, but could have been sub-visible. Whether they existed is unknown, but such factors evidently did not alter antibody quality. It is possible that the cell damage occurred at levels of physical and chemical contaminants far below those damaging to the antibody, and surface interactions may have detrimentally influenced only the cells. No reports in the literature could

be found that considered the influence of such factors during continuous long-duration pumping of cell culture. No reports of chemical leaching from neoprene tubing could be found in the literature. No reports could be found of cell viability and titre diminution by non-visible neoprene or silicone particulates.

Silicone is generally considered stable and non-toxic, but it has been reported that the method used to vulcanize the silicone influences its biocompatibility: peroxide cured silicone tubing was found to be toxic to a suspension of tobacco cells. Platinum cured silicone tubing, as used for the PFR in this study, was found to be non-toxic (Park et al., 2005). In addition, biocompatibility is controlled for assiduously in recent blood pumping studies, and damage from similar pumping occurred (Mulholland et al., 2005). Nevertheless, by their very nature, it is difficult to rule out the influence of such 'difficult-to-identify' factors on *VCN*, viability and titre.

All three factors, heterogeneity, shear and difficult-to-identify could have contributed to the damaging effects of recirculation. Indeed, possible synergistic effects of all three could have exacerbated the negative influence of any other factor that alone may have been negligible. Nevertheless, despite the absence of evidence in the literature for peristaltic pump damage of animal cells at the flow rates used in this study, it is proposed here that 'shear' was the predominant means by which cell damage occurred, perhaps the occlusion mechanism that has been proposed to create damage in blood pumping. Even if the maximum shear stress in the peristaltic pump used in this study was an order an of magnitude less than the expected maximum shear stress (~1000 Pa) calculated by CFD of a peristaltic blood pump, this GS-CHO

cell line need not be especially shear sensitive to have suffered some appreciable damage over the duration of the culture.

In the literature, no study could be found that subjected a fed-batch animal cell culture to continuous peristaltic pumping for the duration of the culture. Comparison with perfusion culture is difficult because of the low flow rates used for perfusion and fact that perfusion itself is intended to alter culture performance. Insensitivity of this GS-CHO cell line to pH and substrate perturbations deliberately introduced to the PFR suggests that heterogeneity created by recirculation alone had little influence. The predominance of silicone and neoprene in cell culture suggest high biocompatibility with cell culture, lowering the probability of difficult-to-indentify factors; clearly, such factors were below the threshold required to damage the antibody.

GS-CHO cell growth and protein production was shown in this study to be robust, in accordance with Werner et al. (1998), and it can be concluded that if pH and substrate perturbations in a large-scale (20 m^3) STR are similar to those created in this scale-down then they are unlikely to affect any important aspect of GS-CHO culture performance.

Chapter 5: Conclusions

Research for this thesis was conducted to test the hypothesis that a two-compartment scale-down model, like that used for scale-down of microbial cell culture, can be used to generate perturbations in pH and substrate that resemble those that occur in a large-scale stirred tank reactor for commercial production of therapeutic proteins from animal cell culture. Further, that these perturbations influence important aspects of the culture performance, such as antibody concentration (titre) and antibody characteristics (antibody quality).

The results of this thesis provide evidence against both parts of this hypothesis and instead support two conclusions, on the basis that the cell line used in this study is not considered to be especially sensitive. Firstly, that recirculation itself is a confounding factor in the creation of similar two-compartment scale-down models for animal cell culture generally. It is considered likely that this is because of their greater sensitivity, compared to microbial cells, to mechanical damage created by some aspect of pumping, but greater sensitivity to other difficult-to-identify factors cannot be excluded. Secondly, that perturbations in pH and substrate have no significant influence to culture of this cell line with this process (e.g., medium composition, feeds composition, feed schedule and reactor control parameters), and, therefore, that perturbations associated with vessel heterogeneity at the large-scale are unlikely to influence culture of the cell line at large-scale. Such perturbations, however, may influence other cell lines more sensitive to pH or feed perturbations.

Experiments using a scale-down model combining a stirred tank reactor and plug flow reactor (STR+PFR) were conducted with the aim of creating pH and

substrate heterogeneity that was similar to the expected heterogeneity in these parameters in a typical poorly mixed large-scale STR used for cultivation of animal cells for therapeutic antibody production. pH and substrate perturbations were found to have no significant effect on any measured parameter of the cell culture, including cell viability, antibody titre and antibody quality (e.g., glycosylation). It was shown that no significant difference existed between all experiments in which culture was recirculated continuously from the STR and through the PFR. Scale-down experiments in which perturbations were created in the PRF at mean residence times (*RT*) of 60 seconds and 120 seconds (s) were all equivalent to the scale-down control experiment, which had continuous recirculation, but pH control and substrate feed to the STR. Thus, this strongly implies that for this scale-down model recirculation is a confounding factor in the investigation of the influence of pH and substrate perturbations.

All experiments with recirculation from the STR though the PFR by continuous pumping with a peristaltic pump were found to have decreased viability and antibody titre. Recirculation was found to decrease specific rate of antibody productivity, *qIgG*, and shorten the rapid growth phase by approximately 48 hours (h). Unlike the fed-batch STR, experiments with recirculation did not have a pronounced stationary phase and cell death and significant viability decline began at the end of the rapid growth phase. Metabolite profiles were unaltered in magnitude and followed cell growth. Antibody quality was consistent for all experiments, with or without recirculation, showing that antibody quality attributes for this cell line were unaltered by deleterious conditions that resulted in considerably decreased cell

viability and, furthermore, likely increased significantly the quantity of extracellular agents considered able to alter antibody-characteristics.

It has not been possible to arrive at any firm conclusions as to the nature of damage created by recirculation. Deleterious oxygen and other substrate deprivations are considered unlikely because of animal cells' low oxygen uptake rate (*OUR*) and glucose uptake rate (*GUR*). (Note: substrate here refers to the nutrients in the medium and feed, and composition was predominantly glucose). Calculations using the expected *OUR* from the literature showed that oxygen limitation was possible only at viable cell numbers (*VCN*) above 86 x 10^6 cells mL^{-1} for 120 seconds (s) mean residence time (*RT*) in the PFR and 170 x 10^5 cell mL^{-1} for the 60 s *RT* case. Substrate consumption for the *RT* in the PFR was negligible. The equivalence of both experimental cases (*RT* of 60 s and 120s), and the very unlikely occurrence of oxygen limitation in the 60 s *RT* case, suggests that neither oxygen nor substrate limitation were significant factors in either case.

The maximum energy dissipation rate generated by laminar flow at the wall of the tubing at the maximum flow rate and minimum tubing diameter, $\varepsilon_{\max, pipe}$, was shown (Section 4.3.3) to be three orders of magnitude below the minimum energy dissipation rate, ε_T, expected to cause damage to typical animal cells. The proven industrial efficacy of the commercial glutamine synthetase Chinese hamster ovary (GS-CHO) cell line used in this study means that greater than typical sensitivity was improbable. Nevertheless, it is proposed that the most likely cause for recirculation damage was some sort of shear, which may have been created by one or several mechanisms, such as bubble entrainment, cavitation and shear stress created by tube compression in the pump head. Several studies of the effects of peristaltic pumping

on blood cells provide evidence that blood cells are damaged by the peristaltic pumping and not oxygen deprivation or biocompatibility issues. Difficult-to-identify uncontrolled factors such as poor biocompatibility of tubing materials may have resulted from chemical leaching and particulate-cell interactions, which may have increased significance with duration of recirculation. It is of course possible that one or multiple types of shear and difficult-to-identify factors were acting synergistically to become more damaging than they would have been alone, but with the high biocompatibility of the materials used in this study this reason is considered less likely.

For the first time, flow cytometer was applied to monitor the effects of the scale-down on multiple parameters. Cell culture viability was measured on the flow cytometer (FC) using a dual stain with Calcein-AM and Propidium Iodide (PI) (Calcein-AM/PI). Calcein-AM was used as a positive control for viability; exclusion stain PI was used to indentify dead cells based on their cytoplasmic membrane integrity. This FC staining protocol was compared to the traditional method for discrimination between live and dead cells: haemocytometer and Trypan Blue (TB) exclusion. Both methods were used for all experiments; this allowed a reliable statistical comparison of viable and dead cell counts by the two methods. This comparison indicated that the flow cytometric method had erroneously included cell debris in the dead cell count, increasing the total cell count above that found by the haemocytometer. The likely cause for the inclusion of cell debris was the large quantities of debris present in all scale-down experiments. No significant difference in the viable cell number (*VCN*) was found between the flow cytometric and haemocytometric methods.

The presence of a small sub-population (~5%) that stained with both Calcein-AM and PI in all experiments, demonstrates that Calcein-AM was an unreliable single indicator of viability, contrary to the claims of some research papers. The likely cause of the dual stained population was relatively slow exclusion of Calcein (the fluorescent product) and/or energy independence of the intracellular esterase reaction. It is thought highly probably that dual stained cells were killed at some point during the staining method. Sample manipulation and a change of environment are thought to have been responsible for cell death during the staining procedure. Dual staining is therefore thought to provide a possible indicator of a sub-population of viable cells that have increased sensitivity to the sub-optimal conditions encountered during sampling and staining.

Dual staining with annexin V conjugated to phycoerythrin (AV-PE) and the exclusion stain, Sytox Green (SG), (AV-PE/SG) was used to identify mode of cell death in all experiments. SG is analogous to PI. AV-PE stains phosphatidylserine (PS) when it translocates from the inside to the outside of the cytoplasmic membrane; in apoptosis, this translocation of PS occurs while the integrity of the cytoplasmic membrane is maintained. AV-PE was shown to be unreliable as a single stain indicator of apoptosis because staining with the exclusion stain, SG, identified cells as having permeable cytoplasmic membrane, and therefore as having died by necrosis, not apoptosis. Indeed, in all experiments, cell death occurred only by necrosis. The proven apoptosis inducer CCCP did not induce apoptotic cell death in this cell line, and caused an increase in cell death by necrosis. The dual staining results emphasise the importance and utility of combined staining with an exclusion stain. Were AV-PE used alone, necrotic cells might easily have been misinterpreted

as apoptotic. Indeed the light scattering properties of the necrotic cells in this study were shown to be similar to those stated for apoptotic cells in one review paper.

An effort was made to develop flow cytometric protocols for monitoring mitochondrial membrane potential ($\Delta\Psi m$) by screening $DiOC_6(3)$ in conjunction with PI, JC-1, and CM-H_2XRos. CCCP was used as a 'decoupler' that has been shown to effectively remove mitochondrial membrane potential in other studies. Dual staining with $DiOC_6(3)$ and PI ($DiOC_6(3)$/PI) showed that cells that stained positive for intact $\Delta\Psi m$ with $DiOC_6(3)$ and positive for permeable cytoplasmic membrane with PI. $\Delta\Psi m$ is very likely lost when the cytoplasmic membrane has lost integrity and become permeable to PI; thus, $DiOC_6(3)$ proved to be an ineffective monitor of $\Delta\Psi m$. Binding of the stain in a $\Delta\Psi m$ independent manner suggests that the lipophilic properties of the stain allowed non-specific cytoplasmic and cell organelle staining.

The efficacy of JC-1 as an indicator of $\Delta\Psi m$ was cast into doubt by the presence of staining indicative of elevated $\Delta\Psi m$ in cells that were shown, by back-gating, to be necrotic in their light scattering properties. The light scattering properties of necrotic cells in the cell line were established with confidence by back gating from the green fluorescence v red fluorescence cytographs (GF-RF) of cells stained with the two different exclusion stains, PI and SG, to forward scatter light v side scatter light cytographs (FS-SS). Based on its ambiguous results, it was concluded that JC-1 was an unreliable indicator of $\Delta\Psi m$.

CM-H_2XRos revealed a subpopulation of cells with elevated fluorescence. By back gating to FS-SS cytographs it was shown that this population was likely dead; however, it should be noted that the staining method involved fixing the cells

in paraformaldehyde, which may have altered the cells' light scattering properties. Assuming that this population was dead, the elevated fluorescence was attributed to increased levels of reactive oxidative species (ROS) created during mitochondrial degradation, as opposed to elevated respiration, perhaps by decoupling. Despite these positive results that suggest the stain could be used to detect elevated ROS, CM-H_2XRos did not pass through the screening stage because recent research by another group had shown that nitrogen storage, which was unavailable, was required for the stain to retain activity over the course of a typical cell culture period. Thus, all of the prospective $\Delta\Psi$m monitoring stains were found unsuitable at the screening stage and were not used for characterisation of the fed-batch stirred tank reactor (STR) or scale-down experiments.

Cell debris was shown by FS-SS cytographs to increase greatly in all experiments with recirculation, indicating that dead cells were rapidly degraded by some process that occurred during recirculation. Flow cytometric analysis of the scale-down experiments showed that the mode of cell death and degree of population heterogeneity was invariant for all experiments and was therefore unchanged by the deleterious conditions created in the scale-down experiments. In view of these results, it is likely that scale-up of this process to a poorly mixed STR would not result in a more than acceptable alteration to antibody titre and antibody quality.

Chapter 6: Recommendations for Future Work

Testing different pumps could establish if type of pump and pump specific shear mechanisms are responsible for damage during continuous recirculation. One mechanism of damage in peristaltic pumping might be the compression of a small proportion of cells as the peristaltic pump's rollers push fluid through the tubing. A peristaltic pump with adjustable occlusion (i.e., the amount the roller compresses the tubing), may surmount this problem. Tube diameter and roller width might also be beneficially varied.

Consideration should also be given to pumps that operate using different mechanisms to move fluid. Modern free flotation magnetically levitated ('MagLev') centrifugal pumps (Hijikata et al., 2008) are purportedly capable of aseptically pumping blood at the flow rates required for the scale-down with reported low levels of haemolysis. In blood pumping, some studies have found that replacement of peristaltic pump with centrifugal pump decreased haemolysis.

Syringe pumping has been used for continuous recirculation similar to that conducted in this study without reported 'shear damage' and could be set-up so that the syringe plunger stopped just short of the end of syringe head, to avoid possible cell compression. However, syringe pumps may be unable to reach the relatively large flow rate required for a 60-second mean residence time in the PFR. To avoid problems of plunger wear, a Teflon plunger used with a glass syringe would likely be required for continuous pumping during a 20-day culture. To identify poor biocompatibility and other difficult-to-identify factors, different types of material for tubing and connectors should be investigated.

Chapter 6: Recommendations for Future Work

Construction of a bespoke plug flow reactor (PFR) that creates turbulent axial mixing at flow rates that would otherwise be in the laminar flow regime in pipe flow would improve attainment of true plug flow. True plug flow would be useful for modelling the scale-down mathematically, but may not significantly improve the validity of the scale-down. Turbulence could be introduced by baffles or a screw/helix. The PFR would need to be robust and either disposable or easily cleaned and sterilised. A disposable option might be simply constructed by the insertion of a reusable flexible plastic helix of appropriate diameter into a length of silicon or neoprene tubing, as used in this study. A stainless steel construction is recommended for any non-disposable option.

Significant and deleterious oxygen limitation was unlikely to have occurred in the PFR, as shown by calculations of oxygen uptake rate (*OUR*); nevertheless, the PFR would be improved by the incorporation of an O_2 probe at its terminus. The scale-down would also benefit by characterisation of the pH perturbation in the PFR. Characterisation could be accomplished by the incorporation of two pH probes in the PFR: one probe immediately down stream of the feeding point and a second probe at the terminus. To accomplish this would probably require several control units.

Further research with a scale-down would benefit from the comparison of several different cell lines, as there is evidence in the literature that sensitivity to perturbations (and ‘shear damage’) varies considerably between different cell lines. Therapeutic proteins, too, have been shown to have varying sensitivity to conditions in the STR, both during intracellular processing and while in the medium after secretion from the cell.

Flow cytometric analysis demonstrated that the cell culture was unlikely to exist as a binary mixture of live and dead cells, and was instead likely composed of a mixture of cells with varying degrees of viability, and perhaps productivity. If cells with elevated productivity were identified this could be used with the scale-down to aid development of an improved process for transfer to the large-scale. Mitochondrial membrane potential ($\Delta\Psi m$) is known to correlate with mitochondrial activity which is may be correlated with protein productivity. It would certainly benefit characterisation of the scale-down if an effective protocol for measurement of $\Delta\Psi m$ were developed for this cell line.

Apoptotic cell death was not observed in the GS-CHO cell line used for this study, using the proven AV-PE/SG staining method. To support further the conclusion that apoptosis does not occur in this cell line, different staining protocols for mode of cell death would have to be developed and investigated. Knowledge of the mode of cell death might permit future studies to optimise the process conditions in the scale-down to favour the most desirable mode of cell death for any particular process, possibly influencing productivity and down stream processing.

References

Akagi Y, Ito K, and Sawada S (1993). Radiation-Induced Apoptosis and Necrosis in Molt-4 Cells: a Study of Dose Effect Relationship and Their Modification. International Journal of Radiation Biology. **64:** 47-56.

Al-Rubeai M (1999). Monitoring Animal Cell Growth and Productivity by Flow Cytometry. In: Animal Cell Biotechnology, (145-153). Humana Press.

Al-Rubeai M and Emery AN (1990). Mechanisms and Kinetics of Monoclonal Antibody Synthesis and Secretion in Synchronous and Asynchronous Hybridoma Cell Cultures. Journal of Biotechnology. **16:** 67-85.

Al-Rubeai M, Emery AN, Chalder S, and Goldman MH (1993). A Flow Cytometric Study of Hydrodynamic Damage to Mammalian Cells. Journal of Biotechnology. **31:** 161-177.

Al-Rubeai M, Kloppinger M, Fertig G, Miltenburg HG, and Emery AN (1992). Monitoring of Biosynthetic and Metabolic Activity in Animal Cell Culture Using Flow Cytometric Methods. In: European Society for Animal Cell Technology, The 11th Meeting., (301-306). Oxford: Butterworth-Heinemann.

Al-Rubeai M, Oh SKW, Musaheb R, and Emery AN (1990). Modified Cellular Metabolism in Hybridomas Subjected to Hydrodynamic and Other Stresses. Biotechnology Letters. **12:** 323-328.

Al-Rubeai M, Singh RP, Goldman MH, and Emery NH (1995). Death Mechanisms of Animal Cells in Conditions of Intense Agitation. Biotechnology and Bioengineering. **45:** 463-472.

Al-Rubeai M, Welsenback K, Lloyd R, and Emery AN (1996). A Rapid Method for Evaluation of Cell Number and Viability by Flow Cytometry. Cytotechnology. **24:** 161-168.

Alberts B, Bray D, Lewis J, Raff M, Roberts K, and Watson JD (1989). Molecular Biology of the Cell. New York: Taylor & Francis.

Altamirano C, Illanes A, Becerra S, Cairo JJ, and Godia F (2006). Considerations on the Lactate Consumption by CHO Cells in the Presence of Galactose. Journal of Biotechnology. **125:** 547-556.

Altman SA, Randers L, and Govind R (1993). Comparison of Typan Blue Exclusion and Fluorometric Assays for Mammalian Cell Viability Determinations. Biotechnology Progress. **9:** 671-674.

Amanullah A (1994). Scale Down Models of Mixing Performance in Large Scale Bioreactors. University of Birmingham.

Amanullah A, McFarlane CM, Emery AN, and Nienow AW (2001). Scale-Down Model to Simulate Spatial PH Variations in Large-Scale Bioreactors. Biotechnology and Bioengineering. **73:** 390-399.

Amanullah A, Nienow AW, and Buckland BC (2003). Mixing in the Fermentation and Cell Culture Industries. In: Handbook of Industrial Mixing; Science and Practice, (1071-1157). New York: Wiley-Interscience.

Amos B, Al-Rubeai M, and Emery AN (1992). Hybridoma Growth and Antibody Production in Extended Stationary States. In: Animal Cell Technology - Developments, Processes and Products, (254-257). Oxford: Butterworth-Heinemann.

Ananthakrishnan V, Gill WN, and Allen JB (1965). Laminar Dispersion in Capillaries: Part 1. Mathematical Analysis. American Institution of Chemical Engineers Journal. **11:** 1063-1072.

Andersen DC and Goochee CF (1994). The Effect of Cell-Culture Conditions on the Oligosaccharide Structures of Secreted Glycoproteins. Current Opinion in Biotechnology. **5:** 546-549.

Andree HA, Reutelingsperger CP, Hauptmann R, Hemker HC, Hermens WT, and Willems GM (1990). Binding of Vascular Anticoagulant Alpha (VAC Alpha) to Planar Phospholipid Bilayers. Journal of Biological Chemistry. **265:** 4923-4928.

Arden and Betenbaugh (2006). Regulating Apoptosis in Mammalian Cell Cultures. Cytotechnology. **50:** 77-92.

Arden N and Betenbaugh MJ (2004). Life and Death in Mammalian Cell Culture: Strategies for Apoptosis Inhibition. Trends in Biotechnology. **22:** 174-180.

Arimochi H and Morita K (2006). Characterization of Cytotoxic Actions of Tricyclic Antidepressants on Human HT29 Colon Carcinoma Cells. European Journal of Pharmacology. **541:** 17-23.

Armstrong JS, Steinauer KK, French J, Killoran PL, Walleczek J and Kochanski J et al. (2001). Bcl-2 Inhibits Apoptosis Induced by Mitochondrial Uncoupling but Does Not Prevent Mitochondrial Transmembrane Depolarization. Experimental Cell Research. **262:** 170-179.

Aubin JE (1979). Autofluorescence of Viable Cultured Mammalian Cells. Journal of Histochemistry and Cytochemistry. **27:** 36-43.

Augenstein DC, Sinskey AJ, and Wang DIC (1971). Effect of Shear on Death of 2 Strains of Mammalian Tissue Cells. Biotechnology and Bioengineering. **13:** 409-418.

Bailey JE and Ollis DF (1986). Biochemical Engineering Fundamentals. New York: McGraw-Hill.

Bajpai RK and Reuss M (1982). Coupling of Mixing and Microbial Kinetics for Evaluating the Performance of Bioreactors. The Canadian Journal of Chemical Engineering. **60:** 384-392.

Barda-Saad M, Zhang AS, Zipori D, and Rozenszajn LA (1997). Adhesion of Thymocytes to Bone Marrow Stromal Cells: Regulation by BFGF and IFN-{Gamma}. Stem Cells. **15:** 229-236.

Barnes LM, Bentley CM, and Dickson AJ (2000). Advances in Animal Cell Recombinant Protein Production: GS-NS0 Expression System. Cytotechnology. **32:** 109-123.

Barron D, Harbottle S, Hoenich NA, Morley AR, Appleton D, and McCabe JF (1986). Particle Spallation Induced by Blood Pumps in Hemodialysis Tubing Sets. Artificial Organs. **10:** 226-235.

Batandier C, Fontaine E, Keriel C, and Leverve XM (2002). Determination of Mitochondrial Reactive Oxygen Species: Methodological Aspects. Journal of Cellular and Molecular Medicine. **6:** 175-187.

Bee JS, Stevenson JL, Mehta B, Svitel J, Pollastrini J, and Platz R et al. (2009). Response of a Concentrated Monoclonal Antibody Formulation to High Shear. Biotechnology and Bioengineering. **103:** 936-943.

Benson RC, Meyer RA, Zaruba ME, and McKhann GM (1979). Cellular Autofluorescence--Is It Due to Flavins? Journal of Histochemistry and Cytochemistry. **27:** 44-48.

Berstein EF, Indeglia RA, Shear MA, and Varco RL (1967). Sublethal Damage to the Red Blood Cell From Pumping. Circulation. **35:** 226-233.

Biddlecombe JG, Craig AV, Zhang H, Uddin S, Mulot S, and Fish BC et al. (2007). Determining Antibody Stability: Creation of Solid-Liquid Interfacial Effects Within a High Shear Environment. Biotechnology Progress. **23:** 1218-1222.

Birch J. (2005). Future Perspectives of Antibody Manufacturing (Lonza).

Birch J, Thompson PW, and Boraston R (1985). Production of Monoclonal Antibodies in Large-Scale Cell Culture. Biochemical Society Transactions 609th Meeting. **13:** 10-11.

Birch JR and Racher AJ (2006). Antibody Production. Advanced Drug Delivery Reviews. **58:** 671-685.

Blackshear PLJ, Dorman FD, and Steinbach JH (1965). Some Mechanical Effects That Influence Hemolysis. American Society for Artificial Internal Organs. **11:** 112-117**.**

Bluestein M and Mockros L (1969). Hemolytic Effects of Energy Dissipation in Flowing Blood. Medical and Biological Engineering and Computing. **7:** 1-16.

Born C, Zhang Z, AlRubeai M, and Thomas CR (1992). Estimation of Disruption of Animal-Cells by Laminar Shear-Stress. Biotechnology and Bioengineering. **40:** 1004-1010.

Borys MC, Linzer DI, and Papoutsaki ET (1993). Culture pH Affects Expression Rates and Glycosylation of Recombinant Mouse Placental Lactogen Proteins by Chinese Hamster Ovary (CHO) Cells. Biotechnology (N Y). **11:** 720-724.

Boulton-Stone JM (1995). The Effect of Surfactant on Bursting Gas Bubbles. Journal of Fluid Mechanics. **302:** 231-257.

Boulton-Stone JM and Blake JR (1993). Gas Bubbles Bursting at a Free Surface. Journal of Fluid Mechanics. **254:** 103-111.

Bourne T, Fossati G, and Nesbitt A (2008). A PEGylated Fab' Fragment Against Tumor Necrosis Factor for the Treatment of Crohn Disease - Exploring a New Mechanism of Action. Biodrugs. **22:** 331-337.

Bratosin D, Mitofan L, Palii C, Estaquier J, and Montreuil J (2005). Novel Fluorescence Assay Using Calcein-AM for the Determination of Human Erythrocyte Viability and Aging. Cytometry Part A. **66A:** 78-84.

Briceño JC and Runge TM (1992). Tubing Spallation in Extracorporeal Circuits. An *In* Vitro Study Using an Electronic Particle Counter. The International Journal of Artificial Organs. **15:** 222-228.

Brodkey RS and Reuss M (1982). Fundamentals of Turbulent Motion, Mixing and Kinetics. Chemical Engineering Communications. **8:** 1-23.

Browing J, Varnedoe NB, and Swinford LR (1951). Fragility of Tetrahymena Geleii in Different Salt Solutions. Texas Reports on Biology and Medicine. **9:** 420-427.

Buchs J and Zoels B (2001). Evaluation of Maximum to Specific Power Consumption Ratio in Shaking Bioreactors. Journal of Chemical Engineering Japan. **34:** 647-653.

Butler M (2004a). Growth and Maintenance of Cells in Culture. In: Animal Cell Culture & Technology, (47-66). Padstow: Garland Science/ BIOS Scientific Publishers.

Butler M (2004b). The Glycosylation of Proteins in Cell Culture. In: Animal Cell Culture & Technology, (113-134). New York: Garland Science/BIOS Scientific Publishers.

Butler M (2005a). Animal Cell Cultures: Recent Achievements and Perspectives in the Production of Biopharmaceuticals. Applied Microbiology and Biotechnology. **68:** 283-291.

Butler M (2005b). Optimisation of the Cellular Metabolism of Glycosylation for Recombinant Proteins Produced by Mammalian Cell Systems. Cytotechnology. **50:** 57-76.

Bylund F, Collet E, Enfors S, and Larsson G (1998). Substrate Gradient Formation in the Large-Scale Bioreactor Lowers Cell Yield and Increases by-Product Formation. Bioprocess Engineering. **18:** 171-180.

Bylund F, Guillard F, Enfors SO, Tragardh C, and Larsson G (1999). Scale Down of Recombinant Protein Production: a Comparative Study of Scaling Performance. Bioprocess Engineering. **20:** 377-389.

Byun T, Zeng A, and Deckwer W (1994). Reactor Comparison and Scale-Up for the Microaerobic Production of 2,3-Butanediol by Enterobacter Aerogenes at Constant Oxygen Transfer Rate. Bioprocess and Biosystems Engineering. **11:** 167-175.

Cacia J, Quan CP, Vasser M, Sliwkowski MB, and Frenz J (1993). Protein Sorting by High Performance Liquid Chromatography. I: Biomimetic Interaction Chromatography of Recombinant Human Deoxyribonuclease I on Polyionic Stationary Phase. Journal of Chromatography. **634:** 229-239.

Campbell NA, Reece JB, and Mitchell LG (1995). Cellular Respiration: Harvesting Chemical Energy. In: Biology, (147-167). New York: Benjamin Cummings.

Capiaumont J, Legrand C, Carbonell D, Dousset B, Belleville F, and Nabet P (1995). Methods for Reducing the Ammonia in Hybridoma Cell Cultures. Journal of Biotechnology. **39:** 49-58.

Carvlhal AV, Marcelino I, and Carrondo MJT (2003). Metabolic Changes During Cell Growth Inhibition by P27 Overexpression. Applied Microbiology and Biotechnology. **63:** 164-173.

Castedo M, Hirsch T, Susin SA, Zamzami N, Marchetti P, and Macho A et al. (1996). Sequential Acquisition of Mitochondrial and Plasma Membrane Alterations During Early Lymphocyte Apoptosis. Journal of Immunological Methods. **157:** 512-521.

Catchpoole DR and Stewart BW (1993). Etoposide-Induced Cytotoxicity in Two Human T-Cell Leukemic Lines: Delayed Loss of Membrane Permeability Rather Than DNA Fragmentation As an Indicator of Programmed Cell Death. Cancer Research. **53:** 4287-4296.

Chaderjian WB, Chin ET, Harris RJ, and Etcheverry TM (2005). Effect of Copper Sulfate on Performance of a Serum-Free CHO Cell Culture Process and the Level of Free Thiols in the Recombinant Antibody Expressed. Biotechnology Progress. **21:** 550-553.

Chance B, Sies H, and Boveris A (1979). Hydrogen Peroxide Metabolism in Mammalian Organs. Physiological Reviews. **59:** 527-605.

Chen P and Harcum SW (2005). Effects of Amino Acid Additions on Ammonium Stressed CHO Cells. Journal of Biotechnology. **117:** 277-286.

Chen Z, Lutkemeyer D, Iding K, and Lehmann J (2001). High-Density Culture of Recombinant Chinese Hamster Ovary Cells Producing Prothrombin in Protein-Free Medium. Biotechnology Letters. **23:** 767-770.

Chi EY, Krishnan S, Randolph TW, and Carpenter JF (2003). Physical Stability of Proteins in Aqueous Solution: Mechanism and Driving Forces in Nonnative Protein Aggregation. Pharmaceutical Research. **20:** 1325-1336.

Chien S (2008). Effects of Disturbed Flow on Endothelial Cells. Annals of Biomedical Engineering. **36:** 554-562.

Choo CY, Tian Y, Kim WS, Blatter E, Conary J, and Brady CP (2007). High-Level Production of a Monoclonal Antibody in Murine Myeloma Cells by Perfusion Culture Using a Gravity Settler. Biotechnology Progress. **23:** 225-231.

Christi Y and Moo-Young M (1994). Clean-in-place systems for industrial bioreactors: design, validation and operation. Journal of Industrial Microbiology. **13**: 201-207.

Chotigeat W, Watanapokasin Y, Mahler S, and Gray PP (1994). Role of Environmental-Conditions on the Expression Levels, Glycoform Pattern and Levels of Sialyltransferase for Hfsh Produced by Recombinant Cho Cells. Cytotechnology. **15:** 217-221.

Cocomartin JM, Oberink JW, Vanderveldendegroot TAM, and Beuvery EC (1992). Viability Measurements of Hybridoma Cells in Suspension-Cultures. Cytotechnology. **8:** 57-64.

Cohen MG, Sun XM, Snowden RT, Dinsdale D, and Skilleter DN (1992). Key Morphological Features of Apoptosis May Occur in Absence of Internucleosomal DNA Fragmentation. Biochemistry Journal. **286:** 331-334.

Cohen SN, Chang ACY, Boyer HW, and Helling RB (1973). Construction of Biologically Functional Bacterial Plasmids *In-Vitro*. Proceedings of the National Academy of Sciences of the United States of America. **70:** 3240-3244.

Cossarizza A, Baccaranicontri M, Kalashnikova G, and Franceschi C (1993). A New Method for the Cytofluorometric Analysis of Mitochondrial Membrane Potential Using the J-Aggregate Forming Lipophilic Cation 5,5',6,6'-Tetrachloro-1,1',3,3'-Tetraethylbenzimidazolcarbocyanine Iodide (JC-1). Biochemical and Biophysical Research Communications. **197:** 40-45.

Cossarizza A, Kalashnikova G, Grassilli E, Chiappelli F, Salvioli S, and Capri M et al. (1994). Mitochondrial Modifications During Rat Thymocyte Apoptosis: A Study at the Single Cell Level. Experimental Cell Research. **214:** 323-330.

Costes J and Couderc JP (1988). Study by Laser Doppler Anemometry of the Turbulent Flow Induced by a Rushton Turbine in a Stirred Tank: Influence of the Size of the Units - II. Spectral Analysis and Scales of Turbulence. Chemical Engineering Science. **43:** 2765-2772.

Coulson JW and Richardson JF (2000). Coulson and Richardson's Chemical Engineering Volume 1: Fluid Flow, Heat Transfer and Mass Transfer. Oxford: Butterworth-Heinemann.

Cromwell MEM, Hilario E, and Jacobson F (2006). Protein Aggregation and Bioprocessing. American Association of Pharmaceutical Scientists. **8:** 572-579.

Cruz HJ, Dias EM, Peixoto CM, Moreira JL, and Carrondo MJT (2000). Product Quality of a Recombinant Fusion Protein Expressed in Immobilised Baby Hamster Kidney Cells Grown in Protein-Free Medium. Biotechnology Letters. **22:** 677-682.

Curtis WR (2000). Hairy Roots, Bioreactor Growth. In: Encyclopedia of Cell Technology, (827-841). New York: John Wiley & Sons.

Cutter LA (1966). Flow and Turbulence in a Stirred Tank. American Institution of Chemical Engineers Journal. **12:** 35-45.

Dang CV, Semenza GL. (1999). Oncogenic Alterations of Metabolism. Trends in Biochemical Sciences. **24:** 68-72.

Darzynkiewicz Z, Bruno S, and Bino G (1992). Features of Apoptotic Cells Measured by Flow Cytometry. Cytometry. **13:** 795-808.

Darzynkiewicz Z, Gloria J, Li X, Gorcyzca W, Murakami T, Traganos F (1996). Cytometry in Cell Necrobiology: Analysis of Apoptosis and Accidental Cell Death (Necrosis). Cytometry. **27:** 1-20.

de Graaf AO, van den Heuvel LP, Dijkman HBPM, De Abreu RA, Birkenkamp KU, and de Witte T et al. (2004). Bcl-2 Prevents Loss of Mitochondria in CCCP-Induced Apoptosis. Experimental Cell Research. **299:** 533-540.

deZengotita VM, Schmelzer AE, and Miller WM (2002a). Characteracterisation of Hybridoma Cell Responses to Elevated pCO_2 and Osmolality: Intracellular pH, Cell Size, Apoptosis, and Metabolism. Biotechnology and Bioengineering. **77:** 369-380.

deZengotita VM, Abston LR, Schmelzer AE, Shaw S, and Miller WM (2002b). Selected Amino Acids Protect Hybridoma and CHO Cells From Elevated Carbon Dioxide and Osmolality. Biotechnolgy and Bioengineering. **78:** 741-752.

Degli Esposti M (2002). Measuring Mitochondrial Reactive Oxygen Species. Methods. **26:** 335-340.

Desa DOJ (2010). Transfer Lag. In: Instrumentation for Process Control Fundamentals, (142-143). New York: Taylor & Francis.

Desagher S and Martinou JC (2000). Mitochondria As the Central Control Point of Apoptosis. Trends in Cell Biology. **10:** 369-377.

Deshpande RR and Heinzle E (2004). On-Line Oxygen Uptake Rate and Culture Viability Measurement of Animal Cell Culture Using Microplates With Integrated Oxygen Sensors. Biotechnology Letters. **26:** 763-767.

Doran PM (1993). Design of Bioreactors for Plant Cells and Organs. In: Bioprocess Design and Control, (115-168). Heidelberg: Springer.

Dove A (2002). Uncorking the Biomanufacturing Bottleneck. Nature Biotechnology. **20:** 777-779.

Duchen MR (2004). Mitochondria in Health and Disease: Perspectives on a New Mitochondrial Biology. Molecular Aspects of Medicine. **25:** 365-451.

Ducommun P, Ruffieux PA, Furter MP, Marison I, and von Stockar U (2000). A New Method for on-Line Measurement of the Volumetric Oxygen Uptake Rate in Membrane Aerated Animal Cell Cultures. Journal of Biotechnology. **78:** 139-147.

Elo MA, Karjalainen HM, Sironen RK, Valmu L, Redpath NT, and Browne GJ et al. (2005). High Hydrostatic Pressure Inhibits the Biosynthesis of Eukaryotic Elongation Factor 2. Journal of Cellular Biochemistry. **94:** 497-507.

Enfors S-O, Jahic M, Rozkov A, Xu B, Hecker M, and KJ Morrow et al. (2001). Physiological Responses to Mixing in Large Scale Bioreactors. Journal of Biotechnology. **85:** 175-185.

Europe AF, Gambhir A, Fu PC, and Hu WS (2000). Multiple Steady States With Distinct Cellular Metabolism in Continuous Culture of Mammalian Cells. Biotechnology and Bioengineering. **67:** 25-34.

Fadok VA, Voelker DR, Campbell PA, Cohen JJ, Bratton DL, and Henson PM (1992). Exposure of Phosphatidylserine on the Surface of Apoptotic Lymphocytes Triggers

Specific Recognition and Removal by Macrophages. Journal of Immunological Methods. **148:** 2207-2216.

Li F, Hashimura Y, Pendleton R, Harms J, Collins E, and Lee B (2006). A Systematic Approach to Scale-Down Model Development and Characterisation of Commercial Cell Culture Processes. Biotechnology Progress. **22:** 696-703.

Fieder J, Schorn P, Bux R, and Noe W (1995). Increase of Productivity in Recombinant CHO by Enhanced Glucose Levels. In: Animal Cell Technology: Development Towards 21st Century, (163-167). Dordrecht: Kluwer Academic Publishers.

Fiore M and Degrassi F (1999). Dimethyl Sulfoxide Restores Contact Inhibition-Induced Growth Arrest and Inhibits Cell Density-Dependent Apoptosis in Hamster Cells. Experimental Cell Research. **251:** 102-110.

Fleischaker RJ and Sinskey A (1981). Oxygen Demand and Supply in Cell Culture. European Journal of Applied Microbiology and Biotechnology. **12:** 193-197.

Frey T (1997). Correlated Flow Cytometric Analysis of Terminal Events in Apoptosis Reveals Absense of Some Changes in Some Model Systems. Cytometry Part A. **28:** 253-263.

Fukuda K, Masamichi K, and Chui JF (1993). Demonstration of Extensive Chromatin Cleavage in Transplanted Morris Hepatoma 7777 Tissue: Apoptosis or Necrosis? American Journal of Pathology. **142:** 935-946.

Garnier A, Voyer R, Rosanne T, Perret S, Barbara J, and Kamen A (1996). Dissolved Carbon Dioxide Accumulation in a Large Scale and High Density Production of TGF Receptor With Baculovirus Infected Sf-9. Cytotechnology. **22:** 53-63.

Geckil H, Stark BC, and Webster DA (2001). Cell Growth and Oxygen Uptake of Escherichia Coli and Pseudomonas Aeruginosa Are Differently Effected by the Genetically Engineered Vitreoscilla Hemoglobin Gene. Journal of Biotechnology. **85:** 57-66.

George S, Larsson G, and Enfors S-O (1993). A Scale-Down Two-Compartment Reactor With Controlled Substrate Oscillations: Metabolic Response of Saccharomyces Cerevisiae. Bioprocess Engineering. **9:** 249-257.

Godoy-Silva R, Chalmers JJ, Casnocha SA, Bass LA, and Ma N (2009a). Physiological Responses of CHO Cells to Repetitive Hydrodynamic Stress. Biotechnology and Bioengineering. **103:** 1103-1117.

Godoy-Silva R, Mollet M, and Chalmers JJ (2009b). Evaluation of the Effect of Chronic Hydrodynamical Stresses on Cultures of Suspended CHO-6E6 Cells. Biotechnology and Bioengineering. **102:** 1119-1130.

Goergen JL, Marc A, and Engasser JM (1993). Determination of Cell Lysis and Death Kinetics in Continuous Hybridoma Cultures From the Measurement of Lactate Dehydrogenase Release. Cytotechnology. **11:** 189-195.

Goldman MH, Ison AP, James DC, and Bull AT (1997). Monitoring Proteolysis of Recombinant Human Interferon-Gamma During Batch Culture of Chinese Hamster Ovary Cells. Cytotechnology. **23:** 103-111.

Goldstein G (1986). An Overview of Orthoclone Okt3. Transplantation Proceedings. **18:** 927-930.

Goochee CF, Gramer MJ, Andersen DC, Bahr JB, and Rasmussen JR (1991). The Oligosaccharides of Glycoproteins: Bioprocess Factors Affecting Oligosaccharide Structure and Their Effect on Glycosylation Properties. Biotechnology (NY). **9:** 1347-1355.

Goochee CF and Monica T (1990). Environmental Effects on Protein Glycosylation. Biotechnology (NY). **8:** 421-427.

Gorenflo VM, Pfeifer TA, Lesnicki G, Kwan EM, Grigliatti TA, and Kilburn DG et al. (2004). Production of a Self-Activating CBM-Factor X Fusion Protein in a Stable Transformed Sf9 Insect Cell Line Using High Cell Density Perfusion Culture. Cytotechnology. **44:** 93-102.

Goswami J, Sinskey AJ, Steller H, Stephanopoulos GN, and Wang DIC (1999). Apoptosis in Batch Cultures of Chinese Hamster Ovary Cells. Biotechnology and Bioengineering. **62:** 632-640.

Gramer MJ, Goochee CF, Chock VY, Brousseau DT, and Sliwkowski MB (1995). Removal of Sialic Acid From a Glycoprotein in CHO Cell Culture Supernatant by Action of an Extracellular CHO Cell Sialidase. Nature Biotechnology. **13:** 692-698.

Gray DR, Chen S, Howarth W, Inlow D, and Maiorella BL (1996). CO_2 in Large-Scale and High-Density CHO Cell Perfusion Culture. Cytotechnology. **22:** 65-78.

Gu X and Wang DIC (1998). Improvement of Interferon Gamma Sialylation in Chinese Hamster Ovary Cell Culture by Feeding of N-Acetylmannosamine. Biotechnology and Bioengineering. **58:** 642-648.

Guile GR, Rudd PM, Wing DR, Prime SB, and Dwek RA (1996). A Rapid High-Resolution High-Performance Liquid Chromatographic Method for Separating Glycan Mixtures and Analyzing Oligosaccharide Profiles. Analytical Biochemistry. **240:** 210-226.

Gupta A and Rao G (2003). A Study of Oxygen Transfer in Shake Flasks Using a Non-Invasive Oxygen Sensor. Biotechnology and Bioengineering. **84:** 351-358.

Haase SB (2004). Cell Cycle Analysis of Budding Yeast Using SYTOX Green. Current Protocols in Cytometry. **7.23**.

Hansbro SD, Sharpe DA, Catchpole R, Welsh KR, Munsch CM, and McGoldrick JP et al. (1999). Haemolysis During Cardiopulmonary Bypass: an in Vivo Comparison of Standard Roller Pumps, Nonocclusive Roller Pumps and Centrifugal Pumps. Perfusion. **14:** 3-10.

Hansen K, Kjalke M, Rasmussen P, Kongerslev L, and Ezban M (1997). Proteolytic Cleavage of Recombinant Two-Chain Factor VIII During Cell Culture Production Is

Mediated by Protease(s) From Lysed Cells. The Use of Pulse Labelling Directly in Production Medium. Cytotechnology. **24:** 227-234.

Hansford GS and Humphrey AE (1966). The Effect of Equipment Scale and Degree of Mixing on Continuous Fermentation Yield at Low Dilution Rates. Biotechnology and Bioengineering. **8:** 85-96.

Harris RJ, Kabakoff B, Macchi FD, Shen FJ, Kwong M, and Andya JD et al. (2001). Identification of Multiple Sources of Charge Heterogeneity in a Recombinant Antibody. Journal of Chromatography B: Biomedical Sciences and Applications. **752:** 233-245.

Haugland RP (2002). Handbook of Fluorescent Probes and Research Products.

Hayter PM, Curling EMA, Baines AJ, Jenkins N, Salmon I, and Strange PG et al. (1991). Chinese Hamster Ovary Cell Growth and Interferon Production Kinetics in Stirred Batch Culture. Applied Microbiology and Biotechnology. **34:** 559-564.

Hayter PM, Curling EMA, Baines AJ, Jenkins N, Salmon I, and Strange PG et al. (1992a). Glucose-Limited Chemostat Culture of Chinese-Hamster Ovary Cells Producing Recombinant Human Interferon-Gamma. Biotechnology and Bioengineering. **39:** 327-335.

Hayter PM, Kirkby NF, and Spier RE (1992b). Relationship Between Hybridoma Growth and Monoclonal Antibody Production. Enzyme and Microbial Technology. **14:** 454-461.

Henzler HJ and Shedel M (1991). Suitability of the Shaking Flask for Oxygen Supply to Microbial Cultures. Bioprocess Engineering. **7:** 121-131.

Hermeling S, Crommelin DJ, Schellekens H, and Jiskoot W (2004). Structure-Immunogenicity Relationships of Therapeutic Proteins. Pharmaceutical Research. **21:** 897-903.

Hewitt CJ, Boon LA, and McFarlane CM (1998). The Use of Flow Cytometry to Study the Impact of Fluid Mechanical Stress on Escherichia Coli W3110 During Continuous Cultivation in an Agitated Bioreactor. Biotechnology and Bioengineering. **59:** 612-620.

Hewitt CJ and Nebe-Von-Caron G (2001). An Industrial Application of Multiparameter Flow Cytometry: Assessment of Cell Physiological State and Its Application to the Study of Microbial Fermentations. Cytometry. **44:** 179-187.

Hewitt CJ, Nebe-Von-Caron G, Axelsson R, Farlane CM, and Nienow AW (2000). Studies Related to the Scale-Up of High-Cell-Density E. Coli Fed-Batch Fermenations Using Multiparameter Flow Cytometry: Effect of a Changing Microenvironment With Respect to Glucose and Dissolved Oxygen Concentration. Biotechnology and Bioengineering. **70:** 381-390.

Hijikata W, Shinshi T, Asama J, Li J, Hoshi H, and Takatani S et al. (2008). A Magnetically Levitated Centrifugal Blood Pump With a Simple-Structured Disposable Pump Head. Artificial Organs. **32:** 531-540.

Hill SS, Shaw BR, and Wu AHB (2001). The Clinical Effects of Plasticizers, Antioxidants, and Other Contaminants in Medical Polyvinylchloride Tubing During Respiratory and Non-Respiratory Exposure. Clinica Chimica Acta. **304:** 1-8.

Hoeks F, Mommers R, Guter D, Willems M, Osman JJ, and Khan M et al. (2004). Industrial Applications of Mixing and Mass Transfer Studies.

Hu WS, Dodge TC, Frame KK, and Himes VB (1987). Effect of Glucose on the Cultivation of Mammalian Cells. Developments in Biological Standardization. **66:** 279-290.

Ifandi V and Al-Rubeai M (2005). Regulation of Cell Proliferation and Apoptosis in CHO-K1 Cells by the Coexpression of C-Myc and Bcl-2. Biotechnology Progress. **21:** 671-677.

Isailovic B (2007). The Use of Multi-Parameter Flow Cytometry for Characterisation of Insect Cell Baculovirus Culture. University of Birmingham.

Isailovic B, Hicks R, Taylor IW, Nienow A, and Hewitt CJ (2007). The Use of Multi-Parameter Flow Cytometry for Characterisation of Insect Cell-Baculovirus Cultures. Cell Technology for Cell Products. In: Cell Technology for Cell Products, (575-577). Dordrecht: Springer.

Ishaque A (2000). Apoptosis in Mammalian Batch Cell Cultures. University of Birmingham.

Ishaque A and Al-Rubeai M (1998). Use of Intracellular PH and Annexin-V Flow Cytometric Assays to Monitor Apoptosis and Its Suppression by Bcl-2 Over-Expression in Hybridoma Cell Culture. Journal of Immunological Methods. **221:** 43-57.

Jacopo U, Rita G, Silvana B, Renato S, Roberto C, Bianca MR et al. (2000). Calcein-AM Is a Detector of Intracellular Oxidative Activity. Histochemistry and Cell Biology. **122:** 499-505.

Jaspe J and Hagen SJ (2006). Do Protein Molecules Unfold in Simple Shear Flow. Biophysical Journal. **91:** 3415-3424.

Jayapal KR, Wlaschin KF, Hu WS, and Yap MGS (2007). Recombinant Protein Therapeutics From CHO Cells - 20 Years and Counting. Chemical Engineering Progress. **103:** 40-47.

Jem JK, Fateen S, and Michaels J (1994). Mixing Phenomena in Industrial Bioreactors With Perfusion Spin Filters. In: Animal Cell Technology: Products of Today, Prospects for Tomorrow, (392-396). Oxford: Butterworth Heinemann.

Jenkins N (2007). Modification of Therapeutic Proteins: Challenges and Prospects. Cytotechnology. **53:** 121-125.

Jenkins N and Curling EM (1994). Glycosylation of Recombinant Proteins: Problems and Prospects. Enzyme and Microbial Technology. **16:** 354-364.

Jenkins N, Parekh RB, and James DC (1996). Getting Glycosylation Right: Implications for the Biotechnology Industry. Nature Biotechnology. **14:** 975-981.

Jiskoot W, Beuvery EC, de Koning AAM, Herron JN, and Crommelin DJA (1990). Analytical Approaches to the Study of Monoclonal Antibody Stability. Pharmaceutical Research. **7:** 1234-1241.

Jolicoeur M, Chavarie C, Carreu PJ, and Archambault J (1992). Development of a Helical Ribbon Impeller Bioreactor for High Density Plant Cell Suspension Culture. Biotechnology and Bioengineering. **39:** 511-521.

Jones PT, Dear PH, Foote J, Neuberger MS, and Winter G (1986). Replacing the Complementarity-Determining Regions in a Human Antibody With Those From a Mouse. Nature. **321:** 522-525.

Kaarinanta K, Elo MA, Sironen RK, Karjalainen HM, Helminen HJ, and Lammi MJ (2003). Stress Responses of Mammalian Cells to High Hydrostatic Pressure. Biorheology. **40:** 87-92.

Katinger HWD (1976). Physiological Response of Candida-Tropicalis Grown on N-Paraffin to Mixing in a Tubular Closed-Loop Fermenter. European Journal of Applied Microbiology. **3:** 103-114.

Kays WM and Crawford ME (1980). Convective Heat and Mass Transfer. New York: McGraw-Hill.

Kenty B, Li Z, Vanden T, and Lee S (2005). Mixing in Laboratory-Scale Bioreactors Used for Mammalian Cell Culture. In: 229th American Chemical Society National Meeting, San Diego, CA, USA.

Kieran PM, O'Donnell HJ, Malone DM, and MacLoughlin PF (1995). Fluid Shear Effects on Suspension Cultures of Morinda Citrifolia. Biotechnology and Bioengineering. **45:** 415-425.

Kim BJ, Oh DJ, and Chang HN (208). Limited Use of Centritech Lab II Centrifuge in Perfusion Culture of RCHO Cells for the Production of Recombinant Antibody. Biotechnology Progress. **24:** 166-174.

Kim DY, Won SJ, and Gwag BJ (2002). Analysis of Mitochondrial Free Radical Generation in Animal Models of Neuronal Disease. Free Radical Biology and Medicine. **33:** 715-723.

Kim NS and Lee GM (2002). Response of Recombinant Chinese Hamster Ovary Cells to Hyperosmotic Pressure: Effect of Bcl-2 Expression. Journal of Biotechnology. **95:** 237-248.

Kimura R and Miller WM (1997). Glycosylation of CHO-Derived Recombinant TPA Produced Under Elevated pCO_2. Biotechnology Progress. **13:** 311-317.

Kimura R and Miller WM (1996). Effects of Elevated pCO_2 and/or Osmolality on the Growth and Recombinant TPA Production of CHO Cells. Biotechnology and Bioengineering. **52:** 152-160.

King MA (2000). Detection of Dead Cells and Measurement of Cell Killing by Flow Cytometry. Journal of Immunological Methods. **243:** 155-166.

Kioukia N, Nienow AW, Emery AN, and Al-Rubeai M (1995). Physiological and Environmental Factors Affecting the Growth of Insect Cells and Infection With Baculovirus. Journal of Biotechnology. **38:** 243-251.

Kiss R, Croughan M, and Trask J (1994). Mixing Time Characterisation in Large-Scale Mammalian Cell Bioreactors. In American Institute of Chemical Engineers Annual Meeting, San Francisco, CA, USA. Paper No. 55c.

Kluck RM, Bossy-Wetzel E, Green DR, and Newmeyer DD (1997). The Release of Cytochrome c From Mitochondria: A Primary Site for Bcl-2 Regulation of Apoptosis. Science. **275:** 1132-1136.

Kohler G and Milstein C (1975). Continuous Cultures of Fused Cells Secreting Antibody of Predefined Specificity. Nature. **256:** 495-497.

Kohler G and Milstein C (2005). Pillars Article: Continuous Cultures of Fused Cells Secreting Antibody of Predefined Specificity. Journal of Immunological Methods. **174:** 2453-2455.

Koopman G, Reutelingsperger CP, Kuijten GA, Keehnen RM, Pals ST, and van Oers MH (1994). Annexin V for Flow Cytometric Detection of Phosphatidylserine Expression on B Cells Undergoing Apoptosis. Blood. **84:** 1415-1420.

Korshunov SS, Skulachev VP, and Starkov AA (1997). High Protonic Potential Actuates a Mechanism of Production of Reactive Oxygen Species in Mitochondria. Federation of European Microbial Societies Letters. **416:** 15-18.

Kozlowski S and Swann P (2006). Current and Future Issues in the Manufacturing and Development of Monoclonal Antibodies. Advanced Drug Delivery Reviews. **58:** 707-722.

Krishna S, Supanaranond W, Pukrittayakamee S, Karter D, Supputamongkol Y, Davis TME, Holloway PA, White NJ (1994). Dichloroacetate for Lactic Acidosis in Severe Malaria: A Pharmacokinetic and Parmacodynamic Assessment. Metabolism. **43**: 974-981.

Kromenaker SJ and Srienc F (1994). Cell Cycle Kinetics of Accumulation of Heavy and Light Chain Immunoglobulin Proteins in Mouse Hybridoma Cell Line. Cytotechnology. **14:** 205-218.

Kroon DJ, Baldwin-Ferro A, and Lalan P (1992). Identification of Sites of Degradation in a Therapeutic Monoclonal Antibody by Peptide Mapping. Pharmaceutical Research. **9:** 1386-1393.

Kubicek CP (2001). Organic Acids. In: Basic Biotechnology, (305-324). Cambridge: Cambridge University Press.

Kumpel BM, Rademacher TW, Rook GA, Williams PJ, and Wilson IB (1994). Galactosylation of Human IgG Monoclonal Anti-D Produced by EBV-Transformed B-Lymphoblastoid Cell-Lines in Dependent on Culture Method and Affects Fc Receptor Mediated Functional Activity. Human Antibodies and Hybridomas. **5:** 143-151.

Kunas KT (1990). Damage Mechanisms of Suspended Animal Cells in Agitated Bioractors With and Without Bubble Entrainment. Biotechnology and Bioengineering. **36:** 476-483.

Kurano N, Leist C, Messi F, Kurano S, and Fiechter A (1990a). Growth Behavior of Chinese Hamster Ovary Cells in a Compact Loop Bioreactor. 2. Effects of Medium Components and Waste Products. Journal of Biotechnology. **15:** 113-128.

Kurano N, Leist C, Messi F, Kurano S, and Fiechter A (1990b). Growth Behaviour of Chinese Hamster Ovary Cells in a Mechanically Stirred Internal Loop Bioreact. 1. Effects of Physical and Chemical Enviroments. Journal of Biotechnology. **15:** 99-110.

Lakhotia SK, Bauer KD, and Papoutsakis ET (1992). Damaging Agitation Intensities Increase DNA Synthesis Rate and Alter Cell-Cycle Phase Distributions in CHO Cells. Biotechnology and Bioengineering. **40:** 978-990.

Lammi MJ, Elo MA, Sironen RK, Karjalainen HM, Kaarniranta K, and Helminen HJ. (2004). Hydrostatic Pressure Induces Changes in Cellular Protein Synthesis. Biorheology. **41:** 309-313.

Langheinrich C and Nienow AW (1999). Control of PH in Large-Scale, Free Suspension Animal Cell Bioreactors: Alkali Addition and PH Excursions. Biotechnology and Bioengineering. **66:** 171-179.

Langheinrich C, Nienow AW, Eddleston T, Stevenson NC, Emery AN, and Clayton TM et al. (1998). Liquid Homogenization Studies in Animal Cell Bioreactors of Up to 8 M_3 in Volume. Food and Bioproducts Processing. **76:** 107-116.

Langheinrich C, Nienow AW, Eddleston T, Stevenson NC, Emery AN, and Clayton TM et al. (2002). Oxygen Transfer in Stirred Bioreactors Under Animal Cell Culture Conditions. Food and Bioproducts Processing. **80:** 39-44.

Lao MS and Toth D (1997). Effects of Ammonium and Lactate on Growth and Metabolism of a Recombinant CHO Culture. Biotechnology Progress. **13:** 688-691.

Laporte C, Kosta A, Klein G, Aubry L, Lam D, and Tresse E et al. (2006). A Necrotic Cell Death Model in a Protist. Cell Death and Differentiation. **14:** 266-274.

LaPorte TL, Shevitz J, Kim Y, and Wang SS (1996). Long Term Shear Effects on a Hybridoma Cell Line by Dynamic Perfusion Devices. Bioprocess and Biosystems Engineering. **15:** 1-7.

Lara AR, Galindo E, Ramirez OT, and Palomares LA (2006). Living With Heterogeneities in Bioreactors. Molecular Biotechnology. **34:** 355-381.

Larsson G, Tornkvist M, Wernersson ES, Tragardh C, Noorman H, and Enfors SO (1996). Substrate Gradients in Bioreactors: Origin and Consequences. Bioprocess Engineering. **14:** 281-289.

Leckie F, Scragg AH, and Cliffe KC (1991). Effect of Bioreactor Design and Agitator Speed on the Growth and Alkaloid Accumulation by Cultures of Catharantus Roseus. Enzyme and Microbial Technology. **13:** 296-305.

Lee H, Homma A, Tatsumi E, and Taenaka Y (2009). Observation of Cavitation Pits on a Mechanical Heart Valve Surface in an Artificial Heart Used in in Vivo Testing. Journal of Artificial Organs. **12:** 105-110.

Lee JC, Chang HN, and Oh DJ (2005). Recombinant Antibody Production by Perfusion Cultures of RCHO Cells in a Depth Filter Perfusion System. Biotechnology Progress. **21:** 134-139.

Lee SY (1996). High Cell-Density Culture of Escherichia Coli. Trends in Biotechnology. **14:** 98-105.

Lehoux S, Castier Y, and Tedgui A (2006). Molecular Mechanisms of Vascular Responses to Haemodynamic Forces. Journal of Interal Medicine. **259:** 381-392.

Levenspiel O (1999). The Dispersion Model. In: Chemical Reaction Engineering, (293-320). Danvers: John Wiley & Sons.

Leverette LB, Hellums JD, Alfrey CP, and Lynch EC (1972). Red Blood Cell Damage by Shear Stress. Biophysical Journal. **12:** 257-273.

Li C and Xu C (2007). Mechanical Stress-Initiated Signal Transduction in Vascular Smooth Muscle Cells in Vitro and in Vivo. Cellular Signaling. **19:** 881-891.

Li J, Vijayasankaran N, Hudson T, Amanullah A, Loong Wong C (2010). Can Lactate Actually be Beneficial to CHO Cell Culture Processes? In: 60th Society for Industrial Microbiology Annual Meeting, San Francisco, CA, USA.

Li YSJ, Haga JH, and Chien S (2005). Molecular Basis of the Effects of Shear Stress on Vascular Endothelial Cells. Journal of Biomechanics. **38:** 1949-1971.

Lin JJ, Meyer JD, Carpenter JF, and Manning MC (2000). Stability of Human Serum Albumin During Bioprocessing: Denaturation and Aggregation During Processing of Albumin Paste. Pharmaceutical Research. **17:** 391-396.

Link T, Backstrom M, Graham R, Essers R, Zorner K, and Gatgens J et al. (2004). Bioprocess Development for the Production of a Recombinant MUC1 Fusion Protein Expressed by CHO-K1 Cells in Protein-Free Medium. Journal of Biotechnology. **110:** 51-62.

Liu H, Gaza-Bulseco G, Faldu D, Chumsae C, and Sun J (2008). Heterogeneity of Monoclonal Antibodies. Journal of Pharmaceutical Sciences. **97:** 2426-2447.

Liu J, Nguyen MD, Andya JD, and Shire SJ (2005). Reversible Self-Association Increases the Viscosity of a Concentrated Monoclonal Antibody Aqueous Solution. Journal of Plant Research. **94:** 1928-1940.

Ljunggren J and Haggstrom L (1994). Catabolic Control of Hybridoma Cells by Glucose and Glutamine Limited Fed-Batch Cultures. Biotechnology and Bioengineering. **44:** 808-818.

Lodish H, Berk A, Zipursky SL, Matsudaira P, Baltimore D, and Darnell J (1999). Protein Structure and Function. In: Molecular Cell Biology, (50-99). New York: WH Freeman and Company.

Loschen G, Floho L, and Chance B (1971). Respiratory Chain Linked H_2O_2 Production in Pigeon Heart Mitochondria. Federation of European Microbial Societies Letters. **18:** 261-264.

Lu SB, Sun XM, and Zhang YX (2005). Insight into Metabolism of CHO Cells at Low Glucose Concentration on the Basis of the Determination of Intracellular Metabolites. Process Biochemistry. **40:** 1917-1921.

Luedeking R and Piret EL (1959). A Kinetic Study of the Lactic Acid Fermentation. Batch Process at Controlled pH. Journal of Biochemical and Microbiological Technology and Engineering. **1:** 393-412.

Ly JD, Grubb DR, and Lawen A (2003). The Mitochondrial Membrane Potential in Apoptosis; an update. Apoptosis. **8:** 115-128.

Ma N, Koelling KW, and Chalmers JJ (2002). Fabrication and Use of a Transient Contractional Flow Device to Quantify the Sensitivity of Mammalian and Insect Cells to Hydrodynamic Forces. Biotechnology and Bioengineering. **80:** 428-437.

Ma N, Chalmers JJ, Auniņš JG, Zhou W and Xie L (2004). Quantitative Studies of Cell-Bubble Interactions and Cell Damage at Different Pluronic F-68 and Cell Concentrations. Biotechnology Progress. **20**: 1183–1191.

Maa YF and Hsu CC (1997). Protein Denaturation by Combined Effect of Shear and Air-Liquid Interface. Biotechnology and Bioengineering. **54:** 503-512.

MacKay DJC (2009). Sustainable Energy - Without the Hot Air. Cambridge: UIT Cambridge.

Madshus IH (1988). Regulation of Intracellular PH in Eukaryotic Cells. Biochemistry Journal. **250:** 1-8.

Maier U and Buchs J (2001). Characterisation of Gas-Liquid Transfer in Shaking Bioreactors. Biochemical Engineering Journal. **7:** 99-106.

Maier U, Losen M, and Buchs J (2004). Advances in Understanding and Modeling the Gas-Liquid Mass Transfer in Shake Flasks. Biochemical Engineering Journal. **17:** 155-167.

Maiorella BL, Winkelhake J, and Young J (1993). Effect of Culture Conditions on IgM Antibody Structure, Pharmacokinetics and Activity. Nature Biotechnology. **11:** 387-392.

Majid FAA (2001). The Fidelity and Reproducibility of Large Scale Animal Cell Cultures: Impact of Bcl-2 Over-Expressions on Product Glycosylation. University of Birmingham.

Malek AM and Izumo S (1994). Molecular Aspects of Signal Transduction of Shear Stress in Endothelial Cells. Journal of Hypertension. **12:** 989-999.

Manning FS, Wolf D, and Keairns DL (1965). Model Simulation of Stirred Tank Reactors. AIChE J. **11:** 723-727.

Mardikar SH and Niranjan K (2000). Observations on the Shear Damage to Different Animal Cells in a Concentric Cylinder Viscometer. Biotechnology and Bioengineering. **68:** 697-704.

Martin SJ, Reutlingsperger CP, McGahon AJ, Rader JA, van Shie RC, LaFace DM et al. (1995). Early Redistribution of Plasma Membrane Phosphatidylserine Is a General Feature of Apoptosis Regardless of the Initiating Stimulus: Inhibition by Over Expression of Bcl-2 Adn Abl. The Journal of Experimental Medicine. **182:** 1545-1556.

Mathews CK, van Holde KE, and Ahern KG (2000). Carbohydrate Metabolism II: Biosynthesis. In: Biochemistry, (560-593). San Francisco: Benjamin Cummings.

Mccormick F, Trahey M, Innis M, Dieckmann B, and Ringold G (1984). Inducible Expression of Amplified Human Beta Interferon Genes in CHO Cells. Molecular and Cellular Biology. **4:** 166-172.

McNeil B and Kristiansen B (1990). Simulated Scale-Up of a Yeast Fermentation Using a Loop Bioreactor. Biotechnology Letters. **12:** 39-44.

McQueen A and Bailey JE (1989). Influence of Serum Level, Cell Line, Flow Type and Viscosity on Flow-Induced Lysis of Suspended Mammalian Cells. Biotechnology Letters. **11:** 531-536.

Mercille S and Massie B (1994). Induction of Apoptosis in Oxygen-Deprived Cultures of Hybridoma Cells. Cytotechnology. **15:** 117-128.

Merten OW (2000). Constructive Improvement of the Ultrasonic Separation Device ADI 1015. Cytotechnology. **34:** 175-179.

Merten OW (2006). Introduction to Animal Cell Culture Technology - Past, Present and Future. Cytotechnology. **50:** 1-7.

Metivier D, Dallaporta B, Zamzami N, Larochette N, Susin SA, Marzo I et al. (1998). Cytofluorometric Detection of Mitochondrial Alterations in Early CD95/Fas/APO-1-Triggered Apoptosis of Jurkat T Lymphoma Cells. Comparison of Seven Mitochondrion-Specific Fluorochromes. Immunology Letters. **61:** 157-163.

Meuwly F, Papp F, Ruffieux PA, Bernard AR, Kadouri A, and von Stockar U (2006). Use of Glucose Consumption Rate (GCR) As a Tool to Monitor and Control Animal Cell Production Processes in Packed-Bed Bioreactors. Journal of Biotechnology. **122:** 122-129.

Midler M and Finn RK (1966). A Model System for Evaluating Shear in Design of Stirred Fermentors. Biotechnology and Bioengineering. **8:** 71-84.

Miller WM, Blanch HW, and Wilke CR (1987). A Kinetic Analysis of Hybridoma Growth and Metabolism in Batch and Continuous Suspension Culture: Effect of Nutrient Concentration, Dilution Rate, and PH. Biotechnology and Bioengineering. **32:** 947-965.

Mlejnek P (2001). Caspase-3 Activity and Carbonyl Cyanide M-Chlorophenylhydrazone-Induced Apoptosis in HL-60 Cells. Atla-Alternatives to Laboratory Animals. **29:** 243-249.

Mollet M, Godoy-Silva R, Berdugo C, and Chalmers JJ (2008). Computer Simulations of the Energy Dissipation Rate in a Fluorescence-Activated Cell Sorter: Implications to Cells. Biotechnology and Bioengineering. **100:** 260-272.

Mollet M, Ma NN, Zhao Y, Brodkey R, Taticek R, and Chalmers JJ (2004). Bioprocess Equipment: Characterization of Energy Dissipation Rate and Its Potential to Damage Cells. Biotechnology Progress. **20:** 1437-1448.

Moore A, Donahue CJ, Hooley J, Stocks DL, Bauer KD, and Mather JP (1995). Apoptosis in CHO Cell Batch Cultures: Examination by Flow Cytometry. Cytotechnology. **17:** 1-11.

Moore A, Mercer J, Dutina G, Donahue CJ, Bauer KD, Mather JP et al. (1997). Effects of Temperature Shift on Cell Cycle, Apoptosis and Nucleotide Pools in CHO Cell Batch Cultues. Cytotechnology. **23:** 47-54.

Morgan IS, Codispoti M, Sanger K, and Mankad PS (1998). Superiority of Centrifugal Pump Over Roller Pump in Paediatric Cardiac Surgery: Prospective Randomised Trial. European Journal of Cardio-Thoracic Surgery. **13:** 526-532.

Morrison SL, Johnson MJ, Herzenberg LA, and Oi VT (1984). Chimeric Human Antibody Molecules: Mouse Antigen-Binding Domains With Human Constant Region Domains. Proceedings of the National Academy of Sciences of the United States of America. **81:** 6851-6855.

Mostafa SS and Xuejun G (2003). Strategies for Improved DCO_2 Removal in Large-Scale Fed-Batch Cultures. Biotechnology Progress. **19:** 45-51.

Mukhopadhyay P, Rajesh M, Hasko G, Hawkins BJ, Madesh M, and Pacher P (2007). Simultaneous Detection of Apoptosis and Mitochondrial Superoxide Production in Live Cells by Flow Cytometry and Confocal Microscopy. Nature Protocols. **2:** 2295-2301.

Mulholland JW, Massey W, and Shelton JC (2000). Investigation and Quantification of the Blood Trauma Caused by the Combined Dynamic Forces Experienced During Cardiopulmonary Bypass. Perfusion. **15:** 485-494.

Mulholland JW, Shelton JC, and Luo XY (2005). Blood Flow and Damage by the Roller Pumps During Cardiopulmonary Bypass. Journal of Fluids and Structures. **20:** 129-140.

Mulukutla BC, Khan S, Lange A, Hu WS (2010). Glucose Metabolism in Mammalian Cell Culture: New Insights for Tweaking Vintage Pathways. Trends in Biotechnology. **28:** 476-484.

Munzert E, Heidemann R, Buntemeyer H, Lehmann J, and Muthing J (1997). Production of Recombinant Human Antithrombin III on 20-L Bioreactor Scale: Correlation of Supernatant Neuraminidase Activity, Desialylation, and Decrease of Biological

Activity of Recombinant Glycoprotein. Biotechnology and Bioengineering. **56:** 441-448.

Munzert E, Muthing J, Buntemeyer H, and Lehmann J (1996). Sialidase Activity in Culture Fluid of Chinese Hamster Ovary Cells During Batch Culture and Its Effect on Recombinant Human Antithrombin III Integrity. Biotechnology Progress. **12:** 559-563.

Namdev KP and Thompson BG (1992). Effect of Feed Zone in Fed-Batch Fermentations of Saccharomyces Cerevisiae. Biotechnology and Bioengineering. **40:** 235-246.

Namdev KP and Yegneswaren PK (1991). Experimental Simulation of Large-Scale Bioreactor Environments Using a Monte Carlo Method. The Canadian Journal of Chemical Engineering. **69:** 513-519.

Narendranathan TJ and Dunhill P (1982). The Effect of Shear on Globular Proteins During Ultrafiltration: Studies of Alcohol Dehydrogenase. Biotechnology and Bioengineering. **24:** 2103-2107.

Natarajan S and Mokhtarzadeh-Dehghan MR (2000). Numerical Prediction of Flow in a Model of a (Potential) Soft Acting Peristaltic Blood Pump. International Journal for Numerical Methods in Fluids. **32:** 711-724.

Nevaril CG, Lynch EC, Alfrey CP, and Hellums JD (1968). Erythrocyte Damage and Destruction Induced by Shearing Stress. Journal of Laboratory and Clinical Medicine. **71:** 784-790.

Newland M, Greenfield PF, and Reid S (1990). Hybridoma Growth Limitations: The Roles of Energy Metabolism and Ammonia Production. Cytotechnology. **3:** 215-229.

Newsholme P, Lima MMR, Procopio J, Pithon-Cur TC, Doi SQ, Bazotte RB, Curi R. (2003a). Glutamine and Glutamate as Vital Metabolites. Brazilian Journal of Medical and Biological Research. **36:**153 – 163.

Newsholme P, Procopio J, Lima MMR, Pithon-Curi TC, Curi R (2003b). Glutamine and Glutamate – Their Central Role in Cell Metabolism and Function. Cell Biochemistry and Function. **21:** 1 – 9.

Nienow AW and Langheinrich C (1996). Homogenisation and Oxygen Transfer Rates in Large Agitated and Sparged Animal Cell Bioreactors: Some Implications for Growth and Production. Cytotechnology. **22:** 87-94.

Nienow AW (1997). On Impeller Circulation and Mixing Effectiveness in the Turbulent Flow Regime. Chemical Engineering Science. **52:** 2557-2565.

Nienow AW (1998). Hydrodynamics of Stirred Bioreactors. Applied Mechanics Review. **51:** 3-32.

Nienow AW (2003). Aeration-Biotechnology. In: Kirk Othmer Encyclopaedia of Chemical Technology New York: Wiley.

Nienow AW (2006). Reactor Engineering in Large Scale Animal Cell Culture. Cytotechnology. **50:** 9-33.

Noguchi Y, Nakai Y, and Shimba N (2004). The Energetic Conversion Competence of Escherichia Coli During Aerobic Respiration Studies by 31P NMR Using a Circulation Fermentation System. Journal of Biochemistry. **136:** 509-515.

Noon GP, Kane LE, Feldman L, Peterson JA, and DeBakey ME (1985). Reduction of Blood Trauma in Roller Pumps for Long-Term Perfusion. World Journal of Surgery. **9:** 65-71.

Oh SKW, Nienow AW, Al-Rubeai M, and Emery AN (1989). The Effects of Agitation Intensity With and Without Continuous Sparging on the Growth and Antibody Production of Hybridoma Cells. Journal of Biotechnology. **12:** 45-61.

Oliva A, Santoveña A, Fariña J, and Llabrés M (2003). Effect of High Shear Rate on Stability of Proteins: Kinetic Study. Journal of Pharmaceutical and Biomedical Analysis. **33:** 145-155.

Omerod MG (1999). Flow Cytometry. Guilford: BIOS Scientific Publishers.

Oosterhuis NMG and Kossen NWF (1984). Dissolved Oxygen Concentration Profiles in a Production-Scale Bioreactor. Biotechnology and Bioengineering. **26:** 546-550.

Oosterhuis NMG, Kossen NWF, Oliver APC, and Schenk ES (1985). Scale-Down and Optimisation Studies of the Gluconic Acid Fermentation by *Gluconobacter Oxydans*. Biotechnolgy and Bioengineering. **27:** 711-720.

Osman JJ, Birch J, and Varley J (2001). The Response of GS-NS0 Myeloma Cells to PH Shifts and PH Perturbations. Biotechnology and Bioengineering. **75:** 63-73.

Osman JJ, Birch J, and Varley J (2002). The Response of GS-NS0 Myeloma Cells to Single and Multiple PH Perturbations. Biotechnology and Bioengineering. **79:** 398-407.

Ozturk SS (1996). Engineering Challenges in High Density Cell Culture Systems. Cytotechnology. **22:** 3-16.

Ozturk SS and Palsson BO (1990). Effect of Medium Osmolarity on Hybridoma Growth, Metabolism, and Antibody Production. Biotechnology and Bioengineering. **37:** 989-993.

Ozturk SS and Polsson BO (1990). Effects of Dissolved Oxygen on Hybridoma Growth, Metabolism and Antibody Production in Continuous Culture. Biotechnology Progress. **6:** 437-446.

Ozturk SS, Riley MR, and Palsson BO (1992). Effects of Ammonia and Lactate on Hybridoma Growth, Metabolism, and Antibody Prodution. Biotechnology and Bioengineering. **39:** 418-431.

Papagianni M, Mattey M, and Kristiansen B (2003). Design of a Tubular Loop Bioreactor for Scale-Up and Scale-Down of Fermentation Processes. Biotechnology Progress. **19:** 1498-1504.

Park ES, Gao X, Chung JM, and Chung K (2006). Levels of Mitochondrial Reactive Oxygen Species Increase in Rat Neuropathic Spinal Dorsal Horn Neurons. Neuroscience Letters. **391:** 108-111.

Park H, Berzin IJL, and Gordana V (2005). Evaluation of Silicone Tubing Toxicity Using Tobacco BY2 Culture. In Vitro Cellular and Developmental Biology. **41:** 555-560.

Passini CA and Goochee CF (1989). Response of Mouse Hybridoma Cell Line to Heat Shock, Agitation and Sparging. Biotechnology Progress. **5:** 175-188.

Pavlou AK and Belsey MJ (2005). The Therapeutic Antibodies Market to 2008. European Journal of Pharmaceutics and Biopharmaceutics. **59:** 389-396.

Perani A, Singh R, Chauhan R, and Al-Rubeai M (1998). Variable Functions of Bcl-2 in Mediating Bioreactor Stress- Induced Apoptosis in Hybridoma Cells. Cytotechnology. **28:** 177-188.

Perkins M, Theiler R, Lunte S, and Jeschke M (2000). Determination of the Origin of Charge Heterogeneity in a Murine Monoclonal Antibody. Pharmaceutical Research. **17:** 1110-1117.

Petersen JF, McIntire LV, and Papoutsakis ET (1988). Shear Sensitivity of Cultured Hybridoma Cells (Crl-8018) Depends on Mode of Growth, Culture Age and Metabolite Concentration. Journal of Biotechnology. **7:** 229-246.

Petit PX, Lecoeur H, and Zorn E (1995). Alterations in Mitochondrial Structure and Function Are Early Events of Dexamethasone-Induced Thymocyte Apoptosis. The Journal of Cell Biology. **130:** 157-167.

Pin S, Chen H, Lein PJ, and Wang MM (2006). Nucleic Acid Binding Agents Exert Local Toxic Effects on Neurites Via a Non-Nuclear Mechanism. Journal of Neurochemistry. **96:** 1253-1266.

Pohorecki R, Nienow AW, Chisti Y, Chalmers JJ, and Baldyag J (1998). Fluid Mechanics Problems in Biotechnology. Applied Mechanics Review. **51:** 1-121.

Poot M, Gibson LL, and Singer VL (1997). Detection of Apoptosis in Live Cells by MitoTracker Red CMXRos and SYTO Dye Flow Cytometry. Cytometry. **27:** 358-364.

Poot M and Pierce RH (1999a). Detection of Changes in Mitochondrial Function During Apoptosis by Simultaneous Staining With Multiple Fluorescent Dyes and Correlated Multiparameter Flow Cytometry. Cytometry. **35:** 311-317.

Poot M and Pierce RH (1999b). Detection of Changes in Mitochondrial Function During Apoptosis by Simultaneous Staining With Multiple Fluorescent Dyes and Correlated Multiparameter Flow Cytometry. Cytometry. **35:** 311-317.

Poot M, Zhang YZ, Kramer JA, Wells KS, Jones LJ, Hanzel DK et al. (1996). Analysis of Mitochondrial Morphology and Function With Novel Fixable Fluorescent Stains. Journal of Histochemistry and Cytochemistry. **44:** 1363-1372.

Porter AJ, Dickson AJ, Barnes LM, and Racher AJ (2007). Antibody Production by GS-CHO Cell Lines Over Extended Culture Periods. Cell Technology for Cell Products. **19:** 137-140.

Qi W, Ding D, and Salvi RJ (2008). Cytotoxic Effects of Dimethyl Sulphoxide (DMSO) on Cochlear Organotypic Cultures. Hearing Research. **236:** 52-60.

Racher AJ, Looby D, and Griffiths JB (1990). Use of Lactate Dehydrogenase Release to Assess Changes in Culture Viability. Cytotechnology. **3:** 301-307.

Rathore AS (2009). Roadmap for Implementation of Quality by Design (QbD) for Biotechnology Products. Trends in Biotechnology. **27:** 546-553.

Rearick JI, Chapman A, and Kornfeld S (1981). Glucose Starvation Alters Lipid-Linked Oligosaccharide Biosynthesis in Chinese Hamster Ovary Cells. Journal of Biological Chemistry. **256:** 6255-6261.

Reuveny S, Velez D, Macmillan JD, and Miller L (1986). Factors Affecting Cell-Growth and Monoclonal-Antibody Production in Stirred Reactors. Journal of Immunological Methods. **86:** 53-59.

Reuveny S, Velez D, Macmillan JD, and Miller L (1987). Factors Affecting Monoclonal Antibody Production in Culture. Developments in Biological Standardization. **66:** 169-175.

Reyes C, Pera C, and Galindo E (2003). Reproducing Shake Flasks Performance in Stirred Fermentors: Production of Alginates by Azotobacter Vinelandii. Journal of Biotechnology. **105:** 189-198.

Reynolds JE, Li J, and Eastman A (1996). Detection of Apoptosis by Flow Cytometry of Cells Simultaneously Stained for Intracellular PH (Carboxy SNARF-1) and Membrane Permeability (Hoechst 33342). Cytometry. **25:** 349-357.

Rhiel M and Murhammer DW (1995). The Effect of Oscillating Dissolved Oxygen Concentrations on the Metabolism of a *Spodoptera Frugiperda* IPLB-Sf21-AE Clonal Isolate. Biotechnology and Bioengineering. **47:** 640-650.

Riley S (2006). The Future of Monoclonal Antibodies Therapeutics. Business Insights Business Report.

Ross DD, Joneckis CC, Ordonez JV, Sisk AM, Wu RK, Hamburger AW et al. (1989). Estimation of Cell-Survival by Flow Cytometric Quantification of Fluorescein Diacetate Propidium Iodide Viable Cell Number. Cancer Research. **49:** 3776-3782.

Rottenberg H and Wu S (1998). Quantitative Assay by Flow Cytometry of the Mitochondrial Membrane Potential in Intact Cells. Biochimica Et Biophysica Acta. **1404:** 393-404.

Ruszkowski S (1995). A Rational Method for Measuring Blending Performance, and Comparison of Different Impeller Types. Institute of Chemical Engineers Symposium Series. **136:** 283-291.

Salvioli S, Ardizzoni A, Franceschi C, and Cossarizza A (1997). JC-1, but Not $DiOC_6(3)$ or Rhodamine 123, Is a Reliable Fluorescent Probe to Assess MMP in Intact Cells: Implications for Studies on Mitochondrial Functionality During Apoptosis. FEBS Letters. **411:** 77-82.

Santos NC, Figueira-Coelho J, Martins-Silva J, and Saldanha C (2003). Multidisciplinary Utilization of Dimethyl Sulfoxide: Pharmacological, Cellular, and Molecular Aspects. Biochemical Pharmacology. **65:** 1035-1041.

Schmelzer AE and Miller WM (2002). Hyperosmotic Stress and Elevated pCO_2 Alter Monoclonal Antibody Charge Distribution and Monosaccaride Content. Biotechnology Progress. **18:** 346-353.

Schugerl K (1993). Comparison of Different Bioreactor Performances. Bioprocess Engineering. **9:** 215-223.

Senger RS and Karim MN (2003). Effect of Shear Stress on Intrinsic CHO Culture State and Glycosylation of Recombinant Tissue-Type Plasminogen Activator Protein. Biotechnology Progress. **19:** 1199-1209.

Senior PJ and Windass J (1980). The ICI Single Cell Protein Process. Biotechnology Letters. **2:** 205-210.

Sgonc R and Gruber J (1998). Apoptosis Detection: an Overview. Experimental Gerontology. **33:** 525-533.

Shafer FQ, Buettner GR (2001). Redox Environment of The Cell as Viewed Through The Redox State of The Glutathione Disulfide/ Glutathione Couple. Free Radical Biology and Medicine. **30:** 1191 – 1212.

Shanker G, Aschner JL, Syversen T, and Aschner M (2004). Free Radical Formation in Cerebral Cortisal Astrocytes in Culture Induced by Methylmercury. Brain Research. Molecular Brain Research. **10:** 48-57.

Shanker G, Syversen T, Aschner JL, and Aschener M. (2005). Modulatory Effect of Glutathione Status and Antioxidants on Methylmercury-Induced Free Radical Formation in Primary Cultures of Cerebral Astrocytes. Brain Research. Molecular Brain Research. **13:** 11-22.

Shapiro HM (2000). Membrane Potential Estimation by Flow Cytometry. Methods. **21:** 271-279.

Shapiro HM (2003a). Parameters and Probes. In: Practical Flow Cytometry, (273-410). New Jersey: John Wiley & Sons.

Shapiro HM (2003b). Practical Flow Cytometry. New Jersey: John Wiley & Sons.

Sheeley DM, Merrill BM, and Taylor LCE (1997). Characterization of Monoclonal Antibody Glycosylation: Comparison of Expression Systems and Identification of Terminal [Alpha]-Linked Galactose. Analytical Biochemistry. **247:** 102-110.

Shultz JS (1964). Cotton Closure as an Aeration Barrier in Shaken Flask Fermentations. Applied Microbiology. **12:** 305-310.

Simpson NH, Milner AE, and AlRubeai M (1997). Prevention of Hybridoma Cell Death by Bcl-2 During Sub-Optimal Culture Conditions. Biotechnology and Bioengineering. **54:** 1-16.

Simpson NH, Singh RP, Perani A, Goldenzon C, and Al-Rubeai M (1998). In Hybridoma Cultures, Deprivation of Any Single Amino Acid Leads to Apoptotic Death, Which Is Suppressed by the Expression of the Bcl-2 Gene. Biotechnology and Bioengineering. **59:** 90-98.

Sinclair AM and Elliott S (2004). Glycoengineering: The Effect of Glycosylation on the Properties of Therapeutic Proteins. Journal of Pharmaceutical Sciences. **94:** 1626-1636.

Singh RP and Al-Rubeai M (1994). Cell Death in Bioreactors: A Role for Apoptosis. Biotechnology and Bioengineering. **44:** 720-726.

Singh RP and Al-Rubeai M (1998). Apoptosis and Bioprocess Technology. Advances in Biochemical Engineering/Biotechnology. **62:** 167-184.

Stacpoole PW (1989). The Pharmacology of Dichloroacetate. Metabolism. **38:** 1124-1144.

Stephanopoulos GN (1984). Dynamic Behaniour of Second-Order Systems. In: Chemical Process Control, (186-211). Upper Saddle River, NJ: Prentice Hall.

Sugita M, Muroya T, Sugishita T, Tenjin Y, and Satoh H (1986). Sorting of Living and Dead Cells by Flow Cytometry-Staining Principle and Basic Experiment. Gan No Rinsho. **32:** 268-273.

Sun X and Zhang Y (2004). Glutamine Cannot Support Recombinant CHO Cell Growth and Maintenance in the Absence of Glucose. Process Biochemistry. **39:** 719-722.

Sutera SP (1977). Flow-Induced Trauma to Blood Cells. Circulation Research. **41:** 2-8.

Sweere APJ, Luyben KChAM, and Kossen NWF (1987). Regime Analysis and Scale-Down: Tools to Investigate the Performance of Bioreactors. Enzyme and Microbial Technology. **9:** 386-398.

Szabo G, Kiss A, and Tron L (1982). Permeabilization of Lymphocytes With Polyethylene Glycol-1000 - Discrimination of Permeabilized Cells by Flow-Cytometry. Cytometry. **3:** 59-63.

Takahama T, Kanai F, Hiraishi M, Onishi K, Yamazaki Z, Suma K et al. (1985). Long-Term Non Heparinized Left Heart Bypass (LHB): Centrigugal Pump or Roller Pump. Transactions - American Society for Artificial Internal Organs. **31:** 372-376.

Takeda H, Goda T, Uzawa S, Matsukura H, Sakai K, and Tanabe TA (1984). A Comparison of Centrifugal and Roller Pumps. An Experimental Study. Japanese Journal for Thoracic Surgery. **37:** 273-277.

Takuma S, Hirashima C, and Piret JM (2007). Dependence on Glucose Limitation of the pCO_2 Influences on CHO Cell Growth, Metabolism and IgG Production. Biotechnology and Bioengineering. **97:** 1479-1488.

Tamari Y, Lee-Sensiba K, Leonard EF, Parnell V, and Tortolani AJ (1993). The Effects of Pressure and Flow on Hemolysis Caused by Bio-Medicus Centrifugal Pumps and Roller Pumps. Guidelines for Choosing a Blood Pump. The Journal of Thoracic and Cardiovascular Surgery. **106:** 997-1007.

Tanzeglock T, Soos M, Stephanopoulos G, and Morbidelli M (2009). Induction of Mammalina Cell Death by Simple Shear and Extensional Flows. Biotechnology and Bioengineering. **104:** 360-370.

Taylor ME and Drickamer K (2006). Introduction to Glycobiology. Oxford: Oxford University Press.

Telling RC and Elsworth R (1965). Submerged Culture of Hamster Kidney Cells in a Stainless Steel Vessel. Biotechnology and Bioengineering. **7:** 417-434.

Terada M, Inaba M, and Yano Y (1998). Growth-Inhibitory Effect of a High Glucose Concentration on Osteoblast-Like Cells. Bone. **22:** 17-23.

Terasaki M, Song J, Wong JR, Weiss MJ, and Chen LB (1984). Localization of Endoplasmic-Reticulum in Living and Glutaraldehyde-Fixed Cells With Fluorescent Dyes. Cell. **38:** 101-108.

Teshima G, Porter J, Yim K, Ling V, and Guzzetta A (1991). Determination of Soluble CD4 at Asparagine-52 Results in Reduced Binding Capacity for the HIV-1 Envelope Glycoprotein Gp120. Biochemistry. **30:** 3916-3922.

Tey BT, Singh RP, Piredda L, Piacentini M, and Al-Rubeai M (2000). Influence of Bcl-2 on Cell Death During the Cultivation of a Chinese Hamster Ovary Cell Line Expressing a Chimeric Antibody. Biotechnology and Bioengineering. **68:** 31-43.

Thaysen-Andersen M, Mysling S, and Hojrup P (2009). Site-Specific Glycoprofiling of N-Linked Glycopeptides Using MALDI-TOF MS: Strong Correlation Between Signal Strength and Glycoform Quantities. Analytical Chemistry. **81:** 3933-3943.

Toth P, El-Shanti H, Eivins S, Rhead WJ, Klein JM (1993). Transient Improvement of Congenital Lactic Acidosis in a Male Infant with Pyruvate Decarboxylase Deficiency Treated with Dichloroacetate. The Journal of Pediatrics. **123:** 427-440.

Trummer E and Fauland K (2006). Process Parameter Shifting: Part I. Effect of *DOT*, PH and Temperature on the Performance of Epo-Fc Expressing CHO Cells Cultivated in Controlled Batch Bioreactors. Biotechnology and Bioengineering. **94:** 1033-1044.

Tsai PK, Bruner MW, Irwin JI, Ip CCY, Oliver CN, and Nelson RW et al. (1993). Origin of the Isoelectric Heterogeneity of Monoclonal Immunoglobulin H1B4. Pharmaceutical Research. **10:** 1580-1586.

Tsao YS, Cardoso AG, Condon RGG, Voloch M, Lio P, and Lagos JC et al. (2005). Monitoring Chinese Hamster Ovary Cell Culture by the Analysis of Glucose and Lactate Metabolism. Journal of Biotechnology. **118:** 316-327.

Tsujino T, Miura M, Komori N, and Inoue K (1999). Cavitational Occurence Around Rotational Bodies in Water and Blood. Natural Science. **48:** 21-27.

Tyagi AK, Randolph TW, Dong A, Maloney KM, Hitscherich C, and Carpenter JF (2009). IgG Particle Formation During Filling Pump Operation: A Case Study of Heterogeneous Nucleation on Stainless Steel Nanoparticles. Journal of Pharmaceutical Sciences. **98:** 94-104.

Tzannis ST, Hrushesky WJM, Wood PA, and Przybycien TM (1997). Adsorption of a Formulated Protein on a Drug Delivery Device Surface. Journal of Colloid and Interface Science. **189:** 216-228.

Tzima E (2006). Role of Small GTPases in Endothelial Cytoskeletal Dynamics and the Shear Stress Response. Circulation Research. **98:** 176-185.

Urlaub G and Chasin LA (1980). Isolation of Chinese Hamster Cell Mutants Deficient in Dihydrofolate Reductase Activity. Proceedings of the National Academy of Sciences of the United States of America. **77:** 4216-4220.

Usami A, Ohtsu A, Takahama S, and Fujii T (1996). The Effect of pH, Hydrogen Peroxide and Temperature on the Stability of Human Monoclonal Antibody. Journal of Pharmaceutical and Biomedical Analysis. **14:** 1133-1140.

Valeri CR, Macgregor H, Ragno G, Healey N, Fonger J, and Khuri SF (2006). Effects of Centrifugal and Roller Pumps on Survival of Autologous Red Cells in Cardiopulmonary Bypass Surgery. Perfusion. **21:** 291-296.

van der Lans RGLM, Vrabel P, Luyben KChAM, Boon L, and Nienow A (2000). Mixing in Large-Scale Vessels With Multiple Radian or Radial and Axial Up-Pumping Impellers: Modelling and Measurements. Chemical Engineering Science. **55:** 5881-5896.

van Reis R and Zydney A (2007). Bioprocess Membrane Technology. Journal of Membrane Science. **297:** 16-50.

Varley J and Birch J (1999). Reactor Design for Large Scale Suspension Animal Cell Culture. Cytotechnology. **29:** 177-205.

Varum S, Bento C, Sousa AP, Gomes-Santos CSS, Henriques P, and Almeida-Santos T et al. (2007). Characterization of Human Sperm Populations Using Conventional Parameters, Surface Ubiquitination, and Apoptotic Markers. Fertility and Sterility. **87:** 572-583.

Vazquez A, Lui J, Zhou Y, and Oltvai ZN (2010). Catabolic Efficiency of Aerobic Glycolysis: The Warburg Effect Revisited. BMC Systems Biology. **4:** 58-70.

Vermes I, Haanen C, and Reutelingsperger C (2000). Flow Cytometry of Apoptotic Cell Death. Journal of Immunological Methods. **243:** 167-190.

Vermes I, Haanen C, Steffens-Nakken H, and Reutellingsperger C (1995). A Novel Assay for Apoptosis Flow Cytometric Detection of Phosphatidylserine Expression on Early Apoptotic Cells Using Fluorescein Labelled Annexin V. Journal of Immunological Methods. **184:** 39-51.

Vivian Md, Albert E.Schmelzer, and Wiliam M.Miller (2002). Characterisation of Hybridoma Cell Responses to Elevated pCO_2 and Osmolarity: Intracellular PH, Cell Size, Apoptosis, and Metabolism. Biotechnology and Bioengineering. **77:** 369-380.

Waldmann TA (2003). Immunotherapy: Past, Present and Future. Nature Medicine. **9:** 269-277.

Wang HY, Bao N, and Lu C (2008). A Microfluidic Cell Array With Individually Addressable Culture Chambers. Biosensors and Bioelectronics. **24:** 613-617.

Warburg O (1930). The Metabolism of Tumours. Constable: London.

Watanabe N, Kataoka H, Yasuda T, and Takatani S (2006). Dynamic Deformation and Recovery Response of Red Blood Cells to a Cyclically Reversing Shear Flow: Effects of Frequency of Cyclically Reversing Shear Flow and Shear Stress Level. Biophysical Journal. **91:** 1984-1998.

Weaver JL (1998). Estimation of Cell Viability by Flow Cytometry. Methods in Molecular Biology. **91:** 77-83.

Werner RG, Noe W, Kopp K, and Schluter M (1998). Appropriate Mammalian Expression Systems for Biopharmaceuticals. Arzneimittel-Forschung-Drug Research. **48:** 870-880.

Wold F (1981). In Vivo Chemical Modifications of Proteins (Prost-Translational Modification). Annual Review of Biochemistry. **50:** 783-814.

Wong, Kathy Tin Kam Wong, Yih Yean Lee, Perer Nissom Morin, Chew Kiat Heng, and Miranda Gek Sim Yap (2006). Transcriptional Profiling of Apoptotic Pathways in Batch and Fed-Batch CHO Cell Cultures. Biotechnology and Bioengineering. **94:** 373-382.

Wong DCF, Wong KTK, Goh LT, Heng KC, and Yap MGS (2004). Impact of Dynamic Online Fed-Batch Strategies on Metabolism, Productivity, and N-Glycosylation Quality in CHO Cell Cultures. Biotechnology and Bioengineering. **89:** 164-177.

Wu J (1995). Mechanisms of Animal Cell Damage Associated With Gas Bubbles and Cell Protection by Medium Additives. Journal of Biotechnology. **43:** 81-94.

Xie LZ and Wang DIC (1994). Fed-Batch Cultivation of Animal-Cells Using Different Medium Design Concepts and Feeding Strategies. Biotechnology and Bioengineering. **43:** 1175-1189.

Xing ZZ, Li ZJ, Chow V, and Lee SS (2008). Identifying Inhibitory Threshold Values of Repressing Metabolites in CHO Cell Culture Using Multivariate Analysis Methods. Biotechnology Progress. **24:** 675-683.

Yang M and Butler M (2000). Effects of Ammonia on CHO Cell Growth, Erythropoietin Production and Glycosylation. Biotechnology and Bioengineering. **68:** 370-380.

Yarborough KA, Mockros LF, and Lewis FJ (1966). Hydrodynamic Hemolysis in Extracorporeal Machines. The Journal of Thoracic and Cardiovascular Surgery. **52:** 550-557.

Yoon SK, Hong JK, and Lee GM (2004). Effect of Simultaneous Application of Stressful Culture Conditions on Specific Productivity and Heterogeneity of Erythropoietin in Chinese Hamster Ovary Cells. Biotechnology Progress. **20:** 1293-1296.

Zabriskie DW and Arcuri EJ (1986). Factors Influencing Productivity of Fermentations Employing Recombinant Microorganisms. Enzyme and Microbial Technology. **8:** 706-717.

Zamai L, Falcieri E, Marhefka G, and Vital M (1996). Supravital Exposure to Propidium Iodide Identifies Apoptotic Cells in the Absence of Nucleosomal DNA Fragmentation. Cytometry. **23:** 303-311.

Zamzami N, Marchetti P, Castedo M, Decaudin D, Macho A, Hirsch T et al. (1995). Sequential Reduction of Mitochondrial Transmembrane Potential and Generation of Reactive Oxygen Species in Early Programmed Cell Death. The Journal of Experimental Medicine. **182:** 367-377.

Zang Z, Al-Rubeai M, and Thomas CR (1993). Estimation of Disruption of Animal Cells by Turbulent Capillary Flow. Biotechnology and Bioengineering. **42:** 987-993.

Zanghi JA, Mendoza TP, Knop RH, and Miller WM (1998). Ammonia Inhibits Neural Cell Adhesion Molecule Polysialylation in CHO and Small Cell Lung Cancer Cells. Journal of Cell Physiology. **177:** 248-263.

Zbinniew Darzynkiewicz, Gloria Juan, and Xun Li (1996). Cytometry in Cell Necrobiology: Analysis of Apoptosis and Accidental Cell Death (Necrosis). Cytometry. **27:** 1-20.

Zettlmeissl G, Conradt HS, Nimtz M, and Karges HE (1989). Characterization of Recombinant Human Antithrombin III Synthesized in Chinese Hamster Ovary Cells. Journal of Biological Chemistry. **264:** 21153-21159.

Zhang F, Sun XM, Yi XP, and Zhang YX (2006). Metabolic Characteristics of Recombinant Chinese Hamster Ovary Cells Expressing Glutamine Synthetase in Presence and Absence of Glutamine. Cytotechnology. **51:** 21-28.

Zhang YB, Howitt J, McCorkle S, Lawrence P, Springer K, and Freimuth P (2004). Protein Aggregation During Overexpression Limited by Peptide Extensions With Large Net Negative Charge. Protein Expression and Purification. **36:** 207-216.

Zhang Z, Al R, and Thomas CR (1993). Comparison of the Fragilities of Several Animal Cell Lines. Biotechnology Techniques. **7:** 177-182.

Zhang Z, Pan H, and Chen X (2009). Mass Spectrometry for Structural Characterisation of Therapeutic Antibodies. Mass Spectrometry Reviews. **28:** 147-176.

Zhang Z and Thomas CR (1993). Modelling of Animal Cell Damage in Turbulent Flows. In: Proc. 3rd Int. Conf. on Bioreactor and Bioprocess Fluid Dynamics, (475-482). London: Mechanical Engineering Publications.

Zhou G and Kresta SM (1996). Impact of Tank Geometry on the Maximum Turbulence Energy Dissipation Rate for Impellers. American Institution of Chemical Engineers Journal. **42:** 2476-2490.

Zhou W, Rehm J, and Hu WS (1995). High Viable Cell Concentration Fed-Batch Cultures of Hybridoma Cells Through on-Line Nutrient Feeding. Biotechnology and Bioengineering. **46:** 579-587.

Zhu MM, Goyal A, Rank DL, Gupta SK, Vanden Boom T, and Lee SS (2005). Effects of Elevated pCO_2 and Osmolality on Growth of CHO Cells and Production of Anibody-Fusion Protein B1: a Case Study. Biotechnology Progress. **21:** 70-77.

Zuliani T, Duval R, Chantal J, Schnebert S, Andre P, Dumas M et al. (2003). Sensitive and Reliable JC-1 and TOTO-3 Double Staining to Assess Mitochondrial Transmembrane Potential and Plasma Membrane Integrity: Interest for Cell Death Investigations. Cytometry Part A. **54A:** 100-108.

}